Proteasomal protein turnover during defense priming in *Arabidopsis*

Dissertation

to obtain the academic degree

Doctor rerum naturalium (Dr. rer. nat.)

in molecular plant physiology

submitted to the

Faculty of Science

Institute of Biochemistry and Biology

of the Universität Potsdam

by

Daniela Spinti

Date of disputation:

Potsdam, 20 April 2021

Supervisor: Prof. Dr. Frederik Börnke (Universität Potsdam)
Reviewers: Prof. Dr. Tina Romeis (Leibniz-Insitut für Pflanzenbiochemie, Halle)
PD Dr. Marcel Wiermer (Georg-August-Universität Göttingen)

Published online on the
Publication Server of the University of Potsdam:
https://doi.org/10.25932/publishup-43571
https://nbn-resolving.org/urn:nbn:de:kobv:517-opus4-435713

Index

Abbreviations

°C	degree Celsius	*N. benthamiana*	*Nicotiana benthamiana*
µg	micro gram	NHP	N-hydroxy pipecolic acid
µl	micro liter	nm	nano meter
A. thaliana	*Arabidopsis thaliana*	OD_{600}	optical density at 600 nm
A. tumefaciens	*Agrobacterium tumefaciens*	P	Primed plants
CFU	Colony forming units	PAGE	polyacrylamide gel electrophoresis
cLSM	confocal laser scanning microscope	PAMP	pathogen associated molecular pattern
Col-0	*Arabidopsis* Columbia-0	PCR	polymerase chain reaction
dpi	Days post infiltration	Pip	Pipecolic acid
E. coli	*Escherichia coli*	PQC	Protein quality control
em.	emission	PRR	pathogen recognition receptor
ET	Ethylene	*Psm*	*Pseudomonas syringae* pv. *maculicola*
EtOH	Ethanol	*Pst*	*Pseudomonas syringae* pv. *Tomato* DC3000
ex.	excitation	PT	Primed and triggered plants
g	gram	RAM	root apical meristem
GFP	green fluorescent protein	rpm	rotation per minute
hpi	Hours post infiltration	*S. cerevisiae*	*Saccharomyces cerevisiae*
HR	hypersensitive response	SA	Salicylic acid
ISR	Induced systemic resistance	SAR	Systemic acquired resistance

JA	Jasmoncic acid	SDS	sodium dodecyl sulfate
kDa	Kilo dalton	T	Triggered plants
M	Mock treated plants	T3E	bacterial type III effector
mA	milli ampere	Ub	ubiquitin
mg	milli gram	UPS	Ubiquitin-proteasome-system
ml	milli liter	V	volt
mM	milli molar	*Xcv*	*Xanthomonas campestris* pv. *vesicatoria*

Summary

The ubiquitin-proteasome-system (UPS) is a cellular cascade involving three enzymatic steps for protein ubiquitination to target them to the 26S proteasome for proteolytic degradation. Several components of the UPS have been shown to be central for regulation of defense responses during infections with phytopathogenic bacteria. Upon recognition of the pathogen, local defense is induced which also primes the plant to acquire systemic resistance (SAR) for enhanced immune responses upon challenging infections. Here, ubiquitinated proteins were shown to accumulate locally and systemically during infections with *Psm* and after treatment with the SAR-inducing metabolites salicylic acid (SA) and pipecolic acid (Pip). The role of the 26S proteasome in local defense has been described in several studies, but the potential role during SAR remains elusive and was therefore investigated in this project by characterizing the *Arabidopsis* proteasome mutants *rpt2a*-2 and *rpn12a*-1 during priming and infections with *Pseudomonas*. Bacterial replication assays reveal decreased basal and systemic immunity in both mutants which was verified on molecular level showing impaired activation of defense- and SAR-genes. *rpt2a*-2 and *rpn12a*-1 accumulate wild type like levels of camalexin but less SA. Endogenous SA treatment restores local *PR* gene expression but does not rescue the SAR-phenotype. An RNAseq experiment of Col-0 and *rpt2a*-2 reveal weak or absent induction of defense genes in the proteasome mutant during priming. Thus, a functional 26S proteasome was found to be required for induction of SAR while compensatory mechanisms can still be initiated.

E3-ubiquitin ligases conduct the last step of substrate ubiquitination and thereby convey specificity to proteasomal protein turnover. Using RNAseq, 11 E3-ligases were found to be differentially expressed during priming in Col-0 of which *plant U-box 54* (*PUB54*) and *ariadne 12* (*ARI12*) were further investigated to gain deeper understanding of their potential role during priming.

PUB54 was shown to be expressed during priming and /or triggering with virulent *Pseudomonas. pub54*-I and *pub54*-II mutants display local and systemic defense comparable to Col-0. The heavy-metal associated protein 35 (HMP35) was identified as potential substrate of PUB54 in yeast which was verified in *vitro* and *in vivo*. PUB54 was shown to be an active E3-ligase exhibiting auto-ubiquitination activity and performing ubiquitination of HMP35. Proteasomal turnover of HMP35 was observed indicating that PUB54 targets HMP35 for ubiquitination and subsequent proteasomal degradation. Furthermore, *hmp35*-I benefits from increased resistance in bacterial replication assays. Thus, HMP35 is potentially a negative regulator of defense which is targeted and ubiquitinated by PUB54 to regulate downstream defense signaling. *ARI12* is transcriptionally activated during priming or triggering and hyperinduced during priming and triggering. Gene expression is not inducible by the defense related hormone salicylic acid (SA) and is dampened in *npr1* and *fmo1* mutants consequently depending on functional SA- and Pip-pathways, respectively. ARI12

accumulates systemically after priming with SA, Pip or *Pseudomonas*. *ari12* mutants are not altered in resistance but stable overexpression leads to increased resistance in local and systemic tissue. During priming and triggering, unbalanced *ARI12* levels (i.e. knock out or overexpression) leads to enhanced *FMO1* activation indicating a role of ARI12 in Pip-mediated SAR. ARI12 was shown to be an active E3-ligase with auto-ubiquitination activity likely required for activation with an identified ubiquitination site at K474. Mass spectrometrically identified potential substrates were not verified by additional experiments yet but suggest involvement of ARI12 in regulation of ROS in turn regulating Pip-dependent SAR pathways.

Thus, data from this project provide strong indications about the involvement of the 26S proteasome in SAR and identified a central role of the two so far barely described E3-ubiquitin ligases PUB54 and ARI12 as novel components of plant defense.

Zusammenfassung

Das Ubiquitin-Proteasom-System (UPS) ist ein in drei Schritten enzymatisch ablaufender Prozess zur Ubiquitinierung von Proteinen, wodurch diese zum proteolytischen Abbau an das 26S Proteasom geschickt werden. Verschiedene Komponenten des UPS sind zentral an der Regulation von Immunantworten während der Infektion mit phytopathogenen Bakterien beteiligt. Beim Erkennen einer Infektion werden lokale Abwehrreaktionen initiiert, wobei auch mobile Signale in distalen Pflanzenteilen verteilt werden, welche die Pflanze *primen* (vorbereiten). Mit dem Erwerb der systemischen Resistenz (SAR) kann die Immunantwort bei einer zweiten Infektion verstärkt aktiviert werden. Es wurde hier gezeigt, dass ubiquitinierte Proteine in lokalem und systemischem Gewebe akkumulieren, wenn *Arabidopsis* mit *Pseudomonas* infiziert oder mit SAR-induzierender Salizylsäure (SA) oder Pipecolinsäure (Pip) behandelt wird. Die genaue Rolle des 26S Proteasoms in der systemischen Immunantwort ist bisher unklar und wurde daher in diesem Projekt mithilfe der Charakterisierung der Proteasommutanten *rpt2a*-2 und *rpn12a*-1 während des Primings genauer untersucht. In Bakterienwachstumsversuchen zeigte sich eine lokal und systemisch erhöhte Suszeptibilität der Proteasommutanten, welche auf molekularer Ebene durch ausbleibende Aktivierung von Abwehrgenen verifiziert wurde. Beide Mutanten akkumulieren ähnliche Mengen Camalexin während einer Infektion, sind aber in der Biosynthese von SA gestört. Die endogene Applikation von SA löst lokale *PR*-Gen Expression aus, kann aber nicht das SAR-Defizit ausgleichen. In einem RNAseq Experiment wurde das Transkriptom von Col-0 und *rpt2a*-2 während des Primings analysiert und zeigte, dass zentrale Abwehr- und SAR-Gene nicht oder nur schwach induziert werden. Es konnte somit gezeigt werden, dass ein funktionales 26S Proteasom zur vollen Induktion aller Teile der lokalen und systemischen Immunantwort benötigt wird, während ausgleichende Prozesse weiterhin aktiviert werden können.

E3-Ubiquitin Ligasen führen den letzten Schritt der Substratubiquitinierung durch und vermitteln dadurch die Spezifität des proteasomalen Proteinabbaus. Mithilfe des RNAseq Experiments konnten 11 differentiell exprimierte Transkripte, annotiert als E3-Ligasen, identifiziert werden. Von diesen wurden *PLANT U-BOX 54* (*PUB54*) und *ARIADNE 12* (*ARI12*) weiter analysiert, um ein tiefergehendes Verständnis ihres Einflusses auf die systemische Immunantwort zu erhalten. *PUB54* wird während des Primings und bei Infektionen mit virulenten *Pseudomonas* exprimiert. Die *pub54*-I und *pub54*-II Mutanten zeigen lokal und systemisch eine wildtyp-ähnliche Resistenz. Das „heavy-metal associated protein 35" (HMP35) wurde in Hefe als potentielles Substrat von PUB54 identifiziert und *in vitro* und *in vivo* verifiziert. PUB54 ist eine aktive E3-Ligase mit Autoubiquitinierungsaktivität, welche HMP35 ubiquitiniert. HMP35 wird außerdem *in planta* proteasomal abgebaut, wodurch eine Ubiquitinierung von HMP35 durch PUB54 zum proteasomalen Abbau nahegelegt wird. Des Weiteren wurde gezeigt, dass *hmp35* Mutanten von erhöhter Resistenz profitieren. HMP35 agiert möglicherweise als negativer Regulator der Immunantwort und wird zur Aktivierung von Abwehrreaktionen durch PUB54 für den proteasomalen Abbau markiert.

ARI12 wird nach Priming oder Infektion mit *Pseudomonas* transkriptionell aktiviert und nach sekundärer Infektion hyperinduziert, wobei die Behandlung mit SA keine Expression induziert. *ARI12* ist jedoch reduziert in *npr1* und *fmo1* Mutanten, wodurch eine Abhängigkeit der Genexpression von funktionalen SA- und Pip-Signalwegen angedeutet wird. ARI12 akkumuliert in systemischem Gewebe nach lokaler Behandlung mit SA, Pip, oder *Pseudomonas.* Die *ari12* Mutante zeigt wildtypähnliche Resistenz gegenüber bakteriellen Infektionen, wohingegen die Überexpression zu einer verstärkten Resistenz in lokalem und systemischem Gewebe führt. Unausgewogene Level von *ARI12* (d.h. knockout oder Überexpression) führen zur erhöhten Expression von *FMO1,* sodass ARI12 potentiell eine regulatorische Rolle in der Pip-vermittelten systemischen Immunantwort übernimmt. Es konnte gezeigt werden, dass ARI12 eine aktive E3-Ligase mit Autoubiquitinierungsaktivität an Lys474 ist, welche vermutlich für die Aktivierung benötigt wird. Massenspektrometrisch identifizierte, mögliche Substrate von ARI12 konnten noch nicht experimentell bestätigt werden, deuten aber auf eine Rolle von ARI12 in der Regulation von reaktiven Oxygen Spezies (ROS) hin, welche wiederum Pip-anhängige Signalwege regulieren.

Zusammengenommen deuten die Daten aus diesem Projekt darauf hin, dass das 26S Proteasom durch den regulierten Proteinabbau zentral ist für die systemische erworbene Resistenz und dass die bisher wenig untersuchten E3-Ligasen PUB54 und ARI12 neue regulatorische Komponenten der pflanzlichen Immunabwehr darstellen.

1. Introduction

Due to their sessile life style, plants cannot escape from fluctuating environmental conditions and stresses. Thus, they are constantly exposed to biotic and abiotic stresses and hence evolved outstanding mechanisms to sense and adapt to these stresses. Some bacteria are potentially pathogenic and may have severe impact on plant health (Danhorn & Fuqua, 2007). However, disease development is mostly an exception because plants possess an efficient multilayered immune system, which enables them to sense the presence of a pathogen and to initiate defense responses *via* an innate immunity to restrict disease establishment at the local infection site (Dangl & Jones, 2001). These local events also impact systemic tissue of the plant by distribution of locally generated signals throughout the plant and consequently primes the plant against future infections (Fu & Dong, 2013; Mishina & Zeier, 2007). The effect of priming is well observable but many aspects of the underlying molecular mechanism remain largely unclear until today.

Proteolytic degradation of proteins *via* the 26S proteasome is a continuously occurring process involving a cascade of enzymes facilitating selective targeting of proteins to maintain protein homeostasis during plant development and response to stresses. Recent findings suggest that the activity of multiple UPS-components is required for full establishment of immune responses (Furniss *et al.*, 2018; Üstün *et al.*, 2013; Yao *et al.*, 2012). However, the role of the proteasome during systemic defense responses is not well understood.

1.1. The plant immune system

1.1.1. Immunity in locally infected tissue

PAMP-triggered immunity (PTI)

Plants developed a sophisticated and multilayered immune system to defend against pathogenic attacks (Jones & Dangl, 2006). When bacteria overcome the preformed physical barriers such as stomata or the plant cuticula virulent pathogens may infect the host (Figure 1). The host plant is susceptible in compatible interactions leading to bacterial propagation and development of disease symptoms. The plant is able to sense the presence of pathogen-associated non-self structures in the apoplast by pattern recognition receptors (PRRs) (Dangl & Jones, 2001). PRRs recognize highly conserved pathogen associated molecular patterns (PAMPs) such as flagellin (represented by the 22 amino acids lone flg22 epitope) and fungal chitin, typically associated with classes of microbes to initiate intercellular defense responses referred to as PAMP-triggered-immunity (PTI) (Boller & Felix, 2009; Nürnberger & Brunner, 2002). PTI restricts development of disease symptoms and confers basal resistance at the local infection site. Within minutes, an oxidative burst is elicited by NADPH oxidase and apoplastic peroxidase mediated production of reactive oxygen species (ROS) such as hydrogen peroxide (H_2O_2) and nitric oxide (NO) (O'Brien *et al.*, 2012). Flagellin-sensitive 2

(FLS2) is a transmembrane PRR interacting with its co-receptor bri1-associated receptor kinase (BAK1) during perception of flg22 (Chinchilla *et al.*, 2007). Dissociation of BAK1 from FLS2 and activation of the downstream receptor-like cytoplasmic kinase (RLCK) botrytis-induced kinase 1 (BIK1) induces a mitogen-activated protein (MAP)-kinase-cascade (Ma *et al.*, 2020; Meng & Zhang, 2013). MAP-kinases (MPKs) in turn induce transcriptional regulation of defense genes via activation of multiple transcription factors (TF) such as WRKY TF (Chen *et al.*, 2019). For instance, the MPK3/MPK6 pathway induces synthesis of the antimicrobial phytoalexin camalexin via transcriptional and post-transcriptional regulation of the transcription factor WRKY33 (Mao *et al.*, 2011). Infections with (hemi-)biotrophic bacteria furthermore induce biosynthesis of defense hormones such as salicylic acid (SA). Accumulation subsequently leads to nonexpressor of pathogenesis-related (NPR)-mediated expression of *pathogenesis related* (*PR*) genes operating at the local infection site and systemically in distal tissue (Ali *et al.*, 2018).

Effector-triggered susceptibility (ETS)

Successful phytopathogens are adapted to their host plants and translocate bacterial effector proteins into the host cell using type III secretion systems to overcome plant immune responses by interference with multiple cellular processes (Beth Mudgett, 2005; Tanaka *et al.*, 2015). The resulting effector-triggered susceptibility (ETS) enhances the bacterial virulence (Jones & Dangl, 2006). For instance, FLS2 is targeted by the *Pseudomonas syringae* effector AvrPtoB harboring an E3-ubiquitin ligase activity (Göhre *et al.*, 2008; Rosebrock *et al.*, 2007). Poly-ubiquitination of the FLS2 kinase domain catalyzed by AvrPtoB likely leads to degradation of the receptor to increase virulence of the pathogen (Göhre *et al.*, 2008). Another example of bacterial effect or protein interfering with plant cellular processes is the targeting of the *Xanthomonas* outer protein J (XopJ) to the proteasomal subunit RPT6 (Üstün *et al.*, 2013). XopJ is proteolytically active and mediates degradation of RPT6 thereby disturbing proteasomal integrity and causing altered degradation of NPR proteins (Üstün & Börnke, 2015)

Effector-triggered immunity (ETI)

The second layer of plant defense is the effector-triggered immunity (ETI) mediated in the host by resistance (R) proteins (Knepper & Day, 2010). The identified mainly intracellular R proteins mostly belong to the nucleotide-binding leucine-rich repeat family (NB-LRR) or to the Toll-like receptors (TLR) (Głowacki *et al.*, 2011). R proteins convey plant resistance by different mechanisms. The gene-for-gene hypothesis is a classic concept basing on the observation that plant resistance depends on *avirulence* (a*vr*) genes deriving from the pathogen and a complement *R* gene from the host (Flor, 1971). In this receptor-ligand model, plants activate immune responses mediated by R-protein dependent recognition of

Avr products. R-proteins may also guard the integrity of host cellular targets for effector action known as the guard hypothesis (Jones & Dangl, 2006). The guard hypothesis was further developed into the decoy model (Van Der Hoorn & Kamoun, 2008). Specific proteins with similarities to the effector targets are generated in the host in order to bind these bacterial effects and mediate the interaction with R proteins. Largely independent on the mode of R-protein action, the recognition of effectors by R proteins leads to a strong and durable defense response which often involves a certain kind of cell death known as the hypersensitive response (HR) to limit pathogen spread (Chisholm *et al.*, 2006).

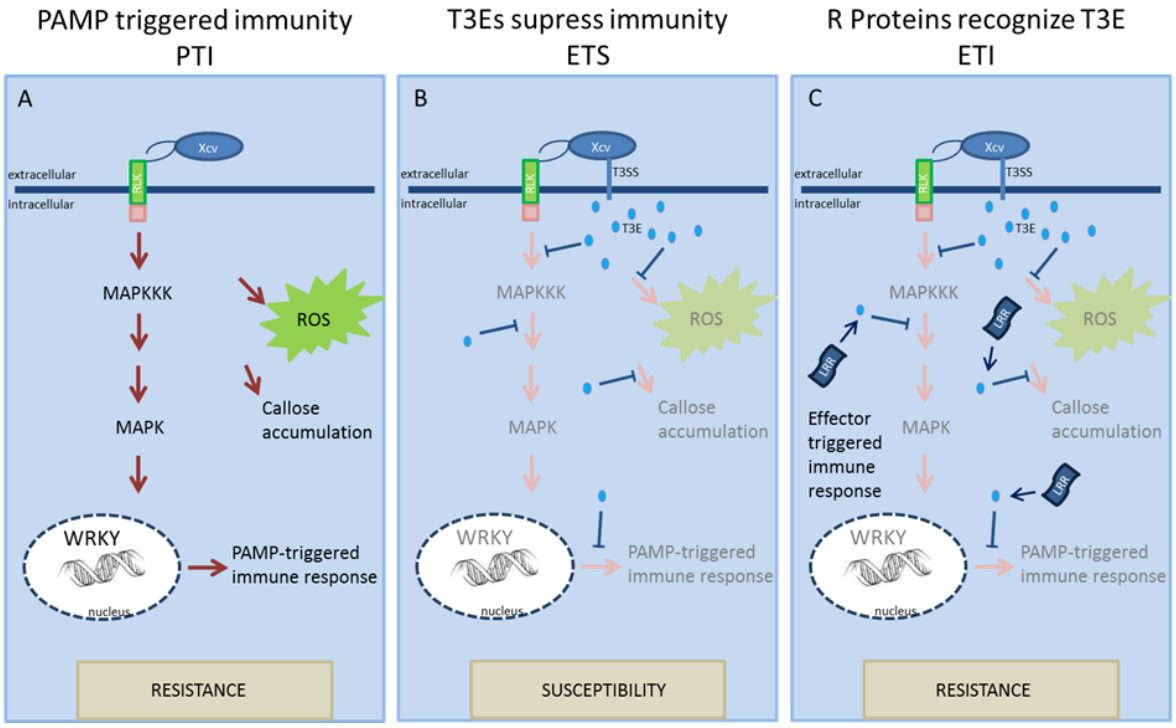

Figure 1: A schematic overview on reactions during plant-pathogen interactions. (A) Presence of PAMPS can be recognized by PRRs to induce intracellular signaling mediating PAMP-triggered immunity (PTI). (B) Translocated bacterial type III effector proteins interfere with host immune signaling leading to effector triggered susceptibility of the host. (C) Type III effector proteins may be recognized by R proteins leading to an effector triggered immunity for increased defense response often resulting in a hypersensitive response. PAMP = pathogen-associated molecular patterns; RLK = receptor like kinase; ROS = reactive oxygen species; T3E = type III effector; T3SS = type III secretion system; Modified after Chisholm *et al.*, 2006.

1.1.2. Systemic immune response

Priming for SAR

Local infection with phytopathogenic bacteria or treatment with PAMPs generate mobile signals that can spread systemically through the plant to distal uninfected tissue where they are perceived and prime the plant's immune system for enhanced responsiveness against future biotic stressors (Conrath *et al.*, 2015). Primed plants may defend faster, earlier and/or stronger upon recognition of a secondary infection (Hilker *et al.*, 2016). The acquired

immunity in distal tissue is termed systemic acquired resistance (SAR). Among other signals, SAR predominantly relies on salicylic acid (SA), pipecolic acid (Pip) and its presumably active derivate N-hydroxy pipecolic acid (NHP) in interdependent and synergistic signaling pathways (Vlot *et al.*, 2020; Westman *et al.*, 2019). The following sections focus on the establishment of SAR upon pathogenic infection including phytohormones, signaling, and the role of other metabolites.

Mobile signals

After local perception and generation of defense induced signals, priming and SAR establishment depends on the systemic distribution to distal tissue followed by activation of defense responses (Transport of Chemical Signals in Systemic Acquired Resistance, 2017). Different potential mobile SAR inducers have been suggested to be involved in the establishment of SAR. Azelaic acid (AzA) was initially identified in petiole exudates from *Arabidopsis* after infection with pathogens and was found to induce systemic SA and Pip-dependent defense responses after application (Jung *et al.*, 2009). AzA is a mobile signal systemically transported via the symplastic route via plasmodesmata-mediated distribution (Lim *et al.*, 2016). The phosphorylated sugar derivative G3P is a glycerol-derived metabolite from the primary metabolism providing basal resistance against the hemibiotrophic fungi *Colletotrichum higginsianum* (Chanda *et al.*, 2008). After treatment with avirulent bacteria, G3P levels increase earlier than other SAR-involved metabolites (Mandal *et al.*, 2011). G3P-defective mutants are compromised in SAR and exogenous application of G3P is capable of systemic defense induction in cooperation with other signals (Chanda *et al.*, 2011). The predicted lipid-transfer protein defective in induced resistance 1 (DIR1) was detected as a mobile molecule during SAR in petiole exudates and is potentially required for transport of AzA, G3P, and other mobile SAR signals to distal leaves and signal amplification (Champigny *et al.*, 2013; Vlot *et al.*, 2020). NAD^+ and NAD^+ phosphate ($NADP^+$) are universal electron carrier which can be released to the extracellular space inducing transcriptional and metabolic changes similar to those occurring during infection with pathogens (Berger *et al.*, 2004; Billington *et al.*, 2006; Pétriacq *et al.*, 2016; Zhang & Mou, 2009). The lectin receptor kinase VI.2 (LecRK-VI.2) was recently identified as a possible $eNAD(P)^+$ receptor functioning with brassinosteroid insensitive 1-associated kinase 1 (BAK1) in complex as central signaling component in SAR in *Arabidopsis* (Wang *et al.*, 2019).

SA-dependent pathway

SA is a phenolic phytohormone with an essential role in local and systemic immune responses mainly synthesized by isochorismate synthase 1 (ICS1, also known as SA-induction deficient 2 (SID2))-dependent pathway in *Arabidopsis* chloroplasts (Garcion *et al.*, 2008; Nawrath & Métraux, 1999). After enhanced disease susceptibility 5 (EDS5) mediated IC

transport to the cytoplasm, the amidotransferase avrPphB SUSCEPTIBLE3 (PBS3) catalyzed the final synthesis step and spontaneous decomposition leads to a release of free SA (Nawrath *et al.*, 2002; Rekhter *et al.*, 2019). Glycosylated SA (SAG) represents the inactive SA and can be stored in the vacuole in large quantities (Dean *et al.*, 2003).

Level of SA increase in response to pathogens in local and systemic tissue during SAR (Hao *et al.*, 2018; Kim & Hwang, 2014). SA is essential for defense activation as *ics1* mutants show a decrease in their potential to establish SAR with moderate resistance responses (Bernsdorff *et al.*, 2016; Hartmann *et al.*, 2018). Exogenous application of SA or chemically active analogues are capable of activating defense responses and SAR (Tripathi *et al.*, 2019). SA is a systemically mobile signal transported via the apoplastic route during SAR (Lim *et al.*, 2016). Methyl-salicylate (MeSA) generated by a SA-methyltransferase (SAMT) might be another long-distance signal initially accumulating in infected tissue. Hydrolysis of MeSA by the methyl esterase SA-binding protein 2 (SABP2) again releases the active SA likely after transportation to systemic tissue (Kumar & Klessig, 2003; Park *et al.*, 2007; Vlot *et al.*, 2008). SABP2 together with SAMT possibly promotes SA-dependent mounting of SAR by regulation of homeostasis (Vlot *et al.*, 2020). In *Arabidopsis*, long light exposure followed by infection reduces the impact of MeSA in the systemic response (Liu *et al.*, 2011). Light exposure generally influences SAR with *Pseudomonas* inoculations in the morning/midday leading to high SA levels, fast PR-gene expression and stronger HR but weak effects in plants infected during night (Griebel & Zeier, 2008; Zeier *et al.*, 2004).

SA is considered as required but not sufficient to mount a full SAR response with nonexpressor of pathogenesis-related 1 (NPR1) being a main player in SA-dependent signaling during SAR (Bernsdorff *et al.*, 2016; Hartmann *et al.*, 2018). *npr1* mutants are impaired in SA-induced *PR* gene expression and are more susceptible towards pathogens (Cao *et al.*, 1994). NPR1 and the paralogues NPR3/ NPR4 share a high sequence similarity and were described as bona fide SA receptors with high SA-binding affinity operating as master regulators of SA-dependent transcriptional reprogramming possibly by interaction with TFs from the TGA family (Ding *et al.*, 2018). TGA TF are involved in regulation of defense genes such as *PR* and mutations of the respective TGA TFs in the triple mutant *tga6-1 tga2-1 tga5-1* leads to loss of SAR responses genes (Shi *et al.*, 2013; Zhang *et al.*, 1999, 2006). Mutants of *npr2* and *npr3* show increased basal *PR*-gene expression and enhanced resistance against infections with *Pst* (Zhang *et al.*, 2006). Likely, NPR proteins and TGA TF prevail as complexes in the nucleus in competition for binding to the promotor regions of defense genes such as *PR* genes, *SARD1* and *WRKY70*. During low SA-levels, NPR3 and NPR4 are active and operate as repressors for defense gene expression (Ding *et al.*, 2018). Increase in SA levels leads to translocation of NPR1 from the cytosol to the nucleus and conformational change of the NPR proteins (Wu *et al.*, 2012). NPR1 subsequently gains activating properties by differential sumoylation and phosphorylation while NPR3 and NPR4 lower their activity as repressors (Ding *et al.*, 2018; Innes, 2018; Withers & Dong, 2016).

Pip-dependent SAR

Pipecolic acid is a non-proteinogenic amino acid which accumulates in local and systemic tissue upon bacterial infection (Návarová *et al.*, 2013). AGD2-like defense response protein 1 (ALD1) was found to be essentially required for establishment of SAR (Jong *et al.*, 2004) and knock out of the gene leads to deficient Pip-biosynthesis (Návarová *et al.*, 2013). Pip-deficient mutants are fully impaired in SAR-induction but treatment with Pip is capable to restore the SAR-deficiency phenotype (Bernsdorff *et al.*, 2016; Hartmann *et al.*, 2018). Pip is produced from Lysine as substrate in a two-step enzymatic reaction involving ALD1 and SAR-DEFICIENT 4 (SARD4) (Ding *et al.*, 2016). N-hydroxy pipecolic acid (NHP) is produced by flavin-dependent monooxygenase 1 (FMO1) and was identified as central metabolite mediating the SAR response (Hartmann *et al.*, 2018). Furthermore, NHP glycosylation (NHPG) by a UDP-glycosyltransferase (UGT76B1) at the local infection site was found to mediate and fine-tune the SAR response by regulation of the NHP/NHPG ratio (Cai *et al.*, 2020).

Pip signaling is involved in positive feedback loops with the MAP kinases (MPK) 3 and 6 activated downstream of Pip which regulate the TF WRKY33. WRKY33 subsequently binds to the promotor region of *ALD1* leading to transcriptional upregulation of the gene and consequent raise of Pip level (Y. Wang *et al.*, 2018). MPK-activation at the local site is sufficient to trigger SAR and is associated with induced *ALD1* and *FMO1* expression and Pip/NHP synthesis (Y. Wang *et al.*, 2018). A cascade involving NO <-> ROS -> Aza -> G3P has been shown to mediate SAR with Pip acting upstream of self-amplifying NO<->ROS (Wang *et al.*, 2014, 2018). Both, G3P and AzA are systemically transported via the plasmodesmata controlled symplastic route (Lim *et al.*, 2016). A positive-feedback loop to induce Pip deriving from G3P and AzA might support defense responses in systemic tissue (HJung *et al.*, 2009; Wang *et al.*, 2018).

Co-regulation of SA- and Pip/NHP pathways

Mutants with deficient Pip-pathway are fully defective in SAR establishment while SA-compromised *sid2* mutants are still capable of moderate SAR induction and Pip/NHP-dependent responses (Bernsdorff *et al.*, 2016; Hartmann *et al.*, 2018). Both, SA and Pip/NHP pathways are essential to mount a systemic immune response and are often considered as parallel pathways (Gao *et al.*, 2015). However, recent studies indicate a tight co-regulation mediated by multiple TFs which are involved in regulation of SA- biosynthesis and Pip/NHP accumulation (Kim *et al.*, 2019; Sun *et al.*, 2018, 2019). The redundant calmodulin-binding transcription factors 1, 2, and 3 (CAMTA1/2/3) negatively regulate the two TF SAR-deficient 1 (SARD1) and calmodulin binding protein 60-like g (CBP60g) thereby regulating SA- and NHP

biosynthesis (Sun *et al.*, 2019). The expression of SARD1 and CBP60g is further modulated by the positively regulating TGACG-binding factor 1 (TGA1) and TGA4 (Sun *et al.*, 2018).

Exogenous application of Pip/NHP induces SA levels and signaling (Návarová *et al.*, 2013). Interestingly, increased Pip levels induce accumulation of NPR1 likely involved in regulation of SA- and Pip biosynthesis genes, SARD1, and CBP60g (Kim *et al.*, 2019). Vice versa, SA increases transcription of Pip and NHP biosynthesis genes (Ding *et al.*, 2018; Sun *et al.*, 2019). Interdependent and synergistic effects of SA and Pip/NHP accumulation therefore lead to the assumption that both pathways are mutually amplifying signals during establishment of systemic defense (Vlot *et al.*, 2020).

SARD1-dependend systemic defense responses are further intensified by Calcium-dependent protein kinase 5 (CPK5) (Guerra *et al.*, 2020). CPKs are calcium sensor proteins operating upstream of SA-dependent local defense responses. In systemic defense, NHP and SAR marker genes (including *SARD1*) accumulate in CPK5-dependent fashion (Guerra *et al.*, 2020). CPK5 phosphorylates ROS-producing RBOHD leading to an increase in ROS levels further activating CPK5 (Dubiella *et al.*, 2013; Miller *et al.*, 2009). CPK5 and ROS possibly promote SAR by induction of *SARD1* in distant tissue (Guerra *et al.*, 2020). Consequently, the before mentioned SA-Pip/NHP feed forward loop might be activated (A. Corina Vlot *et al.*, 2020).

1.2. Protein quality control *via* the ubiquitin-proteasome-system (UPS)

Homeostasis of the cellular proteome during protein quality control (PQC) in plants is maintained by autophagy and the ubiquitin-proteasome-system (UPS) both tightly linked and conducting degradation of damaged, misfolded, or unwanted proteins (Xiong *et al.*, 2018; Yoon & Chung, 2019; Zientara-Rytter & Subramani, 2019). Ubiquitination serves as efficient degradation signal in both systems (Ciechanover, 1998; Kirkin *et al.*, 2009). The proteolytic mechanistic of the UPS plays an essential role in manifold cellular processes by degradation of misfolded proteins and cellular regulators controlling growth, development, circadian rhythm, abiotic, and biotic stress responses (Hershko *et al.*, 1980; Sadanandom *et al.*, 2012). Ubiquitin is the major modifier required for specific degradation of target proteins and is one of the most abundant post-translational modifications in eukaryotes (Khoury *et al.*, 2011). Free ubiquitin is attached to substrates by an ATP-dependent enzymatic cascade involving E1-ubiquitin activating enzyme, E2-ubiquitin conjugating enzyme, and E3-ubiquitin ligases. The UPS is shown in Figure 2 and described in detail in the following section.

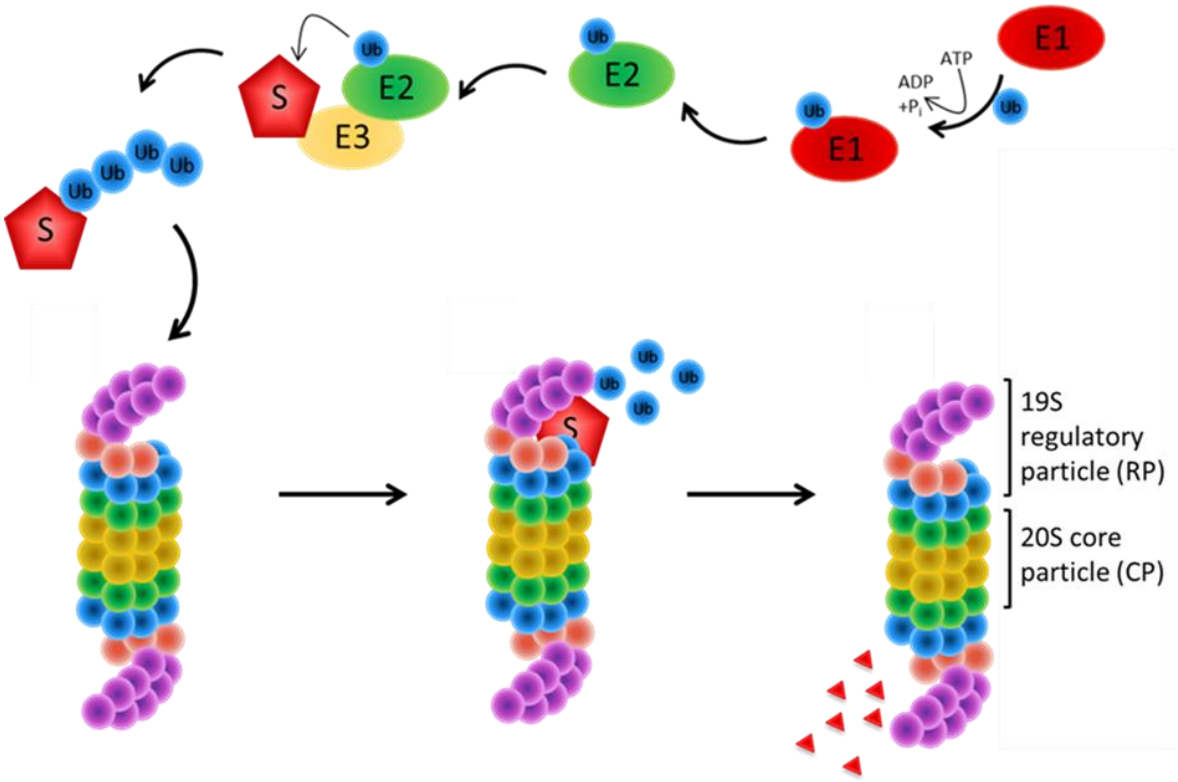

Figure 2: The UPS is a stepwise enzymatic cascade for protein ubiquitination and subsequent 26S proteasome mediated protein degradation. The E1-ubiquitin activating enzyme catalyzed the binding of ubiquitin in an ATP-dependent manner and mediates the ubiquitin transfer to the E2-ubiquitin conjugating enzyme. E3-ubiquitin ligases specifically bind to substrate proteins and ubiquitin-loaded E2 and catalyze the ubiquitin transfer. Ubiquitinated proteins may be send to the 26S proteasome for degradation. The proteins are recognized by the 19S regulatory particle and proteolytically degraded in the 20S core particle.

Ubiquitin

Ubiquitin (Ub) is a small (~8.5 kDa), highly conserved, and abundant protein prevalent in eukaryotic cells and applicable as reusable recognition signal (Callis *et al.*, 1995; Smalle & Vierstra, 2004). In *Arabidopsis*, *ubiquitin* gene family members (*UBQs*) are typically synthesized as polymers of four to six copies of the coding sequence (Callis *et al.*, 1995). Most commonly, the c-terminal glycine of Ub is bound to the ε-amino group of lysine residues of the substrate through a covalent isopeptidebond (Avram Hershko *et al.*, 2000). With the type of ubiquitination defining the fate of a protein, mono-ubiquitination of proteins may determine location or activity (Hicke, 2001). Various configurations of poly-Ub chains confer diverse consequences on substrates including stabilization or degradation (Pickart & Fushman, 2004). Each UB contains seven lysines (K6, K11, K27, K29, K33, K48, and K63) and polyubiquitin linkages between all lysines have been observed *in vitro*. Poly-Ub linkages through K48 prevails in cells and targets the substrate for proteasomal degradation (Pickart & Fushman, 2004). Recent data suggest a key regulatory role of K63-linages in DNA-repair, immune response and during iron deficiency (Wenfeng Li & Schmidt, 2010; Mural *et al.*, 2013; Wen *et al.*, 2008).

E1- ubiquitin activating enzymes

In *Arabidopsis*, the E1-family consist of two members, namely At*UBA1* and At*UBA2* catalyzing the formation of a phosphoanhydride bond between the c-terminal glycine carboxyl group of Ub and the ATP-moiety adenosine monophosphate (AMP) (Hatfield *et al.*, 1997). Both proteins, At*UBA1* and At*UBA2*, harbor a conserved cysteine in their active site which directly binds the AMP-Ub-intermediate via thiol-ester linkage (Hatfield *et al.*, 1997). E1 is a highly efficient enzyme only required at low concentrations to provide sufficient amount of activated Ub concentrations (Haas *et al.*, 1983; Hershkos *et al.*, 1983).

E2- ubiquitin conjugating enzymes

Analysis of the *Arabidopsis* proteome predict 37 ubiquitin conjugating-enzymes (E2-enzymes, UBC) divided into 12 groups based on their sequence similarity (Kraft *et al.*, 2005). In addition to the UBC domain, several E2s carry a c- or n-terminal acidic or basic extension, or a predicted transmembrane domain likely supporting association with E3s or target recognition (Bachmair *et al.*, 2001). The UBC domain itself is a conserved 150-amino acid catalytic domain including an active site cysteine required for transfer of the activated Ub from the E1 to the E2 (Hamilton *et al.*, 2001; Hershkos *et al.*, 1983). E2s are therefore key enzymes by mediating the catalytic step during the ubiquitination cascade and by determining the type of substrate ubiquitination (Ye & Rape, 2009).

E3-ubiquitin ligases

E3-ubiquitin ligases comprise most of the enzymes involved in ubiquitination of proteins with over 1400 E3-ligases identified in *Arabidopsis* by now (Vierstra, 2009). E3s are a very heterogeneous class of enzymes and are central in conferring specificity to the ubiquitination cascade by specific identification of substrates and catalyzation of the isopeptide bond formation between Ub and the substrate (Vierstra, 2012). Depending on the presence of characteristic protein domains and the used mechanism for ubiquitin transfer to the substrate E3s are currently categorized in 3 main classes, namely Really Interesting New Gene (RING), RING-between RING-RING (RBR), and homologous to the E6AP carboxyl terminus (HECT) (Spratt *et al.*, 2014).

The most abundant and diverse group across eukaryotes are RING E3-ligases carrying a cysteine-rich zinc-binding motif called RING (Freemont, 1993). The RING domain mediates protein-protein-interactions and provides functional specificity to the E3 ligases (Borden & Freemont, 1996). The domains are generally defined by a RING-fold comprising of conserved cysteine and histidine residues binding zinc atoms. Zinc binding is central for proper protein folding and biological activity of the RING-enzyme (Borden, 2000). The RING domain is

essential for the binding of the appropriate Ub-loaded E2 and directly mediates the transfer of Ub to the substrate. RING-E3s may be present as monomers, as homo- , or heterodimers (Linke *et al.*, 2008). A particular RING-related domain is the U-box domain consisting of the RING-fold without zinc-chelating properties but is instead stabilized by hydrogen bonds and salt bridges (Aravind & Koonin, 2000). The *Arabidopsis* genome contains 64 U-box genes (Yee & Goring, 2009). Overall, RING-finger and related U-box E3s act as passive scaffolds by sustaining the proximity between Ub-loaded E2 and the substrate protein (Passmore & Barford, 2004). Another family of RING-E3s are *Arabidopsis* Tóxicos en Levadura (ATL) enzymes with over 80 members (Serrano *et al.*, 2006). These proteins contain a variation of the canonical cysteine-histidine structure and a n-terminal transmembrane domain (Aguilar-Hernández *et al.*, 2011). ATLs have been found to function in various processes associated with defense responses during infections, regulation of cell death in root development, or endosperm development (Guzmán, 2012). Also, cullin-RING ligases (CRLs) are a specific type of RING E3 ligases as multi-subunit complexes assembled on a cullin (CUL) scaffold (Hua & Vierstra, 2011). CUL1, CUL2a/b, CUL3a/b, and CUL4 prevail in *Arabidopsis* (Shen *et al.*, 2002). CUL3 has been shown to constitutively target NPR1 for proteasomal degradation thereby regulating SAR (Spoel *et al.*, 2009). The region n-terminal of the CUL scaffold harbors a substrate-receptor mediating substrate specificity. The catalytic active RING-domain locates at the c-terminus. Here, also the Ub-loaded E2 is bound (Petroski & Deshaies, 2005). The c-shaped structure of the hollo-complex mediates the contact between E2 and substrate (Hua & Vierstra, 2011).

A second class of E3-ubiquitin ligases containing 42 members in *Arabidopsis* are RBR E3s containing two predicted RING domains (RING1 and RING2) surrounding an in-between-RING domain (IBR) (Marín, 2010). The ubiquitin transfer from E2 to the substrate is catalyzed in a two-step reaction. RING1 is required for the recruitment of the Ub-charged E2. Subsequently, the Ub is transferred to the catalytic cysteine in the RING2-domain in a RING/HECT mechanism (Dove *et al.*, 2016; Dove & Klevit, 2017; Wenzel & Klevit, 2012). Among the *Arabidopsis* RBR E3-ligases, the ariadne (ARI) E3s are a dominant group with 14 expressed genes and 2 pseudogenes (Mladek *et al.*, 2003). Molecular data regarding the function of RBR E3s were mostly obtained from humans with the Human homolog of ariadne (HHARI) being involved in regulation of translation in Parkinson's (Dove *et al.*, 2016; Wenzel *et al.*, 2011).

HECT E3s represent the third major group composing two lobes with the E2 binding domain located in the n-terminal lobe and the catalytic cysteine in the c-terminal lobe (Spratt *et al.*, 2014). A flexible region connects both lobes and mediates the Ub transfer from E3 to the substrate (Huang *et al.*, 1999; Verdecia *et al.*, 2003). Some HECT E3s ubiquitinate partially proteolyzed substrates and thereby increase the proteasome processivity (Chu *et al.*, 2013). In *Arabidopsis*, a HECT-type ubiquitin protein ligase (UPL) mediates proteasome-derived elongation of ubiquitin chains and thereby promotes immunity-related proteasome processivity (Furniss *et al.*, 2018).

The 26S proteasome

The 26S proteasome is a 2,5 MDa multi-subunit protease complex comprising the 20S core particle (CP) and the 19S regulatory particle (RP) (Figure 3A) which binds, deubiquitinates, and unfolds ubiquitin-marked substrates before degradation (Hartmann-Petersen *et al.*, 2003; Tomko & Hochstrasser, 2013; Voges *et al.*, 1999). Multiple studies indicate that proteins can also be degraded without prior attachment of a poly-Ub chain in Ub-independent manner only requiring the 20S proteasome for degradation (Asher *et al.*, 2006; Davies, 2001). For example, turnover of oxidized proteins is Ub-independent (Shringarpure *et al.*, 2003). Protein damage by oxidation is mainly caused by ROS generated in stress conditions and needs to be degraded to avoid accumulation and cytotoxicity (Cohen *et al.*, 2006; Poppek & Grune, 2006).

The barrel shaped and catalytic active CP is composed of four stacks of α and β subunits containing an ATP- and ubiquitin-independent peptidase activity (Groll *et al.*, 2000). The outer α-rings form a pore flanking the inner β-rings and regulating the entrance of target proteins and removal of degradation products. Proper organization and activation of the gate highly depends on the α3-subunit, since deletion leads to constant opening of the gate (Groll *et al.*, 2000). The β-rings possess specific proteolytic activities, i.e., caspase-like, trypsin-like, and chymotrypsin-like activity for degradation of the substrate (Dick *et al.*, 1998).

The ATP-dependent RPs cap the CP at one or both ends and recognize ubiquitinated target proteins thereby conferring substrate specificity to the proteasome (Glickman, 2000). Furthermore, the substrates are deubiquitinated before unfolding and translocation to the CP (Hartmann-Petersen *et al.*, 2003). In total, the RP combines 18 subunits forming the lid and the base as sub-particles (Figure 3B). The base connects the RP to the α-subunit ring of the CP and channels the target protein to the proteolytic core after unfolding. Non-ATPase subunits (Rpn1, Rpn2, and Rpn10) and a ring of AAA-ATPase subunits (Rpt1-6) represent the base (Fu *et al.*, 2001). RPT2 and RPT5 are required for channel opening of the ring to the CP in yeast (Groll *et al.*, 2000; Smith *et al.*, 2007). Serving as ubiquitin receptors, Rpn10 and Rpn13 recognize ubiquitinated substrates targeted to the proteasome (Husnjak *et al.*, 2008; Shi *et al.*, 2016). Rpn10 and Rpn2 connect lid and base and are required for full proteasome activity (Sun *et al.*, 2004). The lid of the RP consists of nine subunits (Rpn3, Rpn5–9, Rpn11–12, and Rpn15) organized in a horse-shoe-like structure centrally involved in recognition and de-ubiquitination of ubiquitinated target proteins (Verma *et al.*, 2002). During lid assembly, a core module is formed (Rpn5-6, Rpn8-9 and Rpn11) and extended by a second module (Rpn3, Rpn7 and Rpn15) and completed by Rpn12 incorporation (Tomko *et al.*, 2015).

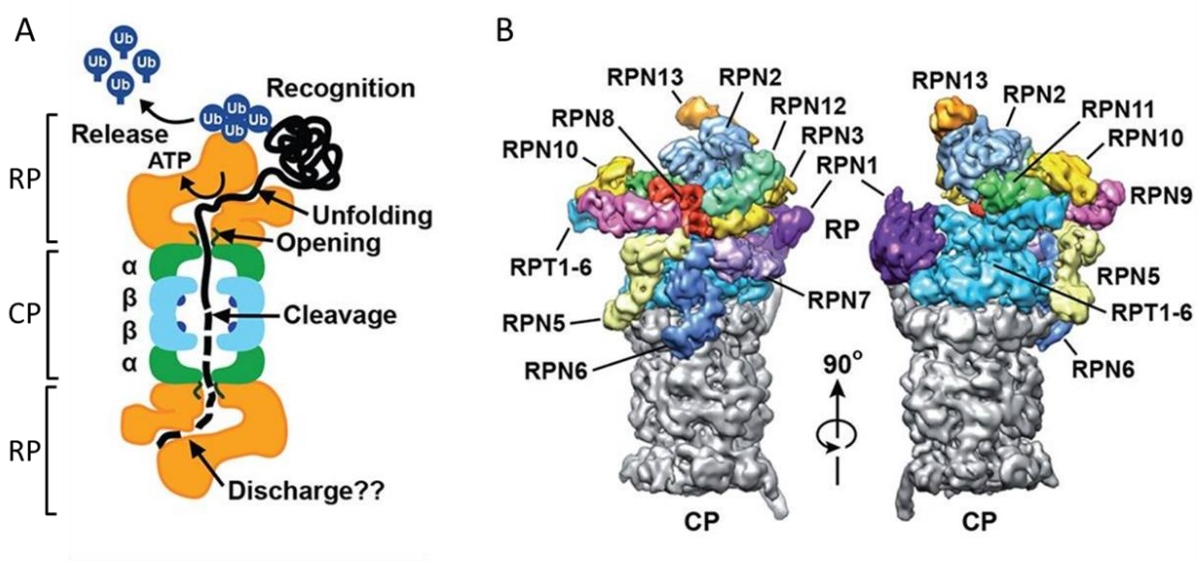

Figure 3: Structure of the 26S proteasome. The 3-dimensional structure of the yeast proteasome has been determined by Cryogenic electron microscopy (Lasker *et al.*, 2012). (A) The regulatory particle (RP) and core particle (CP) are involved in substrate recognition, release of ubiquitin, substrate unfolding and cleavage after channel opening. (B) The subunit architecture of the RP is illustrated. The ATPase ring of the regulatory particle is shown in blue, the no-ATPase Rpn subunits are multicolored, the CP is shown in grey. RP = 19 S regualtory particle; CP = core particle; Ub = ubiquitin. Modified after Marshall and Vierstra, 2019.

Proteasome subunits

Attenuation of RP-genes leads to a widespread transcriptional upregulation of 26S related genes indicating a feedback mechanism to ensure regulation of proteasome levels (Yang *et al.*, 2004). Additionally, *Arabidopsis* genome encodes for paralogous subunits implying that incorporation of these paralogues may confer altered target specificity and/or properties of the holoprotease (Yang *et al.*, 2004). Indications accumulate that many individual subunits of the proteasome (such as Rpt2) have individual functions and specifically identify targets thereby regulating development and hormone pathways (Smalle *et al.*, 2002, 2003; Ueda *et al.*, 2004)

RPT2 plays a pivotal role in Ub-dependent turnover of proteins by controlling the substrate entry in the CP in yeast (Groll *et al.*, 2000). The capacity for Ub-dependent protein degradation is consequently decreased in *rpt2a*-2 but Ub-independent protein turnover increases allowing for higher tolerance of oxidative stress. The mutation leads to loss of 60% wild-type 26S proteasome activity (Kurepa *et al.*, 2008). The RPT2 paralogues *RPT2a* and *RPT2b* share an amino acid sequence identity of 99,1% and double knock out of *rpt2a rpt2b* is lethal in gametophytes (Ueda *et al.*, 2004, 2011). When expression is under control of the *RPT2a* promotor RPT2b is capable of rescuing *rpt2a* indicating that RPT2b is likely a minor redundant of RPT2a (Ueda *et al.*, 2011). RPT2a (also known as halted root (HLR)) was identified as central component involved in various processes including maintenance of meristems and leaves and regulation of leaf organ size in *Arabidopsis* (Sonoda *et al.*, 2009;

Ueda *et al.*, 2004). Both, *rpt2a*-2 and *rpt5a* fail to maintain the root apical meristem (RAM) resulting in shortened roots. However, *rpt2b* and *rpt5b* do not show altered root growth when compared to wildtype (Ueda *et al.*, 2004). RPT2a was also found to be involved in epigenetic changes during which transcriptional gene silencing is often associated with DNA methylation with *rpt2a* leading to DNA hypermethylation and subsequent silencing (Finnegan & Kovac, 2000; Sako *et al.*, 2012). More recently, physical interaction with RPT2a and components of the RNA quality control were described thereby promoting post-transcriptional gene silencing to control foreign RNA during RNA homeostasis (Kim *et al.*, 2019).

The *Arabidopsis* genome encodes for two paralogues of RPN12 with *RPN12a* encoding for the full polypeptide whereas *RPN12b* is n-terminally truncated (Smalle *et al.*, 2002). The *rpn12a*-1 mutant assembles a RPN12a-NPTII fusion in the 26S proteasome but also wildtype RPN12a was also found to incorporate in the proteasome in this line. The mutation likely causes a subtle change in proteasome activity affecting RPN12a-related functions instead of global 26S proteasome perturbation (Smalle *et al.*, 2002). *rpn12a*-1 shows decreased sensitivity to auxins and cytokinins in comparison to wildtype and increased sensitivity towards heat stress (Kurepa *et al.*, 2008; Smalle *et al.*, 2002). Comparable *rpt2a*-2, the 26S proteasome activity is 60% decreased related to wild type in *rpn12a*-1 enhancing oxidative stress tolerance by increased Ub-independent 20S degradation rate (Kurepa *et al.*, 2008). Proposedly, mutants like *rpt2a* and *rpn12a* experience attenuation of RP assembly resulting in a shifted ratio between 26S and 20S proteasomes (Kurepa *et al.*, 2008).

1.3. UPS components in immune responses

The UPS is centrally involved in perception of abiotic and biotic stresses as well as respective downstream responses to cope with these stresses including suppression of signaling pathways during growth, removal of negative regulators signaling pathways, and attenuation of pathways during stresses (Serrano *et al.*, 2018; Stone, 2014). E3-ubiquitin ligases confer specificity to proteasomal protein degradation. Hence, it is not surprising that ubiquitination of substrates by multiple E3 ligases were found to be involved in fine tuning immunity regulating processes (Adams & Spoel, 2018; Marino *et al.*, 2012; Trujillo & Shirasu, 2010).

Regulation of PRRs

The plant U-box E3 ligase 22 (PUB22) was shown to negatively regulate PTI by specifically targeting and mediating the degradation of a subunit of the octameric exocyst complex (Exo70B2) involved in trafficking of FLS2 to the plasma membrane (He & Guo, 2009; Stegmann *et al.*, 2012; Wang *et al.*, 2020). PUB22 has been shown to regulate its own activity by autoubiquitination which is in turn controlled by MPK3-mediated phosphorylation leading to accumulation due to reduced autoubiquitination activity (Furlan *et al.*, 2017). In

turn, degradation of substrates like Exo70B is mediated to negatively regulate plant immunity (Furlan *et al.*, 2017). PUB23 was identified as homologue of PUB22 with 75% amino acid identity and physical interaction (Seok *et al.*, 2008). The 26S proteasome subunit RPN12a is ubiquitinated *in vitro* and *in vivo* by PUB22 and PUB23 which alters stability or activity of RPN12a upon water stress (Seok *et al.*, 2008). Interestingly, PUB22 and PUB23 also ubiquitinate RPN6 and therefore target the proteasomal subunit for proteasomal degradation during drought stress (Cho *et al.*, 2015). Both E3 ligases act in concert with PUB24 and contribute additively during PTI responses in *Arabidopsis* (Trujillo *et al.*, 2008). Responses to various PAMPs (i.e., flg22, chitin, and elf18) are negatively regulated by the E3 ligase triplet by downregulation of amplitude and duration of the oxidative burst (Trujillo *et al.*, 2008).

Regulation of PRRs such as FLS2 by the UPS is a common mechanism in plants to regulate defense responses and is therefore also targeted by bacterial AvrPtoB during infection with *Pst* DC3000 (Göhre *et al.*, 2008). AvrPtoB possesses E3 ligase activity *in planta* and obtain full virulence of *Pst* by poly-ubiquitination of the FLS2 kinase domain (Göhre *et al.*, 2008; Rosebrock *et al.*, 2007). During infections, the FLS2 co-receptor BAK1 interacts with and activates downstream signaling via the receptor-like cytoplasmic kinase (RLCK) botrytis-induced kinase 1 (BIK1) (Lu *et al.*, 2010). PUB25 and PUB26 target BIK1 for degradation and thereby negatively regulate immune signaling. The phosphorylation status of PUB25 and PUB26 mediated by the Calcium-dependent protein kinase 28 (CPK28) in turn regulates ligase activity (Wang *et al.*, 2018). Additionally, BIK1 is monoubiquitinated by the E3 ligases RING-H2 finger A3A (RHA3A) and RHA3B inducing dissociation from the FLS2/BAK1 complex and initiating downstream signaling (Ma *et al.*, 2020).

Transcriptional regulation

An important strategy to regulate immune responses is the homeostasis of nuclear localized proteins, mainly transcription factors (Serrano *et al.*, 2018). In *Arabidopsis*, *botrytis susceptible 1* (*BOS1*) encodes the R2R3MYB transcription factor involved in tolerance to certain abiotic stresses and required for resistance to pathogens (Mengiste *et al.*, 2003). *BOS1 interactor* (*BOI1*) and three *BOI-related genes* (*BRG*s) encode for RING-E3 ligases which physically interact with and ubiquitinate BOS1 for proteasomal degradation *in vitro* (Luo *et al.*, 2010). The *bos1* mutant shows increased susceptibility to fungal infections and *boi1* RNAi *Arabidopsis* plants show increased susceptibility although the BOS1 protein is expected to accumulate (Luo *et al.*, 2010; Mengiste *et al.*, 2003).

The master co-activator of SA-dependent gene expression NPR1 was found to be a substrate of the nuclear localized cullin-RING ligase 3 (CRL3) continuously and subsequently degraded by the proteasome to prevent activation of autoimmunity and premature SAR (Spoel *et al.*, 2009). Interestingly, nuclear activation of NPR1 and recruitment to CRL3 involves a tightly regulated interplay between SUMOylation and (de)phosphorylation. Unmodified NPR1

associates with the transcriptional repressor WRKY70 whereas SUMOylated NPR1 interacts with the transcriptional activator TGA3 (Saleh *et al.*, 2015). SUMOylation or interaction with TGA3 is required for phosphorylation which is in turn required for recruitment by CRL3 (Saleh *et al.*, 2015; Spoel *et al.*, 2009). Thus, NPR1 accumulates in the nucleus for activation of basal resistance and the subsequent turnover mediated by CUL3 is required for establishment of SAR (Fu *et al.*, 2012).

Regulation of hormone levels

In pepper (*Capsicum annuum*), *Ca*RING1 was characterized as active E3 ligase (Lee *et al.*, 2011a). *RING1* expression is induced upon treatment with the avirulent stain *Xanthomonas campestris* pv. *vesicatoria* (*Xcv*) and overexpression of RING1 enhances resistance to *Pst* and *Hyaloperonospora arabidopsidis*. Virus-induced gene silencing of *Ca*RING1 decreases resistance to *Xcv*, expression of *PR1*, SA levels and hypersensitive cell death (Lee *et al.*, 2011a). Further experiments showed a plasma membrane localization of *At*RING1 in lipid rafts (Lin *et al.*, 2008). These results suggest a critical role of RING1-mediated ubiquitination processes during regulation of defense responses regulating programmed cell death.

Role of the 26S proteasome

The 26S proteasome itself was identified to be involved in interactions with both beneficial and pathogenic bacteria including maintenance of proteostasis and on the contrary targeting of the proteasome by pathogenic effector proteins (Banfield, 2015; Üstün & Börnke, 2014). Beneficial endophytic colonization of *Arabidopsis* with *Kosakonia radicincitans* DSM 16656 interferes with Ub-dependent turnover of proteins (Witzel *et al.*, 2017). XopJ, a T3E from the phytopathogenic bacterium *Xanthomonas campestris* pv. *vesicatoria* (*Xcv*), was identified to target the proteasomal subunit RPT6 in pepper for proteolytic degradation leading to an attenuated degradation of SA-master regulator NPR1 (Üstün *et al.*, 2013; Üstün & Börnke, 2015). As a consequence, SA-dependent signaling is altered and cell death induction is delayed (Üstün *et al.*, 2013). *Pst* has been shown to stimulate autophagy of proteasomes (proteaphagy) in a T3E-dependent manner to increase virulence (Üstün *et al.*, 2018).

Furthermore, accumulating evidence suggest a substantial role of single 26S subunits in resistance against pathogens such as RPN1a being required for immune response upon infection with the biotrophic powdery mildew resistance pathogen (Yao *et al.*, 2012). Mutation of the subunit leads to increased susceptibility and defects in SA accumulation upon infection with virulent *Pst* DC3000 (Yao *et al.*, 2012). Based on the analysis of additional proteasome subunit mutants it appears that many but not all proteasome subunits play a similar role in immunity (Yao *et al.*, 2012).

1.4. Aims of this study

Data indicate a pivotal contribution of the ubiquitin-proteasome-system (UPS) to defense responses of plants towards pathogenic bacteria. Infections of *Arabidopsis thaliana* with *Pseudomonas syringae* pv. *tomato* DC3000 is an excellent combination of model organisms to study plant-bacterial interactions especially regarding disease susceptibility of plants (Xin & He, 2013). During infections, a central role of the 26S proteasome activity emerged for systemic acquired resistance (SAR) with a decreased priming capacity when proteasomal protein turnover is impaired (Üstün *et al.*, 2016). Hence, this project was performed to advance knowledge on the underlying mechanisms of this observation on how proteasomal activity interferes with priming.

One part of the project therefore aims to unravel signal transduction pathways, transcriptional modules and metabolic cues governed by proteasomal protein turnover. Characterization of *Arabidopsis* proteasome mutants during priming will be performed using molecular, biochemical, and genomic approaches (RNAseq). A second part of the project addresses the identification and characterization of novel components and targets of the UPS functioning in the establishment of defense priming and SAR. This includes mainly the molecular and biochemical characterization of E3-ubiquitin ligases possibly involved in mediating local and systemic defense responses to draw a comprehensive picture of UPS-dependent mechanisms during priming.

In order to analyze *Arabidopsis* during priming, a standardized experimental setup as schematically shown in Figure 4 will be used.

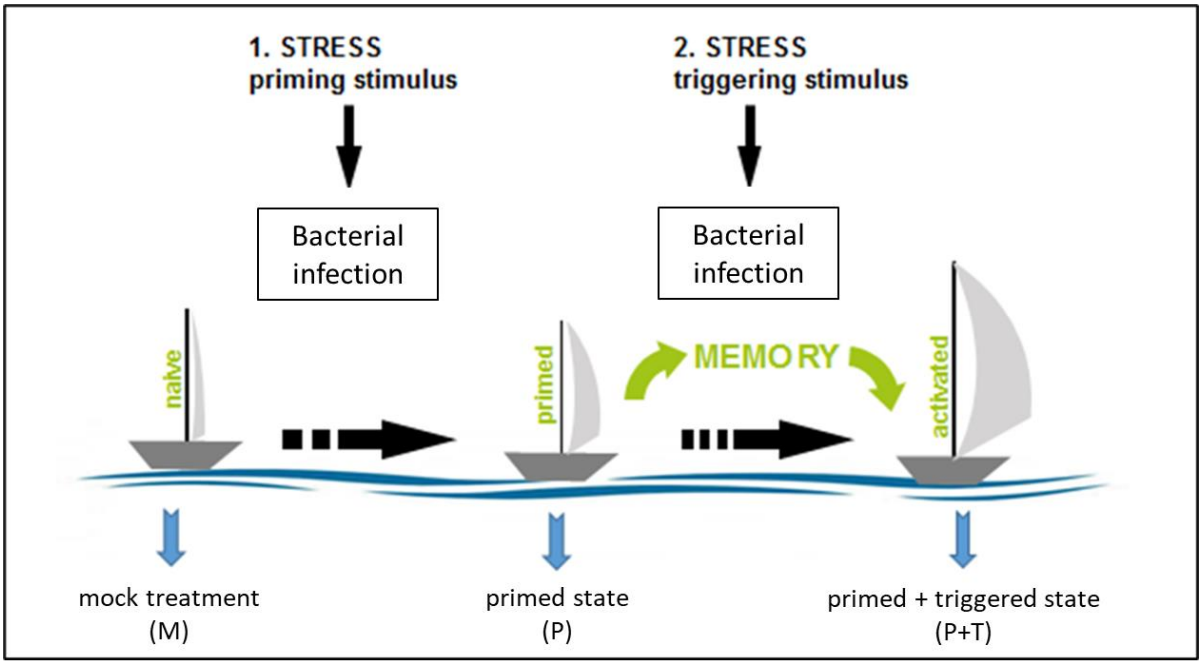

Figure 4: Scheme of the experimental setup. *Arabidopsis thaliana* will be infected with *Pseudomonas syringae* or treated with elicitor to induce priming (P). Triggering by challenge infection will be performed after a memory phase (P+T). Plants will be analyzed during systemic defense responses regarding their resistance towards pathogens, defense gene expression, metabolic markers, and protein ubiquitination.

2. Material and Methods

2.1. Material

2.1.1. Vectors and constructs

Table 1: Vectors used in this study

Vector	Application/ properties	Resistance in bacteria/plant	Origin
pENTR™/D-TOPO®	"Entry"-Vektor for Gateway® cloning	Kan^R	Invitrogen™
pMALc2-GW	N-terminal MBP fusion, protein induction and purification	Amp^R	New England Biolabs® GmbH
pDEST15-GW	N-terminal GST fusion, protein induction and purification	Amp^R	Invitrogen™
pGAD424-GW	Prey for direct interaction in yeast	Amp^R	Clontech
pGBT9-GW	Bait for direct interaction in yeast	Amp^R	Clontech
pRB-35S-GW $VENUS^{N173}$	Bimolecular fluorescence complementation	$Spec^R$ $Strep^R$	Üstün *et al.*, 2013
pRB-35S-$VENUS^{N173}$-GW	Bimolecular fluorescence complementation	$Spec^R$ $Strep^R$	Üstün *et al.*, 2013
pRB-35S-GW $VENUS^{C155}$	Bimolecular fluorescence complementation	$Spec^R$ $Strep^R$	Üstün *et al.*, 2013
pRB-35S-	Bimolecular	$Spec^R$ $Strep^R$	Üstün *et al.*, 2013

VENUS^{C155}-GW	fluorescence complementation		
pK7WGF2-GW	Binary vector, n-terminal GFP-tag, 35S promotor	Spec^R Strep^R	Karimi *et al.*, 2002
pK7FWG2-GW	Binary vector, c-terminal GFP-tag, 35S promotor	Spec^R Strep^R	Karimi *et al.*, 2002
pGWB615-GW	Binary vector, n-terminal 3x HA-tag, 35S promotor	Spec^R	Nakamura *et al.*, 2010

Table 2: Generated and used constructs

Name	**Vector**	**Resistance**	**Application**
3xHA-HMP35	pGWB615-GW	Spec^R	Binary construct for expression of HMP35 with n-terminal 3xHA-tag
AD-HMP35	pGAD424	Amp^R	HMP35 with n-terminal activation domain, prey for direct interaction in Y2H
ARI12-GFP	pK7FWG2-GW	Spec^R Strep^R	Binary construct for expression of ARI12 with c-terminal GFP-tag
BD-PUB54	pGBT9	Amp^R	PUB54 with n-terminal binding domain, bait for direct interaction in Y2H
GFP-HMP35	pK7WGF2-GW	Spec^R Strep^R	Binary construct for expression of HMP35 with n-terminal GFP-tag
GFP-PUB54	pK7WGF2-GW	Spec^R Strep^R	Binary construct for expression of PUB54 with n-

			terminal GFP-tag
GST-HMP35	pDEST15-GW	Amp^R	IPTG-inducible protein expression of recombinant HMP35 with n-terminal GST-tag
MBP-PUB54	pMALc2	Amp^R	IPTG-inducible protein expression of recombinant PUB54 with n-terminal MBP-tag
MBP-PUB54ΔU	pMALc2	Amp^R	IPTG-inducible protein expression of recombinant PUB54ΔU with n-terminal MBP-tag
pENTR-ARI12	pENTR™/D-TOPO®	Kan^R	"Entry"-Vector for GW-cloning
pENTR-HMP35	pENTR™/D-TOPO®	Kan^R	"Entry"-Vector for GW-cloning
pENTR-PUB54	pENTR™/D-TOPO®	Kan^R	"Entry"-Vector for GW-cloning
pENTR-PUB54ΔU (provided by Feke *et al.*, 2019)	pENTR™/D-TOPO®	Kan^R	"Entry"-Vector for GW-cloning
$VENUS^C$-HMP35	pRB-35S-$VENUS^{C155}$-GW	$Spec^R$ $Strep^R$	Binary construct for expression of HMP35 with n-terminal $Venus^C$, BiFC
$VENUS^N$-PUB54	pRB-35S-$VENUS^{N173}$-GW	$Spec^R$ $Strep^R$	Binary construct for expression of PUB54 with n-terminal $Venus^N$, BiFC

2.1.2. Oligonucleotides

Table 3: Oligonucleotides used for RT-qPCR

Target	Sequence
ALD1 fw	GTGCAAGATCCTACCTTCCCGGC
ALD1 rev	CGGTCCTTGGGGTCATAGCCAGA
ARI12 fw	ACGTATCGCAGCTTAAGTTCATCC
ARI12 rev	AATCCTTTGACGGTTCCTCCTCG
EDS5 fw	GGACAAGAAAGAAGCGCAAC
EDS5 rev	GCTGCAGGGACAATCTCAAT
FMO1 forward	CTTTCCGAACTTGGCTTGAG
FMO1 reverse	AAGTTCGAGCTGCTTTGGAC
ICS1 fw	TTCTCAATTGGCAGGGAGAC
ICS1 rev	AAGCCTTGCTTCTTCTGCTG
PAD3 fw	GGCTGAAGCGGTCATAAGAG
PAD3 rev	TCCAGGCTTAAGATGCTCGT
PR1 fw	TTCTTCCCTCGAAAGCTCAA
PR1 rev	CATGGGACCTACGCCTACC
PUB23 fw	CATAGCGGTGGTGTGCAAGAAG
PUB23 rev	ACCCTAACCGCTCTATCGCTTG
PUB54 fw	TGGCTGCTGATGGTTTCACCTAC
PUB54 rev	TTTGGAGAGGTTCGACCTCCTGAC
SARD4 fw	CAAGTGCTGATCATGGTTGG
SARD4 rev	GGATCCTTGGAGAGGGTTTC

Table 4: Oligonucleotides used for cloning and genotyping

Name	Target	Purpose	Sequence
D21	LP SALK_005596 *rpt2a*-2	genotyping	GGAATTGTTTTACCGGAGGAG
D22	RP SALK_005596 *rpt2a*-2		GCGAGAAATTTGTTCTCATGG
D23	LB SALK-Lines	genotyping	TGGTTCACGTAGTGGGCCATCG
D24	*rpn12a*-1 Kan^R rev	genotyping	CCCCTGCGCTGACAGCCCGGAACA
D25	*rpn12a*-1 fw	genotyping	CGAGCTTGAATTACTTTCATCAGC
D26	*rpn12a*-1 rev		ACGATACGCTCCAGCTCTCTGGCGTA
D117	*ARI12* fw	cloning (GW)	CACCATGGATAATAATTCTGTAATCG
D118	*ARI12* rev		TTATTGATTACGGCCTGAACC
D119	*PUB54* fw	cloning (GW)	CACCATGGAAGACGCCATAT
D120	*PUB54*		TCA ACG TTT ATA ATT TGG GTT CTT
D123	LP *pub54-I* SALK_055772	genotyping	TAAATGGCCCATACTGAATGC
D124	RP *pub54-I* SALK_055772		TAGGGTTGAAACCAAATTTGG
D125	LP *pub54-II* SALK_035556	genotyping	GTGCATTTTCAGCAAGTAGGC
D126	RP *pub54-II* SALK_035556		GGTTCGACCTCCTGACCTTAG
D129	LP *ari12* SALK_136787	genotyping	AGCGTCTTCTCTGCACTGAAG
D130	RP *ari12* SALK_136787		CAACGCAGCTTTAGAAGATGG
D213	LP *hmp35*-I SALK_105737	genotyping	TTTGTCCATGATCCTCTCAGG
D214	RP *hmp35*-I SALK_105737		ATTGAATTATGCCGACTCACG
D215	LP *hmp35*-II	genotyping	GGGAACTTGCAAAGAACCTTC

	SALK_105737		
D216	RP *hmp35*-II SALK_105737		ATTGAATTATGCCGACTCACG
D219	*HMP35* fw	cloning (GW)	CACCGCCGAGAAGGGCAA
D220	*HMP35* rev		TCACATGATGGAACAGCTCTGTGGA
D229	pMALc2-*ARI12* fw	cloning (NEBuilder)	GATCGAGGGAAGGATTTCAGAAGATAATAATTC TGTAAT
D230	pMALc2-*ARI12* rev		GGTCGACTCTAGAGGATCCGTTATTGATTACGGC CTGAA

LP = left primer; RP = right primer; LB = left border; fw = forward; rev = reverse.

2.1.3. Enzymes and chemicals

All enzymes and chemicals were purchased from ThermoScientific (Massachusetts, USA), New England Biolabs (Frankfurt a. M.), Roche (Mannheim), Sigma-Aldrich (Steinheim), Biorad Laboratories (München), Fermentas (St. Leon-Rot), GE Healthcare (Freiburg), Duchefa Biochemie (Haarlem, Niederlande), Difco Laboratories (Detroit, USA), Macherey & Nagel (Düren), Solis BioDyne (Tartu, Estonia), Bioline GmbH (Luckenwalde) Carl Roth GmbH + Co. KG (Karlsruhe), and Promega (Mannheim).

2.1.4. Antibodies

Table 5: Antibodies

Antibody	**Origin**	**Host species**	**Dilution**
α-GFP-HRP (B-2)	Santa Cruz Biotechnology	Mouse	1:1000
α-GST-HRP (B-14)	Santa Cruz Biotechnology	Mouse	1:1000
α-HA-HRP (3F10)	Roche	Rat	1:1000
α-MBP	New England Biolabs	Mouse	1:10000
α-mouse-HRP	Thermo Fischer Scientific	Goat	1:10000
α-Ubiquitin-HRP (P4D1)	Santa Cruz Biotechnology	Mouse	1:500

2.1.5. Bacterial strains

Table 6: Bacterial strains

Bacterial strain	Genotype / genetic properties
Agrobacterium tumefaciens GV3101::pMP90RK	T-DNA^{-e}, Rif^{R}, Gm^{R}, Kan^{R}
Escherichia coli BL21/Rosetta pRARE	F^{-} *ompT hsdS*$_B$(r_B^- m_B^-) *gal dcm* (DE3) pRARE (Cam^{R})
E. coli DH5α	F^{-} ϕ80*lac*ZΔM15 Δ(*lac*ZYA-*arg*F)U169 *rec*A1 *end*A1 *hsd*R17(r_K^-, m_K^+) *pho*A *sup*E44 λ^{-} *thi*-1 *gyr*A96 *rel*A1
E. coli TOP10	F^{-} *mcr*A Δ(*mrr-hsd*RMS-*mcr*BC) ϕ80*lac*ZΔM15 Δ*lac*X74 *rec*A1 *ara*D139 Δ(*ara-leu*)7697 *gal*U *gal*K λ^{-} *rps*L(Str^{R}) *end*A1 *nup*G
Pseudomonas syringae pv. maculicola ES4362	Rif^{R}
Pseudomonas syringae pv. tomato DC3000	Rif^{R}, Cor +
Saccharomyces cervisiae Y187	MATα, ura3-52, his3-200, ade2-101, trp1-901, leu2-3, 112, gal4Δ, met–, gal80Δ, URA3::GAL1$_{UAS}$-GAL1$_{TATA}$-lacZ
S. cervisiae Y190	*MATa, ura3-52, his3-D200, lys2-801, ade2-101, trp1-901, leu2-3, 112, gal4Δ, gal80Δ, URA3::GAL1UAS-GAL1TATA-lacZ, cyhr2, LYS2::GALUAS-HIS3TATA-HIS3*
S. cervisiae AH109 (*A. thaliana* cDNA library CD4-30)	*MATa, trp1-901, leu2-3, 112, ura3-52, his3-200, gal4Δ, gal80Δ, LYS2::GAL1UAS-GAL1TATA-HIS3, GAL2UAS-GAL2TATA-ADE2, URA3::MEL1UAS-MEL1TATA-lacZ*

2.1.6. Plant genotypes

Table 7: Plant lines used in this study

Line	Source
Arabidopsis thaliana Col-0	
A. thaliana ARI12 K8 & *IIB1*	Xie *et al.*, 2015
A. thaliana ari12 SALK_136787	NASC
A. thaliana ARI12-OX1 and 2 *(35S::ARI12-GFP*)	This work
A. thaliana fmo1-1 SALK_026163	NASC
A. thaliana hmp35-I SALK_105737	NASC
A. thaliana hmp35-II SALK_108494	NASC
A. thaliana npr1-1 N3726	NASC
A. thaliana pub54-I SALK_055772	NASC
A. thaliana pub54-II SALK_035556	NASC
A. thaliana rpn12a-1	Kurepa, Toh-E and Smalle, 2008
A. thaliana rpt2a-2 SALK_ 005596	Nottingham Arabidopsis Stock Centre (NASC) (Kurepa *et al.*, 2008)
A. thaliana wrky40	SLAT collection of dSpm insertion lines (Q. H. Shen *et al.*, 2007)
Nicotiana benthamiana	

2.1.7. Media for cultivation

Table 8: Media for bacteria, yeast, and plant cultivation

Medium	Cultivated organism	Components
½ MS	*Arabidopsis*	MS-Salt (Duchefa) 2,2 g/l; pH 5,7 with KOH; if required plant agar 0,8%
King's B	*Pseudomonas*	Glycerol 20 g/l; peptone 40 g/l; 10% (w/v) K_2HPO_4 10 ml/l; 10% (w/v) $MgSO_4$ 10m/l; if required agar-agar 15 g/l
LB	*E. coli*	Bacto tryptone 10 g/l; yeast extract 5 g/l; NaCl 5 g/l; 1N NaOH 0,2 g/l; if required agar-agar 15 g/l
M9 minimal medium	*E. coli* K8	Glucose 20 g/l; amino acid mix 0,67 g/l (Table 9); agar-agar 15 g/l; added after autoclaving: Na_2HPO_4 6 g/l, KH_2PO_4 3 g/l; NaCl 0,5 g/l; NH_4Cl 1 g/l
SCAD	Yeast	Yeast nitrogen base 6,7 g/l; glucose 20 g/l; amino acid mix 0,67 g/l (Table 9); adenine hemisulfate 200 mg/l; pH 5,8 with NaOH; if required agar-agar 15 g/l
YEB	*A. tumefaciens*	Bacto beef extract 5 g/l; yeast extract 1 g/l; Bacto tryptone 5 g/l; sucrose 5 g/l; 2mM $MgSO_4$ 0,439 ml/l; if required agar-agar 15 g/l
YPAD	Yeast	Peptone 20 g/l; yeast extract 10 g/l; glucose 20 g/l; adenine hemisulfate 200 mg/l; pH 5,8; if required agar-agar 15 g/l

For selection of bacteria, the respective antibiotics (Table 10) were added to the autoclaved media after cooling to appx. 50°C.

Table 9: Amino acid mix for yeast cultivation. For preparation of selective media amino acid mixtures missing the respective amino acids were used.

Amino acid		**Amino acid**	
Adenine hemisulfate	2,0 g	Myo-inositol	2,0 g
p-Aminobenzoic acid	0,2 g	Phenylalanine	3,0 g
Arginine-HCl	2,0 g	Serine	2,0g
Histidine-HCl	2,0 g	Threonine	2,0 g
Isoleucine	2,0 g	Tryptophan	3,0 g
Leucine	4,0 g	Tyrosine	2,0 g
Lysine-HCl	2,0 g	Uracil	1,2 g
Methionine	2,0 g	Valine	9,0 g

2.1.8. Antibiotics

Table 10: Antibiotics used for selection

Antibiotic	**Final concentration**
Ampicillin	200 µg/ml
Chloramphenicol	30 µg/ml
Gentamycin	15 µg/ml
Kanamycin	50 µg/ml
Rifampicin	50 µg/ml
Spectinomycin	50 µg/ml
Streptomycin	20 µg/ml

2.2. Methods

2.2.1. Work with plants

2.2.1.1. Surface sterilization and stratification of seeds

Seeds of *Arabidopsis thaliana* were surface sterilized prior to germination. Seeds were treated twice with 70% ethanol and 0,05 % Tween20 for 1 min. After washing with sterile water, the seeds were sowed on soil or on plates with sterile ½ MS medium. Alternatively, seeds were sterilized in a desiccator for 4 h containing chloric gas by adding 5 ml HCl to 100 ml sodium hypochlorite. All seeds were exposed to stratification for 3 days at 4°C and subsequently transferred to climate chambers for germination.

2.2.1.2. Cultivation of *Arabidopsis thaliana* and *Nicotiana benthamiana*

Arabidopsis thaliana was grown under controlled short-day conditions in climate chambers (relative humidity 70%, day: 8 h light, intensity: 80 µmol/s/m^2, 22°C; night: 16 h, 18°C). Seedlings were transplanted in pots containing p-soil, 25% sand and 10 % perlite after 10 days. For experiments, 5 weeks old plants were used.

Nicotiana benthamiana was grown under controlled conditions in walk-in growth chambers (relative humidity 40%, day: 8 h light, intensity: 100 µmol/s/m^2, 25°C; night: 16 h, 20°C. Seedlings were transplanted to bigger pots containing t-soil after 2 weeks. Plants were used for experiments at the age of 5 weeks.

2.2.1.3. Stable transformation of *Arabidopsis thaliana*

Stable transformation of *A. thaliana* was achieved using the floral-dipping method (Bent & Clough, 1998). *Agrobacterium tumefaciens* carrying the construct of interest was suspended in a solution with 5% (w/v) sucrose and 0,05 % Silwet L-77 (Lehle Seeds, USA). *A. thaliana* shoots carrying closed buds were dipped in the solution for 30 s and subsequently covered with a plastic bag. The bags were removed after incubation for 24 h under reduced light conditions. Plants were then cultivated under long-day conditions (16 h light, 8 h darkness). Collected seeds were sowed on ½ MS-plates containing the appropriate antibiotic for selection.

2.2.1.4. Infiltration of *Arabidopsis thaliana* with bacteria to investigate systemic immune responses

All infiltration experiments were performed in 5 weeks old *A. thaliana* plants. In this project, systemic defense responses upon a primary local bacterial infection with *Pseudomonas syringae* pv. *maculicola* ES4362 (*Psm*) were investigated. Three local leaves were infiltrated

using a needleless syringe with *Psm* (OD_{600} 0,005 in 10 mM $MgCl_2$) or, as control, with 10 mM $MgCl_2$. These plants were considered primed (P) or mock infiltrated (M), respectively.

Priming

To investigate the priming response, samples were taken from local (M or +*Psm*) and systemic tissue (M or P) 48 h after the first infiltration.

Systemic acquired resistance (SAR)

Full-factorial experiments were performed to investigate SAR. Systemic leaves of M or P plants were infiltrated with *Psm* ES4362 /*Pst* DC3000 or 10 mM $MgCl_2$ after 48 h. This results in four different treatments (mock, M; primed, P; triggered, T; primed and triggered, P+T; Table 11). Depending on subsequent analyses, the titer of *Psm*/*Pst* suspension and the time point of sampling after the challenging infection differed. When bacterial replication in systemic leaves of M or P plants was assayed 3 dpi, *Psm* or *Pst* was infiltrated with a low titer (10^4 cfu/ml) in 10 mM $MgCl_2$. For all other experiments, *Psm*/*Pst* was infiltrated with OD_{600} 0,005 in 10 mM $MgCl_2$. Samples were taken 10 h after systemic infiltration for assessment of changes in transcript levels (qPCR) or 24 h after infiltration for measurement of SA and camalexin accumulation.

Table 11: Treatments during priming experiments

Abbreviation	Local treatment	Systemic treatment
M	$MgCl_2$	$MgCl_2$
P	*Psm*	$MgCl_2$
T	$MgCl_2$	*Psm* or *Pst*
P+T	*Psm*	*Psm* or *Pst*

M = mock; P = primed; T = triggered; P+T = primed and triggered

2.2.1.5. Bacterial replication assays *in planta*

Quantification of bacterial replication in systemic tissue was performed in bacterial growth assays using 5 weeks old primed and unprimed plants. At least 6 plants were inoculated per *Arabidopsis* line and treatment.

Per plant, two challenge infected systemic leaves (2°) were harvested 3 d post infiltration. The leaves were surface sterilized for 30 s in 70% EtOH and washed for 30 s in ddH_2O. Two leaf discs (diameter 0,5 cm) were punched out from each leaf and homogenized in 200 µl

10 mM $MgCl_2$. 10 µl of the bacterial suspension was plated on King's B plates in dilution series. The plates were incubated at 28°C for 2 days. Finally, CFU were determined.

2.2.1.6. Infiltration of *Nicotiana benthamiana* for transient protein expression

Transient expression of proteins in *N. benthamiana* was performed by infiltration of *A. tumefaciens*. Cultures of transformed *A. tumefaciens* were incubated overnight. Additionally, *Agrobacteria* containing the silencing inhibitor p19 (Voinnet *et al.*, 2003) were inoculated. All bacterial overnight cultures were harvested and resuspended in infiltration medium (10 mM $MgCl_2$ with 200 µM acetosyringone). The OD_{600} of bacterial suspensions were determined. The *Agrobacteria* were mixed in the desired combination with a final OD_{600} of 0,5 for each construct and OD_{600} of 0,3 for p19. The bacteria were incubated at room temperature for 2 h and infiltrated in *N. benthamiana* using a needleless syringe. Samples were taken after 1-3 day and frozen in liquid nitrogen. The leaf material was stored at -80°C until use.

2.2.1.7. Confocal laser scanning microscopy (cLSM)

The Zeiss LSM 510 Axioplan2i was used for visualization of fluorescent proteins. All pictures were taken using the LD LCI-Plan-Neofluar 25x/0.8 Imm Korr DIC M27 objective. Fluorescent proteins were excited by using appropriate lasers, i.e., for GFP (ex. 488 nm, em. 705 nm) and YFP (ex. 514, em. 791).

2.2.1.8. Extraction of salicylic acid and camalexin

Total salicylic acid (SA), i.e., free and conjugated SA, and camalexin levels were analyzed after methanol extraction (Nawrath & Métraux, 1999). Quantification was facilitated by addition of an internal standard (Meuwly & Métraux, 1993). 50 mg of leaf material were ground in nitrogen. 600 µl of 70% MeOH and 300 ng of the internal standard SA-d4 were added. After incubation for 1 h at 65°C and centrifugation for 5 min at 13.000 rpm the supernatant was transferred to a glass vial. The MeOH extraction was repeated and both fractions were combined. The MeOH was vaporized in nitrogenated atmosphere. Afterwards, 500 µl 5% TCA (w/v) were added for resuspension. After centrifugation at 6000 rpm for 10 min 600 µl cyclohexane/ ethyl acetate (1:1) was added to the supernatant. Centrifugation for 10 min at 6000 rpm separates the upper organic phase containing free SA and the aqueous phase used for extraction of conjugated SA. The separation was repeated with the aqueous phase and both fractions of organic phases were combined. The solution was vaporized in nitrogenated atmosphere but not fully dried. 100 µl of 80% formic acid / 20% acetonitrile were added to the sample for storage at -20°C. To extract conjugated SA, the residual aqueous phase was complemented with 1 vol. formic acid and incubated at 80°C for 1 h. Again, organic phases were twice separated with cyclohexane/ ethyl acetate (1:1) and combined. 20 µl acetonitrile were added to the solution and subsequently vaporized in nitrogenated atmosphere but not fully dried. 100 µl of 80% formic acid / 20% acetonitrile

were added to the sample. 5 µl of each were injected for LC-MS/MS measurement. Additionally, a SA-calibration curve ranging from 0,1 ng/µl to 20 ng/µl was measured.

2.2.2. Microbiological methods

2.2.2.1. Cultivation and selection of bacteria and yeast

Escherichia coli strains

E. coli strains DH5α, BL21 (Rosetta) and KC8 were cultivated at 37°C in LB liquid medium or on plates. During identification of protein-interaction partners using the Y2H system, plasmids were extracted from yeast and transformed into *E. coli* KC8. Separation of colonies carrying the bait or prey plasmid was achieved by incubation on M9 medium leu^- or trp^-.

Agrobacterium tumefaciens

A. tumefaciens was cultivated on YEB liquid medium with respective antibiotics for 2-3 days at 28°C. If in liquid culture, bacteria were shaken at 250 rpm overnight.

Saccharomyces cerevisiae

Both, *S. cerevisiae* Y190 and Y187 were incubated on YPAD medium without antibiotics for 2 days at 28°C. The auxotroph yeast strains were incubated at 28°C on selective SCAD medium for complementation by a transformed plasmid.

2.2.2.2. Transformation of bacteria and yeast

E. coli DH5α

Chemo competent DH5α (aliquots of 50 µl each) were thawed on ice and 1 µl of plasmid DNA was added. After incubation on ice for 30 min, a heat shock at 42°C was applied for 90 s. The cells were immediately transferred on ice for 1 min. For recovery, 1 ml LB medium was added and the tube was shaken for 1 h at 37°C. Afterwards, the tube was centrifuged at 6000 rpm for 1 min and the supernatant was poured off. The remaining supernatant was used to resuspend the pellet. The suspension was plated on LB plates containing the according antibiotics. Bacteria were incubated over night at 37°C.

E. coli BL21 (Rosetta)

The transformation of *E. coli* BL21 (Rosetta) was performed as described above. Different from E. coli DH5*α*, the heat shock was applied for 30 s.

E. coli KC8

Electro competent *E. coli* KC8 was thawed on ice and incubated with 1 µl plasmid DNA for 5 min. After transfer into a pre-chilled electroporation cuvette an electric pulse was applied

(2,2 kV). 1 ml of LB medium was added and bacteria were incubated at 37°C for 1 h. Afterwards, the bacteria were incubated on selective M9 plates for 1 day at 37°C.

Agrobacterium tumefaciens

A 50 µl aliquot electro competent *A. tumefaciens* GV3101 was thawed on ice. 1 µl of plasmid DNA was added to the bacteria. Next, the cells were transferred to a pre-chilled electroporation cuvette (0,2 cm gap). Application of an electric pulse (2,2 kV) was followed by addition of 1 ml YEB media. The suspended cells were transferred to a tube and allowed to recover at 28°C for 1 h. The tube was centrifuged at 6000 rpm for 1 min and the supernatant was poured off. The remaining supernatant was used to resuspend the pellet. The suspension was plated on YEB plates containing appropriate antibiotics and incubated at 28°C for 2-3 days.

Saccharomyces cerevisiae

S. cerevisiae Y187 and Y190 were transformed using the Lithium acetate-ssDNA-PEG-method (Gietz & Woods, 2002). Selection of positive colonies was achieved by cultivation on SCAD medium lacking the amino acid complemented by the transformed plasmid.

2.2.2.3. IPTG induction of recombinant proteins in *E. coli* BL21 (Rosetta)

Recombinant proteins were expressed in *E. coli* BL21 (Rosetta) after induction with isopropyl β-D-1-thiogalactopyranoside (IPTG). A single colony carrying the desired vector was inoculated overnight in 2 ml LB media containing suitable antibiotics. The main culture of 50 ml was inoculated with the overnight culture and incubated until an OD_{600} of 0,5. Expression of target proteins was induced by application of 0,5 mM IPGT. The culture was grown at 37°C for 3 h or at 16°C for 24 h. To harvest the culture, cells were centrifuged at 6000 rpm for 10 min at 4°C. Pellets were stored at -20°C until use.

2.2.2.4. Yeast2Hybrid system to test for protein-protein interaction

In order to identify novel putative interaction partner of a protein of interest or to confirm the potential interaction of two proteins the yeast-2-hybrid system (Y2H) was used (Fields & Song, 1989). The Y2H system is a powerful and fast approach to investigate protein-protein interactions. The system relies on a transcriptional activator with separable functional domains, i.e., DNA-binding and activation domain. These domains are fused to a protein of interest (bait) and potential interaction partners (prey). Interaction of bait and prey leads to transactivation of biosynthetic genes and allows auxotroph yeast strains to replicate on medium lacking essential amino acids.

Test for direct interaction of proteins

To test direct interaction of two proteins, competent *S. cerevisiae* Y190 was transformed with two plasmids as described above. The cells were cultivated on SCAD trp^-leu^- plates to

select for colonies carrying both, bait and prey plasmid. After 2-3 days, positive colonies were transferred to SCAD $trp^-leu^-his^-$ + 25 mM 3-AT-plates with gene screen membrane. The activation of the LacZ-reporter gene was tested with a LacZ-filter–assay (Breeden & Nasmyth, 1985).

Y2H-screen to identify potential interaction partner

In order to identify potential interaction partner of a protein of interest the coding sequence of the bait protein was cloned into the vector pGBT9. The plasmid was transformed into S: cerevisiae Y187 and cultivated on SCAD trp^- medium at 28°C. A liquid overnight culture (5 ml) was used to inoculate the main culture (150 ml). After incubation overnight, the cells were harvested by centrifugation at 4000 rpm for 5 min and washed twice with sterile water. Meanwhile, *S. cerevisiae* AH101 carrying the *Arabidopsis* cDNA gene library CD4-30 was thawed and resuspended in 20 ml YPAD medium. The cells were allowed to recover for 10 min at 28°C. Both yeast strains were combined and resuspended in 2 ml YPAD after additional centrifugation. Aliquots of 400 ml each were plated on YPAD plates and incubated for 4 h at 28°C for mating. The cells were three times rinsed off the plates with liquid YPAD medium and collected. After centrifugation for 5 min at 4000 rpm, the cells were resuspended in sterile water. Aliquots of 1 ml each were plated on large petri dishes with SCAD $trp^-leu^-his^-$ +4 mM 3-AT-plates and incubated at 28°C for 1-2 weeks. Positive colonies were then transferred to SCAD $trp^-leu^-his^-$ +4 mM 3-AT-plates with gene screen membrane. The expression of the second reporter was verified by a LacZ-filter assay.

2.2.2.5. LacZ-filter assay

Interaction of bait and prey proteins fused to the activation- or binding domain of the GAL4-transcriptionfactor allow auxotroph yeast to grow on SCAD-leu^- trp^- his^- medium. The interaction can be verified by an additional reporter performing the LacZ-filter assay. Yeast was grown on SCAD $trp^-leu^-his^-$ plates with gene screen membrane. The membrane was placed into liquid nitrogen to disrupt the cells and subsequently placed on Whatman filter paper soaked with LacZ-buffer [(60 mM Na_2HPO_4; 40 mM NaH_2PO_4; 10 mM KCl; 1 mM $MgSO_4$; pH 7,0); 0,064% X-Gal (w/v) in dimethylformamide), 0,26% ß-mercaptoethanol (v/v)]. Blue staining of the colony indicates interaction of bait and prey after incubation for 4-6 h at 28°C.

2.2.3. Molecular biological methods

2.2.3.1. Extraction of genomic DNA from *Arabidopsis thaliana*

Genomic DNA (gDNA) from *A. thaliana* was isolated using the protocol from (Edwards *et al.*, 1991). Isolated gDNA was used as template for genotyping PCRs of overexpression lines and SALK-knock out lines.

2.2.3.2. Extraction of total RNA from *Arabidopsis thaliana*

Total RNA from plant material was extracted using NucleoZOL (Macherey & Nagel, Düren). All steps were performed as described in the product manual. The RNA concentration was determined by spectrophotometric measurement (plate reader infinite 200Pro, Tecan).

RNAsequencing required RNA of highest quality. This was accomplished by using a RNA extraction kit (RNeasy Mini Kit, Qiagen). The RNA was extracted following the supplied protocol. The concentration and integrity of the isolated RNA was determined (2100 Bioanalyzer, Agilent). Samples with RIN>9 were diluted to 100 ng/µl and sent for sequencing.

2.2.3.3. DNase-digestion of RNA

Potentially remaining DNA in RNA samples was digested by DNase. 2 µg RNA were incubated with 2 µl DNaseI (1 U/µl) and 1x DNase-Buffer (Thermo scientific™) at 37°C for 1h. DNaseI was inactivated by addition of 1 µl 50 mM EDTA and subsequent incubation at 65°C for 15 min.

2.2.3.4. Synthesis of cDNA

First strand cDNA was synthesized from 2 µg DNase digested RNA using the RevertAid Reverse Transcriptase (200 U/µl) with supplemented buffer and RNase inhibitor RiboLock RNase-Inhibitor (40 U/µl) (Thermo scientific™).

Table 12: Reaction components required for cDNA synthesis from RNA

RNA	1 µg
Oligo(dT)$_{18}$ primer (50 µM)	1 µl
dNTP Mix, 10 mM each	2,5 µl
Reverse Transcriptase	1 µl
RiboLock	0,5 µl
RNase free H_2O	ad 10 µl

The reaction was incubated at 37°C for 1 h and the enzyme was subsequently inactivated by heating at 70°C for 15 min. The obtained cDNA was 1:10 diluted in RNase free water for analysis in RT-qPCR.

2.2.3.5. Real Time Quantitative -PCR (RT-qPCR)

Synthesized cDNA was used for gene expression analysis in RT-qPCRs. cDNA was amplified with SensiFAST™ SYBR® Lo-ROX Mix (Bioline GmbH, Luckenwalde) using the AriaMx Real-time PCR system (Agilent Technologies Deutschland GmbH& Co. KG, Waldbronn). The relative transcript level of the target genes was normalized to the reference gene UBC9 (UBIQUITIN CARRIER PROTEIN 9). Each sample was measured in technical duplicates.

Table 13: Components and program for two-step RT-qPCRs

Component	Volume		Temperature	Time	
SensiFAST SYBR Lo-ROX Mix	5 µl	Denaturation	95°C	2 min	
Fwd primer (1mM)	0,8 µl				
Rev primer (1mM)	0,8µl	Denaturation	95°C	5 s	40x
cDNA (1:10 diluted)	1 µl	Annealing and elongation	60°C	10 s	
		Melting curve	65°C – 95°C	0,5°C /5s	

The melting curve was essential for detection of undesired byproduct during the RT-qPCR. The relative quantity (RQ) was determined with the following formula following (Rieu & Powers, 2009).

$RQ = \frac{1}{E^{Cq}}$ RQ= relative quantity; E= primer efficiency ($E=10^{1/\text{slope of standard curve}}$);

Cq= measured cycle in which fluorescence exceeds threshold

The relative transcript level of the target genes was normalized to the reference gene UBC9 (UBIQUITIN CARRIER PROTEIN 9). Each sample was measured in technical duplicates.

2.2.3.6. Polymerase chain reaction (PCR)

Table 14: Components and program used for cloning purposes

Component	Volume		Temperature	Time
Phusion® High Fidelity	0,25 µl	Denaturation	95°C	5 min

DNA Polymerase					
DNA template	1 µl	Denaturation	95°C	30 s	35x
dNTPs (2,5 mM)	5 µl	Annealing	T_{anneal}	30 s	
5x HF buffer	5 µl	Elongation	72°C	30s/kb	
Fwd primer (5 µM)	1,25 µl	Final elongation	72°C	10 min	
Rev primer (5 µM)	1,25 µl				
ddH_2O	11,25 µl				

Table 15: Components and program for genotyping purposes

Component	**Volume**		**Temperature**	**Time**	
FIREPol® 5x master mix	4 µl	Denaturation	95°C	5 min	
gDNA	1 µl	Denaturation	95°C	30 s	35x
Fwd primer (5 µM)	0,8 µl	Annealing	T_{anneal}	30 s	
Rev primer (5 µM)	0,8 µl	Elongation	72°C	60 s/kb	
ddH_2O	1,25 µl	Final elongation	72°C	10 min	

2.2.3.7. Plasmid-preparation from Escherichia coli

Plasmid DNA from *E. coli* was isolated from overnight cultures. The pellet of a 2 ml culture was resuspended in 100 µl solution I (50 mM TRIS HCl, pH 8,0; 10 mM EDTA, pH 8,0; RNase 50 µg/ml). Bacteria were lysed by addition of 200 ml solution II (0,2 M NaOH; 1% (w/v) SDS) and inverting the tube. The reaction was stopped with 150 µl solution III (3 M Potassium acetate, pH 4,8). After mixing, the samples were centrifuged for 10 min at 13.000 rpm. Plasmid DNA present in the supernatant was precipitated in 1 ml pure ethanol. After centrifugation for 10 min at 13.000 rpm the pellets were washed twice in 70 % EtOH. Dried pellets were resuspended in 30 µL dd H_2O.

2.2.3.8. Agarose gel electrophoresis

Amplified DNA-fragments and digested vectors were separated in 1% (w/v) agarose gels. Addition of 4 µl ROTI® GelStain per 100 ml agarose gel allowed for visualization of DNA under UV-light. Electrophoresis was performed for 30 min at 140 V in 1x TAE buffer (40 mM Tris base; 1 mM EDTA; 20 mM acetic acid).

2.2.3.9. Elution of DNA from agarose gels

In order to elute DNA from agarose gels, the QIAquick Gel Extraction Kit (Qiagen) was used. The corresponding standard protocol was applied.

2.2.3.10. Cloning strategies

Two different cloning systems were used in this study dependent on the properties of the desired destination vector.

Gateway® system

The pENTR™/D-TOPO™ (Invitrogen™) cloning kit was used to generate Gateway®-compatible entry-clones according to the manufacturers protocol.

NEBuilder® HiFi DNA Assembly

The NEBuilder® HiFi DNA Assembly system was used for non-Gateway® compatible vectors and assembly of multiple DNA fragments. All steps were performed according to the NEBuilder® HiFi DNA Assembly Reaction protocol. The required primers were designed using the NEBuilder® Assembly Tool v2.2.7.

2.2.3.11. Digestion of plasmids using restriction enzymes

Extracted plasmids from *E. coli* were tested for the insertion of the desired fragment. In der to test this, 1 µl plasmid DNA was incubated 0,2 µl of each required restriction enzyme and the corresponding buffer. The digestion was inoculated at 37°C for 1 h. Digested plasmids were separated in agarose gels.

2.2.3.12. Sequencing of DNA

Sequencing of plasmid DNA was performed by Eurofins genomics or LCG genomics according to their specific conditions.

2.2.4. Biochemical methods

2.2.4.1. Protein extraction from plant material

Deep frozen plant material expressing the protein of interest was ground in liquid nitrogen. 2 vol (v/w) protein extraction buffer (50 mM Tris-HCl pH 7,5; 150 mM NaCl; 10% (v/v) glycerol; 10 mM DTT; 10 mM EDTA; 1 mM NaF; 1 mM N_2MoO_4; 0,5% (v/v) NP40) were added to the homogenized sample. After thawing, the samples were kept on ice and centrifuged at 13000 rpm for 15 min at 4°C. The supernatant containing all soluble proteins was transferred to a new reaction tube.

2.2.4.2. (Co-) immunoprecipitation of fusion proteins from plant material

GPF- or HA-tagged proteins and their interacting factors can be isolated by immunoprecipitation (IP). First, proteins were extracted from plant tissue as described above. IPs were performed according to the protocol GFP-TRAP®_MA (ChromoTek GmbH, Planegg-Martinsried).

2.2.4.3. Protein digestion and sample preparation for MS-analysis

Purified proteins were digested with trypsin on filter (Microcon®10K green top 42407) following the manufacturer's manual. The resulting peptides were desalted and washed via Thermo Scientific™ Zeba™ Spin Desalting Columns following the recommended protocol. Prepared peptides were stored at -20°C until measurement using LC-MS/MS was started.

2.2.4.4. Affinity purification of recombinant proteins from bacteria

MBP- and GST-tagged recombinant proteins were purified from bacteria with the aid of affinity matrixes. Production of these recombinant proteins in *E. coli* BL21 Rosetta was induced by IPTG. Frozen pellets were thawed on ice in 1 ml MBP-column buffer (50 mM TRIS HCl pH 7,5) or for GST-tagged proteins with 1 ml IPP50 (10 mM TRIS-HCl, pH 8,0; 150 mM NaCl; 0,1% NP40 (v/v)). One "spatula tip" Lysozyme was added. The suspension was incubated on ice for 10 min and 10 min at RT. In the following, the suspension was sonicated 8 times at 29-33% intensity. A sample was taken from the raw extract for further analysis in SDS-PAGE. The raw extract was centrifuged at 4°C and 13.000 rpm for 15 min. In the meantime, the appropriate affinity matrix was prepared, i.e., 300 µl amylose resin for MBP-tagged proteins or 350 µl glutathione sepharose beads were transferred to a new tube. The matrixes were equilibrated by 3-fold washing with 600 µl MBP-column buffer or 600 µl IPP50. The cleared supernatant was added to the tube containing the equilibrated affinity matrix. Samples were taken from the supernatant and the pellet for testing with SDS-PAGE. The proteins were allowed to bind to the matrix by incubation at 4°C for 2 h. Next, the matrixes loaded with the bound proteins were washed 4 times. Proteins were eluted with 300 µl MBP-column buffer with 50 mM maltose or 300 µl 50 mM reduced glutathione by incubation for 1h. A sample was taken from the eluate to control efficiency of the purification.

2.2.4.5. Measurement of protein concentration

The concentration of extracted proteins was measured using Bio-Rad Protein Assay Dye Reagent Concentrate (Bio-Rad laboratories GmbH, München). The concentrate was diluted with water (1:5) and bovine serum albumin was used a standard. The extinction was measured at 595 nm with a plate reader (Synergy HT, BioTek Instruments GmbH, Bad Friedrichshall).

2.2.4.6. Sodium dodecyl sulfate-polyacrylamide-gel electrophoresis (SDS-PAGE)

Polyacrylamide-gel electrophoresis was performed with gels containing SDS and 12% polyacrylamide. All components (

Table 16) were mixed in the given order. Gels were loaded with samples. Initially, 100 V were applied to the gel to line up the proteins at the border to the resolving gel. Once the proteins start migration the resolving gel, the electric potential was increased to 140 V.

Table 16: Components for SDS-PA gels

Component	resolving gel	stacking gel
Acrylamide/Bis-acrylamide 30:0	7,5 ml	1,25 ml
3 M TRIS-HCl pH 8,8	2,25 ml	-
1 M TRIS HCl pH 6,8	-	1,25 ml
H_2O	7,9 ml	3,6 ml
10 % SDS (w/v)	180 µl	100 µl
10 % APS (w/v)	135 µl	50 µl
TEMED	9 µl	5 µl

2.2.4.7. Coomassie stain of SDS-gels

SDS-gels were irreversibly stained with coomassie by incubation in 20 ml InstantBlue® Coomassie Protein Stain for 30 min. Excessive stain was removed by washing in $_{dd}H_2O$ for 1 h.

2.2.4.8. Western blot

The semi-dry wester blotting method was used in order to transfer proteins from a SDS-gel to a membrane (nitro cellulose or PVDF). Briefly, a stack of 3 Whatman filter papers, the membrane (nitro cellulose or PVDF), the SDS-gel and another 3 Whatman filter papers were placed in a semi-dry blotting device. All components were previously wetted with 1x transfer buffer (25 mM TRIS pH 8,2; 192 mM glycine; 20 % MeOH (v/v)). A current of 60 A was applied for 90 min to blot the proteins to the membrane (6 x 8 cm).

2.2.4.9. Immuno-detection of tagged proteins

Blotted membranes were blocked either in 5% milk powder in TBS-T for 1 h or in 3% milk powder in TBS-T over night. The blocked membranes were incubated with the appropriate antibodies diluted in TBS-T. If the use of a secondary antibody was required the membranes

were at least 3x washed with TBS-T for 5 min after incubation of the primary antibody. Next, blots were washed 3x with TBS-T for 5 min and 2x with TBS for 5 min. Detection was performed by application of 800 µl Clarity Western ECL Substrate to the membrane and imaging using the Bio-Rad ChemiDoc™ Imaging System.

2.2.4.10. *In vitro* ubiquitination assay

In vitro ubiquitination assays may be performed with recombinant proteins to analyze auto-ubiquitination of E3-ubiquitin ligases and their ability to transfer ubiquitin to potential substrate proteins. All components required for a ubiquitination reaction (25 mM Tris-HCl pH 7,5; 5 mM MgCl2; 50 mM KCl; 0,6 mM DTT; 2 mM ATP; 2 µg ubiquitin; 0,2 µg E1; 1,2 µg E2; 2 µg E3; if required: 0,3 µg substrate protein) are combined in one reaction tube and incubated for 1h at 30°C. Control reactions were simultaneously performed lacking one of the following components each: -ATP, - ubiquitin, -E1, -E2, -E3, -substrate protein. The reactions were stopped by addition of 10 µl loading buffer (240 mM Tris-HCl pH 6,8; 0,5 M DTT; 10% SDS (w/v); 50% glycerol (v/v); 0.005% bromphenol blue (w/v)). Samples were denaturated for 10 min at 68°C and directly load on an SDS-polyacrylamide gel.

2.2.5. RNA-sequencing and bioinformatics methods

Sanger sequencing of DNA (Sanger *et al.*, 1977) is an extensively used method with continuous developed throughout the following years. With development of the Next Generation Sequencing technology (NGS) in 2005 capacity of sequencing increased dramatically. Prior to NGS, DNA is fragmented to smaller DNA fragments, which allows for shorter and parallel sequencing runs of high quality.

A specific variant of NGS is RNA-sequencing (RNAseq). Total mRNA is extracted from samples and fragmented prior to cDNA synthesis. Individual adapters with random but know sequences are ligated to the cDNA fragments. The fragments are subsequently immobilized on the surface of a chip. Using bridge amplification, each cDNA fragment is amplified multiple times in proximity and therefore creates a cluster. The cluster intensifies the signal during each step of the following sequencing reactions. The nucleotide sequence of each cluster is detected and emerge in reads corresponding to the fragments. The total number of all reads represents the sequencing depth for each sample.

In this project RNAseq was used to gain a global overview of transcriptional changes during systemic immunity. The used script can be found in the appendix with exemplary data names. In the following paragraphs all conducted steps are described in more detail.

2.2.5.1. Quality control of *reads*

The sequencing was performed by ATLAS Biolabs, Berlin. The received sequencing data provide information about the total number of sequenced reads per sample and information about the individual reads. A good quality of the sequencing process is essential for subsequent bioinformatics steps. This includes successful clipping of the used adapter. The subsequent quality control was performed by the company and included e.g., analysis of the per base sequence quality and proper clipping of the adapters. A general quality control of the data and adapter clipping was performed by the company before submitting the sequencing data.

2.2.5.2. Mapping und quantification of reads

The first step in RNAseq analysis is the alignment of the obtained reads to an index genome. Here, the *A. thaliana* TAIR10 genome was used as reference genome for the mapping. The LINUX based program *STAR* was used to align the reads to the genome. Subsequently, the output files were compressed using *samtools sort*. The mapped reads were then counted with *htseq-count*. Counted reads from each sample were combined into one file before proceeding with statistical analysis.

2.2.5.3. Differentially expressed genes

RNAseq provides quantitative approximations of the abundance of transcripts. In this study per-gene based counts were statistically analyzed using the R package DEseq2 from the Bioconductor project (Love *et al.*, 2014). The basic concept of DEseq2 allows a gene-based identification of transcriptional differences between conditions bigger than the biological variance. The underlying assumption of DEseq2 is that most genes are not differentially expressed. Furthermore, normalization on raw counts assumes a negative binominal distribution and accounts for sequencing depth of each sample.

For determination of DEG the standard workflow of DESeq2 was applied. Initially, a DESeqDataSet (*dds*) was designed. The *dds*-object contains the matrix of un-normalized counts derived from htseq (*countData*) and metadata defining the conditions of the experimental design (*colData*). Additionally, the data from control samples were specified as reference level. The standard analysis of DEG is implemented in a single function including normalization on raw counts. In this study, genes with base read > 10 and padj < 0,1 were considered as differentially expressed.

2.2.5.4. Assessment of data quality / exploratory data analysis

In order to assess the data quality several methods of visualizations can be used. The R packages *ggplots* and *RColorBrewer* were used to generate plots. Analysis of Cook's distances were performed from *dds* to exclude experimental artefacts or read mapping

problems. A regularized log transformation (using the *rlogTransform* function) was applied to the count data from *dds* for transformation to the log2 scale. *DESeq* therewith minimizes differences between samples for genes with low count and normalizes to the library size to approximate a normal distribution of the data. To study inter-sample consistency a principal component analysis (PCA) was performed on *rlogTransformed* data. Additionally, hierarchical clustering was applied taking distance between *rlogTransformed* data into account. The cluster was plotted as heatmap.

2.2.5.5. GO-term analysis

The Gene Ontology is a bioinformatics initiative aiming to unify description of genes across species (Harris *et al.*, 2008). Annotated genes are assigned to three domains, i.e., biological process, molecular function, and cellular component. The *Arabidopsis* database org.At.tair.db provides information regarding the annotation of genes to a certain GO term. The R package *topGO* was used to identify enriched GOterms. In a list of DEG, analysis of enriched GOterms gives additional information on the shift and relevance of processes.

3. Results

3.1. Characterization of the proteasome mutants *rpt2a-2* und *rpn12a-1*

3.1.1. Large scale ubiquitination of proteins occurs upon pathogenic infection in local and systemic tissue.

The Ubiquitin-proteasome-system is involved in defense responses on several levels. Additionally, bacterial type-3 effectors interfere with diverse immune related processes during infection and lead to decreased proteasome activity. To study if ubiquitinated proteins accumulate in local and systemic tissue of primed plants during pipecolic acid (Pip), salicylic acid (SA), or *Psm*-induced priming, samples were taken after 48 h from local and systemic tissue and probed on a western blot using an α-ubiquitin antibody for immunodetection of ubiquitinated proteins (Figure 5).

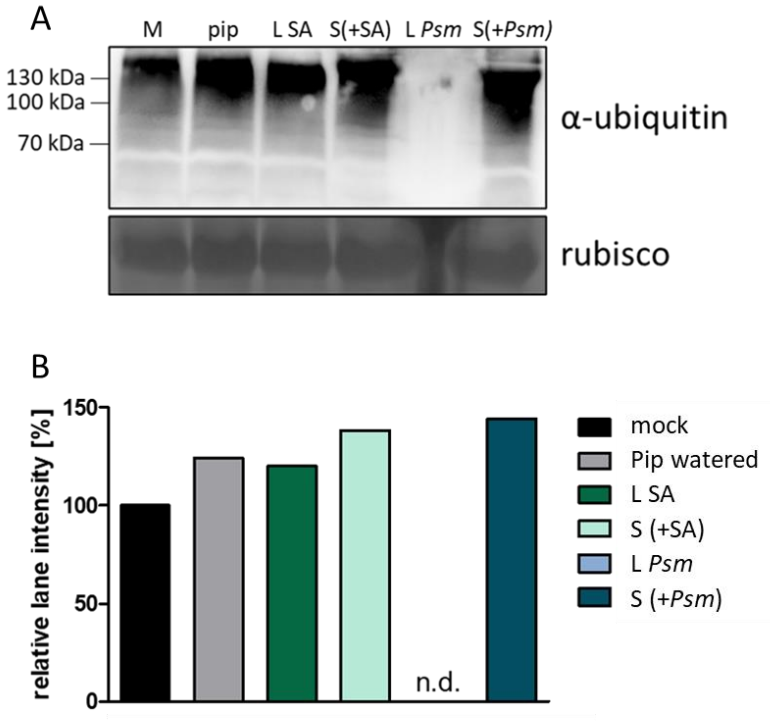

Figure 5: Ubiquitinated proteins accumulate during priming with Pip, SA, and *Psm* in Col-0. *Arabidopsis* Col-0 was locally mock infiltrated with 10 mM $MgCl_2$, primed by infiltration of 200 µM SA or *Psm* (OD_{600} = 0,005) or by watering with 10 mL 1 mM Pip. Samples were taken from locally treated tissue (mock, L SA, L *Psm*) and from systemic tissue (Pip, S(+SA), S(+*Psm*)) 48 h after local application. (A) Accumulation of ubiquitinated proteins was analyzed in crude extracts by SDS-gel electrophoresis and subsequent western blot using an α-ubiquitin antibody for immunodetection. (B) Signal intensity deriving from immunodetection with an α-ubiquitin antibody was quantified and plotted as relative lane intensity [%] with local mock treated samples considered

as basal 100% of ubiquitinated proteins. Each sample consists of two leaves from 4 biological replicates. Statistical analysis was not applied due to pooled samples. The experiment was only conducted once. Pip = pipecolic acid, SA = salicylic acid, M = mock, L = local, S = systemic n = 4

Pip-watered plants accumulate more ubiquitinated proteins than mock treated plants. Leaves of locally SA treated plants show a comparable level of ubiquitination as in Pip-watered plants. Interestingly, ubiquitination is increased in systemic tissue of SA-primed plants. *Psm* infiltrated tissue was highly damaged and therefore no intact proteins could be extracted from this material. Highest ubiquitination levels are reached in systemic tissue of *Psm* primed plants suggesting that bacterial infections lead to accumulation of ubiquitinated proteins during systemic defense responses. These data furthermore indicate a regulation elicited by Pip- and SA-mediated mechanisms.

3.1.2. Proteasome mutants are impaired in local and systemic immunity

Accumulation of ubiquitinated proteins during SAR and the involvement of many E3 ubiquitin ligases in defense responses (Adams & Spoel, 2018; Trujillo & Shirasu, 2010) imply a central role of the UPS during development of resistance towards pathogens. However, the underlying mechanism on how the 26S proteasome itself contributes to onset and/or maintenance of systemic defense responses remain unclear. Therefore, the proteasome mutants *rpt2a*-2 and *rpn12a*-1 were characterized regarding their defense responses during infections with *Psm*.

To investigate the basal resistance and susceptibility after priming in wildtype Col-0, *rpt2a-2,* and *rpn12-a1*, a bacterial growth assay was performed. Plants were either locally primed with *Psm* (OD_{600} 0,005) or mock infiltrated. After 48 h, all plants were triggered with *Psm* ($1x10^4$ CFU/ml) in systemic tissue with the same bacterial titer. Bacterial replication in systemic leaves was assayed after 3 days. Significant differences in bacterial replication emerge between the genotypes (Figure 6). In unprimed conditions, proteasome mutants are significantly more susceptible when compared to wildtype where *rpt2a-2* shows even higher bacterial replication than *rpn12a-1*. Thus, both genotypes show weaker basal resistance. Wildtype plants strongly benefit from a previous priming stimulus. The capacity of the priming benefit is slightly decreased in *rpt2a-2*. Primed *rpn12a-1* do not acquire systemic resistance. These data indicate that a functional 26S proteasome is required to display local and systemic resistance against infections with *Psm*.

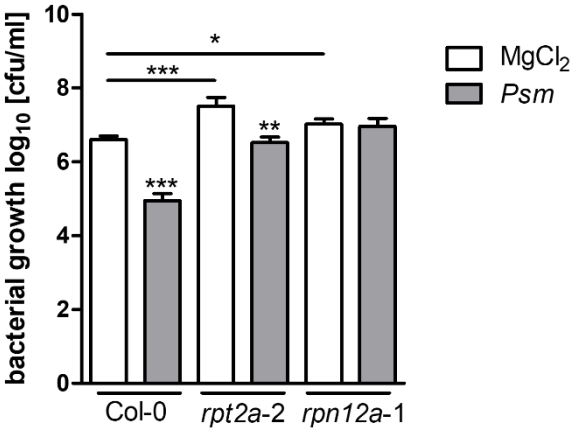

Figure 6: Basal resistance is decreased and the effect of priming is dampened in the proteasome mutants *rpt2a*-2 and *rpn12a*-1. Three lower leaves (1°) of Col-0, *rpt2a*-2, and *rpn12a*-1 were infiltrated with 10 mM $MgCl_2$ as control or *Psm* (OD_{600} = 0.005) for priming. Two days later, three upper leaves (2°) were triggered with *Pst* ($1x10^4$ cfu/ml). Bacterial replication in 2° was assayed 3 dpi. Asterisks indicate statistically significant differences between the treatments within the same genotype. Included bars display statistically significant differences across the genotypes (***P < 0.001; **P <0.01; *P < 0.05, two-tailed *t* test). Data represent mean ± SEM. The experiment was performed three times with similar results. N=12

To analyze the impact of proteasome components on the establishment and maintenance of SAR, *rpt2a*-2 and *rpn12a*-1 were further analyzed on the molecular level during a priming and triggering infection. Plants were primed/mock treated in local leaves and after 48 h systemic leaves were triggered or mock infiltrated and subsequently sampled 10 h after the second treatment. Thus, 4 different treatments including only mock infiltrated (M), triggered (T), primed (P) as well as primed and triggered (PT) were applied. The expression of defense and priming marker genes was quantified using qRT-PCR (Figure 7). *Pathogenesis-related gene 1* (*PR1*) was tested as marker for SA-dependent defense responses. *PR1* expression is induced upon triggering in wildtype. The priming stimulus elicits even higher gene expression in systemic tissue. A tendency of enhanced response in triggered plants which received a previous priming stimulus is seen here. *Flavin-dependent monooxygenase 1* (*FMO1*) and *AGD2-like defense response protein 1* (*ALD1*) are well established marker genes upregulated during priming (Hartmann *et al.*, 2018). The expression of these genes in distal plant parts is slightly induced upon local priming and stronger upon triggering, which is strongly exceeded when a prior priming stimulus is applied.

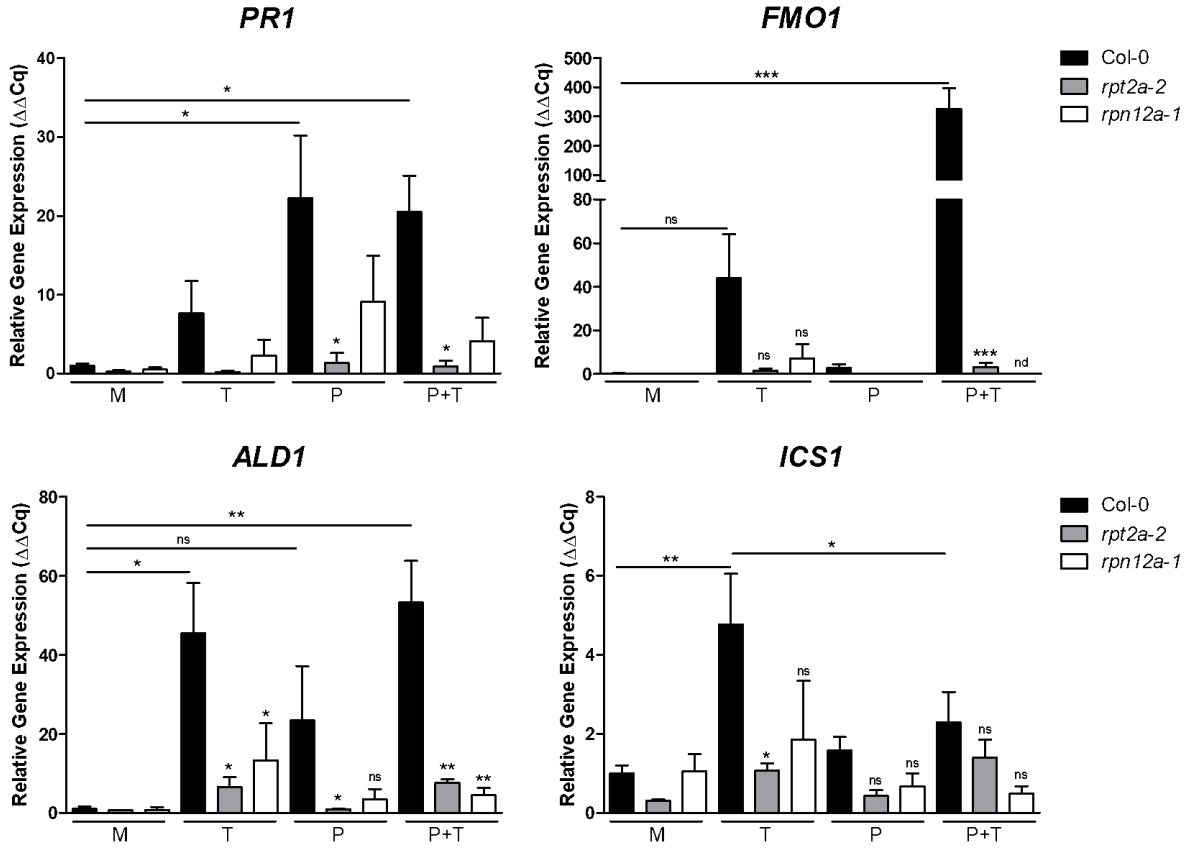

Figure 7: SAR marker genes are weakly expressed during priming and triggering in the proteasome mutants. Three lower leaves (1°) of Col-0, *rpt2a*-2, and *rpn12a*-1 were infiltrated with 10 mM $MgCl_2$ as control or *Psm* (OD_{600} = 0.005) for priming. Two days later, three upper leaves (2°) were triggered with *Pst* (OD_{600} = 0.005) or infiltrated with 10 mM $MgCl_2$. Samples were taken from systemic tissue (2°) 10 h after triggering. Relative Gene Expression (ΔΔCq) displays fold-induction in relation to mock-treated Col-0. Asterisks indicate statistically significant differences between genotypes within the same treatment. Included bars display statistically significant differences within one genotype across the treatments (***P < 0.001; **P <0.01; *P < 0.05, ns = not significant, nd = not detectable, 1way ANOVA with Bonferroni's post-test). M = mock; T = triggered; P = primed; P+T = primed and triggered. Data represent mean ± SEM. The experiment was performed three times with similar results. N=4

Arabidopsis isochorismate synthase 1 (*ICS1*, also known as *SID2*), *enhanced disease susceptibility 5* (*EDS5*), *phytoalexin deficient 3* (*PAD3*), and plant-U-box E3 ubiquitin-protein ligase (*PUB23*) were additionally tested (integrated in Figure 8). Gene expression is weakly induced in priming and strongly induced after triggering in Col-0. Plants being additionally challenging infected react with hyper-induction of these genes. Interestingly, *rpt2a*-2 and *rpn12a*-1 shows an overall alleviation in gene expression of all genes during all treatments. Solely *PUB23* (which is not a classical SAR-marker gene but involved in defense responses) is induced in *rpn12a*-2 in T and P+T plants.

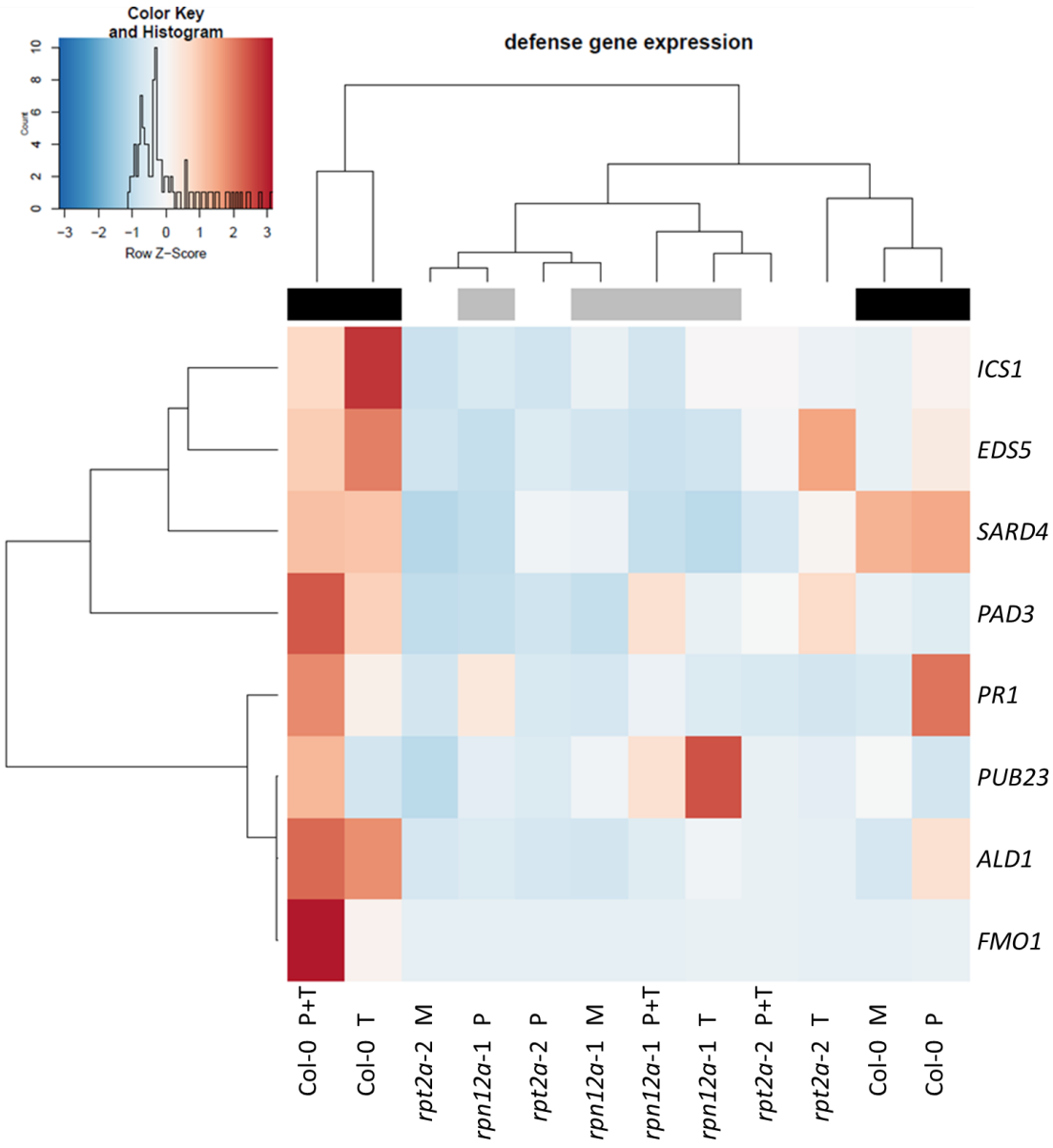

Figure 8: Heatmap of defense gene expression after priming and triggering reveals differences in defense gene expression between Col-0 and proteasome mutants *rpt2a*-2 and *rpn12a*-1. A heatmap was created from the mean values of gene expression data (ΔCq) from Col-0, *rpt2a*-2 and *rpn12a*-1 during mock treatment, primed and/or triggered conditions. High (red) or low (blue) defense gene expression within one gene (scaling =row) and clustering of similar expression patterns across the samples (dendogram on the left) are illustrated. The dendogram (top) indicates clustering of samples across the analyzed genes. The colored bars indicate the respective genotypes, i.e., black for Col-0, grey for *rpt2a*-2, and white for *rnp12a*-1. M = mock; T = triggered; P = primed; P+T = primed and triggered. N=4

To visualize the changes in transcript levels during priming and/or triggering in the proteasome mutants compared to Col-0, a heatmap was created from the mean values of

gene expression data (ΔCq) from defense genes tested above (Figure 8). The plot visualizes that the expression of the two Pip/NHP biosynthesis genes *FMO1* and *ALD1* cluster closely with the E3 ligase *PUB23* and are located in the same branch with *PR1*. The other SA-marker genes *ICS1, EDS5*, *SARD4*, and *PAD3* are clustered in a separate branch. Two genes involved in SA-biosynthesis, i.e., *ICS1* and *EDS5*, appear tightly co-regulated. Interestingly, the heatmap reveals a quite distinct clustering of T and P+T plants in Col-0. Gene expression of M and P wild type plants is considerably separated from the proteasome mutants. Almost all samples taken from the proteasome mutants are clustered in a separate branch. Therein, M and P plants are combined. Gene expression of P and P+T plants is distinctly separated. Interestingly, triggering of *rpt2a*-2 leads to transcriptional shift of the tested genes which is comparable to M and P conditions in Col-0.

Overall, the molecular data indicate a weak responsiveness of essential defense genes in *rpt2a*-2 and *rnp12a*-1 during priming and/or triggering. Thus, the obtained molecular data support previous findings of enhanced bacterial replication in the proteasome mutants in primed tissue.

3.1.3. Proteasome mutants accumulate less SA but wild type like levels of Cam

Bacterial growth assays supported by molecular analyses showed a central role of a functional proteasome during establishment of systemic defense responses. In order to assess if the proteasome mutants are generally defective in defense responses or if these defects are restricted to specific pathways of immunity, the accumulation of defense related metabolites salicylic acid (SA) and camalexin (Cam) were quantified in primed (P) and/or triggered tissue (T and P+T).

SA is a central metabolite essentially involved in systemic defense responses with free SA acting as active metabolite. Conjugated, i.e., glycosylated SA (SAgluc) is the stored and inactive metabolite (Dean *et al.*, 2003). Free SA accumulates in local tissue of Col-0 after infection with *Psm* (Figure 9A). Strikingly, SA contents are strongly decreased in local tissue of both proteasome mutants. A similar pattern was measured for SAgluc (Figure 9B). SA content in systemic tissue is equal in Col-0 T and P+T plants. Measurements revealed a decreased but statistically insignificant difference in SA levels in *rpt2a*-2. *rpn12a*-1 accumulates significantly less free SA. Interestingly, Col-0 and *rpt2a*-2 contain similar contents of SAgluc in T and P+T plants. The previous priming stimulus leads to further increase of SAgluc levels in both lines. However, *rpn12a*-1 is not capable to enrich SAgluc in T or P+T plants.

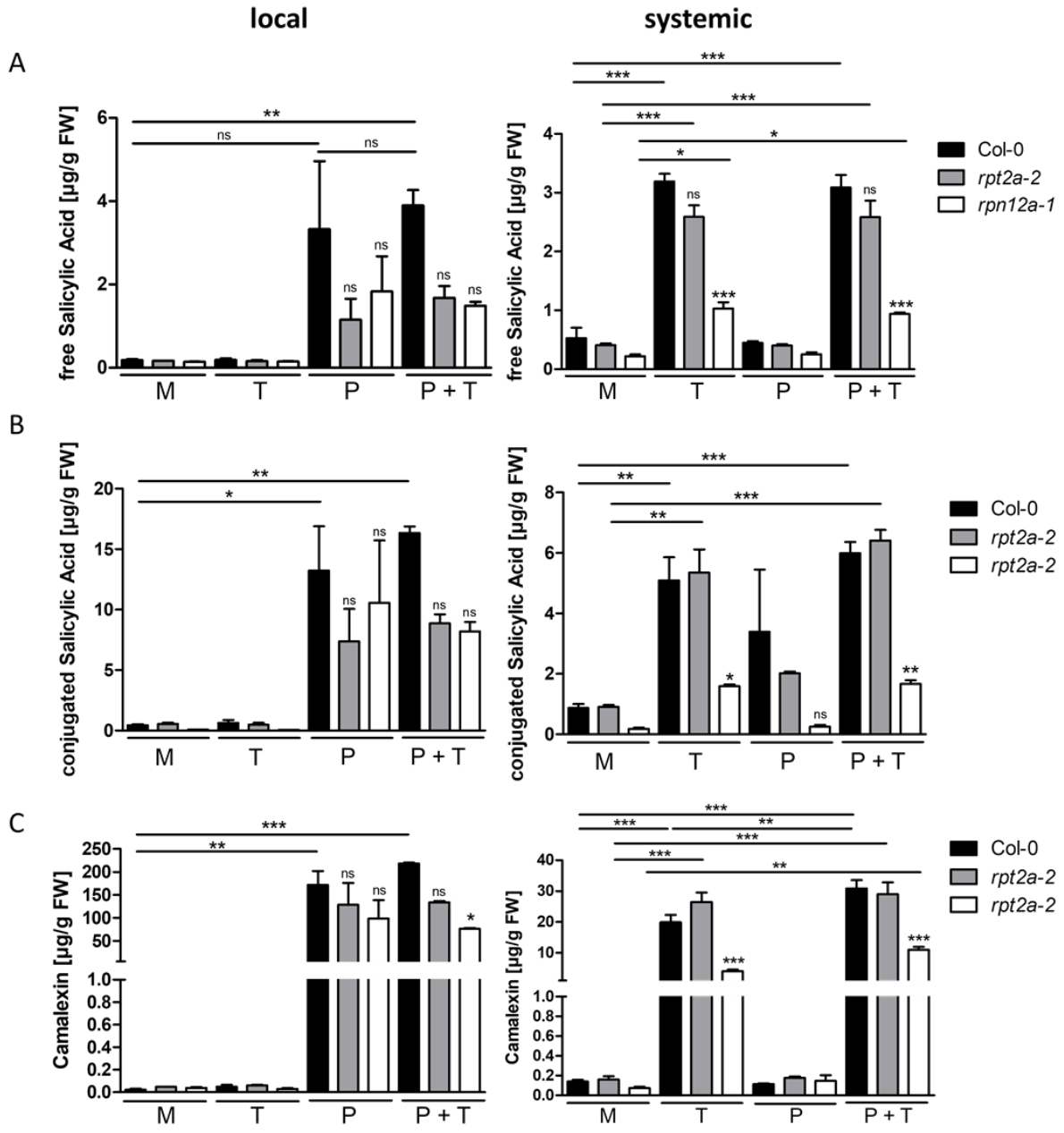

Figure 9: Proteasome mutants accumulate less SA during infections while camalexin biosynthesis is mildly affected. Col-0, *rpt2a*-2 and *rpn12a*-1 were locally (1°) mock treated with 10 mM $MgCl_2$ or primed with *Psm* (OD_{600} = 0.005). Challenging *Psm*-infections (OD_{600} = 0.005) or mock treament with 10 mM $MgCl_2$ in systemic tissue (2°) were performed 48 h after priming. Accumulation of (A) free SA, (B) conjugated SA, and (C) Cam in local and systemic tissue was determined at 24 hpi. Data represent mean ± SEM of four replicates each consisting of two leaves from at least six plants. Asterisks indicate statistically significant differences between genotypes when compared to Col-0. Included bars display statistically significant differences within one genotype across the treatments (***P < 0.001; **P <0.01; *P < 0.05, ns = not significant, 1way ANOVA with Bonferroni's post-test). M = mock; T = triggered; P = primed; P+T = primed and triggered. Repetition of the experiment showed similar results. N=4

Camalexin (Cam) is a phytoalexin with antimicrobial properties synthesized in *A. thaliana* and other *Brassicaceae*. The *de novo* synthesis of Cam increase during infections with pathogens such as *P. syringae* and mainly depends on two cryptochrome p450 enzymes, CYP71A13 and CYP71B15 (also known as PAD3) (Nafisi *et al.*, 2007; Schuhegger *et al.*, 2006). Cam strongly accumulates in local tissue of Col-0 plants infected with *Psm* (Figure 9C). Despite decreased *PAD3* expression, Cam levels of the mutants are insignificantly lower. Comparable Cam concentrations were determined in primed and triggered plants in local tissue of *rpt2a*-2 and *rnp12a*-1. Due to a higher content of Cam in P+T Col-0, the difference to *rpn12a*-1 is statistically significant in local tissue. Cam levels are generally lower in systemic tissue and are increased in P+T WT-plants when compared to triggered plants. Interestingly, *rpt2a*-2 contains more Cam in triggered tissue when compared to WT but equal levels in P+T tissue. However, *rpn12a*-1 contains significantly less Cam in T and P+T tissue. The measurement indicates a slightly decreased capacity of the mutants to synthesize Cam in response to bacterial infections. This defect is more pronounced in *rpn12a*-1.

These data indicate that the proteasome mutants are strongly impaired in SA synthesis during defense against *Psm*. However, the camalexin levels are comparable to wild type in *rpt2a*-2.

3.1.4. Treatment with salicylic acid partially restores SAR-phenotype

Previous investigations revealed decreased levels of free SA in both mutants with the lowest level observed in *rpn12a*-1. By contrast, both proteasome mutants are less impaired in the mainly SA-independent camalexin biosynthesis. The following experiments were performed to gain deeper insights into the role of SA-dependent signaling in *rpt2a*-2 and *rpn12a*-1 during priming.

The impaired defense signaling in *rpt2a*-2 and *rpn12a*-1 may arise from insufficient SA-biosynthesis or downstream signaling. To test if the mutants can perceive SA as signal and initiate downstream signaling, SA was exogenously applied. Gene expression of central and established SAR marker genes *ALD1*, *FMO1*, *ICS1*, and *PR1* was subsequently monitored 10 h after application (Figure 10). *ALD1* and *FMO1* expression slightly increased in Col-0 upon SA-treatment. *ICS1* transcript levels did not change in comparison to mock treated plants. In contrast, the proteasome mutants only show a weak increase in transcript levels. The SA-responsive marker gene *PR1* is 52-fold induced in Col-0 after application of SA. Intriguingly, also both proteasome mutants strongly respond to SA-infiltration. Direct application of SA might be able to restore the observed SAR-phenotype. Thus, the proteasome mutants are able to perceive SA as signal when it is present. Hence, reduced capacity for SA-biosynthesis could be causal for the observed SAR-phenotype in both mutants.

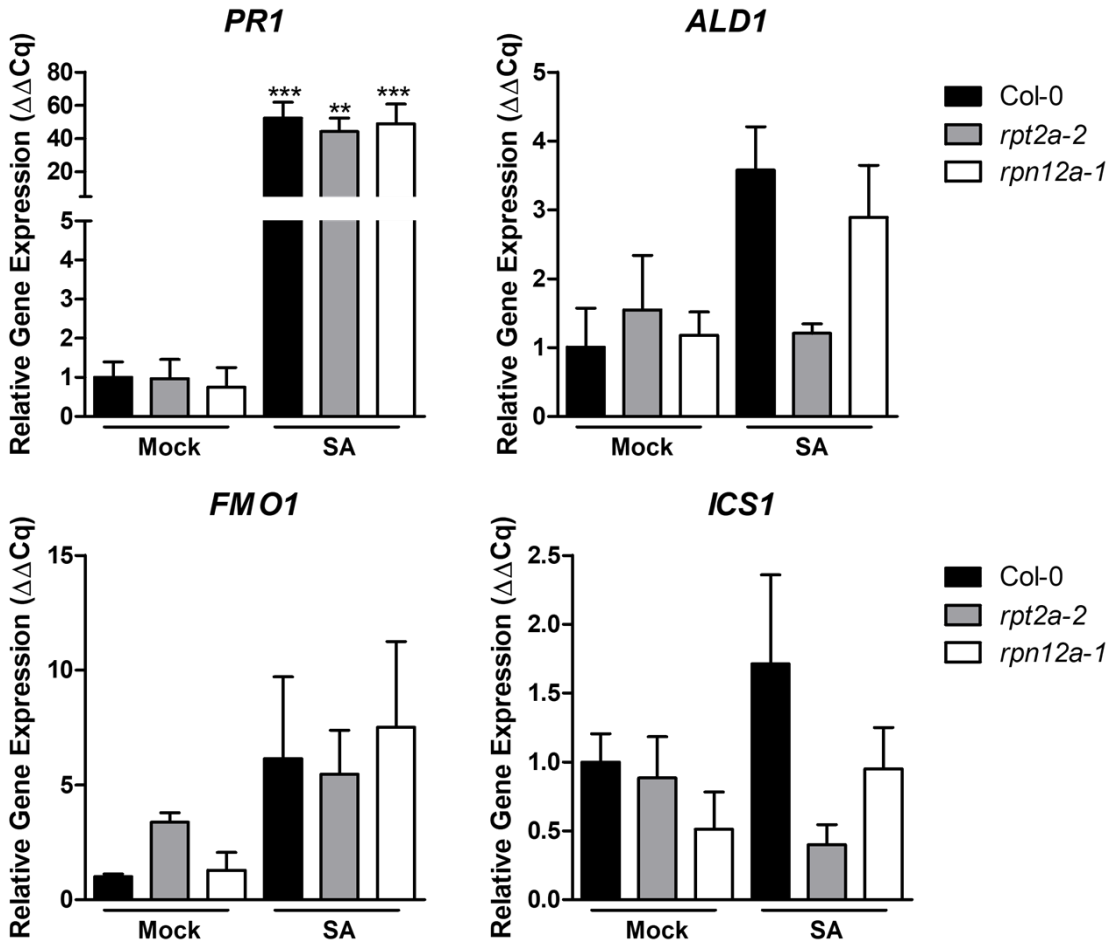

Figure 10: *PR1* is induced in proteasome mutants after exogenous application of SA. Three lower leaves (1°) of Col-0, *rpt2a*-2, and *rpn12a*-1 were infiltrated with 10 mM $MgCl_2$ as control or SA (200µM). Samples were taken from infiltrated leaves after 10 h. Relative Gene Expression (ΔΔCq) displays fold-induction in relation to mock-treated Col-0. Asterisks indicate statistically significant differences of SA-treated samples within one genotype when compared to mock samples (***P < 0.001; 1way ANOVA with Bonferroni's post-test). SA = salicylic acid. Data represent mean ± SEM. Repetition of the experiment showed similar results. N=4

To investigate if a local *PR*-gene activation by application of SA is sufficient to mount a systemic immune response in the proteasome mutants, defense gene expression was screened 10 h after triggering in SA-primed plants (Figure 11A). As expected, systemic *PR1* expression is activated in SA-primed wild type and further elevated in challenge infected tissue. Triggered plants induce *FMO1* expression in systemic tissue with elevated gene expression in SA-primed wild type plants. Interestingly, *PR1* and *FMO1* are not significantly induced in *rpt2a*-2 and *rpn12a*-1. This is reminiscent to the earlier observation of impaired defense gene induction in *Psm*-primed and/or triggered proteasome mutants (Figure 7 and Figure 8). Hence, exogenous application of SA does not induce systemic defense responses on molecular level.

It was furthermore tested, if *rpt2a*-2 is rescued for systemic resistance after local application of SA (Figure 11B).

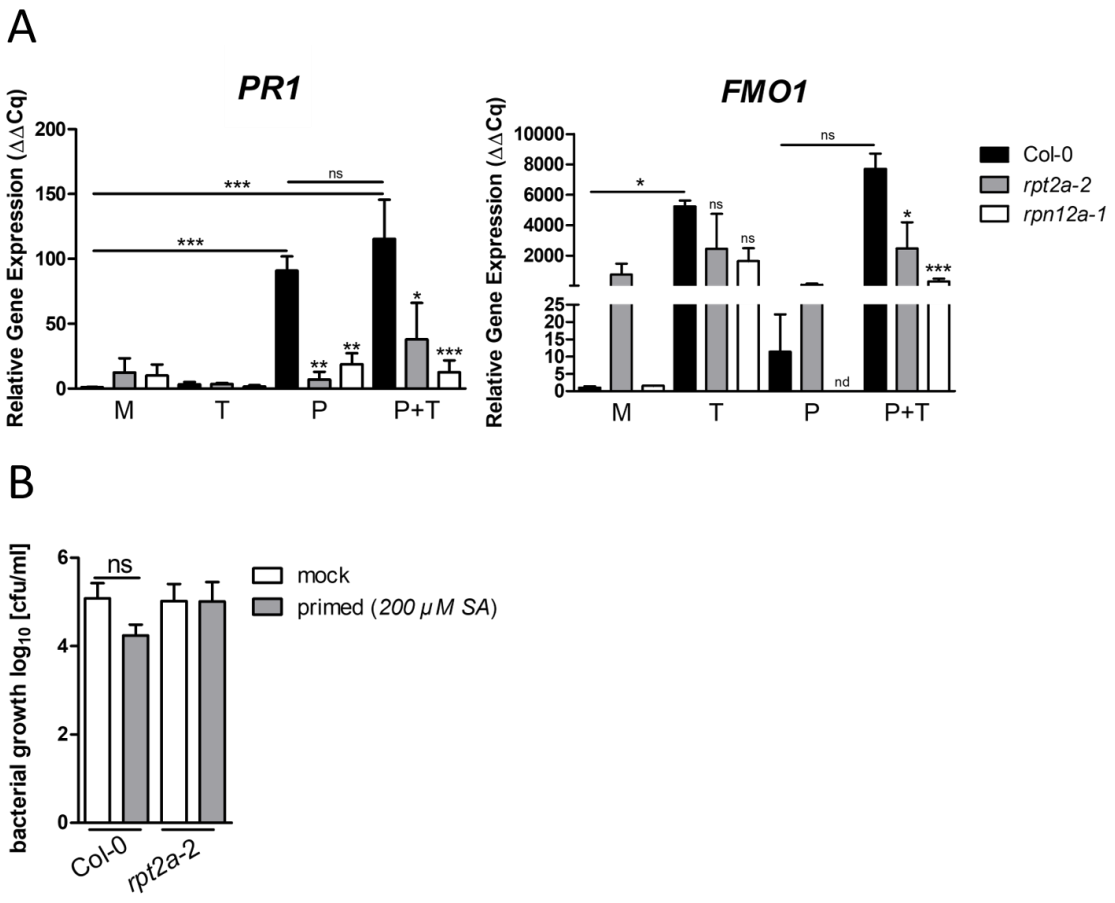

Figure 11: Application of SA does not induce priming responses in the proteasome mutants. (A) Bacterial growth in 6-week-old Col0 and *rpt2a*-2 plants with or without prior priming stimulus. Three lower leaves (1°) of Col-0 and *rpt2a*-2 were infiltrated with 10 mM $MgCl_2$ as control or 200 µM SA in 10 mM $MgCl_2$. Two days later, upper leaves (2°) were triggered with *Pst* ($1x10^4$ CFU/ml). Bacterial replication in 2° was assayed 3 dpi. (ns, not significant, two-tailed *t* test). Data represent mean ± SEM. N=10. (B) Three lower leaves (1°) of Col-0 and *rpt2a*-2 were infiltrated with 10 mM $MgCl_2$ as control or 200 µM SA in 10 mM $MgCl_2$. Two days later, upper leaves (2°) were triggered with *Psm* (OD_{600} = 0,005) or control infiltrated with 10 mM $MgCl_2$. Samples were taken from systemic tissue 10 h after triggering. Relative Gene Expression (ΔΔCq) displays fold-induction in relation to mock-treated Col-0. Asterisks indicate statistically significant differences between genotypes within the same treatment. Included bars display statistically significant differences within one genotype across the treatments (***P < 0.001; **P <0.01; *P < 0.05, ns = not significant, nd = not detectable, 1way ANOVA with Bonferroni's post-test). M = mock; T = triggered; P = primed; P+T = primed and triggered. Data represent mean ± SEM. Repetition of the experiment showed similar results. N=4

Priming with SA activates systemic defense responses in wild type. The replication of *Pst* is strongly decreased when compared to mock treated plants. However, this difference is not

significant. Mock treated and SA-primed *rpt2a*-2 show similar susceptibility towards *Pst*. The bacterial replication is comparable to unprimed wild type plants. Thus, priming with SA and therefore activation of *PR*-genes is not sufficient for *rpt2a*-2 to overcome limitations in the SAR phenotype. This additionally supports the molecular data indicating that SA-application alone is not sufficient to rescue the SAR-phenotype of the proteasome mutants.

3.1.5. RNA-sequencing to analyze global changes in transcriptome during priming

Previous experiments indicate that proteasome mutants are impaired in initiation of local and systemic defense responses leading to increased susceptibility towards infection with *Psm*, decreased defense gene expression and dampened biosynthesis of the phytohormone salicylic acid. However, the underlying molecular mechanism remain elusive. Therefore, a RNAseq approach was followed to gain a global view on transcript changes in both, wild type and the proteasome mutant *rpt2a*-2 during priming. Plants were locally primed with *Psm* or mock infiltrated. After 48 h, leaves were sampled in triplicates from local (mock, M and infected, +*Psm*) and systemic (mock, M and primed, P) tissue. Extracted total RNA was subsequently assessed for quantity and quality using the Agilent 4150 TapeStation System. All tested samples were evaluated with RNA integrity number (RIN) ≥9 and are therefore of high quality. LGC Genomics (Berlin) prepared the cDNA library and performed the sequencing. The raw reads were then mapped to the *Arabidopsis* genome and subsequently counted. It was required to confirm a coherent sample set with high quality prior to analysis of differentially expressed genes.

A principal component analysis (PCA) was performed to evaluate the relation between the samples (Figure 12A). Principal component (PC) 1 comprises 89% of variance in the dataset. PC2 explains another 3 % of variation. Within the specific groups the biological replicates cluster along PC2. Local *Psm*–intiltrated tissue from Col-0 and *rpt2a*-2 are separated from the other samples indicating that PC1 depicts probably the heavy transcriptional changes in infected tissue after 48 h. The variance of PC2 may composite of treatment (mock or *Psm*), sampling site (local or systemic tissue), or genotype (Col-0 or *rpt2a*-2). Taken together, the PCA of the whole dataset shows a strong and coherent response to the applied stimuli. In contrast, the within-group variability is very low.

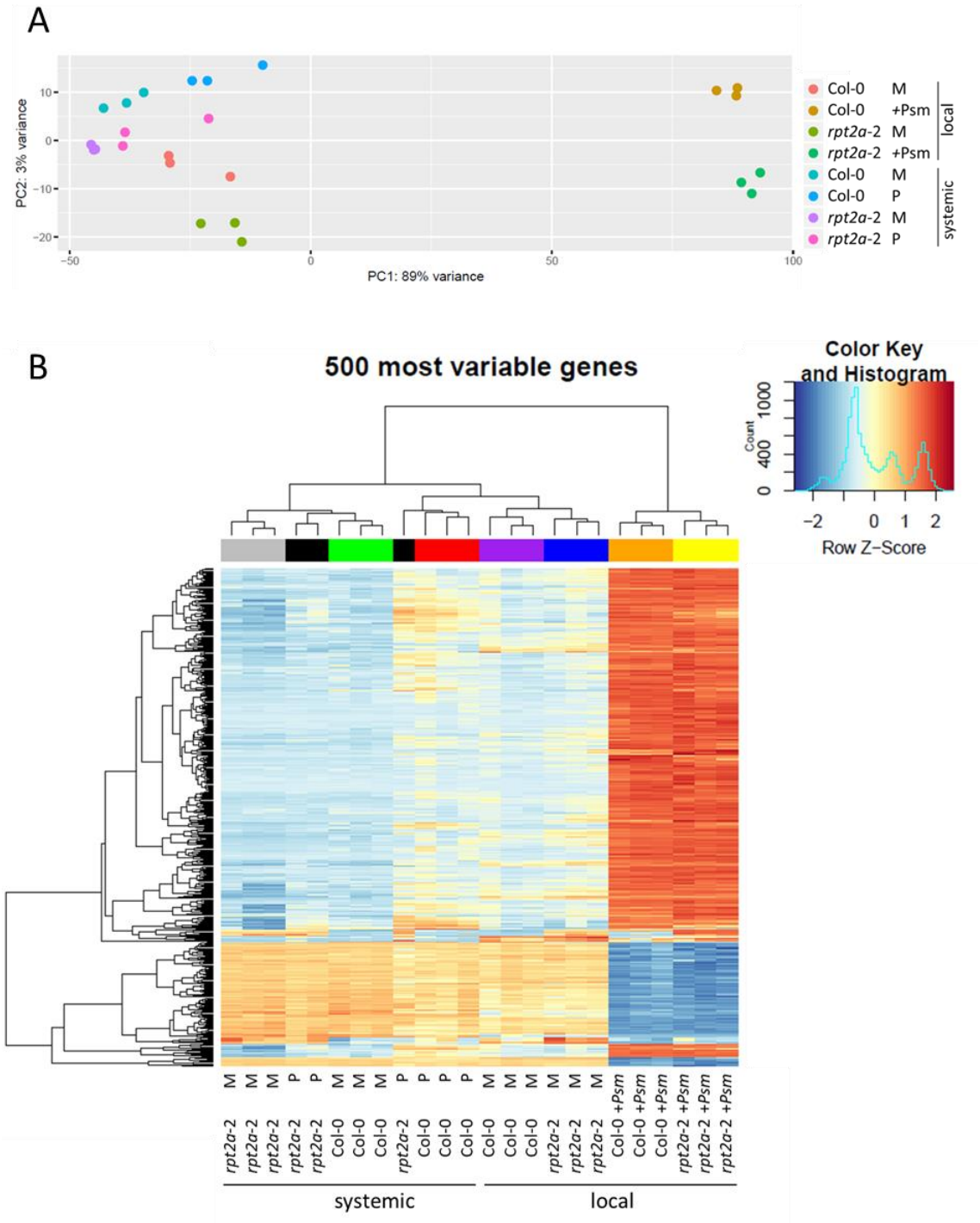

Figure 12: Quality control of RNAseq data indicates a coherent RNAseq data set. A RNAseq experiment was performed to analyze global changes in the transcriptome of Col-0 and *rpt2a*-2. Three lower leaves (1°) of Col-0 and *rpt2a*-2 were infiltrated with 10 mM $MgCl_2$ as control or *Psm* (OD_{600} = 0.005) for priming. 48h later, local (1°) and systemic leaves (2°) were sampled. (A) A PCA was performed to study inter-sample consistency and (B) the 500 most viarble genes were hierachically clustered in a heatmap. Both analyses rely on the *rlogTransformed* data from the DESeqDataSet (*dds*) object. M = Mock, *+Psm* = *Psm* infiltrated, P = primed with *Psm*.

In the next step, the 500 most variable genes of all samples were illustrated in a heat map with hierarchical clustering (Figure 12B). This allows for visualization of genes with relatively higher or lower transcript levels across all 24 samples. Among these highly variable genes, most transcripts are strongly increased in local infected tissue from Col-0 and *rpt2a*-2.

Interestingly, local mock treated samples from wild type and *rpt2a*-2 cluster in proximity with systemic samples from primed Col-0. Systemic mock treated plants from both lines cluster in a separate branch with two of three systemic samples from primed *rpt2a*-2. The third sample clusters with primed tissue from wild type. The hierarchical clustering underlines previous observations that the direct infection of tissue elicits a massive transcriptional change. The influence of a priming stimulus is weaker, but leads to distinct transcriptional changes. It further indicates that overall, the proteasome mutant is able to induce gene expression during defense responses as well but is well distinguishable from Col-0. Next analyses therefore target to identify genes required for priming and triggering which are not induced in *rpt2a*-2. Furthermore, quantification of transcript levels is important to potentially analyze genes which are induced during defense but to a lower extend when compared to wild-type.

Calculation of Cook's distances within samples was then applied to identify potential outliers from the sample dataset to verify the coherency of the dataset (Figure 13). These potential outliers may derive from experimental artefacts or read mapping problems in genetically differing samples. The observed cook's distances are similar for all 24 samples which does not point towards outliers. Therefore, the detected within-group variability in the PCA and observed differences between the sample groups in further analyses can be considered as biological effects. Thus, all subsequent steps were performed taking all samples into account.

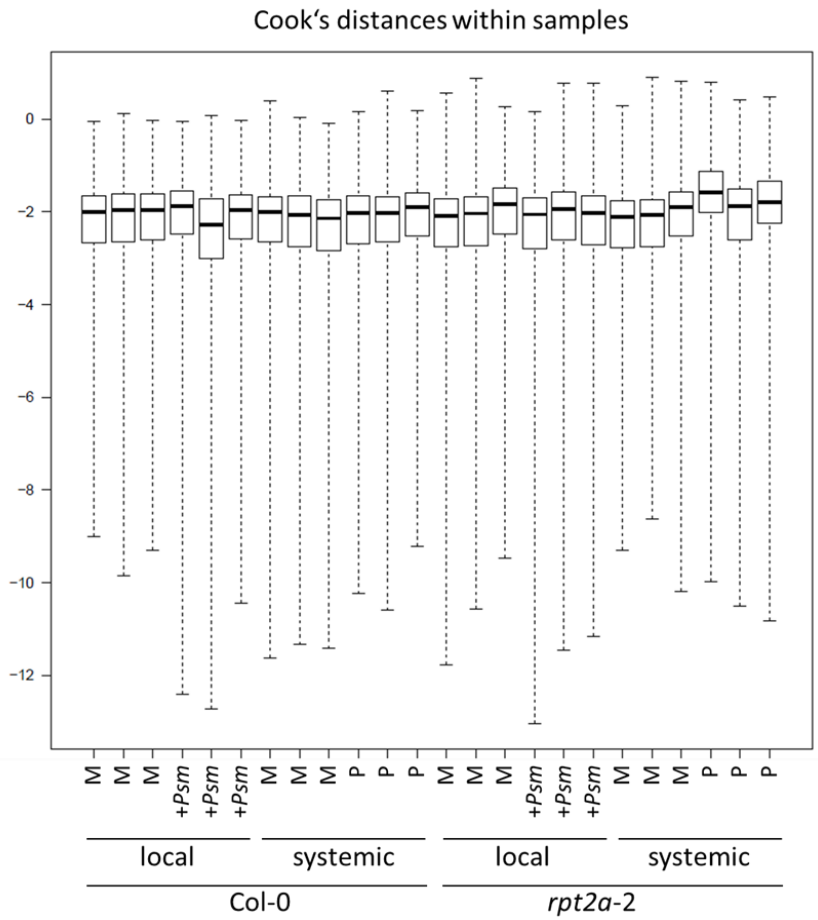

Figure 13: The RNAseq data set does not contain outliers deriving from experimental artefacts. Three lower leaves (1°) of Col-0 and *rpt2a*-2 were infiltrated with 10 mM $MgCl_2$ as control or *Psm* (OD_{600} = 0.005) for priming. 48h later, local (1°) and systemic leaves (2°) were sampled. Calculation of cook's distances was applied to the DESeqDataSet (*dds*) containg un-normalized counts and illustrated in a boxplot to identfy potential experimental artefacts or read mapping problems.

3.1.5.1. Differentially expressed genes in Col-0 during priming

The RNAseq data set was initially statistically analyzed to identify global changes in the transcriptome during priming in wild type plants. The comparison of locally infected tissue from Col-0 compared to mock treated leaves (local P Col-0 over local M Col-0) using the *contrast* argument in DESeq2 gives insights into transcriptional regulation 48h after infections. In total, 27416 protein coding genes are annotated in TAIR10 of which 8844 genes were found in this data set to be differentially expressed (Table 17). Among these, 4033 are higher expressed and 4811 are down regulated in infected tissue than in the control plants. This indicates a massive transcriptional reprogramming during infections with virulent bacteria.

Table 17: Differentially Expressed Genes in wild type Col-0 during infections and priming. The contrast argument indicates the compared condition. All data were analyzed with the same statistical cutoff (padj <0,1; BaseMean > 10, up-regulated: log2FC > 1; down-regulated: log2FC < -1; total DEG: up- and down-regulated genes). FC = fold change; M = mock; P = primed; DEG = differentially expressed genes.

contrast	Up-regulated (log2FC > 1)	Down-regulated (log2FC < -1)	Total DEGs
local P over local M	4033	4811	8844
systemic P over systemic M	749	268	1017

Data were similarly processed to dissect genes relevant for priming responses. To do so, systemic samples from primed plant were compared to leaves at comparable developmental stage from unprimed plants (systemic P over systemic M). Overall, 1017 genes are differentially expressed with 268 repressed genes (log2FC < -1). 749 genes are higher expressed in primed tissue (log2FC >1). Typical SAR-related genes like *FMO1*, *ALD1*, and *PR1* were found to be highly induced in these samples (appendix, Table 25).

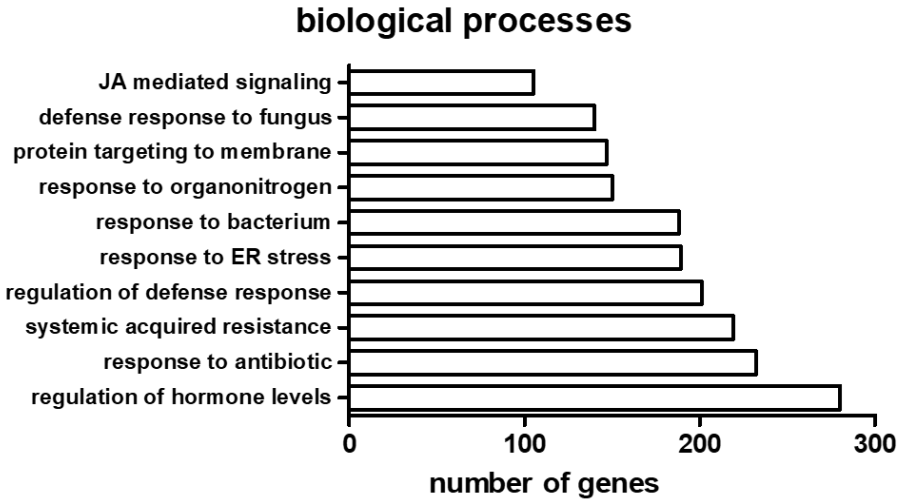

Figure 14: GOterm analysis of biological processes during priming in systemic tissue reveal appearance of defense related processes in Col-0. Results of GO enrichment analysis for 'Biological Process' using 'topGO' indicating the number of differentially expressed genes annotated with the corresponding GO term. GO, Gene Ontology.

The genes upregulated in systemic tissue during priming were further grouped by *topGO* analysis to gain an overview on the affected processes. The *topGO* analysis was focused on

the biological processes (BP) in the GOterm analysis illustrating the top 10 BPs here (Figure 14). Among these BPs most genes are related to regulation of hormone levels. SAR, regulation of defense responses, response to bacteria, defense response to fungi and JA-mediated signaling directly link the observed events to ongoing defense responses. Taken together, data analysis reveals that a massive transcriptional reprogramming occurs during infection and appearance of known SAR-marker genes confirms the reliability of the dataset.

3.1.5.2. Differentially expressed genes in *rpt2a-2* during priming

Further statistical analyzes of the RNAseq data were performed to gain deeper insights in gene transcription during local infections and systemic priming in *rpt2a*-2. Severe changes in the transcriptome of *rpt2a*-2 occur mainly in local tissue after infection (Table 18). 9052 of 271416 protein coding genes are differentially expressed during local infections. Among these, about 1/3 is downregulated with a log2FC < -1 and 3983 genes are upregulated with a log2FC > 1.

Table 18: Differentially Expressed Genes in *rpt2a*-2 during infection and priming. The contrast argument indicates the compared condition. All data were analyzed with the same statistical cutoff (padj <0,1; BaseMean > 10, up-regulated: log2FC > 1; down-regulated: log2FC < -1; total DEG: up- and down-regulated genes). FC = fold change; M = mock; P = primed; DEG = differentially expressed genes.

contrast	**Up-regulated (log2FC > 1)**	**Down-regulated (log2FC < -1)**	**Total DEGs**
local P over local M	3983	5069	9052
systemic P over systemic M	948	132	1080

In systemic tissue during priming, less transcriptional reprogramming was observed in *rpt2a*-2. 1080 genes are differentially expressed of which only 132 are down regulated. However, the vast majority (i.e., 948 genes) are up regulated in primed tissue (appendix, Table 26). These genes are - among others- involved in BPs assigned to SAR, SA biosynthetic processes and regulation of defense responses (Figure 15).

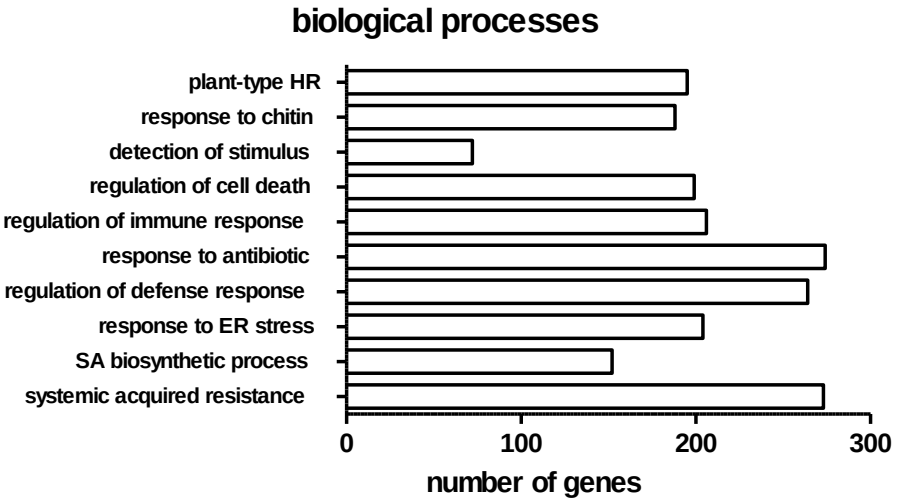

Figure 15: GOterm analysis of biological processes during priming in systemic tissue reveal appearance of defense related processes in *rpt2a*-2. Results of GO enrichment analysis for 'Biological Process' using 'topGO' indicating the number of differentially expressed genes annotated with the corresponding GO term. GO, Gene Ontology.

For both, local infected and systemic primed *rpt2a*-2 tissue, the numbers are comparable to the analyzed DEGs in Col-0. This hints to an overall ability of *rpt2a*-2 to induce transcriptional reprogramming during stress without giving information on the transcribed genes. Furthermore, the number of up regulated genes in systemic tissue of primed plants is larger than the repressed genes indicating that priming of distal tissue requires *de novo* gene expression.

3.1.5.3. The transcriptome differs between Col-0 and *rpt2a*-2 during priming

The phenotype of the proteasome mutant *rpt2a*-2 is distinct from Col-0 including plant appearance and stress resistance. The RNAseq dataset was used to analyze differences of the transcriptome between Col-0 and *rpt2a*-2 in untreated plants (Table 19). Interestingly, 428 genes were significantly differentially expressed between naïve Col-0 and *rpt2a*-2 plants. Many of these genes affect biological processes involved in proteasomal protein catabolic process, ubiquitin-dependent protein catabolic process, and catabolic process. These data strongly indicate that the mutation of the proteasome subunit alone already causes changes in the expression of genes related to basal cellular functions and suggest a compensatory effect in the proteasome mutant by upregulating proteasomal and catabolic processes.

Table 19: Differentially Expressed Genes comparing untreated Col-0 and *rpt2a*-2. All data were analysed with the same statistical cutoff (padj <0,1; BaseMean >10, up-regulated: log2FC >1; down-regulated: log2FC <-1; total DEG: up- and down-regulated genes). FC = fold change; M = mock; DEG = differentially expressed genes.

contrast	**Up-regulated (log2FC >1)**	**Down-regulated (log2FC <-1)**	**Total DEGs**
Local M Col-0 over Local M *rpt2a*-2	276	152	428

To take these general differences between Col-0 and *rpt2a*-2 into account, systemic primed tissue of Col-0 and *rpt2a*-2 were not analyzed using the *contrast* argument to identify sectors of impaired immune responses in *rpt2a*-2. Instead, the analyzed data from DEG in primed systemic tissue of Col-0 were compared to primed systemic *rpt2a*-2 in a Venn diagram.

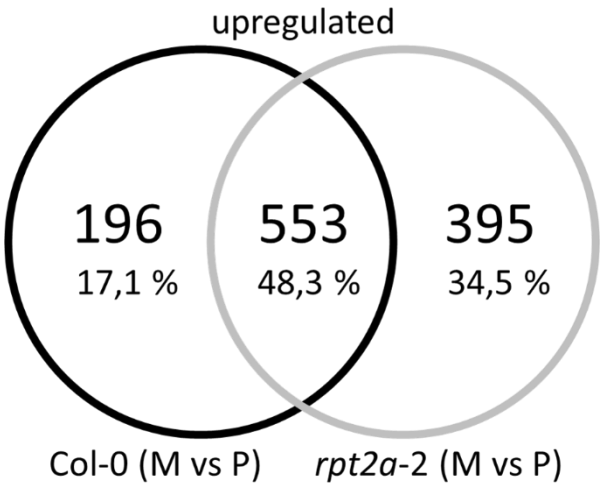

Figure 16: Venn diagram illustrates a high overlap of differentially expressed genes and reveals differences in transcriptional changes between Col-0 and *rpt2a*-2. The Venn diagram depicts numbers of differentially expressed genes (padj <0,1; log2FC >1, base mean >10) between primed tissue in Col-0 (left, black circle) and *rpt2a*-2 (right, grey circle) and indicates overlap of genes.

A Venn diagram was generated to identify larger proportions of affected defense processes. Here, up-regulation of genes was assumed as a prerequisite for an induced priming response. Therefore, up-regulated genes during priming in systemic tissue from Col-0 and *rpt2a*-2 were compared. The Venn diagram signifies an overlap of almost 48,3 % in these DEGs up-regulated in both lines. However, the diagram does not give information about the amplitude of gene induction. Genes with lower transcript levels in *rpt2a*-2 than Col-0 but statistical significance are also included in this proportion. 395 genes (34,5 %) have an

increased transcript level in the proteasome mutant which are not induced in the wild type plant. Of these 395 genes, only 11 can be found to be up-regulated in untreated *rpt2a*-2 when compared to Col-0 (Table 19) indicating the ability of flexible gene activation in the proteasome mutants in response to fluctuating conditions. Most interestingly, 196 are only differentially expressed in Col-0 during priming making 17 % of the transcriptional changes.

This observation is highly interesting regarding the conditional assumption that induced expression of genes is related to the specific priming response. Thus, the 196 genes not responding in the proteasome mutant screened to identify interesting candidates which might explain the observed SAR-phenotype. These genes were in in the next step further studied in context with genes that are differentially expressed in *rpt2a*-2 but with a lower amplitude than in wild type. With this approach a set of co-regulated genes with low expression in *rpt2a-2*, i.e., *FMO1*, *PAD3*, and *CYP71A13*. These genes are commonly regulated by the TF WRKY40 which was described as negative regulator of defense (Brotman *et al.*, 2013).

3.1.6. Altered degradation of WRKY40 has an additive effect on the SAR-phenotype of *rpt2a*-2

Transcription of genes negatively regulated by transcription factors require degradation of these TFs for activation. *FMO1*, *PAD3*, and *CYP71A13* are genes jointly regulated by the negatively regulating TF WRKY40 during Trichoderma colonization in *Arabidopsis* (Brotman *et al.*, 2013). Expression of these genes was found to be repressed in *rpt2a*-2 during priming compared to Col-0. Furthermore, WRKY40 was shown to be degraded via the 26S proteasome (Raffeiner, unpublished). Taking these aspects into account one can postulate that impaired turnover of WRKY40 might lead to suppression of target genes such as *FMO1*, *PAD3*, and *CYP71A13* in proteasome mutants during infections (Figure 17). WRKY40 represses the expression of defense genes in uninfected and unprimed tissue (Figure 17A). During priming, WRKY40 might be ubiquitinated by so far unknown E3 ligases and subsequently degraded by the 26S proteasome to induce defense gene expression (Figure 17B). However, degradation of WRKY40 is potentially impaired in the proteasome mutant which could lead to an accumulation or reduced release of WRKY40 from the promotor regions of target genes like *FMO1*, *PAD3*, and *CYP71A13*. Subsequently, these genes may be weakly expressed or fully repressed as a consequence of insufficient turnover of the TF (Figure 17C).

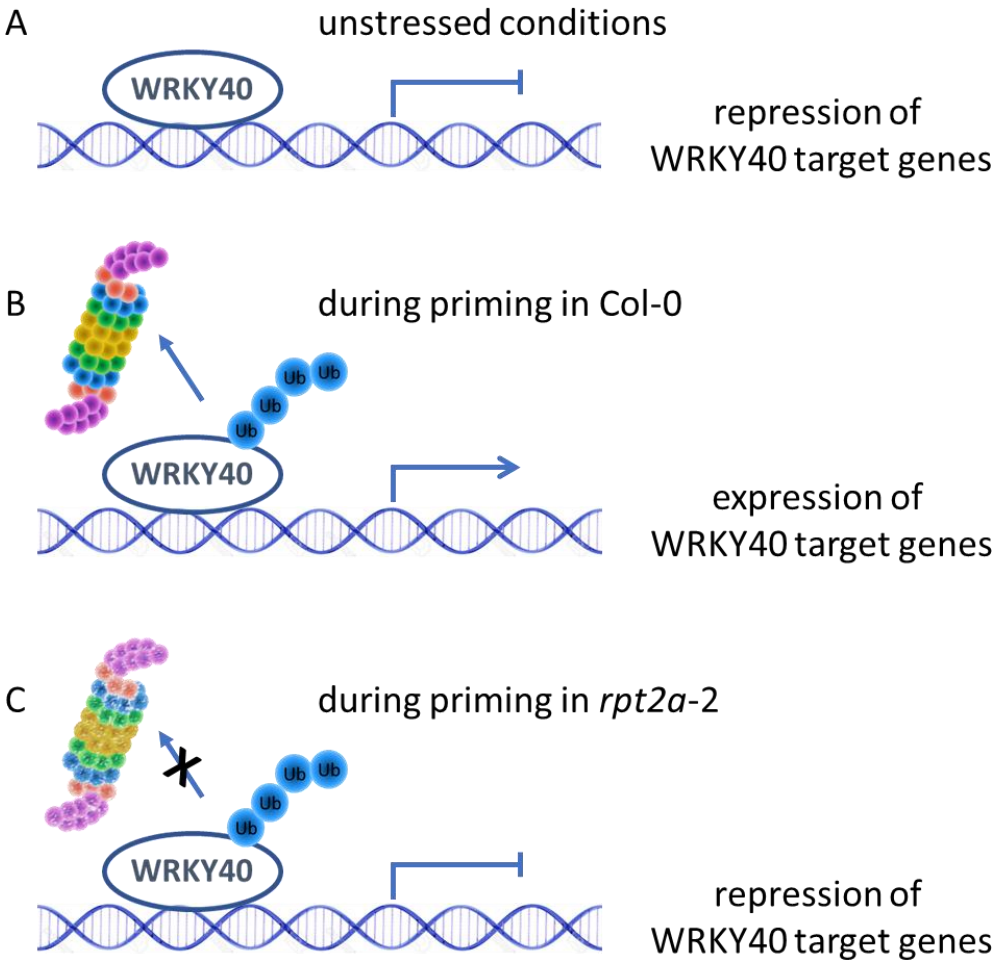

Figure 17: A hypothesis was formulated to illustrate the possible role of WRKY40 during priming. (A) In unstressed conditions, the negative regulator WRKY40 binds to promotors of target defense genes and inhibits gene expression. (B) During priming in Col-0, WRKY40 might be ubiquitinated and subsequently degraded via the 26S proteasome to activate gene expression. (C) During priming in *rpt2a*-2, WRKY40 might still be ubiquitinated for proteasomal degradation but cannot be released or degraded due to insufficient protein turnover leading to dampened gene expression.

To test if the gene repression observed in the RNAseq experiment arises from impaired turnover of TFs, a line carrying the double mutation of *rpt2a*-2 x *wrky40* was generated by crossing of *rpt2a*-2 and *wrky40*-1. The presence of the tDNA insertion in *rpt2a*-2 x *wrky40* was tested by PCR using genomic DNA as template from T3 plants (Figure 18A). Plants #2 and #5 from line *rpt2a*-2 x *wrky40* 1.1 were found to be homozygous lines only carrying the tDNA insertion in the *rpt2a* gene and no WT-*RPT2a* gene. Due to unsuccessful genotyping PCR using gDNA as template, knock out of *wrky40* was tested by RT-PCR after treatment with 5 mM SA for 4 h in the T4 generation (Figure 18B). Progeny #6 from line *rpt2a*-2 x *wrky40* #1.1-2 was found to be a full knock out of *wrky40*. This line was therefore used for subsequent experiments.

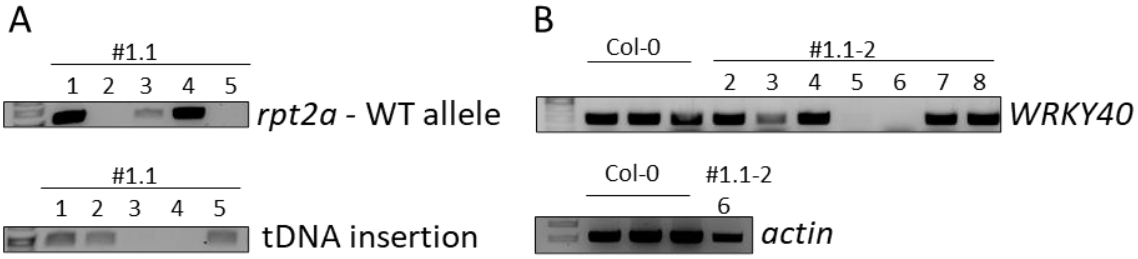

Figure 18: Genotyping of *rpt2a*-2 x *wrky40* by PRC using gDNA as template and transcript quantification via RT-qPCR. (A) Genomic DNA was extracted from *rpt2a*-2 x *wrky40* (#1.1, T3 generation) and used as template for a PCR testing the presence of *RPT2a* wildtype-gene (upper panel) and tDNA insertion (lower panel) in five individual plants each. (B) cDNA was synthesized from Col-0 and *rpt2a*-2 x *wrky40* (#1.1-2, T4 generation) samples taken 4 h after treatment with 5 mM SA and probed for *WRKY40* transcription in seven individual plants. *Actin* expression (lower panel) served as control in all three Col-0 samples as well as the #6 from *rpt2a*-2 x *wrky40* #1.1-2.

Transcription of the WRKY40 regulated genes *FMO1*, *PAD3*, and *CYP71A13* was found to be repressed in *rpt2a*-2 during defense responses. Bacterial replication was assayed in Col-0, *rpt2a*-2, *wrky40*, and *rpt2a*-2 x *wrky40* to test the hypothesis if impaired degradation of the negatively regulating TF WRKY40 is causal or partially involved in the defective defense responsiveness in the proteasome mutant (Figure 19). Interestingly, *rpt2a*-2 x *wrky40* unprimed plants are more susceptible than wild type and do not benefit from prior priming with *Psm.* Overall, these plants are more susceptible towards infection with virulent *Pseudomonas* than *rpt2a*-2 or *wrky40* single mutants alone. *Psm* primed WT plants are more resistant to *Pst* when compared to mock infiltrated plants. The single knock out of *wrky40* does not impact basal resistance of the plants. However, the priming effect is strongly decreased indicating that the overall priming capacity of *wrky40* is decreased. As observed earlier, the proteasome mutant is slightly more susceptible to *Pst* than wild type and priming with *Psm* does not induced systemic resistance. Taken together, double knock out of r*pt2a*-2 x *wrky40* does not lead to a reversal of the SAR-phenotype observed in *rpt2a*-2. Instead, the data indicate an additive effect of both mutations.

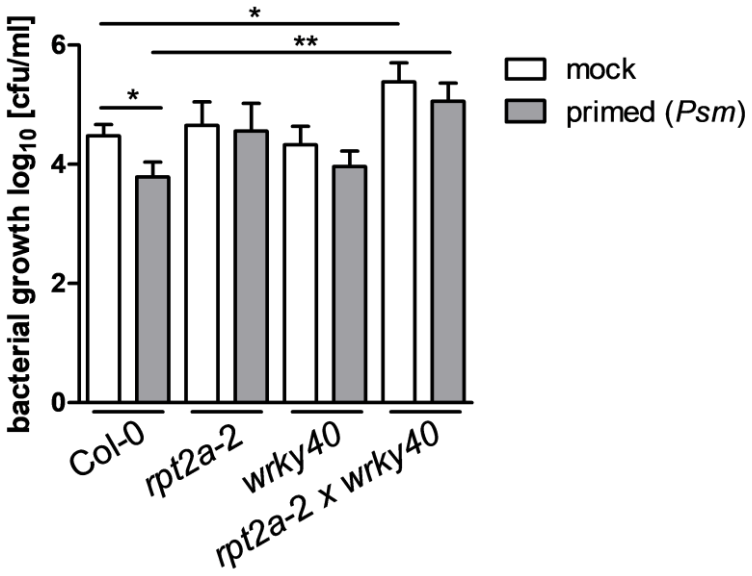

Figure 19: Bacterial replication indicates an additive effect of *rpt2a*-2 and *wrky40* on plant susceptibility against *Pseudomonas*. Three lower leaves (1°) of Col-0, *rpt2a*-2, *wrky40*, and *rpt2a*-2 x *wrky40* were infiltrated with 10 mM $MgCl_2$ as control or *Psm* (OD_{600} = 0.005) for priming. Two days later, upper leaves (2°) were triggered with *Pst* ($1x10^4$ CFU/ml). Bacterial replication in 2° was assayed 3 dpi. Asterisks indicate statistically significant differences between mock treated and *Psm*-primed samples (**P < 0.01; *P < 0.05, two-tailed *t* test). The experiment was only conducted once. N=12

3.2. Role of single E3-ubiquitin ligases during priming

Degradation of proteins is centrally involved in maintaining processes in all stages of the cell's lifecycle. Misfolded proteins or proteins exceeding their half-life may be degraded via the 26S proteasome. Also, targeted degradation of proteins allows the cell to fine-tune responses to stresses (Sadanandom *et al.*, 2012). The specificity of this process is conferred by E3-ubiquitin ligases which are able to bind specific substrates to mark them for degradation. The *Arabidopsis* genome encodes for more than 1400 E3 ligases of which many E3-ligases remain uncharacterized regarding their function in cellular processes (Vierstra, 2009). Several E3-ligases from the RING, RING_between-RING_RING and HECT E3-ligase families were already described with central regulatory roles at different levels during local immunity (Adams & Spoel, 2018; Trujillo & Shirasu, 2010).

This part of the project aimed to identify E3 ligases with potential role in onset or maintenance in proteasomal protein turnover during SAR. The data obtained from the RNAseq experiment were used to select E3 ligases that might play an important role during priming based on the transcriptional profile.

3.2.1. Selection of E3 ubiquitin ligases with potential roles during priming

Initiated systemic defense responses are considered to be effective for the plant at lowest energy costs (Hilker *et al.*, 2016). Since priming is an active process, it is very likely that the plant invests in required signaling pathways indicated by upregulation of genes. Therefore, data obtained from the RNAseq experiment were used to make an educated guess on which E3 ubiquitin ligases might be involved in priming signaling. DEGs in primed Col-0 plants were surveyed for upregulation (log2FC > 1; padj < 0,05; base mean > 10) of annotated E3 ligases (Table 20).

Table 20: 11 candidate genes of E3-ligases with potential role in priming responses based on the transcriptional upregulation during priming in systemic tissue

	Locus	Name	E3 ligase family	Log 2 FC	padj.	references
1	AT1G01680	PUB54	Plant U-box	4,1	1,65E-25	(Wiborg *et al.*, 2008)
2	AT3G60966	ATL91	RING/U-box superfamily protein	3,42	0,00024	
3	AT5G53110	ATL96	RING/U-box superfamily protein	3,19	5,33E-12	
4	AT1G05880	ARI12	RING_between_ RING domain proteins	3,18	0,03114	(Xie *et al.*, 2015)
5	AT5G10380	ATL55/ RING1	RING finger domain protein	2,85	3,73E-36	(D. H. Lee *et al.*, 2011b; S. S. Lin *et al.*, 2008)
6	AT1G08050		Zinc finger (C3HC4-type RING finger) family protein	2,10	4,69E-17	
7	AT4G28270	RMA2	RING finger domain protein	1,67	6,39E-08	(Y. Liu & Li, 2014)

8	AT1G65040	Hrd1B	RING domain	1,41	1,57E-11	(Su *et al.*, 2011a)
9	AT1G63840		RING/U-box superfamily protein	1,2	0,02253	
10	AT5G41400		RING/U-box superfamily protein	1,15	0,01472	
11	AT3G05200	ATL6	RING/U-box superfamily protein	1,09	1,33E-05	(Maekawa *et al.*, 2012)

In total, 11 E3-ubiquitin-ligases with significant increase in transcript levels were chosen for detailed research. The ligases are annotated to different classes of RING (i.e., RING, ATL and PUB) and RING_between-RING_RING (RBR) E3-ubiquitin ligases. *PUB54*, *ATL91*, *ATL96*, and *ARI12* undergo the highest transcriptional induction regarding the Log2FC (Table 20). Interestingly, RING1 is an E3-ubiquitin ligase with already described function for cell death and SA-dependent defense responses in pepper (Lee *et al.*, 2011b). ARI12 is an active E3-ubiquitin ligase which is regulated during UV-B exposure (Xie *et al.*, 2015). The RING-HECT hybrid mechanism of ARI12 is highly interesting as its function and role is not well understood yet. Furthermore, plant U-box type E3 ubiquitin ligases (PUBs) have been described in defense responses. The expression of PUB22/23/24 triplet negatively regulated PAMP-induced defense responses (Trujillo *et al.*, 2008). Additionally, PUB12/13 ubiquitinate the PRR FLS2 to attenuate immune signaling (Lu *et al.*, 2011). PUB54 is not further characterized but the highly induced transcription during priming indicates a potential involvement in immune responses.

Both, the appearance of E3 ligases described in defense responses and E3 ligases belonging to families with relevance in immunity supports the assumption that additional E3 ligases can be identified following this approach. Among others, *PUB54* and *ARI12* transcripts were also identified as DEGs during priming in publicly available datasets (Bernsdorff *et al.*, 2016). Based on these initially existing information and high transcriptional regulation, PUB54 and ARI12 were chosen as promising candidates with possible roles in priming responses. Following experiments were performed to functionally characterize these E3-ligases and to elucidate their potential role in immune responses.

3.2.2. Knock-out lines of *pub54* were identified and overexpressing lines were generated.

ARI12 and *PUB54* were chosen for further analysis to evaluate their potential role in defense responses. Initially, knock-out lines for both genes were identified.

Knock-out lines for *PUB54* were identified as described above. SALK_055772 and SALK_035556, hereafter *pub54*-I and *pub54*-II, were confirmed as homozygous knock-out lines for *PUB54* (Figure 20A). A RT-PCR showed the absence of *PUB54* transcript in *pub54*-I and *pub54*-II (Figure 20B).

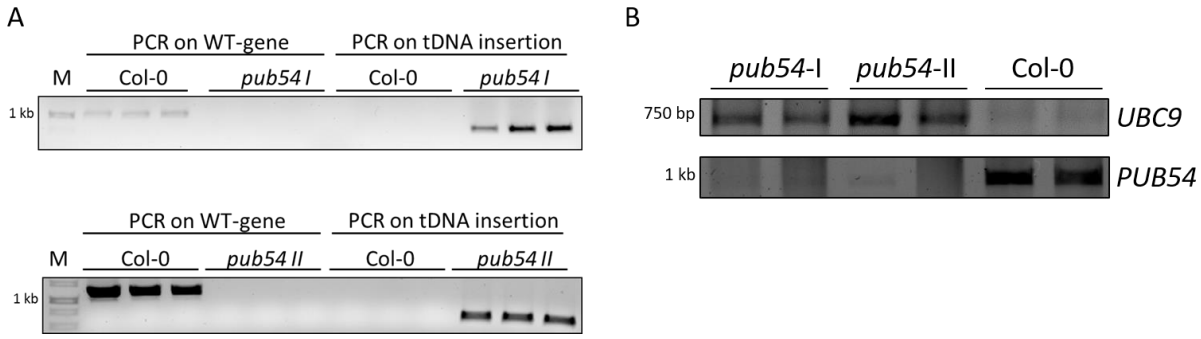

Figure 20: Genotyping of *pub54*-I and II and quantification of *PUB54* transcript levels identify full knock out lines. (A) Genotyping PCRs were performed with different primer sets to analyze the presence or absence of the *PUB54* wild-type gene and the tDNA insertion using genomic DNA from *pub54*-I (upper panel), *pub54*-II (lower panel), and Col-0 as template. (B) cDNA was synthesized from naïve Col-0, *pub54*-I and *pub54*-II and probed for *UBC9* expression (upper panel) as control and *PUB54* transcription in 2 individual plants each.

3.2.2.1. *PUB54* specifically responds to bacterial infection and is required for full priming capacity

The gene expression of *PUB54* was quantified in qRT-PCR to obtain molecular data on gene activation during infections and to verify data from the RNAdeq analysis (Figure 21). Systemic samples were taken 10 h after priming /and or triggering with *Psm*. *PUB54* gene expression is induced in primed plants verifying the data from the RNAseq-analysis. Transcription is highest in triggered plants. A priming stimulus does not lead to hyperinduction of the gene and gene expression is comparable to triggered plants. This indicates that *PUB54* might play a role at the infection site but also during priming in systemic tissue.

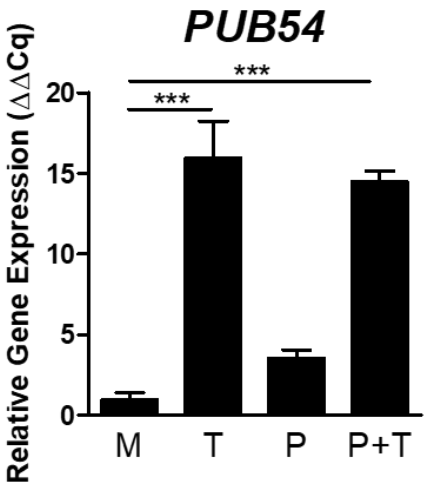

Figure 21: Transcription of *PUB54* is differentially regulated during priming and/or triggering. Three lower leaves (1°) of Col-0 were infiltrated with 10 mM $MgCl_2$ as control or *Psm* (OD_{600} = 0.005) for priming. Two days later, three upper leaves (2°) were triggered with *Psm* (OD_{600} = 0.005) or infiltrated with 10 mM $MgCl_2$. Samples were taken from systemic tissue 10 h after triggering. Relative Gene Expression (ΔΔCq) displays fold-induction in relation to mock-treated samples. Asterisks indicate statistically significant differences between the treatments. (***P < 0.001, 1way ANOVA with Bonferroni's post-test). M = mock; T = triggered; P = primed; P+T = primed and triggered. The experiment was conducted three times with similar results. Data represent mean ± SEM. N=4

To further evaluate the potential role of PUB54 during local and systemic defense responses, bacterial replication in mock infiltrated and primed Col-0, *pub54*-I and *pub54*-II plants was assayed (Figure 22). Data from day 0 confirm infiltration of equal titer of *Pst* to all plants. After 3 days a clear effect of priming emerges in Col-0 plants. More specifically, the bacterial replication of *Pst* is significantly reduced in plants previously primed with *Psm* when compared to mock infiltrated plants. Basal resistance of *pub54*-I and *pub54*-II is comparable to WT-plants. In both lines, the benefit of priming emerges to a smaller extend than in Col-0. The statistic difference between primed und unprimed plants is not significant but shows a WT-like tendency. These observations were confirmed in 2 further independent experiments. The experiment points to a requirement of PUB54 in the plant to exploit full capacity of priming. However, basal resistance is not impacted by single knock out of *pub54*.

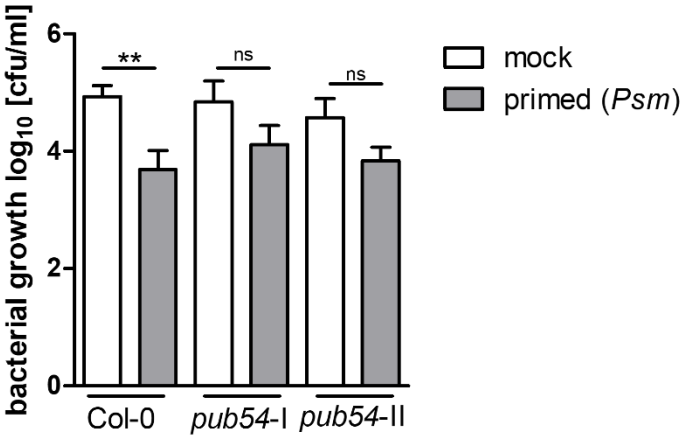

Figure 22: Systemic bacterial resistance is weakly repressed in *pub54*-I and II. Three lower leaves (1°) of Col-0, *pub54*-I, and *pub54*-II were mock infiltrated with 10 mM $MgCl_2$ as control or *Psm* (OD_{600} = 0.005) for priming. Two days later, three upper leaves (2°) were triggered with *Pst* ($1x10^4$ CFU/ml). Bacterial replication in 2° was assayed 3 dpi. Asterisks indicate statistically significant differences between mock treated and *Psm*-primed (PT) samples (**P < 0.01; ns, not significant, two-tailed *t* test). Repetition of the experiment showed similar results. N=10

3.2.2.2. HMP35 is potentially interacting with PUB54

PUB54 was found to be transcriptionally activated during local and systemic defense. To elucidate a potential role of PUB54 in immune responses the identification of potential substrates is crucial. In order to do so, PUB54 fused to the GAL4 binding domain (BD-PUB54, plasmid coding for leucine synthesis gene) was used as bait to screen for interacting proteins against a cDNA library from *Arabidopsis* using the Yeast-Two2-Hybrid system (Y2H). The screen revealed a potentially interacting protein which was identified as AT4G16380. The gene product was recently designated as Heavy meatal-associated protein 35 (HMP35) (Li *et al.*, 2020). The full-length gene was fused to the GAL4 activation domain (ACT-HMP35, plasmid coding for tryptophane synthesis gene) and thereafter tested for direct interaction with BD-PUB54 in yeast (Figure 23).

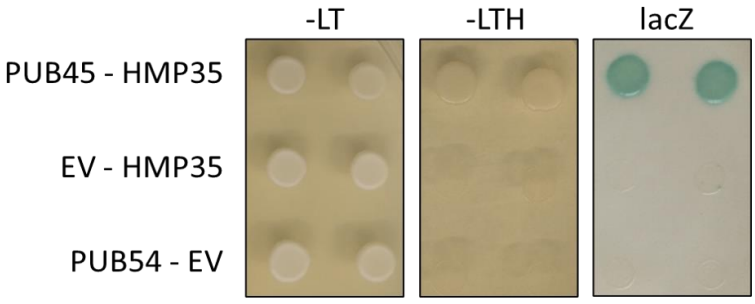

Figure 23: HMP35 was identified as potential interactor of PUB54 in a yeast screen. PUB54 was n-terminally fused with the binding domain (BD) of the GAL4-TF and co-transformed in auxotroph yeast with HMP35

n-terminally fused to the GAL4 activation domain (AD). Additionally, AD-HMP35 and BD-PUB54 were each co-transformed with the corresponding empty vector controls (EV) AD-EV and BD-EV, respectively. Colonies were cultivated on SCAD drop-out media for selection (-LT and -LTH) for 3 days and a lacZ-test was performed. Growth on -LT indicates successful transformation of BD-PUB54 and AD-HMP35. Growth -LTH and blue staining in the lacZ assay show interaction of the co-transformed potential interaction partners. L = Leucine; T = Tryptophan, H = Histidine; EV = empty vector.

Growth on –LT media displays that the plasmids coding for the GAL4 BD and ACT are expressed in all three approaches including the co-transformation of PUB54 with HMP35 and each of the proteins with the corresponding empty vector (EV) control. Both, growth on selective media (-LTH) and blue staining in the LacZ assay suggest that BD-PUB54 interacts with ACT-HMP35 in yeast reported by reconstitution of the GAL4 transcription factor allowing for histidine synthesis and activity of the ß-galactosidase. Co-transformation of each protein with the EV does not rescue the auxotroph yeast. Based on the data from yeast, HMP35 is an interacting protein of the E3- ubiquitin ligase PUB54 and thus could potentially represent a substrate for ubiquitination.

3.2.2.3. PUB54 interacts with HMP35 *in planta*

Before continuing to specify the possible role of PUB54 and HMP35 during immunity, the potential interaction identified in yeast needed to be verified *in planta*. PUB54 and HMP35 are both predicted to localize in the nucleus. Indeed, GFP-PUB54 and GPF-HMP35 locate to the nucleus and the cell periphery when transiently expressed in tobacco (Figure 24).

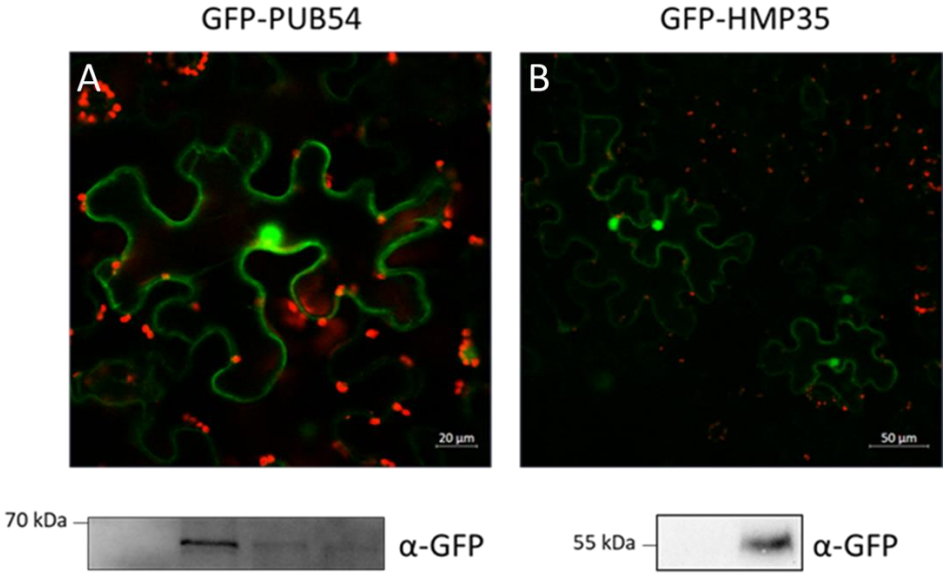

Figure 24: Transiently expressed PUB54 and HMP35 localize to the nucleus and cell periphery in tobacco. (A) GFP-PUB54 was transiently expressed in *Nicotiana benthamiana* via *Agrobacteria*-mediated transformation. Pictures were taken 2 dpi using laser scanning microscopy for localization studies (Scale bar: 20 µm). A representative picture is shown here. Protein expression was verified in crude extracts by western blots using

an α-GFP antibody for immunodetection. (B) GFP-HMP35 was transiently expressed in *Nicotiana benthamiana* via *Agrobacteria*-mediated transformation. Pictures were taken 3 dpi using laser scanning microscopy for localization studies (Scale bar: 50 µm). A representative picture is shown here. Protein expression was verified in crude extracts by western blot using a α-GFP antibody for immunodetection.

Appearance of Hechtian strains suggest that PUB54 and HMP35 might localize to the cytosol. Interestingly, the detected GFP-signal of GFP-HMP35 is stronger in the nucleus than in the dell periphery suggesting that it prevalently localizes to the nucleus. A common cellular localization of PUB54 and HMP35 indicates that both proteins might also interact *in planta*.

Bimolecular fluorescence complementation (BiFC) is an *in vivo* method performed in tobacco which allows for detection of weak protein-protein-interactions. Shortly, two proteins of interest are fused to a split-VENUS fragment which irreversibly reconstitutes upon interaction of the proteins of interest. Thus, the fluorescent signal accumulates over time when both co-expressed proteins localize to the same cellular compartment.

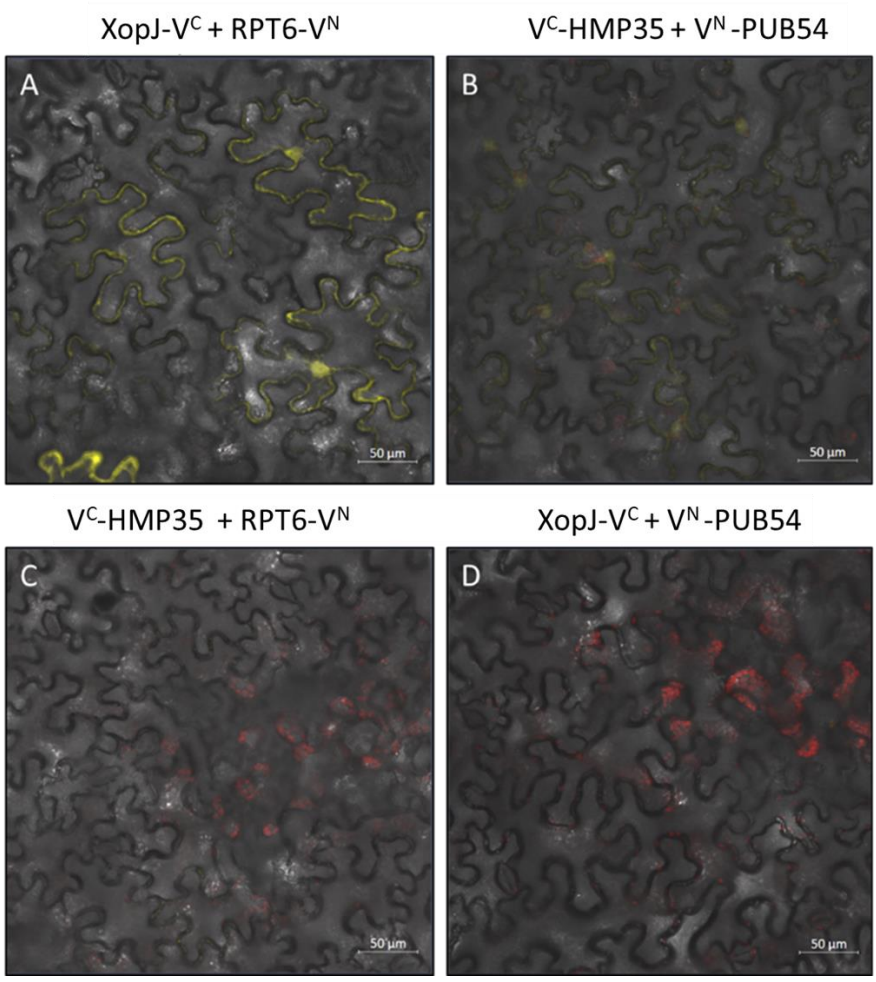

Figure 25: BiFC experiment indicates interaction between PUB54 and HMP35 in *planta*. *Nicotiana benthamiana* was co-infiltrated with split-VENUS fusion constructs as indicated above each picture. (A) Positive control using XopJ-V^C and RPT6-V^N. (B) Interaction approach with V^C-HMP35 and V^N-PUB54. (C) Control

approach combining V^C-HMP35 and RPT6-V^N. (D) Control approach combining XopJ-V^C and V^N-PUB54. All pictures were taken 3 dpi using laser scanning microscopy with the same microscope settings. Pictures show an overlay of transmitted light (grey shades), reconstituted VENUS-fragments (yellow), and autofluorescence of chloroplasts (red). Scale bar = 50µm.

The nuclear and cytosolic localized proteins XopJ-Venus^C and RPT6-Venus^N are known for their interaction and are therefore implemented as positive control in a BiFC experiment (Figure 25A) (Üstün *et al.*, 2013). All other samples, i.e., Venus^N-PUB54 coexpressed with Venus^C-HMP35 (Figure 25B) and the respective controls (Figure 25C and Figure 25D) were screened using the same microscope settings to allow for qualitative comparison between the individual samples. An interaction between PUB54 and HMP35 was detectable although the overall signal strength is weaker than in the positive control. The interaction localizes in dot-like structures in the nucleus indicating a possible interaction in the nucleus. Additionally, the shape of the epidermis cell became apparent without detection of Hechtian strands. This indicates a localization to the cell membrane or the cytosol.

Negative controls (combining RPT6 with HMP35 and XopJ with PUB54) were performed to exclude positive signals deriving from abundance effects due to different expression levels of the proteins. Both controls do not show fluorescent signals indicating that the detected singal in the positive control and the interaction approach do mot derive from abundance effects but rely on interaction events.

3.2.2.4. PUB54 is an U-box domain dependent E3-ubiquitin-ligase and ubiquitinates HMP35 *in vitro*

PUB54 was already shown to be an active E3 ubiquitin ligase *in vitro* (Mural *et al.*, 2013). Here, an *in vitro* ubiquitination assay was performed to test if PUB54 produces free poly-ubiquitin chains and if it performs auto-ubiquitination. Recombinant MBP-PUB54 (42 kDa MBP + 35,4 kDa PUB54) was therefore deployed in a reaction mixture with UBC9 as E2 ubiquitin conjugating enzyme and E1 (AtUBA1). When all components required for the ubiquitination cascade are combined in one reaction a smear at high molecular size appears after immunodetection with α-ubiquitin antibody. When one component is missing, i.e., E1, E3, or ATP, the smear is absent. The assay therefore strongly indicates that PUB54 is an active E3 ligase *in vitro* which is able to produce poly-ubiquitin chains (Figure 26).

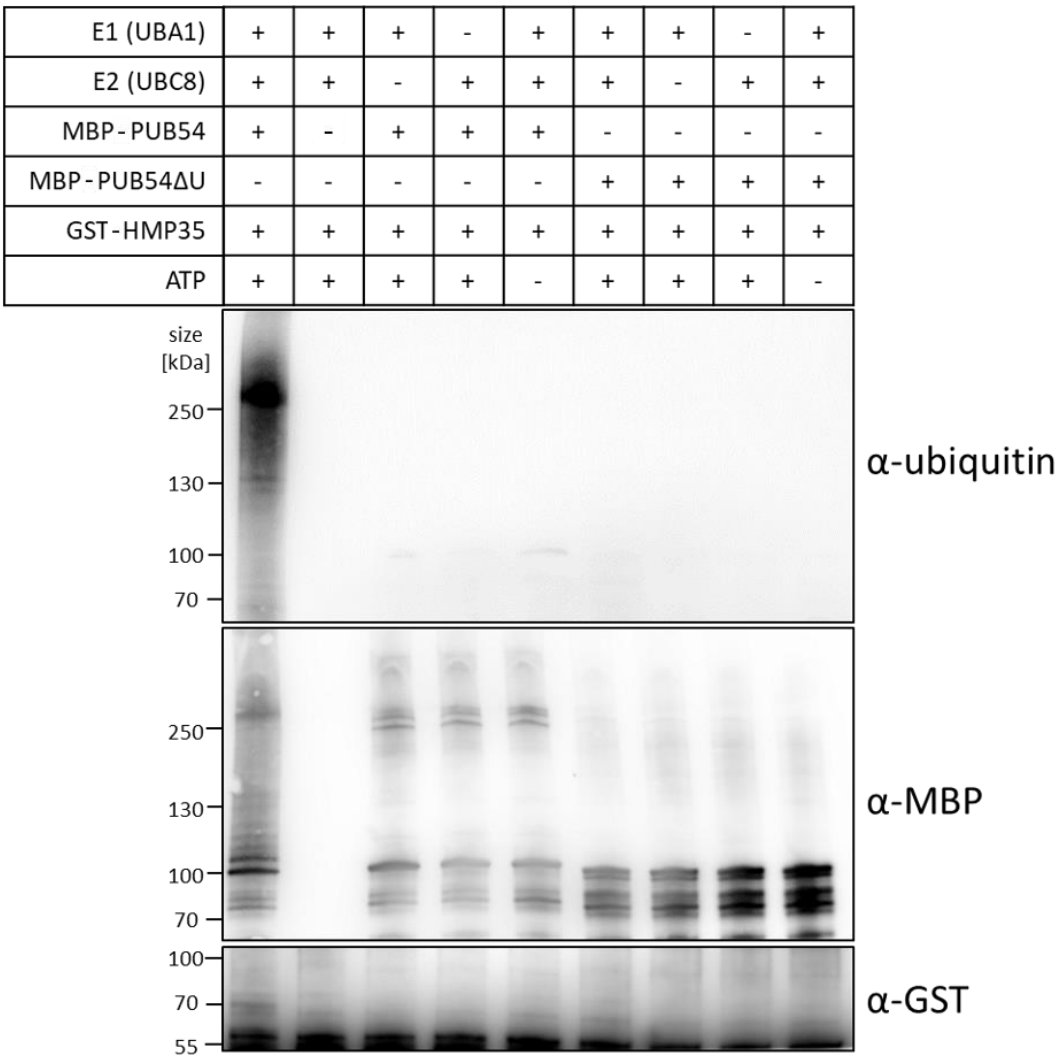

Figure 26: Ubiquitination assay underlines U-box dependent E3-ligase activity of PUB54 and potential PUB54-mediated ubiquitination of HMP35 *in vitro*. An *in vitro* ubiquitination assay was performed combining all compounds required for a successful ubiquitination cascade to test E3-ubiquitin ligase activity of PUB54 and the decoy protein PUB54ΔU. All recombinant proteins (i.e., UBA1, UBC8, MBP-PUB54, MBP-PUB54ΔU, and GST-HMP35) were expressed in *Escherichia coli* BL21/Rosetta and subsequently purified. Controls of the ubiquitination assay were performed by exclusion of single compounds as indicated. All samples were equally treated and incubated at 37°C for 1 h and subsequently run on separate SDS-gels in parallel. Signals were detected using α-ubiquitin, α-MBP, and α-GST antibodies. Repetition of the experiment showed similar results.

PUB54 is a Plant U-box containing protein which is considered to mediate the E3-ligase activity. To further characterize PUB54, a decoy variant of PUB54 with deleted U-box domain (MBP-PUB54ΔU) was tested *in vitro* for E3-ligase activity. Immunodetection with an α-ubiquitin antibody reveals that no free polyubiquitin chains are present when PUB54ΔU is incubated with all components potentially required for creation of ubiquitin chains. The detected signal is comparable to the control reactions. The *in vitro* ubiquitination assay supports the general characteristics of plant U-box containing proteins. Consequently, the

ligase activity of PUB54 depends on the functionality of its U-box domain. Furthermore, immune detection with an α-MBP antibody was performed. Reactions with MBP-PUB54 displays a smear at molecular weights ≥ 75 kDa when all components are added to the reaction. This shift typically appears in ubiquitination assays when varying numbers of ubiquitin moieties are bound to a protein. Hence, PUB54 presumably mediates auto-polyubiquitination *in vitro*. Furthermore, MBP-PUB54ΔU is detected but no protein shift or smear emerges at ≥ 75 kDa in reactions containing all components required for the ubiquitination cascade. Hence, PUB54 is an active E3-ubiquitin ligase with (auto-) ubiquitination activity *in vitro* whose E3-ligase activity depends on the U-box domain. The GST-antibody detects GST-HMP35 at 55 kDa. Interestingly, a distinct band emerges at 70 kDa indicating a shift of HMP35 implying (mono-)ubiquitination. Importantly, the reaction containing MBP-PUB54ΔU as well as all corresponding controls do not show this signal. The assay therefore indicates that HMP35 is targeted by PUB54. HMP35 is potentially (mono-) ubiquitinated by the U-box domain dependent E3-ligase-activity of PUB54.

The samples deriving from the *in vitro* ubiquitination assay were prepared for further LC-MS/MS-analysis with the aim to identify the auto-ubiquitination site of PUB54 and the ubiquitination site of HMP35. The peptides deriving from a tryptic digestion were analyzed in regard of a mass shift caused by a di-glycine residue. *In silico* digestion with trypsin performed using the Expasy PeptideMass online tool (Wilkins *et al.*, 1997). A theoretical sequence coverage of 88,6% was predicted (Table 21). However, HMP35 could not be identified in the measured sample.

Table 21: *In silico* digestion of HMP35.

Mass [Da]	Position	Peptide sequence
7047,1	168-233	QPGPPPQAIPMMPQGQPAMCCGPYYDGYGGPAFNGYGMPP QPYECYGRPVYESWGGGCPP PPPAYR
2601,4	75-97	TIEIVEPPKPPQPQPQQPPQKPK
2588,4	139-167	QPAPAPAPAPAPAAKPAPAPAPAPAPAPK
1752,6	240-254	CDYFSEENPQSCSIM
894,4	39-45	DQLFDEK
892,4	53-60	VVCCSPER
786,5	46-52	SNIVIIK
763,3	16-22	VDLDCAK
743,3	234-239	QCHVTR
727,3	109-114	EPEKPK
727,4	121-126	EPEKPK

726,4	127-132	QPEKPK
669,4	103-108	APEKPK
660,4	34-38	FPQIR
609,3	9-13	VTMMK
558,3	98-102	DAQPK
518,3	69-74	GGGSIK
506,3	61-64	IMDK
502,2	133-136	EPEK
501,3	115-118	QPEK

In silico analysis of PUB54 predicted a possible sequence coverage of 85,7%. In this MS-analysis, sequence coverage of 40 % was reached when FDR 0,5 was applied (Table 22). Among the detected peptides (grey shaded), one peptide was identified with addition of the GlyGly-specific monoisotopic mass of about 114 Da. Interestingly, this peptide was identified with and without di-glycine residue. It is consequently reasonable to assume that auto-ubiquitination of PUB54 is mediated at K181 and/or K185.

Table 22: *In silico* digestion and MS analysis of PUB54. Peptides detected during LC-MS/MS analysis are grey shaded.

Mass [Da]	Position	Modification	Peptide sequence
4301,0	86-125		DVDTSMISGHDVGEGIVELI YQNIITNLVMGAAADPHYSR
2625,2	162-185	GlyGLy	SFYLGNPSDSFSEFSTSAE**K** PIS**K**
2596,2	50-72		LEQSEIDAIQDSELNTSVNS LYK
2055,1	32-49		IFLLHVHLPFSLTTSSSR
1997,0	277-293		TNKPLENHNLVPNHTLR
1953,8	248-264		DPHVAADGFTYEAEEFR
1647,8	200-213		EHPGWILEPEESPK
1622,7	1-14		MEDAIYVAVNQDVR
1456,6	134-146		AEYVSQHAPHSCK
1188,4	190-199		DEEEEPESPK
1079,5	239-247		CPISMEIMR
1048,4	225-233		SNESDEDPR
844,5	19-25		TLLWALK
809,4	147-152		IWFICK
751,3	126-132		GMSITSR

705,3	75-80	DICINK
690,3	298-302	DWLEK
651,3	234-238	LEDFK
635,3	303-307	NPNYK
619,3	218-222	ETIEK
601,3	26-30	NLQVK
546,2	81-85	GVNEK

3.2.2.5. Single knock out of *HMP35* increases resistance towards infection with *Pseudomonas*

The HMP35 protein is not well described and its function is not understood. To test the potential role of HMP35 in defense responses, the two available independent SALK lines (SALK_105737 and SALK_108494, hereafter called *hmp35*-I and hmp*35*-II) were identified as tDNA insertion lines (Figure 27). The tDNA insertion of *hmp35*-I is located to an annotated exon and was tested as homozygous knock out in a PCR using genomic DNA as template. No residual transcript was detected in RT-PCR consequently identifying *hmp35*-I as full knock-out. In *hmp35*-II, the tDNA is inserted in the promotor region of the gene and therefore presumably alters the expression profile of *hmp35* with residual transcript in the RT-PCR. Indeed, RT-PCR analysis revealed residual HMP35 transcript in *hmp35*-II. Therefore, *hmp35*-II is not a knock-out line but a tDNA insertion line with presumably altered transcript levels and regulation of *HMP35*.

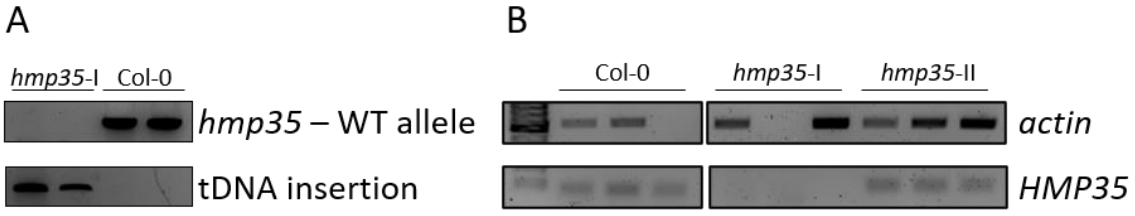

Figure 27: Genotyping of *hmp35* SALK lines analyzing genomic DNA and transcript levels. (A) Genomic DNA was extracted from Col-0 and *hmp35*-I and used as template for a PCR testing the presence of *HMP35* wildtype-gene (upper panel) and tDNA insertion (lower panel) in two individual plants each. (B) cDNA was synthesized from naïve Col-0, *hmp35*-I, and *hmp35*-II and probed for *Actin* expression (upper panel) as control and *HMP35* transcription in 3 individual plants each.

Col-0, *hmp35*-I, and *hmp35*-II were probed for bacterial replication of *Pst* in *Psm*-primed and unprimed plants (Figure 28). *hmp35*-I shows increased basal resistance and interestingly primed tissue does not benefit additionally. Hence, mock treated and primed *hmp35*-I shows equal bacterial replication comparable to primed wildtype plants. However, *hmp35*-II is

highly susceptible in unprimed plants. Previous priming leads to similar bacterial replication in *hmp35*-II and Col-0. Wildtype plants show a higher resistance towards *Pst* 3dpi in primed tissue. Although the difference between primed and unprimed conditions is not significant, a clear trend is visible and is comparable to previously performed bacterial growth assays with a statistically significant priming. These data indicate that HMP35 is involved in local and systemic defense responses and might act as negative regulator of (local) defense.

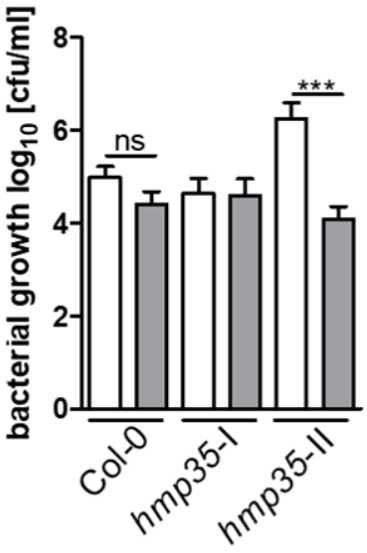

Figure 28: HMP35 is involved in plant resistance during infection with *Psm*. Three lower leaves (1°) of Col-0, *hmp35*-I, and *hmp35*-II were infiltrated with 10 mM $MgCl_2$ as control or *Psm* (OD_{600} = 0.005) for priming. Two days later, three upper leaves (2°) were triggered with *Pst* ($1x10^4$ CFU/ml). Bacterial replication in 2° was assayed 3 dpi. Asterisks indicate statistically significant differences between unprimed control and *Psm*-primed samples (***P < 0.001; ns = not significant, two-tailed *t* test). Data represent mean ± SEM. Repetition of the experiment showed similar results. N=12

3.2.2.6. HMP35 is degraded by the 26S proteasome

Prior experiments suggest that HMP35 is ubiquitinated by PUB54 and thereby possibly targeted to the 26S proteasome for degradation. To test this, the proteasomal turnover of HA-HMP35 was tested in tobacco transiently overexpressing HA-HMP35. 10 µM bortezomib was infiltrated 3 dpi to inhibit proteasomal activity (Figure 29A). Samples were subsequently taken in a time course. The western blot reveals a decent expression of HA-HMP35 in the control (0 h). The signal strength increases over time and is strongest after 24 h. Additionally, a smear appears above the detected protein indicating a mass shift deriving from accumulation of ubiquitinated HMP35. Increased accumulation of HMP35 cannot be observed when the proteasomal inhibitor Bortezomib is not applied (Figure 29B). This

experiment therefore strongly indicates a permanent turnover of HMP35 mediated by the 26S proteasome.

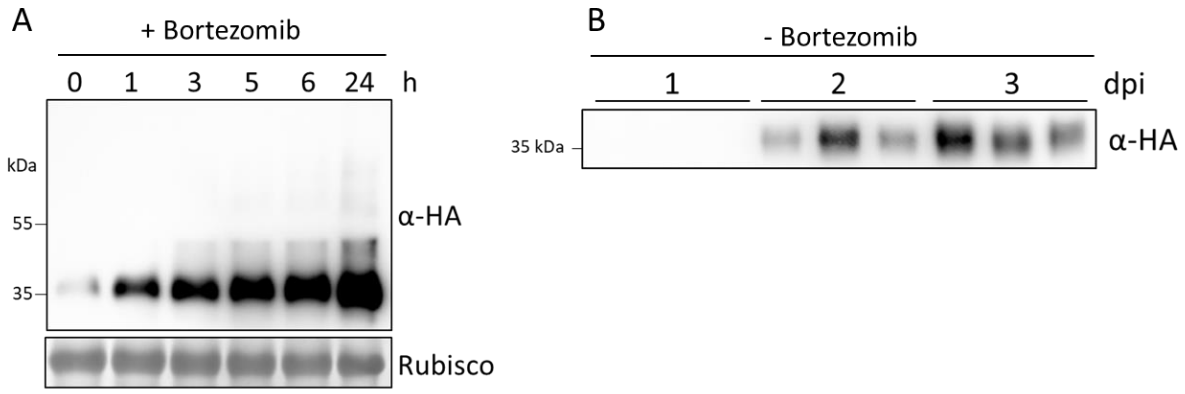

Figure 29: HMP35 accumulates during proteasomal inhibition. (A) 35S::3xHA-HMP35 was transiently expressed in tobacco. 2 dpi, 10 µM Bortezomib was infiltrated in the same leaves. Samples were taken in a time course between 0 and 24 h after infiltration as indicated and pooled from four individual plants. Protein accumulation was detected in crude extracts using an α-ubiquitin antibody. N=4 (B) As control, *35S::3xHA-HMP35* was transiently expressed in tobacco without infiltration of Bortezomib. Samples were taken 1-3 days post infiltration from 3 individual plants each. Protein accumulation was detected in crude extracts using an α-ubiquitin antibody. (A) and (B) derive from separate experiments. Repetition of the experiment showed similar results.

3.2.3. Identification of an *ari12* knock out line and generation of overexpression lines.

Analysis of the RNAseq data identified the RING-betweenRING_RING (RBR) E3-ubiquitin ligase *ARI12* to be transcriptionally upregulated during priming in systemic tissue. RBR E3-ubiquitin ligases have so far not been described for a potential role in defense responses and thus ascertains ARI12 as an interesting candidate for further investigations. As a basis for further investigations, genotyping of knock out lines was performed and overexpression lines were generated. The Salk Institute Genomic Analysis Laboratory indexes 2 tDNA insertion lines located in the exon region of *ARI12*, i.e., SALK_053919 and SALK_136787. Seeds from SALK_053919 did not germinate. gDNA from the SALK_136787 line (hereafter *ari12*) was used as template to verify the insertion of tDNA in the expected region and transcript level of *ARI12* was determined in a RT-PCR identifying *ari12* as homozygous knock out line (Figure 30).

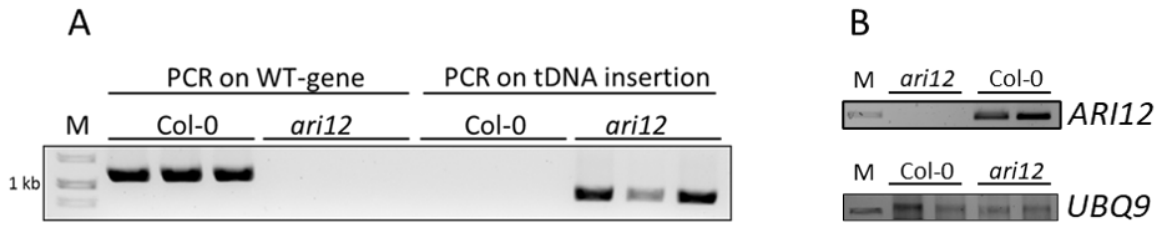

Figure 30: Genotyping of *ari12* and RT-PCR. (A) Genomic DNA was extracted from Col-0 and *ari12* and used as template for a PCR testing the presence of *ARI12* wildtype-gene and tDNA insertion in three individual plants each. (B) cDNA was synthesized from naïve Col-0 and *ari12* and subsequently probed for *ARI12* (upper panel) and *UBC9* transcription (lower panel) as control in two individual plants each.

Additionally, two independent overexpression-lines of ARI12 (hereafter *ARI12*-OX1 and *ARI12*-OX2) were generated in a Col-0 background by floral dipping. The stably transformed lines carry *ARI12* c-terminally tagged with *GFP* driven by a 35S promotor (*35S::ARI12-GFP*). The expression of the protein was proven with a western blot (Figure 31).

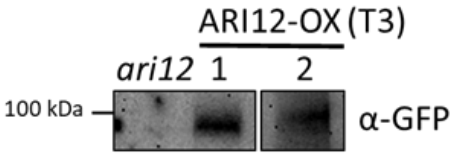

Figure 31: Verification of independent ARI12-OX lines. Stable expression of 35S::*ARI12-GFP* in *Arabidopsis* in the T3 generation was confirmed by western blot analysis of plant crude extracts from two independent lines using an α-GFP antibody. *ari12* was used as control.

3.2.4. *ARI12* is induced during infections and is regulated in SA- and Pip-dependent manner

Due to its transcriptional upregulation during priming and a by now unclear potential function in immunity, *ARI12* was chosen as interesting candidate for further molecular analyses from the RNAseq experiment and therefore initially subjected for molecular analyses. A priming and triggering experiment was performed with *Arabidopsis* Col-0 and expression of *ARI12* was thereafter measured in systemic tissue 10 h after triggering (Figure 32). In primed plants, 2.3-fold upregulated expression of *ARI12* shows a slight but not statistically different tendency of induction. *ARI12* is induced 10 h after triggering. A previous priming stimulus highly increases gene expression (P+T) and leads to hyperinduction of the gene. The overall expression pattern is reminiscent of classical SAR marker genes. Thus, the experiment indicates a potential role of *ARI12* during priming.

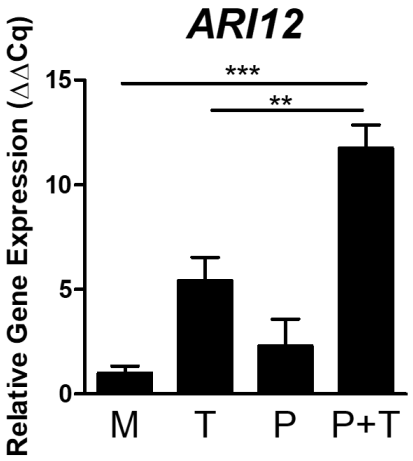

Figure 32: Transcription of *ARI12* is differentially activated in systemic tissue during priming and/or triggering. Three lower leaves (1°) of Col-0 were infiltrated with 10 mM $MgCl_2$ as control or *Psm* (OD_{600} = 0.005) for priming. Two days later, three upper leaves (2°) were triggered with *Psm* (OD_{600} = 0.005) or infiltrated with 10 mM $MgCl_2$. Samples were taken from systemic tissue 10 h after triggering. Relative Gene Expression (ΔΔCq) displays fold-induction in relation to mock-treated samples. Asterisks indicate statistically significant differences between the treatments. (***P < 0.001, **P < 0.01; 1way ANOVA with Bonferroni's post-test). M = mock; T = triggered; P = primed; P+T = primed and triggered. Data represent mean ± SEM. The experiment was conducted three times with similar results. N=4

SA is a central metabolite in systemic resistance and exogenous application induces gene expression of SA-responsive genes. To test if *ARI12* expression is regulated by SA- mediated signaling, SA was exogenously applied to *Arabidopsis* WT plant. The relative gene expression of *ARI12* and *PR1* as control was then quantified by qRT-PCR (Figure 33). Local application of SA strongly induces *PR1* in local and systemic tissue verifying the expected onset of SA-dependent signaling in the tested plants. *ARI12* expression is not elevated in local and systemic tissue when compared to mock treated plants. The overall expression of *ARI12* is high in systemic tissue when compared to local leaves. This indicates an impact deriving from the developmental stage of the tissue. Consequently, the weak responsiveness of *ARI12* on transcriptional level indicates that SA might not be the causal stimulus for priming related gene expression of *ARI12*.

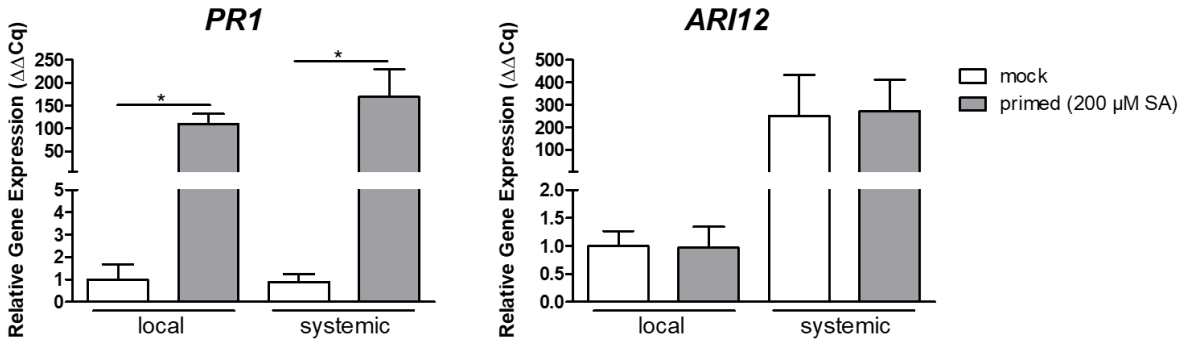

Figure 33: *ARI12* expression is not induced by SA treatment. Three lower leaves (1°) of Col-0 were locally infiltrated with 10 mM MgCl2 as control or 200 µM SA for priming. Two days later, samples were taken from local and systemic leaves. Relative Gene Expression (ΔΔCq) displays fold-induction in relation to mock-treated samples. Asterisks indicate statistically significant differences between the treatments (*P < 0.5; 1way ANOVA with Bonferroni's post-test). Repetition of the experiment showed similar results. Data represent mean ± SEM. N=6

Lines with mutations in *npr1* and *fmo1* were included in this experiment to assess the potential dependency of *ARI12* on SA- or Pip/NHP-dependent defense responses, respectively (Figure 34). SA is required but not sufficient to induce full capacity of systemic resistance whereas NHP was found to be capable of inducing a full priming response (Bernsdorff *et al.*, 2016; Hartmann *et al.*, 2018).

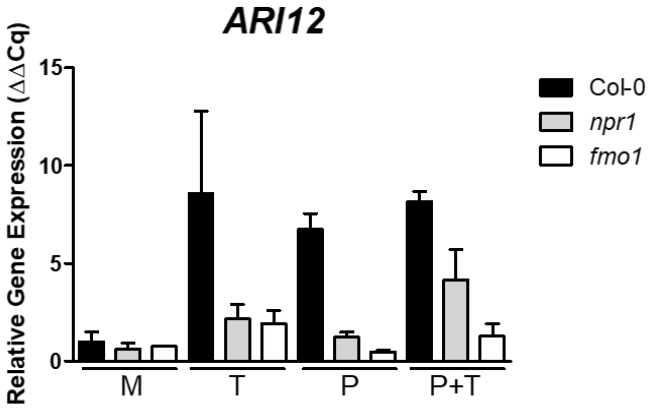

Figure 34: ARI12 expression after priming and/or triggering in npr1 and fmo1. Three lower leaves (1°) of Col-0, *npr1*-1, and *fmo1*-1 were infiltrated with 10 mM MgCl2 as control or *Psm* (OD_{600} = 0.005) for priming. Two days later, three upper leaves (2°) were triggered with *Psm* (OD_{600} = 0.005) or infiltrated with 10 mM $MgCl_2$. Samples were taken from systemic tissue 10 h after triggering. Relative Gene Expression (ΔΔCq) displays fold-induction in relation to mock-treated Col-0. No significant differences were observed within these data (1way ANOVA with Bonferroni's post-test). M = mock; T = triggered; P = primed; P+T = primed and triggered. Data represent mean ± SEM. Repetition of the experiment showed similar results. N=3

Molecular data show here that in both, *npr1* and *fmo1* expression of *ARI12* is weakly induced during priming with *Psm* and/or triggering in systemic tissue. Surprisingly, *ARI12* expression is stronger abolished in *fmo1*. The elevated gene expression can only be seen in Col-0. This consequently suggest that functional SA- and Pip-pathways are required for full gene induction and indicate that *ARI12* activation is possibly stronger influenced by the Pip-/HNP-pathway than SA pathway. Summarized, these data suggest that *ARI12* expression is induced by infection with *Psm* and previous priming leads to hyperinduction upon a secondary infection (Figure 32). Likely, accumulation or application of SA alone is not sufficient for induction of *ARI12* but functional *nrp1*- and *fmo1*-dependent pathways are required for gene expression (Figure 33 and Figure 34).

3.2.5. ARI12 accumulates systemically during priming and localizes to the cytoplasm and the nucleus.

Local infections with *Psm* induces SAR with salicylic acid (SA) and pipecolic acid (Pip) acting as central metabolites required for the onset of systemic defense responses (Bernsdorff *et al.*, 2016). Molecular data indicate that *ARI12* is induced during priming and hyperinduced in priming and triggering but not by SA application (Figure 32 and Figure 33). It was therefore tested whether the ARI12 protein accumulates in systemic tissue after priming with *Psm*. The experiment was conducted with Arabidopsis *K8* and *IIB1* lines (stably transformed lines expressing *ARI12*-GFP driven by the native *ARI12* promotor) (Xie *et al.*, 2015) to examine the dynamics of ARI12 protein abundance in local and systemic tissue during priming. The samples were probed on western blots and relative band intensity was subsequently quantified. The abundance of ARI12-GFP is very low in non-treated plants well correlating with the low transcript levels of *ARI12* (Figure 35A).

To evaluate protein levels of ARI12 mediated by the endogenous SAR-signals SA and Pip and independent of pathogen derived signals such as T3E derived effects, *K8* and *IIB1* were locally infiltrated with SA or watered with Pip (Figure 35 B and C). ARI12-GFP levels increase in both lines after Pip treatment. Local SA treatment leads to enhanced ARI12-GFP abundance only in *K8*. However, both lines accumulate more ARI12-GFP in systemic tissue of SA primed plants. This effect is also detectable in systemic tissue after local priming with *Psm* verifying the initial experiment (Figure 35A). ARI12-GFP protein levels cannot be determined in local *Psm* infected tissue because of progressed cell death emerging in the coomassie stain. The overall intensity is higher in *K8* than in *IIB1*. However, both lines independently indicate that ARI12 accumulates in systemic tissue after priming with *Psm*, SA and Pip. These data consequently suggest that ARI12 protein level is regulated during priming via SA- and Pip-mediated mechanisms.

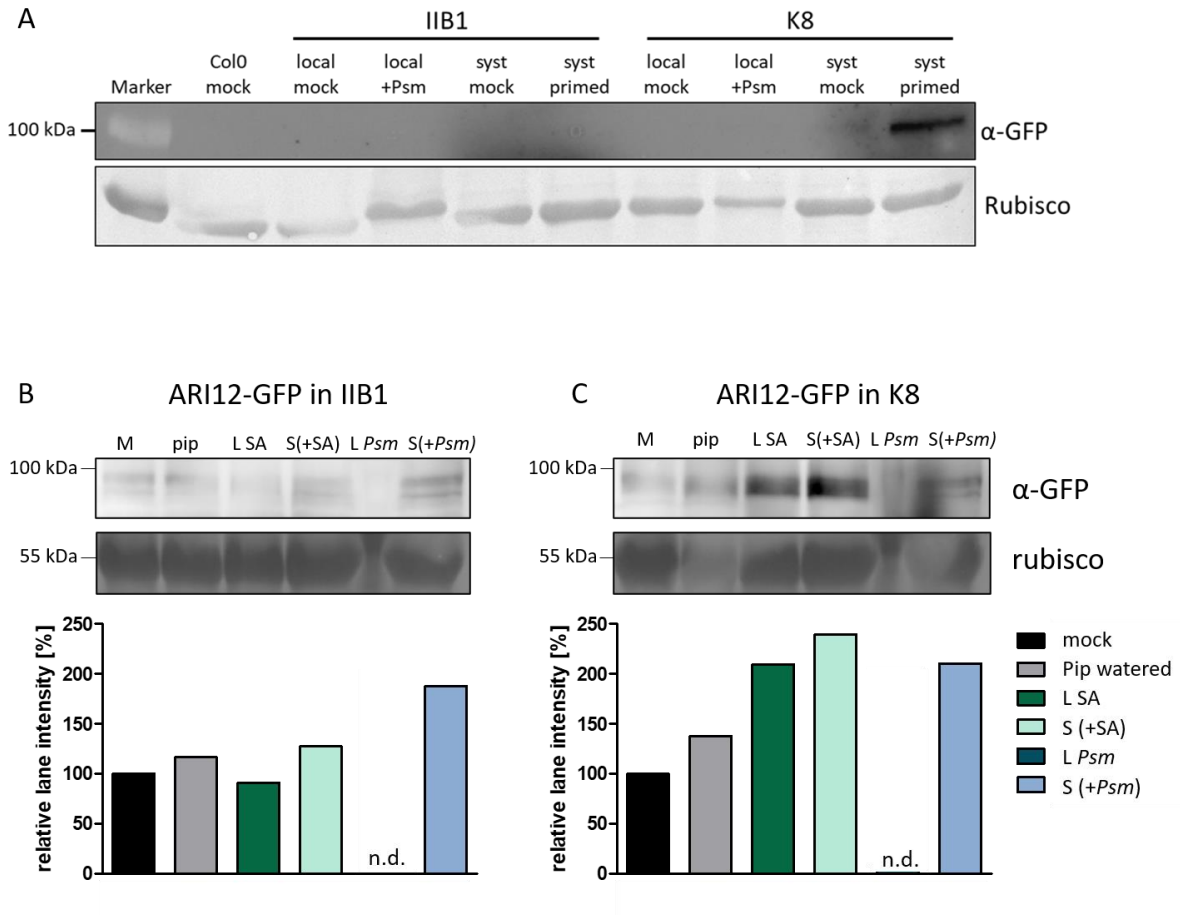

Figure 35: ARI12 accumulates during priming with *Psm*, SA and Pip in local and systemic tissue. Stable lines *IIB1* and *K8* expressing ARI-GFP were used for protein expression analysis in local and systemic tissues with different local stimuli. An α-GFP antibody was used for immunodetection of GFP-tagged ARI12 expressed under native promotor (*pmARI12::ARI12-GFP*) in crude extract of the stable *Arabidopsis* lines *IIB1* and *K8*. (A) Samples from Col-0 were used as control. Plants were locally (1°) mock treated with 10 mM $MgCl_2$ or primed with *Psm* (OD_{600} = 0,005). Samples were taken 48 hpi from local (local mock and local +*Psm*) and systemic tissue (systemic mock and systemic primed). (B) *IIB1* and (C) *K8* plants were locally mock infiltrated with 10 mM $MgCl_2$, primed by infiltration of 200 µM SA or *Psm* (OD_{600} = 0,005) or by watering with 10 mL 1 mM Pip. Samples were taken from locally treated tissue (mock, L SA, L *Psm*) and from systemic tissue (Pip, S(+SA), S(+*Psm*)) 48 h after local application. (A) Accumulation of ubiquitinated proteins was analyzed in crude extracts by SDS-gel electrophoresis and subsequent western blot using an α-ubiquitin antibody for immunodetection. (B) Signal intensity deriving from immunodetection with an α-ubiquitin antibody was quantified and plotted as relative lane intensity [%] with local mock treated samples considered as basal 100% of ubiquitinated proteins. Each sample consists of two leaves from 4 biological replicates. Statistical analysis was not applied due to pooled samples. The experiment was only conducted once. Pip = pipecolic acid, SA = salicylic acid, M = mock, L = local, S = systemic. Repetition of the experiment showed similar results. n = 4

In order to evaluate the cellular protein localization using laser-scanning-microscopy, samples were taken from tobacco plants transiently expressing ARI12-GFP. Expression is very low 1 dpi and peaks at 2 and 3 dpi (Figure 36A). A nuclear and cytoplasmic localization is

predicted according to the GO annotation. Indeed, the pictures taken from tobacco leaves indicate localization of ARI12 to thenucleus and the cell periphery. The overview pictures visualize the shape of epidermis cells and one dot shaped structure per cell indicating nuclear localization. Additionally, in close up images Hechtian strains emerge suggesting a potential cytoplasmic localization of ARI12-GFP. Samples were taken to verify the protein expression on a western blot and validate that the detected GFP signal derives from ARI12-GFP and not free GFP (Figure 36B).

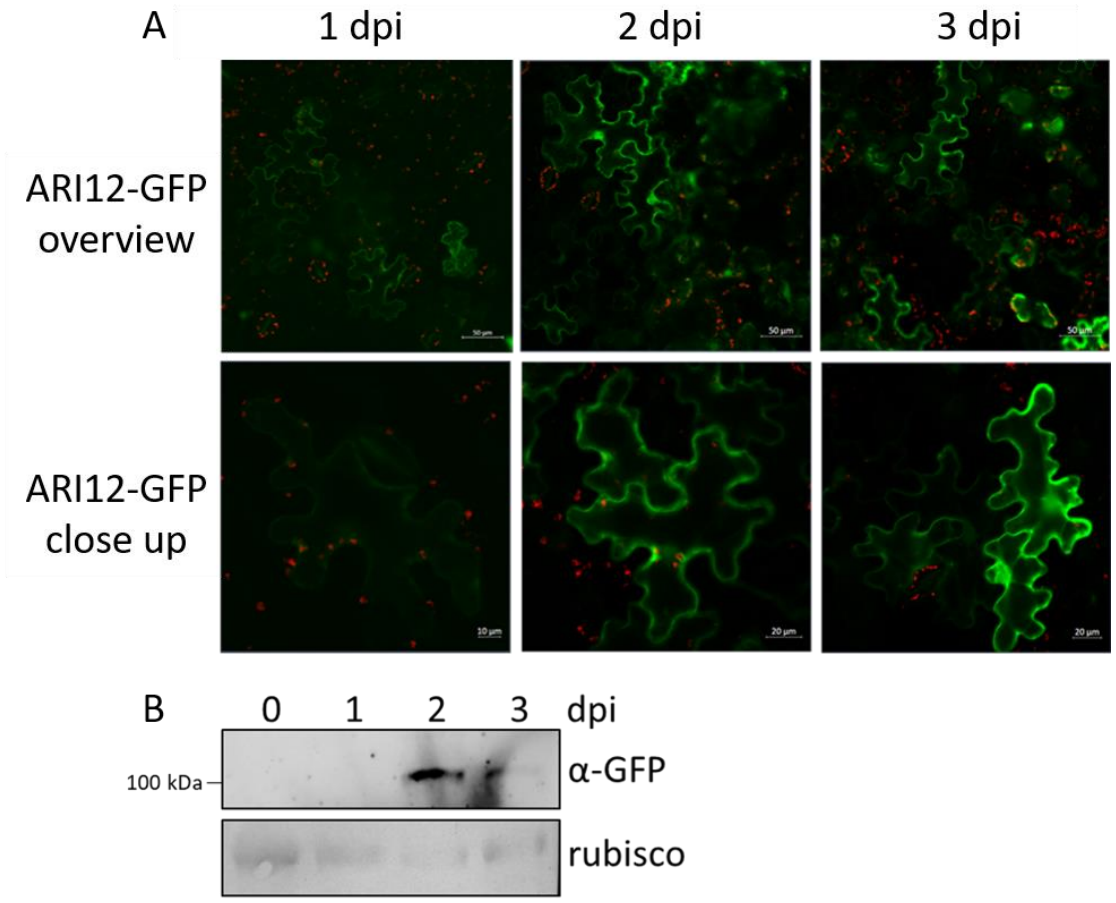

Figure 36: ARI12-GFP localizes to the cell periphery and the nucleus during transient expression in tobacco. (A) 35S::ARI12-GFP was transiently expressed in *Nicotiana benthamiana* by *Agrobacteria*-mediated transformation. Pictures were taken 1-3 dpi using laser scanning microscopy for localization studies. Scale bar = 50 µm (upper panel, overview pictures) and 20 µm (lower panel, close up pictures). Representative pictures are shown here. (B) Protein expression was verified in plant crude extracts by western blot using a α-GFP antibody for immunodetection.

3.2.6. ARI12 is involved in regulation of basal and systemic defense

Examination of *ARI12* transcript levels during priming indicate a role of ARI12 during priming as the expression pattern is reminiscent of central SAR marker genes. To investigate the involvement of ARI12 in defense responses bacterial replication was assessed in Col-0, *ari12* and two independent stable overexpression lines of GFP-tagged ARI12 (*ARI12*-OX1 and *ARI12*-OX2) (Figure 37). Immunodetection of GFP-tagged proteins from *ARI12*-OX1 and ARI12-OX2 confirms the high abundance of ARI12-GFP in both lines (Figure 31).

Bacterial replication of *Pst* DC3000 was assessed in *Psm* primed and non-primed plants. The basal resistance of *ari12* plants is comparable to Col-0 but priming appears slightly more effective than in WT. Both lines stably overexpressing ARI12-GFP show a different phenotype. Bacterial replication in *ARI12*-OX1 is equal in primed and mock infiltrated plants. The difference in bacterial growth is not statistically significant to primed Col-0 plants, but strongly indicates a higher overall resistance. *ARI12*-OX2 unprimed plants are significantly more resistant than the WT during local infections. Priming does not further increase the plant's resistance toward the pathogen. Hence, both overexpression lines show higher basal resistance and do not additionally benefit from previous priming. Primed WT plants show a significant decrease of bacterial replication in systemically infected leaves when compared to unprimed plants. It is therefore highly likely, that the observed phenotype of *ARI12*-OX1 and *ARI12*-OX2 is caused by the increased levels of ARI12-GFP. Thus, data from this experiment support the initial assumption that ARI12 is involved in resistance.

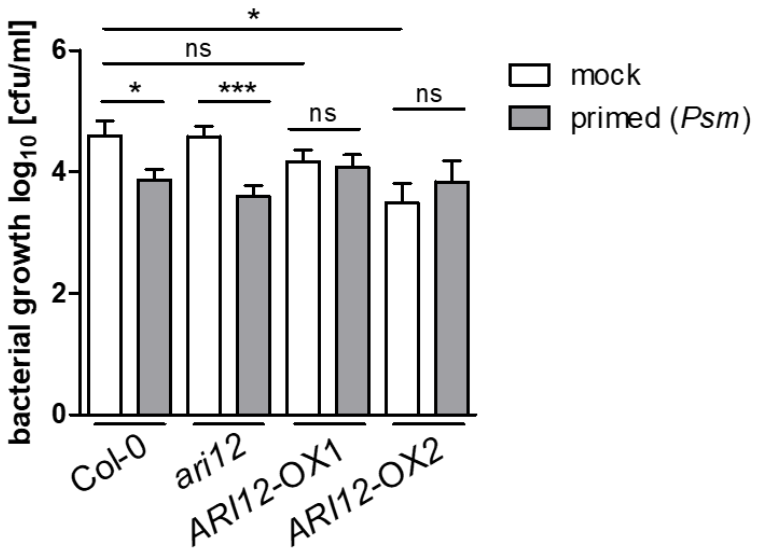

Figure 37: Bacterial replication in *ari12* is decreased in primed conditions but *ARI12* overexpression increases overall resistance. Three lower leaves (1°) of Col-0, *ari12, ARI12-OX1*, and *ARI12-OX2* were mock infiltrated with 10 mM $MgCl_2$ or *Psm* (OD_{600} = 0.005) for priming. Two days later, three upper leaves (2°) were triggered

with *Pst* (1x10^4 CFU/ml). Bacterial replication in 2° was assayed 3 dpi. Asterisks indicate statistically significant differences between unprimed control and *Psm*-primed samples as well as differences between genotypes (***P < 0.001; *P < 0.05, two-tailed *t* test). Data represent mean ± SEM. Repetition of the experiment showed similar results. N=12

It was next tested on molecular level if SAR marker genes are differentially expressed when *ARI12* transcription is altered in the *ari12* mutants and during *ARI12* overexpression (*ARI12*-OX1) compared to Col-0 (Figure 38). Expression of the SA-marker *PR1* was analyzed to get insights if *ARI12* could be involved in SA-dependent defense response. In mock plants, the gene expression of *PR1* is 10-fold higher in *ARI12*-OX1 than in wild type. Interestingly, during all infection treatments the *PR1* expression in *ari12* and *ARI12*-OX1 is highly comparable to WT except in triggered OX-plants. Triggering with *Psm* in *ARI12*-overexpressing plants does not induce *PR1* expression. Furthermore, there is a significant increase in *PR1* transcription in P + T plants in Col-0, *ari12*, and *ARI12*-OX1.

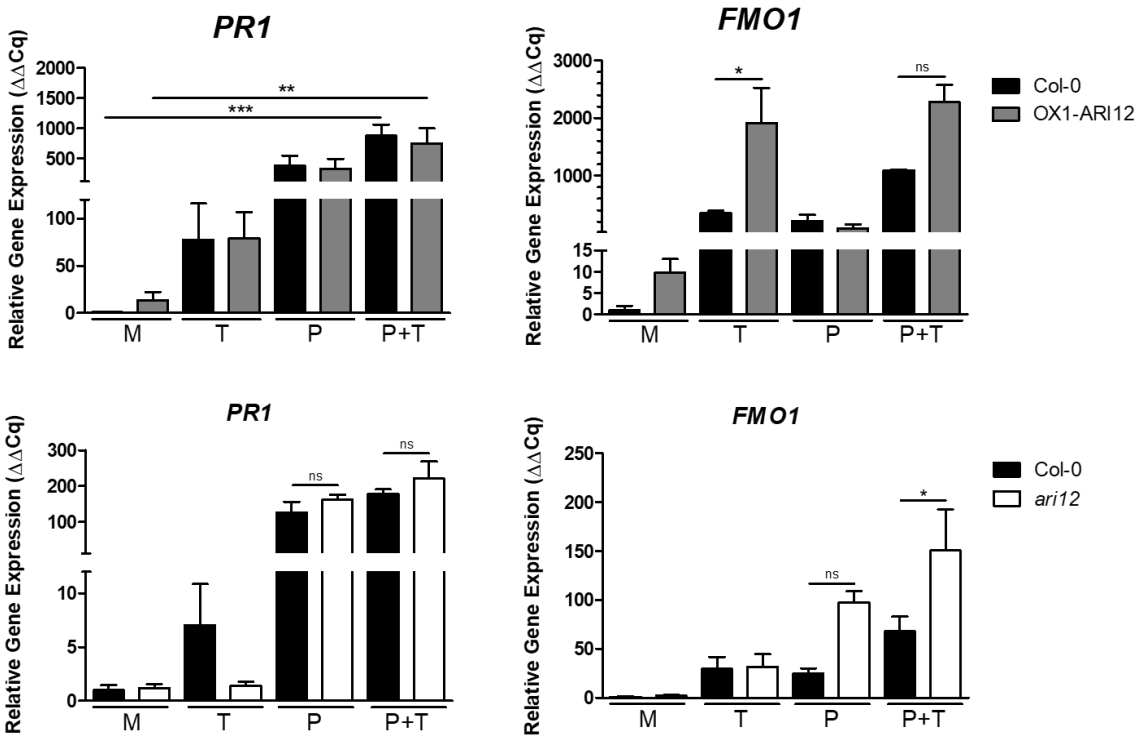

Figure 38: *ARI12* levels influence transcriptional activation of *FMO1* in priming and/or triggering. Three lower leaves (1°) of *ARI12-OX1* (upper panel), *ari12* (lower panel), and Col-0 were infiltrated with 10 mM $MgCl_2$ as control or *Psm* (OD_{600} = 0.005) for priming. Two days later, three upper leaves (2°) were triggered with *Psm* (OD_{600} = 0.005) or infiltrated with 10 mM $MgCl_2$. Samples were taken from systemic tissue 10 h after triggering. Relative Gene Expression (ΔΔCq) displays fold-induction in relation to mock-treated Col-0. Asterisks indicate statistically significant differences (***P < 0.001; **P <0.01; *P < 0.05; 1way ANOVA with Bonferroni's post-

test). M = mock; T = triggered; P = primed; P+T = primed and triggered. The experiment was conducted three times with similar results Data represent mean ± SEM. N=3

The next marker gene tested was *FMO1* to determine a potential involvement of *ARI12* in regulation of Pip-dependent defense responses. The *fmo1* mutant shows a strong SAR deficiency. The quantity of *FMO1* is 10-fold higher in mock treated *ARI12-OX1*. *FMO1* is strongly induced during infection and shows hyperinduction during P + T in wild type. This effect is even more pronounced in *ARI12*-OX1. The differences in gene expression during all treatments is statistically not significant. In contrast, mock treated and triggered *ari12* plants induce *FMO1* to WT-level. Interestingly, priming or priming and triggering cause significantly elevated *FMO1* transcription in *ari12*. The experiment suggests that the expression level of *ARI12* does not impact SA-dependent systemic defense. However, increased transcript levels of *ARI12* alters *FMO1* expression during local and systemic infection. In contrast, absence of *ari12* raises *FMO1* expression in systemic tissue during priming suitable to the observed increased resistance in systemic tissue of primed plants (Figure 37). These data consequently indicate that balanced *ARI12* transcription is involved in regulation of *FMO1* expression during priming and triggering.

3.2.7. ARI12 is an active E3 ligase *in vitro* and *in planta*

It has been shown that ARI12 is a functional E3-ubiuiqitin ligase *in vitro* (Xie *et al.*, 2015). This observation was verified in an *in vitro* ubiquitination assay (Figure 39). Addition of all components required for the ubiquitination reaction (i.e., Buffer, ATP, recombinant enzymes E1, E2, and E3) enables the ubiquitination reaction. The ubiquitin antibody shows a distinct band for GST tagged ARI12 with an increase in band width when all components are included in the reaction indicating a size shift caused by mono-ubiquitination (Figure 39A, left). Upon adjustment of brightness and contrast across the entire image, a high molecular smear emerges suggesting poly-ubiquitination of ARI12 (Figure 39A, right). This signal is not detectable in the control reactions. The signal of GST-ARI12 is slightly enhanced in the sample containing all components when detected with an α-ubiquitin antibody (Figure 39B). Additionally, a smear appears above GST-ARI12 indicating ubiquitination of GST-ARI12 in this sample. Hence, the *in vitro* ubiquitination assay confirms that ARI12 is an active E3- ubiquitin ligase with auto-ubiquitination activity.

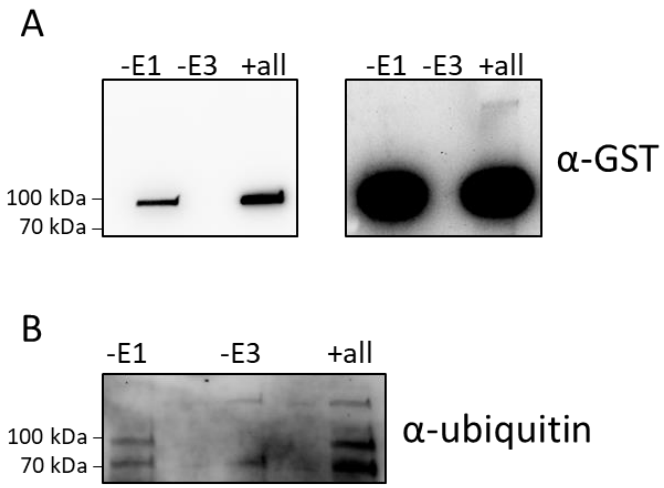

Figure 39: ARI12 possesses E3-ubiquitin ligase activity *in vitro*. An *in vitro* ubiquitination assay was performed combining all compounds required for a successful ubiquitination cascade to test E3-ubiquitin ligase activity of ARI12 (+all). All recombinant proteins (i.e., E1 = UBA1, E2 = UBC8, and E3 = MBP-ARI12) were expressed in *Escherichia coli* BL21/Rosetta pRARE and subsequently purified. Controls of the ubiquitination assay were performed by exclusion of single compounds as indicated (-E1, -E3). All samples were equally treated and incubated at 37°C for 1 h and subsequently run on separate SDS-gels in parallel. Signals were detected using (A) α-GST and (B) α-ubiquitin antibodies. (A) Shows the same blot with the original image (left) and adjusted brightness and contrast settings across the entire image (right).

To test if ARI12 is also an active E3 ligase *in planta*, *35S::ARI12-GFP* was transiently expressed in tobacco (Figure 40A). The transient overexpression peaks at 2 and 3 dpi. Additionally, the α-ubiquitin westernblot shows a high molecular smear in samples with expressed ARI12-GFP (Figure 40B) strongly indicating E3-ubiquitin ligase activity *in planta* and therefore substantiating the data from the *in vitro* assays (Figure 39).

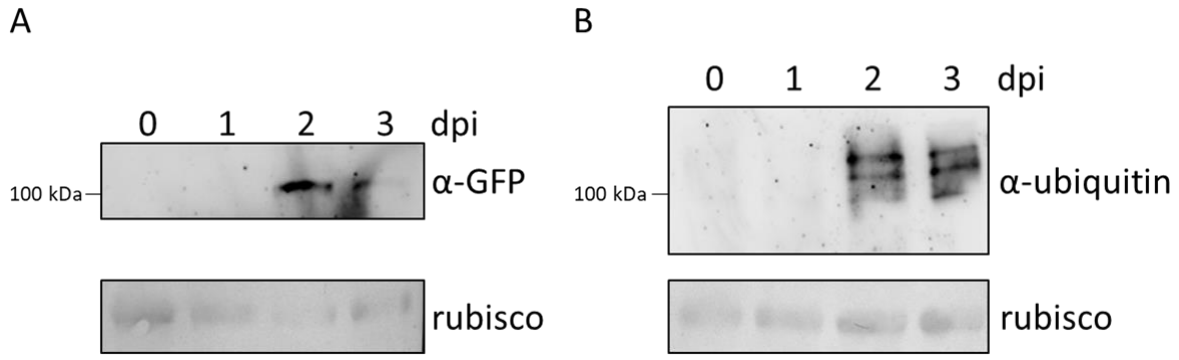

Figure 40: ARI12 is an active E3 ligase *in planta*. 35S::ARI12-GFP was transiently expressed in *Nicotiana benthamiana* by *Agrobacteria*-mediated transformation. Samples were taken and pooled from two individual plants 0-3 dpi. Protein expression was verified and probed for accumulation of ubiquitinated proteins in crude extract by parallel SDS-gel electrophoresis and subsequent western blot using (A) α-GFP and (B) α-ubiquitin antibodies for immunodetection.

ARI12 functions with a RING-HECT mechanism and therefore likely requires (auto-) mono-ubiquitination for activation (Xie *et al.*, 2015). MS-analysis was used to identify the potential auto-ubiquitination sites of ARI12. In order to do so, transiently expressed ARI12-GFP was precipitated using a GFP-trap and digested with trypsin. Unique peptides were identified using MaxQuant after LC-MS/MS measurement (Table 23). Theoretically, 90,7% of the sequence may be covered. 25 peptides were identified for ARI12 and covered the sequence by 47% in this analysis. Interestingly, one peptide was identified with a GlyGly modification indicating a potential ubiquitination site at K474. Hence, K474 is potentially the auto-ubiquitination site of ARI12 to mediate self-regulation of activity.

Table 23: *In silico* digestion and MS analysis of ARI12. Peptides detected in LC-MS/MS analysis are grey shaded

Mass [Da]	Position	Modification	Peptide sequence
4671,9	286-325		CLPCNYVFCWFCHVDWIEDM EGTGGDLHFCTFDAVLSDQR
3228,4	01-31		MDNNSVIGSEVDAEADESYVNAALEDGQTGK
3131,3	96-124		DSVGLLELDPPSDDNEYFCGACGESHPHK
2286,2	360-379		LDTIIQELSNTQLENVSQLK
2179,8	336-352		YEDCYENWDSNELLMQK
1969,9	49-66		ALMEIDVQSVSDFTSLSK
1919,8	475-494		DVENGLASVVSEGEASGSGR
1824,9	166-183		VGLHASCPASVGLDTIER
1797,9	147-161		IISEKPAAEWNLWLK
1773,8	218-235		CAIDLSPGSGNASVSCHR
1724,8	394-406		VLEWTYVYGYYLR
1504,8	380-392		FILEAGLQIIECR
1423,7	37-48		NYATVLTEEDIR
1357,6	432-442		HCLETNLQPFR
1269,6	259-269		WLLENAVPCPK
1230,6	191-199		FNYNQYLLR
1223,7	67-77		AEATLLLSHLR
1100,4	245-254		EDAHSPVDCK
1089,5	86-95		QWSAGAQSVR
1043,5	125-134		NLASVSCGHR
1033,5	458-466		LTELTSLTR
1002,5	467-474	GlyGly (K474)	NHYENVV**K**
988,4	139-146		CWTSHINK

980,5	210-217	WHPIQGSR
980,4	78-85	WNVDCICK
925,3	328-335	MSESDSNR
881,3	443-449	YEEEPSK
828,3	239-244	FCWNCR
818,4	277-283	NQDNSLK
799,4	353-359	EQANLPK
769,3	450-455	DFNAFR
753,3	200-205	SYVDNR
749,4	426-431	FVENLK
676,3	407-412	EDEVGK
648,2	418-422	DTQER
615,3	413-417	QNLLK
508,2	206-209	ETMK

3.2.8. Identification of potential ARI12 substrates

Data deriving from priming experiments suggest that ARI12 is involved in defense and priming responses. ARI12 has been described as an active E3- ubiquitin ligase *in vitro* and is inducible by UV-B light (Xie *et al.*, 2015). Transcript and protein levels are inducible by priming with *Psm*. During transient overexpression of ARI12-GFP ubiquitinated proteins accumulate *in planta*. However, this experiment does not provide information on which proteins are ubiquitinated and how ARI12 could contribute to immune priming. Screening for potential ARI12 substrates was performed *in planta* by transient expression of ARI12-GFP in *N. benthamiana* (Figure 40). Next, immunoprecipitation was performed using a GFP-trap. Non-infiltrated leaf material from tobacco served as a negative control to distinguish specifically interacting proteins from false positive bound ones. Additionally, plants from the *Arabidopsis K8* (*pmARI12::ARI12-GFP*) line were primed and samples were taken from local and distal tissue after 48 h. Purified and desalted trypsin digested peptides were subsequently analyzed *via* MS in technical triplicates.

In samples taken from *N. benthamiana* GFP and ARI12 were successfully identified. GFP harbors 26 cleaving sites of trypsin and the protein sequence may be covered up to 90,8 % according to ExPASy biomass calculator (Wilkins *et al.*, 1997). In this experiment, 21 unique peptides of GFP were detected and cover 68% of the full sequence. The ExPASy biomass calculator predicts 90,7% sequence coverage of tryptic digested ARI12 under optimal conditions. 19 peptides covering 40 % of ARI12 were identified and implies an overall reasonable sample quality. The identified peptides could be assigned to 21 proteins with high confidence (Table 24). Ubiquitin3 and 4 (UBQ3 and UBQ4) were identified with 11

individual peptides and coverage of 94 %. All other proteins were detected with 2-7 individual peptides each and sequence coverage of 4-14%. These values are relatively low but are reasonable enough to clearly identify potential substrates of ARI12. Grey shaded proteins were identified with highest confidence.

Table 24: Identified protential substrates of ARI12.

Description	Gene Symbol	Gene ID	Coverage [%]	# Peptides
Ubiquitin 3;4	*UBQ3; UBQ4*	AT5G03240; AT5G20620	94	11
Green fluorescent protein	*GFP*		68	21
RBR-type E3 ubiquitin transferase	*ARI12*	AT1G05880	40	19
Catalase 2	*CAT2*	AT4G35090	14	7
Glyceraldehyde-3-phosphate dehydrogenase	*GAPA-2*	AT1G12900	12	7
Actin 2	*ACT2*	AT3G18780	10	3
Ribosomal protein L13 family protein		AT3G07110	10	3
Phosphoglycerate kinase		AT1G56190	9	2
GF14 protein phi chain	*GF14 PHI*	AT1G35160	8	2
Heat shock cognate protein 70-1	*HSC70-1*	AT5G02500	8	3
Ribosomal L29 family protein		AT5G02610	8	2
Rubisco activase	*RCA*	AT2G39730	8	6
Cold, circadian rhythm, and rna binding 2	*CCR2; GRP7*	AT2G21660	7	2
Fructose-bisphosphate aldolase	*FBA1*	AT2G21330	6	3
GTP binding Elongation factor Tu family protein		AT1G07930	6	2
Ribosomal protein	*RP1*	AT1G43170	6	2
Tubulin alpha chain	*TUA6*	AT4G14960	5	2
Catalase 3	*CAT3*	AT1G20620	5	3
Heat shock protein 81-2	*HSP81-2*	AT5G56030	5	3
Ribosomal protein S5/Elongation		AT3G12915	5	2

factor G/III/V family protein				
ATP synthase subunit alpha	*ATP1*	ATMG01190	4	2
Glutamine synthetase	*GSR2*	AT1G66200	4	2
S-adenosyl-L-homocysteine hydrolase	*MEE58; HOG1*	AT4G13940	4	2

4. Discussion

4.1. Underlying 26S proteasome-dependent mechanisms during priming

4.1.1. Ubiquitinated proteins accumulate systemically during SAR depending on endogenous SAR-signals

In recent years, evidence has accumulated that the conserved ubiquitin-proteasome system (UPS) occupies a central role during defense responses towards bacterial infections (Adams & Spoel, 2018; Duplan & Rivas, 2014; Marino *et al.*, 2012). In an arms-race between bacteria and the host, bacterial type-II effectors (T3E) are translocated to host cells to target specific proteins which potentially have a substantial role in the host defense response. The T3E XopJ from *Xanthomonas* targets the proteasomal subunit RPT6 for proteolytic degradation (Üstün *et al.*, 2013; Üstün & Börnke, 2015). Consequently, proteasomal protein turnover is reduced and the required degradation of transcription factors such as nonexpresser of PR genes 1 (NPR1) is impaired which potentially increases the pathogen's virulence and decreases the effectiveness of the host immune responses (Üstün & Börnke, 2015). However, not only the 26S proteasome but also ubiquitin itself is targeted during pathogenic infections. It was recently shown that plant begomoviruses directly interact with ubiquitin to hijack ubiquitin-mediated degradation to regulate plant defense (Li *et al.*, 2019). These findings strongly indicate that dampened plant defense signaling regulated by the UPS proteasome is highly favorable for pathogens and that a balanced UPS function is crucial for the host immunity. However, it is not well examined yet if elevated ubiquitination and thus accumulation of ubiquitinated proteins also derives from endogenous signals and therefore mirror a requirement for the plant to induce immunity.

It was shown here, that local infection of *Arabidopsis thaliana* with *Pseudomonas syringae* pv. *maculicola* also induces accumulation of ubiquitinated proteins in systemic tissue (Figure 5). Regarding the local infection site, it is favorable for bacterial virulence to interfere with proteasomal protein turnover in T3E-dependent manner (such as XopJ) consequently leading to accumulation of ubiquitinated proteins. However, in systemic tissue no bacteria were applied which strongly indicates that accumulation of ubiquitinated proteins is conveyed by plant internal defense mechanisms such as the defense related metabolites pipecolic acid (Pip) and salicylic acid (SA). Indeed, exogenous application of SA increases protein ubiquitination levels which is even more pronounced in systemic tissue (Figure 5). This finding is in line with the observation that plants impaired in SA-signaling are dampened in induction of proteasome activity (Üstün *et al.*, 2013). Furthermore, proteasome activity is induced in *N. benthamiana* upon treatment with SA (Üstün *et al.*, 2013). Pip watered plants accumulate higher levels of ubiquitinated proteins as well when compared to mock treated plants. Thus, endogenous plant SAR-related signals not only influence proteasome activity

but activate the whole UPS to allow regulated defense responses. It has been observed that loss of or shifted 26S proteasome function lead to an increase of 20S proteasome biogenesis increasing tolerance of oxidative stress occurring during infections (Kurepa, Wang, Li, Zaitlin, *et al.*, 2009). However, the 26S proteasome is required for ubiquitin-dependent proteolysis (Kurepa *et al.*, 2008). On the assumption, that proteins that negatively regulate immunity such as transcription factors should be degraded to allow high defense output, it is possible that elevated ubiquitination of proteins exceed the proteolytic capacity of the 26S proteasome.

Since substrate ubiquitination and specificity of the process highly depend on E3-ubiquitin ligases (Vierstra, 2009) it is highly likely that Pip and SA mediated pathways are involved in regulation of E3-ubiquitin ligase activity. Indeed, multiple E3-ubiquitin ligases as specificity conferring components of the UPS were shown to play a role in plant defense against pathogens (Devoto *et al.*, 2003). The plant U-box E3-ubiquitin ligases PUB22 and PUB23 have been shown to target Rpn12a (a non-ATPase subunit of the 19S regulatory particle in the 26S proteasome) for degradation during drought stress (Seok *et al.*, 2008). Possibly, levels of 26S proteasomes are thereby regulated in response to stresses (Kurepa, Wang, Li, & Smalle, 2009). PUB17 was shown to be a positive regulator of defense, primarily functioning downstream of R protein signaling during effector-triggered immunity. Substrates of PUB17 are likely key signaling molecules whose degradation is required to generate a hypersensitive response (HR) and to establish resistance (Yang *et al.*, 2006). Thus, upregulated E3-ligases and their potential substrates should be identified to gain deeper understanding on the ubiquitylome of the plant during local and systemic defense responses.

4.1.2. The proteasome is required for full local and systemic immunity

The involvement of the ubiquitin-proteasome-system (UPS) on many different levels of plant immunity has already been demonstrated in multiple studies (Adams & Spoel, 2018; Trujillo & Shirasu, 2010). However, the underlying mechanism on how the 26S proteasome itself is involved in defense responses and specifically systemic acquired resistance (SAR) is not well understood. To examine the role of the proteasome during priming, mutants of the proteasome subunits *rpt2a*-2 and *rnp12a*-1 were probed for their capability to trigger systemic defense responses upon priming with virulent *Psm* (Figure 6). Wildtype plants benefit from priming by reduced bacterial replication during a secondary infection (Fu & Dong, 2013; Mishina & Zeier, 2006; Shah & Zeier, 2013). Locally increased susceptibility to *Pst* and decreased priming capacity of systemic tissue was observed in both mutants with more pronounced defects in *rpn12a*-1. RPT2a and its minor redundant isoform RPT2b are located in the regulatory particle of the proteasome and are essential for channel opening

and substrate entry to the proteolytic active core particle (Groll *et al.*, 2000; Ueda *et al.*, 2011). Incorporation of RPN12a finalizes the lid formation of the regulatory particle (Tomko *et al.*, 2015). The T-DNA insertion line *rpn12a*-1 was identified after exon-trap mutagenesis and found to carry the translational fusion gene *RPN12a-NPTII* (*neomycin phosphotransferase II*) mediating a kanamycin resistance and creating a pool of altered 26S proteasomes by outcompeting residual RPN12a wild-type protein (Babiychuk *et al.*, 1997; Smalle *et al.*, 2002). Not surprisingly, both mutations lead to phenotypic changes including alteration in leaf organ size in *rpt2a*-2 and decreased sensitivity to auxins and cytokinins in *rpn12a*-1 (Smalle *et al.*, 2002; Ueda *et al.*, 2004). Thus, mutations of the single subunits may also have severe impact on the ability to induce immunity in locally infected and systemic tissue. At this point it is not clear by which underlying mechanism the reduced resistance of both mutants is mediated.

The capacity for ubiquitin-dependent protein degradation is decreased in *rpt2a*-2 (40% reduction) and *rpn12a*-1 (60% reduction) but ubiquitin-independent protein turnover is increased enhancing resistance to oxidative stress (Kurepa *et al.*, 2008). A proposed shifted ratio between 26S and 20S proteasomes in *rpt2a* and *rpn12a* may depend on attenuation of RP assembly, explaining the increased tolerance to oxidative stress but higher sensitivity to temperature stress (Kurepa *et al.*, 2008). This 26S and 20S ratio shift might also explain the observed SAR phenotype of both proteasome mutants. Proteasomes regulate sensitive processes which are now imbalanced in *rpt2a* and *rpn12a* by altered 20S proteasome prevalence and activity (Kurepa *et al.*, 2008). The proteasome mutants might cope better with the occurring oxidative stress elicited during PAMP-triggered immunity (PTI). Simultaneously, degradation of proteins whose turnover is required for the onset of local defense and SAR is reduced, potentially leading to insufficient immunity towards *Pst*. This assumption coincides with the observation that resistance is strongly dampened in *rpn12a*-1 with high loss of proteasome activity and an intermediate SAR-phenotype in *rpt2a*-2 with less impaired proteasome activity (Kurepa *et al.*, 2008).

To further evaluate the observed SAR-phenotype of *rpt2a*-2 and *rpn12a*-1, their defense response was tested on molecular level by RT-qPCR quantifying transcript levels of defense- and SAR-related genes in systemic tissue of primed and unprimed plants 10 h after triggering with *Pst* (Figure 7 and Figure 8). These data suggest a strongly reduced responsiveness of the tested genes (such as *PR1*, *FMO1*, *ALD1*, and *SARD4*) in both proteasome mutants when compared to Col-0 and supports previous findings of enhanced bacterial replication in *rpt2a*-2 and *rpn12a*-1 with 40 % and 60% reduced ubiquitin-dependent proteasome activity, respectively (Kurepa *et al.*, 2008). The impaired gene induction is likely a consequence of the highly reduced proteasome activity with several possible scenarios to explain this observation. The degradation of negatively regulating transcription factors is possibly inhibited which consequently represses defense gene activation (Collins & Tansey, 2006). For

example, full expression of NPR1 target genes depends on the proteasomal turnover of phosphorylated NPR1 (Spoel *et al.*, 2009).

Alternatively, synthesis of phytohormones such as Pip and SA might be impaired and therefore downstream signaling and induction of self-enhancing feed-forward loops cannot be induced. It was found that SAR cannot be induced by application of Pip in mutants deficient in SA-signaling (*sid2, npr1, or pad4*) because both branches are required at basal levels for SAR induction (Wang *et al.*, 2018).

4.1.3. Defense-related biosynthesis of phytohormones is altered but exogenous SA-application partially restores SAR-phenotype

The proteasome mutants *rpt2a*-2 and *rpn12a*-1 were shown to be more susceptible towards pathogenic infections with virulent *Pseudomonas* and cannot induce SAR which is associated with impaired defense- and SAR-gene induction. To further characterize the proteasome mutants and to dissect a potential pleiotropic from specific effect, accumulation of defense related metabolites during priming and/or triggering was determined. The antimicrobial phytoalexin camalexin (Cam) is synthesized in *A. thaliana* and other *Brassicaceae* mainly dependent on two cytochrome p450 enzymes, CYP71A13 and CYP71B15 (also known as PAD3) (Nafisi *et al.*, 2007; Schuhegger *et al.*, 2006). SA is a phytohormone accumulating in local and systemic tissue upon infection with (hemi-)biotrophic bacteria and is required but not sufficient to induce full SAR responses (Bernsdorff *et al.*, 2016; Hartmann *et al.*, 2018). Increased SA-levels activate *PR* gene expression in *NPR1*-dependent manner to mount defense responses (Cao *et al.*, 1994).

The proteasome mutants were found to accumulate less SA than Col-0 during priming and/or triggering. However, camalexin levels are more comparable to wildtype (Figure 9). Enhanced disease susceptibility 5 (EDS5) also known as SA induction deficient 1 (SID1) is an essential and SA-responsive component of SA-dependent signaling during defense. *eds5*-1 shows increased susceptibility to virulent *Psm*, is unable to activate *PR1* gene expression, and exhibits decreased SAR responses but accumulates camalexin to wild-type levels (Nawrath *et al.*, 2002; Nawrath & Métraux, 1999). The authors discuss that camalexin accumulation is an SA-independent compensatory pathway as a result of impaired SA-defense responses (Nawrath & Métraux, 1999). Camalexin accumulation and hormone signaling including SA are generally considered as largely independent or complementary mechanisms (Contreras-Cornejo *et al.*, 2011; Ferrari *et al.*, 2007). Interestingly, the defense phenotype of both proteasome mutants with decreased *PR* gene expression and SA accumulation but normal camalexin synthesis is highly reminiscent of *eds5*-1. Thus, defense signaling of the proteasome mutants is likely impaired upstream of defense gene expression.

Dampened gene expression of Pip/NHP-related genes such as *FMO1* and *ALD1* indicate that further SAR pathways are affected but not as a pleiotropic effect mediated by an overall alleviation of protein degradation. Instead, the proteasome mutants appear to be defective in more specific aspects since compensatory mechanisms such as camalexin biosynthesis can still be activated. Present data do not indicate which sector of the signaling cascade from pathogen perception, signal transduction, phytohormone biosynthesis and defense gene expression is impaired. It was therefore tested if local application of SA may rescue the SAR phenotype. Indeed, exogenously applied SA induces expression of the SA-marker gene *PR1* to wild type levels indicating that perception of the signal is not impaired (Figure 10). These data therefore suggest a defect upstream of SA-biosynthesis.

SA was most recently found to be a mobile signal required for signal transduction to non-infected tissue (Lim *et al.*, 2016). However, local application of SA as priming stimulus does not lead to rescue of the priming phenotype in the proteasome mutants upon challenging infections with *Psm* (Figure 11). This might be due to insufficient long-distance transport of SA or impaired signal transduction in the systemic tissue. SA-compromised sid2 mutants can still induce moderate SAR induction and Pip/NHP-dependent responses while Pip-deficient mutants are fully defective in SAR establishment (Bernsdorff *et al.*, 2016; Hartmann *et al.*, 2018). Taking this into account, it appears that the proteasome mutant might also be impaired in Pip/NHP-mediated pathways. Additional measurement of Pip/NHP levels should be performed to verify this assumption. However, the present data hint towards an impaired SAR-signaling deriving from a defect upstream of the biosynthesis of defense metabolites such as SA and Pip/NHP.

4.1.4. Shifted gene transcription and impaired degradation of negatively regulating proteins dampen immune responses in *rpt2a*-2

The current data suggest a central role of a functional UPS for local defense responses and onset of SAR but the underlying molecular mechanism remain unknown. Global transcriptomic changes were therefore investigated by RNAseq comparing Col-0 and the proteasome mutant *rpt2a*-2 in local (un-)infected and systemic primed tissue 48 h after local infiltration with *Psm* (chapter 3.1.5).

Untreated Col-0 and *rpt2a*-2 were compared to reveal general transcriptomic differences in naïve plants. 428 differentially expressed genes (DEGs) were found mainly assigned to proteasomal protein catabolic processes, ubiquitin-dependent protein catabolic process, and catabolic processes indicating severe changes in basal cellular functions (Table 19). Increased transcripts of proteasomal components indicate a compensatory effect to maintain the 26S proteasome function despite the lack of *rpt2a*-2. *RPT2b* is paralogue of *RPT2a* with 99.1% amino acid sequence identity (Ueda *et al.*, 2004). The double knock out of *rpt2a rpt2b* is

lethal in gametophytes but expression of *RPT2b* under control of the *RPT2a* promotor may rescue *rpt2a* (Ueda *et al.*, 2011). *RPT2b* and another 32 proteasomal subunits were found to be transcriptionally upregulated in *rpt2a*-2 consequently indicating a certain equalizing effect. Compensatory effects are common responses to knock out of genes as earlier described for camalexin and SA in *enhanced disease susceptibility* (*eds5*) (Nawrath *et al.*, 2002; Nawrath & Métraux, 1999). Despite the transcriptional upregulation of several proteasomal subunits in *rpt2a*-2, a full compensation of the knock out cannot be reached. Proteasome activity has been found to be reduced about 40% when compared to wild type (Kurepa *et al.*, 2008). Thus, proteasome activity can be maintained but is reduced in unstressed conditions. Furthermore, defense related genes such as the *cysteine-rich receptor-like protein kinase* (*CRK6*) are downregulated in *rpt2a*-2. *CRK6* has been found to positively influence stomatal immunity and improve PTI responses by association with the pattern recognition receptor FLS2 (Yeh *et al.*, 2015). Thus, naïve *rpt2a*-2 differs from wild type plants despite undergoing compensatory mechanisms. These differences have to be kept in mind regarding following experiments.

Immune priming has been described as a mechanism allowing the plant to respond faster and /or stronger to secondary infections in a resource effective manner (Hilker *et al.*, 2016). One mechanism for onset of systemic defense after priming includes induction of SAR-related gene transcripts in systemic tissue (Bernsdorff *et al.*, 2016; Conrath, 2011; Mishina & Zeier, 2006). These transcriptional changes have been studied in several projects using multiple priming stimuli such as bacteria or pipecolic acid unraveling large transcriptional changes (Bernsdorff *et al.*, 2016; Hartmann *et al.*, 2018). In this project, plants were primed with *Psm* to induce systemic immunity and data from systemic tissue of primed Col-0 were compared to mock-treated plants. In total, 749 DEGs were detected containing a range of previously described upregulated defense- and SAR-related genes such as *FMO1*, *ALD1*, and *PR1* also present in other publicly available SAR transcriptome datasets (Bernsdorff *et al.*, 2016; Hartmann *et al.*, 2018). Hence, the RNAseq can be considered as reliable dataset.

Considering the basal variations between Col-0 and *rpt2a*-2, DEGs from Col-0 and *rpt2a*-2 during priming were not directly compared to analyze differences in differential gene expression. Instead, DEGs in primed tissue from Col-0 and *rpt2a*-2 were separately compared to mock conditions and subsequently opposed in a Venn diagram (Figure 16). 196 genes are induced in wild-type during priming but not in *rpt2a*-2, indicating compromised gene activation. Known defense- and SAR regulating genes such as *avrPphB susceptible 3* (*PBS3*, centrally involved in SA-biosynthesis) and the E3-ubiquitin ligases *ATL2 and ATL6* (both early activated PAMP-responsive genes) are included in the list of DEGs (Chang *et al.*, 2019; Maekawa *et al.*, 2012; Salinas-Mondragón *et al.*, 1999). These data therefore indicate that central steps in phytohormone biosynthesis and defense response are impaired in the proteasome mutants. This finding is in line with the observed lower accumulation of SA in

rpt2a-2 during infections (Figure 9). Surprisingly, Col-0 and *rpt2a*-2 share about 50% of the transcriptional changes in systemic tissue during priming. Genes included here are for example well known defense- and SAR-related genes such as *PR, FMO1,* and *PAD3*. These genes are differentially expressed in both lines but the amplitude of gene induction is lower in *rpt2a*-2 than in Col-0. Gene regulation is often controlled by several TFs orchestrating gene expression which only gives a rough suggestion about the expectable protein levels and different proteins require different proteins levels for execution of their biological function (Vogel & Marcotte, 2012). Thus, differences in transcript levels may lead to different biological outputs. This effect is likely observed here for example displayed by reduced SA accumulation in the proteasome mutant leading to dampened *PR* gene expression (Figure 7). Redundant WRKY TFs may act in concert to regulate target gene expression, e.g. observed for WRKY40 and WRKY18 (Ng *et al.*, 2018; Pandey *et al.*, 2010). Furthermore, synthesis and degradation of TFs allow specific adjustment of gene transcription in response to stresses including infections (Desterro *et al.*, 2000; Ng *et al.*, 2018). Due to the impaired function of ubiquitin-dependent protein degradation in *rpt2a*-2 it is feasible to assume that also degradation of TFs which require turnover for defense activation is impaired. A similar effect has been observed in *Xanthomonas* infected pepper plants by XopJ-mediated proteolytic degradation of the proteasomal subunit Rpt6 leading to reduced proteasome activity and accumulation of the TF NPR1 (Üstün *et al.*, 2015; Üstün & Börnke, 2015). *CYP71A13*, *FMO1* and *PAD3* are genes commonly regulated by the TF WRKY40 (Brotman *et al.*, 2013) and were found here to be weakly or not induced in *rpt2a*-2 during priming. The stress responsive TF WRKY53 is a positive regulator in pathogen responses and was shown to be regulated by the E3-Ubiquitin protein ligase 5 (UPL5) by polyubiquitination and subsequent proteasomal degradation (Miao & Zentgraf, 2010). In pepper, continuous ubiquitination and proteasomal degradation of WRKY40 has been shown (Raffeiner *et al.*, unpublished data). Hence, shifted gene transcription in the proteasome mutant presumably depends (partially) on impaired turnover of the negatively regulating TF WRKY40.

4.1.5. WRKY 40 contributes to establishment of systemic resistance and enhances the *rpt2a*-2 SAR-phenotype

Data deriving from the RNAseq experiment suggested that priming might be impaired in *rpt2a*-2 due to insufficient turnover of negatively regulating TFs leading to dampened expression of target defense genes. The WRKY-TF family has been found to be involved in regulation of host defense against phytopathogenic infections (Eulgem & Somssich, 2007; Pandey & Somssich, 2009). The TF *WRKY40* has been found to negatively regulate the expression of positive regulators of defense in *Arabidopsis* during infections with powdery mildew while positively influencing JA-signaling simultaneously (Pandey *et al.*, 2010). Among

others, defense related genes such as A*rabidopsis isochorismate synthase 1* (*ICS1* or *EDS16*, involved in SA-biosynthesis), *avrPphB susceptible 3* (*PBS3*, involved in SA-biosynthesis), *Arabidopsis phytoalexin deficient 4* (*PAD4*, involved in SA-signaling), *AGD2-like defense response protein 1* (*ALD1*, involved in Pip-biosynthesis), and a *cytochrome p450* (*CPY71A13*, involved in camalexin biosynthesis) have been found to be directly targeted by WRKY40 (Birkenbihl *et al.*, 2017). These genes are involved in central SAR-regulating mechanisms and also emerge in the present RNAseq dataset as weakly or not induced genes during priming in *rpt2a*-2 when compared to Col-0. WRKY40 has been shown to be continuously ubiquitinated and degraded via the UPS in pepper (Raffeiner *et al.*, unpublished data). Assuming that WRKY40 degradation is required for a branch of SAR, accumulation of WRKY40 might occur in *rpt2a*-2 during priming caused by insufficient proteasomal degradation (Figure 17). Hence, knock out of *wrky40* in proteasome mutants (*rpt2a*-2 x *wrky40*) could positively influence the ability to increase priming capacity. Surprisingly, bacterial replication assays with a *rpt2a*-2 x *wrky40* double mutant revealed an additive effect of the double knock out when compared to *rpt2a*-2 and *wrky40* alone. The SAR-phenotype of the proteasome mutant is not reversed (Figure 19). WRKY40 was found to act redundantly with its closest relative WRKY18 and to control its expression by binding to the *WRKY18* promotor (Pandey *et al.*, 2010). Thus, single knock out of *wrky40* may not show a full biological effect due to redundant activity of WRKY40 and WRKY18. Possibly, WRKY18 can no more be repressed by WRKY40 leading to an accumulation of WRKY18 which in turn further represses defense gene activation. However, the synergistic effect found here supports the assumption, that WRKY40 is indeed involved in systemic defense in *Arabidopsis*.

Taken together, the analysis of the defense response in the proteasome mutants suggest that a functional 26S proteasome is required for defense gene expression and synthesis of SA for full SAR induction. Dampened proteasome activity results in large scale impaired defense gene expression as observed in the RNAseq potentially due to altered and/or decreased proteasomal turnover of regulating proteins. Exogenous application of SA partially restores SAR in *rpt2a*-2 indicating a defect in phytohormone-dependent signal generation in local and impaired signal transduction in systemic tissue.

4.2. Regulatory role of E3-ubiquitin ligases during defense responses

4.2.1. E3-ubiquitin ligases undergo transcriptional regulation during priming in systemic tissue

Targeted turnover of proteins via the 26S proteasome is a central mechanism to maintain cell processes and allow cells to fine-tune stress responses (Sadanandom *et al.*, 2012). More than 1400 E3 ubiquitin ligases encoded in the *Arabidopsis* genome confer specificity to the

UPS (Vierstra, 2009). However, the function of the vast majority of E3 ligases remains to be investigated. The project aimed to identify previously uncharacterized E3 ligases with a potential role in immunity particularly focusing on SAR. E3-ligases from the RING, HECT, and RING_between-RING_RING E3-ligase families were described to have central regulatory roles at different levels during local immunity (Adams & Spoel, 2018; Trujillo & Shirasu, 2010). To identify E3 ligases with potential role in onset or maintenance of systemic immunity, the transcriptome data obtained from primed Col-0 plants was screened for transcriptional upregulation of E3 ligase genes. Priming and initiation of systemic defense responses are considered to be effective for the plant at lowest energy costs but include measurable reactions such as transcriptional upregulation (Hilker *et al.*, 2016). Thus, the data obtained from the RNAseq experiment were used to select differentially expressed genes (DEGs) annotated to E3 ligases that might play an important role during priming based on the transcriptional profile.

Among the DEGs during priming identified in the RNAseq experiment, 11 upregulated E3 ubiquitin ligases annotated to diverse families were chosen (Table 20). Remarkably, 4 of these genes code for E3 ligases belonging to the *Arabidopsis* toxicos en levadura (ATL) family, namely ATL91, ATL 96, and ATL6. The *ATL* gene family contains at least 91 members of conserved RING zinc-finger proteins (Guzmán, 2014). Different ATL E3-ubiquitin ligases such as *ATL1*, *ATL2, ATL6*, *ATL9, and ATL31* were shown to play a role in defense responses (Berrocal-Lobo *et al.*, 2010; Maekawa *et al.*, 2012; Salinas-Mondragón *et al.*, 1999; Serrano *et al.*, 2014).

As one example, ATL9 is involved in signaling upon PAMP perception and *ATL9* gene expression is partially SA-dependent. ATL9 is inserted into the ER membrane and purposely targets an inhibitor of plant defense for proteasomal degradation (Berrocal-Lobo *et al.*, 2010). ATL isoforms are also involved in defense responses in other species, e.g. EL5 and BIRF in rice and ACRE132 in tobacco (Durrant *et al.*, 2000; Liu *et al.*, 2008). Hence, it is tempting to speculate that the transcriptional induction of so far uncharacterized ATL E3 ligases is involved in systemic defense responses. Really interesting new gene 1 (RING1, also known as ATL55) is a membrane bound protein with E3 ligase activity. Expression is induced by pathogen infection and knock down leads to hypersensitivity accompanied with lower *PR1* gene expression (Lin *et al.*, 2008). The overexpression of pepper *RING1* (*CaRING1*) in *Arabidopsis* enhances resistance to infections with virulent *Pseudomonas*. Hence, RING1 is likely involved in ubiquitination processes during immune responses (Lee *et al.*, 2011). RMA2 and Hrd1B were characterized as endoplasmic reticulum (ER)-associated E3-ligases involved as integral part of ER-associated degradation (ERAD) to remove toxic and misfolded proteins via the UPS (Son *et al.*, 2010; Su *et al.*, 2011). ER-stress response by the unfolded protein response (UPR) was shown to be central for resistance to bacterial infections and establishment of SAR both dependent on the ER membrane-located

kinase/endoribonuclease IRE1 as a key regulator (Moreno *et al.*, 2012). Although a specific role of RMA2 and Hrd1B has not been shown it seems possible that these E3-ligases contribute to local and/or systemic defense responses during ERAD in *Arabidopsis*.

Appearance of transcripts coding for E3 ligases with roles in defense responses can consequently be seen as proof of concept for the approach to screen transcriptionally upregulated genes for potential roles in defense responses. The E3 ligases plant U-box 54 (PUB54) and ariadne 12 (ARI12) were chosen for further investigations to unravel underlying mechanism. Several PUBs such as PUB12 and 13, PUB17, PUB22, PUB23, and PUB24 have been found to be involved in responses to different stresses including infections with pathogenic bacteria and oomycetes (Trujillo *et al.*, 2008; Lu *et al.*, 2011; Antignani *et al.*, 2015; He *et al.*, 2015; reviewed in Trujillo, 2018) but the function of PUB54 has not been investigated yet. The RBR E3-ubiquitin ligase ARI12 is a scarcely characterized E3 ligase previously suggested to be involved in the response to UV-B radiation (Lang-Mladek *et al.*, 2012; Xie *et al.*, 2015). Investigation of ARI12 would immensely expand the current understanding of how RBR E3-ligases might contribute to immunity. Both proteins and their potential role during defense signaling/priming will be discussed in more detail in the following chapters.

4.2.2. PUB54 is differentially expressed during infections and targets HMP35 for ubiquitination and proteasomal degradation

PUB54 was found to be differentially expressed in systemic tissue during priming in the analyzed RNAseq dataset (Table 20). Transcriptional regulation during stresses does not necessarily imply increased protein abundance and direct influence of the expressed gene in coping with the stress but energy investment for gene expression may lay the foundation for faster responses during priming (Hilker *et al.*, 2016). It is therefore intriguing to analyze the biological relevance of *PUB54* expression during priming and triggering in distal leaves after local infections. Transcriptional quantification in a priming and triggering experiment verified the induction of *PUB54* expression during priming and showed high gene expression after triggering without additional benefit from previous priming (Figure 21). It is feasible to postulate that *PUB54* is involved in local defense. Furthermore, *PUB54* transcription in primed but not triggered plants also suggest that systemic signaling associated with SAR is sufficient to induce gene activation. This is reminiscent of other priming involved genes such as *PR1*, *SARD4*, and *EDS5*. However, typical SAR marker genes such as *PR1* and *FMO1* are hyperinduced after triggering in primed Col-0 when compared to unprimed plants which cannot be seen here with *PUB54* (Figure 7) (Kiefer & Slusarenko, 2003; Mishina & Zeier, 2006). *PUB54* was found to be differentially regulated during defense related responses in several studies. Transcriptional downregulation of *PUB54* was observed in *enhanced stress*

response 1 (*esr1-1*) mutants defective in JA-mediated defense signaling (Thatcher *et al.*, 2015). *PUB54* is systemically activated 7 d after local infections with *Hyaloperonospora arabidopsidis* (Coker *et al.*, 2015) and after treatment with Pip (Hartmann *et al.*, 2018). These data thus indicate relevance of *PUB54* during biotic stresses.

Bacterial replication was assayed in *pub54*-I and *pub54*-II to evaluate the role of *PUB54* in defense. Basal resistance was comparable to Col-0 and systemic resistance could still be acquired but with reduced priming capacity (Figure 22). Hence, knock out of *pub54* leads to a specific but not very pronounced effect. In *Arabidopsis*, 64 genes are predicted to encode for plant U-box proteins of which 41 PUBs (but not PUB54) contain armadillo (ARM) repeats as additional domain (Mudgil *et al.*, 2004). ARM repeats are exclusively found in plants and mediate the interaction between ligase and substrate (Trujillo, 2018). Data deriving from *in vitro* ubiquitination assays investigating the role of PUB10 ARM repeats indicate a role for dimerization (Jung *et al.*, 2015). Other PUBs such as PUB22 and PUB24 dimerize via the U-box domain (Furlan *et al.*, 2017). The observation of dimerization events therefore suggest that PUBs may act in concert complementing each other. Furthermore, it is not clear to date if other ligases act with a certain redundancy to PUB54 targeting the same proteins during defense. Functional redundancy among E3-ubiquitin ligases is a wide spread phenomenon with PUB59 and PUB60 recently having been identified to redundantly regulate circadian period by controlling splicing (Feke *et al.*, 2019). Within the same work, a 'decoy' approach was followed (i.e., dominant-negative expression of PUBs lacking the U-box domain required for recruitment the E2 conjugating enzyme) showing that *PUB56* is potentially a redundant gene for *PUB54* in clock rhythmicity (Feke *et al.*, 2019). *Mutation of the highly similar* PUB22*,* PUB23*, and* PUB24 has been shown to lead to an enhanced ROS burst after treatment with flg22 in *pub22/pub23/pub24* triple mutant and increased resistance to *Pst* which is comparable to wildtype in single knock out lines (Trujillo *et al.*, 2008). Hence, the weak but specific *impact as observed* in *pub54*-I and *pub54*-II during defense might rely on functional redundancy of PUB54 with other E3 ligases. Generation of a *pub54* x *pub56* mutant line and subsequent characterization with phytopathologic and molecular methods would be worth investigating potential redundancy and involvement in systemic defense responses of both PUBs.

4.2.3. HMP35 is ubiquitinated by PUB54 and degraded via the 26S proteasome

4.2.3.1. HMP35 was identified as interacting protein of PUB54

A Yeast2Hybrid screen identified the product of AT4G16380 as potential interacting protein of PUB54 (Figure 23). AT4G16380 encodes for the *heavy metal associated protein 35*

(*HMP35*) and harbors a heavy metal-associated (HMA) domain containing two conserved cysteines that are probably involved in metal binding and transfer (Bull & Cox, 1994; Gitschier *et al.*, 1998). A recent study aimed to characterize the HMA-containing protein family in rice and *Arabidopsis* (J. Li *et al.*, 2020). 55 HMPs were identified in *Arabidopsis* and are categorized in four different groups depending on their protein structure: HPPs (heavy metal-associated plant proteins), HIPPs (heavy metal-associated isoprenylated plant proteins), ATX1-like and P1B-ATPase (De Abreu-Neto *et al.*, 2013; Pedersen *et al.*, 2012; Puig *et al.*, 2007). Of these, HPPs and HIPP clades have the largest number of family members of which only a few were functionally described so far. HMA domain-containing proteins have been shown to play diverse rolls in plant development and stress resistance (De Abreu-Neto *et al.*, 2013; Williams *et al.*, 2000). Most investigations so far concern the involvement of HMPs in heavy metal detoxification with more data accumulating that HMPs might also affect immune-related processes. For example, yeast antioxidant protein1 (ATX1) is a small homeostasis factor which protects cells against reactive oxygen species by mediating transport and/or partitioning of copper (Lin & Culotta, 1995). The yeast ATX1 homologue in *Arabidopsis* (AtHMP14) is transcriptionally upregulated in response to *Pseudomonas syringae* according to the eFP browser (Winter *et al.*, 2007). *AtHIPP3* (also known as *AtHMP52*) was shown to be an negative regulator of SA-dependent immunity (Zschiesche *et al.*, 2015). During overexpression of *HIPP3*, expression of SA-target genes such as *NIM1-INTERACTING 1* (*NIMIN1*) is repressed. Furthermore, *HEAVY METAL ASSOCIATED PROTEIN 9* (*AtHMAD1* or *AtHMP09*) was shown to be involved in plant immunity as negative regulator with *hmad1* mutants being more resistant and showing induction of SAR genes (Imran *et al.*, 2016).

The *in vivo* performed BiFC experiment validated the data from the Y2H and showed *in planta* interaction of PUB54 and HMP35 (Figure 23 and Figure 25). Colocalization is a prerequisite for direct interaction between E3-ligase and substrate and could be identified to occur mainly in the nucleus (Figure 24). Also other E3 ligases such as CUL3 were shown to function in the nucleus ubiquitinating NPR1 (Spoel *et al.*, 2009). PUB17 is located in the nucleus positively regulating programmed cell death mediated by interaction with the BTB-BACK domain protein POB1 resulting in degradation of PUB17 (He *et al.*, 2015; Orosa *et al.*, 2017). Thus, PUB54 might be another PUB operating in regulation of nuclear localized proteins. Several HMA containing proteins such as heavy metal-associated isoprenylated plant proteins 26 (HIPP26) were described to be localized in the nucleus interacting with the drought stress related TF ATHB29 mediated by the HMA domain (Barth *et al.*, 2009). Furthermore, rice HIPP41 is localized to the nucleus and is involved in abiotic stress responses (De Abreu-Neto *et al.*, 2013). Thus, the localization of the PUB54/HMP35 interaction in the nucleus suggests the involvement of HMP35 in a nuclear process.

4.2.3.2. PUB54 is an active E3-ligase *in vitro* and directly targets HMP35 for ubiquitination

Biochemical studies using an *in vitro* ubiquitination assay proved PUB54 to be an active U-box dependent E3-ubiquitin ligase supporting previous reports (Mural *et al.*, 2013). Furthermore, PUB54 is capable for auto-ubiquitination and directly targets HMP35 for ubiquitination (Figure 26). Auto-ubiquitination is observable for most E3-ligases *in vitro* and interestingly, K181 and K185 located in the N-terminal domain were identified via MS analysis as potential auto-ubiquitination sites of PUB54 (Table 22). Auto-ubiquitination is a common mechanism to self-regulate protein prevalence and thereby regulate activity. The membrane bound E3-ubiquitin ligase really interesting new gene 1 (RING1, also known as ATL55) is a positive regulator of programed cell death in response to fungal pathogens and was found to be capable of auto-regulation by auto-ubiquitination (Lin *et al.*, 2008). The proteasome itself undergoes auto-ubiquitination at the proteasomal subunit Rpn13 to regulate breakdown of ubiquitin conjugates (Besche *et al.*, 2014). The PrDOS server for prediction of natively unordered protein regions predicts a large unordered region in PUB54 between amino acids 164-229 containing K181 and K185 (Ishida & Kinoshita, 2007) (appendix, Figure 43). Mainly studied in mammalian cells, posttranslational-modifications of E3-ubiquitin ligases within disordered regions were shown to influence localization, conformation, and enzymatic activity (Guharoy *et al.*, 2016). Therefore, auto-ubiquitination of PUB54 could potentially be a factor influencing E3 ligase activity by self-regulation of protein levels. To test if K181 and K185 are auto-ubiquitination sites of PUB54, an *in vitro* ubiquitination assay might be conducted with PUB54 bearing the lysine residues 181 and/or 185 mutated to arginine ("K-to-R" mutants), i.e., PUB54-K181R, PUB54-K185R, and PUB54-K181R-K185R.

The E2-binding cleft of the PUB54 U-box domain (Amino acids 232-306) has an essential function for E2 selectivity (Wiborg *et al.*, 2008). Substitution of Trp^{266} (located in the E2 binding cleft) with Ala eliminates enzyme activity and substitution with His altered selectivity. Wiborg and colleagues also assume that the E3 specificity is not solely determined by E2-E3 interactions but also other parameters such as interaction with additional domains or proteins (Wiborg *et al.*, 2008). PUB54 has been shown to interact with the E2 ubiquitin-conjugating enzyme Ubc13 and the *Solanum lycopersicum* Ubc13-homologue Fni13 to mediate Lys-63-linkase formation of polyubiquitin chains (Mural *et al.*, 2013; Wiborg *et al.*, 2008). Lys63 linkage is the second most abundant ubiquitin linkage in *Arabidopsis* but its biological role is not well understood (Kim *et al.*, 2013). Likely, Lys63-linked ubiquitin chains do not target substrates for proteolytic degradation but mediate regulatory roles in DNA-repair or immune response, during iron deficiency, or promotes endosome trafficking (Wenfeng Li & Schmidt, 2010; Mural *et al.*, 2013; Romero-Barrios & Vert, 2018; Wen *et al.*, 2008; Yu & Xie, 2017). Taken these data together, it is possible that

PUB54 mediates Lys63-linkages during auto-ubiquitination and substrate ubiquitination which can possibly be influenced by changed E2 selectivity allowing flexibility in PUB54-mediated ubiquitination in fluctuating environmental conditions.

Phosphorylation mediated by kinases is another PTM often acting in interplay with auto-ubiquitination to regulate PUB E3-ligase localization, stability, and activity *in vivo* (discussed in Trujillo, 2018). The A*rabidopsis* receptor kinases 1 and 2 (ARK1 and ARK2) phosphorylate PUB9 at its ARM domain and thereby altering its subcellular localization (Samuel *et al.*, 2008). PUB1 is phosphorylated by the lysin motif receptor-like kinase 3 (LYK3) in *Medicago truncatula* and negatively regulates the LYK3 pathway which is not mediated by PUB1-dependent ubiquitination of LYK3 (Mbengue *et al.*, 2010). PUB13 is so far the only described E3 ligase mediating ubiquitination of the interacting kinase while most reports highlight phosphorylation of the E3 ligase by the kinase in PUB-kinase interactions. In this specific case the lysin motif receptor-like kinase 5 (LYK5) is ubiquitinated and subsequently targeted for proteasomal degradation by PUB13 (Liao *et al.*, 2017). PUB22, a negative regulator of PTI, is phosphorylated by MPK3 at Thr62 and Thr88 but does not ubiquitinate MKP3 (Furlan *et al.*, 2017). PUB22 undergoes homodimerization and *trans*-ubiquitination mediating its degradation (Stegmann *et al.*, 2012). It was suggested that the phosphorylation at Thr62 at the rear site of the U-box domain inhibits homodimerization consequently leading to accumulation of PUB22 and substrate ubiquitination (Furlan *et al.*, 2017). Thus, phosphorylation events can be causal for E3-ligases to switch from auto-ubiquitination to substrate-ubiquitination. The *in vitro* ubiquitination assay of PUB54 using HMP35 as substrate showed high u-box dependent auto-ubiquitination activity and weak but specific substrate ubiquitination. (Figure 26) Considering the requirement for PUB22 to be phosphorylated by MKP3 for activity (Furlan *et al.*, 2017) it is conceivable that also PUB54 requires upstream kinases for full activation and therefore only weakly ubiquitinates HMP35 *in vitro* without addition of the appropriate kinase. The auto-ubiquitination activity was observed *in vitro* and *in vivo* in this project but the phosphorylation status was not investigated and thus remains unknown so far. Due to lacking knowledge of a potential upstream kinase, MS analysis of *in planta* expressed PUB54 would identify if PUB54 is phosphorylated *in vivo*.

However, interaction between PUB54 and HMP35 including ubiquitination of HMP35 could be observed *in vitro* and *in vivo*. One can consequently assume that ubiquitinated HMP35 is directed for proteasomal degradation possibly mediated by PUB54. Indeed, proteasome inhibition using bortezomib leads to accumulation of HA-HMP35 and appearance of a protein smear during transient expression indicating that HA-HMP35 is continuously degraded by the 26S proteasome under native conditions *in vivo* (Figure 29). A similar effect was observed in the degradation process of TF NPR1 mediated by the E3 ligase CUL3 when

the proteasome is inhibited by MG132 (Spoel *et al.*, 2009). The RING E3-ubiquitin ligase XBAT35 in tobacco ubiquitinates and targets its defense related substrate Accelerated Cell Death11 (ACD11) for proteasomal degradation. Inhibition of the 26S proteasome leads to an accumulation of ubiquitinated ACD11 (Liu *et al.*, 2017). Due to shown interaction and *in vitro* ubiquitination of HMP35 by PUB54, it is reasonable to assume that PUB54 is involved in the observed ubiquitination and proteasomal degradation of HMP35 *in vivo*.

4.2.4. HMP35 possesses a regulatory function in immunity during infections with *Pseudomonas*

4.2.4.1. HMP35 plays a role in defense responses

The single knock out of *pub54* leads to weak but distinct alterations in local and systemic immune responses in *Arabidopsis* and data obtained during this project strongly indicate that PUB54 targets HMP35 and thereby might influence defense responses. The role of HMP35 was therefore investigated during infections with *Psm* in *hmp35*-I and *hmp35*-II. *hmp35*-I was identified as knock out mutant and shows increased basal resistance but no further benefit from a previous priming stimulus. It seems that *hmp35*-I has a preformed immune status like primed wild type plants under both, primed and unprimed conditions (Figure 28). The open question is consequently, if *hmp35*-I displays increased resistance due to a constitutive priming status and is impaired to further react to triggering or if the enhanced immunity is a result of preformed PTI. As an example, the nucleotide hydrolyzing Nudix domain-containing protein 7 (NUDT7) shows enhanced resistance towards infections with virulent *Pseudomonas* when knocked out (in *nudt7*) and thus identified NUDT7 as negative regulator of basal defense resulting in increased resistance (Ge *et al.*, 2007). This observation is comparable to *hmp35*-I strongly indicating that HMP35 is a negative regulator in local defense. Consequently, PUB54-mediated ubiquitination and proteasomal degradation of HMP35 represents a feasible mode of action for defense activation. NUDT7 dampens salicylic acid (SA) accumulation and subsequent gene expression (Ogawa *et al.*, 2016). Similarly, *nudt7* was found to exhibit enhanced NPR1- and SA-dependent *PR1* expression (Ge *et al.*, 2007). SA is a central metabolite during local defense responses and induction of SAR (Bernsdorff *et al.*, 2016; Hartmann *et al.*, 2018; Kim & Hwang, 2014). Thus, interference with SA-dependent pathways might link a protein's involvement in basal as well as systemic immunity. It was discussed that the observed defense phenotype of *nudt7* is not caused by a constitutive disease resistance but rather by a constantly primed state leading to an accelerated defense reaction (Ge *et al.*, 2007). Molecular data are not available for *hmp35*-I and thus cannot suggest possible involvement of Pip/NHP or SA-mediated pathways. Assumed, that also HMP35 is involved in negative regulation of defense responses by a so far unknown mode of action, one could speculate that the outcome of *hmp35* is potentially comparable to *nudt7*. Future measurements of SA- and SAR-marker gene

expression such as *PR1* and *FMO1* as well as quantification of SA and Pip levels should be performed to evaluate the plant's state in local and systemic tissue of *hmp35*-I during infections. Priming sets the plant to an alert-state for future challenging infections accompanied by induction of genes (e.g. *PR1*) and phytohormone accumulation in systemic tissue distant from the local infection site (Delaney *et al.*, 1994; Durrant & Dong, 2004; Gaffney *et al.*, 1993; Ryals *et al.*, 1996). Thus, if investigations of phytohormone levels and defense gene expression show decreased defense responses in distal tissue (i.e., weak *PR1* and *FMO1* gene expression and low SA levels) it is a likely explanation that *hmp35*-I is set to a generally primed state in a comparable manner like *nudt7*. Increased basal resistance by absence of the negative regulator *HMP35* could be the consequence of a primed state and explains that *hmp35*-I does not further benefit from a previous priming stimulus due to a fully utilized priming potential. Generation of HMP34 overexpression lines is also desirable to further elucidate the impact of HMP35. If bacterial replication assays show increased susceptibility in comparison to Col-0, the negative regulatory role of HMP35 could be confirmed.

Future experiments should also aim to analyze a potential autoimmune phenotype in *hmp35*-I. Loss-of-function mutations of native regulators often lead to autoimmunity causing compromised organ development, elevated SA levels and constitutive defense activation (van Wersch *et al.*, 2016). The plant U-box E3-ubiquitin ligase PUB13 is a negative regulator of SA-mediated defense and knock out (*pub13*) leads to an autoimmune phenotype (Wei Li *et al.*, 2012; Zhou *et al.*, 2015). However, autoimmunity is not supported by the recent observation regarding the wild-type like appearance of *hmp35*-I.

hmp35-II is possibly affected in promotor function by tDNA insertion in the promotor region and is highly susceptible to *Pst* in unprimed conditions (Figure 27 and Figure 28). Supporting observations with *hmp35*-I that *HMP35* is a negative regulator of local defense, *HMP35* expression might be elevated in infected tissue leading to increased susceptibility. However, bacterial replication in systemic tissue of primed *hmp35*-II is comparable to *hmp35*-I and primed wild type plants. Either priming is not functional anymore due to the lack of HMP35 as positive regulator in systemic defense in *hmp35*-I or the plant already reached highest possible resistance and does not benefit from further priming. Knock out or overexpression of immune related components such as the calcium-dependent protein kinase 5 (CPK5) results in distinct resistance patterns (Guerra *et al.*, 2020). CPK5 was found to elicit a constitutive SA-dependent defense when overexpressed (Dubiella *et al.*, 2013). CPK5 positively regulates immunity resulting in enhanced local resistance comparable to primed wild type plants and hyper-resistance during priming (Guerra *et al.*, 2020). An effect for SAR as reported for CPK5 is not detectable for *hmp35* leading to the assumption that HMP35

either does not play a role in systemic defense or that HMP35 does not function as negative regulator in systemic defense, contrary to local immunity.

4.2.4.2. The HMA domain possibly mediates the function of HMP35

According to the analyzed *hmp35*-I mutant, HMP35 is possibly a negative regulator of basal resistance and *hmp35* might lead to constitutive priming. If HMP35 is also involved in establishment or maintenance of SAR remains unclear at this point of investigations. HPM35 is annotated as protein containing a predicted HMA domain. It is feasible to presume that the HMA domain conveys a main role in the function of the protein since no further domains could be identified. The mode of action of HMP35 mediated by the HMA domain is still an open question.

HMPs were initially described as proteins mainly involved in heavy metal transport and detoxification processes acting as metalloproteins or metallochaperone-like proteins (Tehseen *et al.*, 2010; Zorrig *et al.*, 2011). Heavy metal associated isoprenylated plant proteins (HIPPs) are centrally involved in Cd-detoxification (Tehseen *et al.*, 2010). Interestingly, HIPP3 (also known as HMP53) was found to be located to the nucleus and to be involved in transcription regulation by interaction with zinc-finger TFs. Functioning as zinc-binding metallochaperone, HIPP3 likely provides zinc to activate the TF LSD1 which is a negative regulator of basal defense and upstream of SA-dependent responses (Rustérucci *et al.*, 2001; Zschiesche *et al.*, 2015). With HMP35 being annotated as heavy metal transport and detoxification protein it may also function in transcriptional regulation by mediating activation of negatively regulating TFs.

Harold Henry Flor proposed the gene-for-gene model host-pathogen-interactions (Flor, 1971). The model describing disease causing avirulence (*Avr*) genes from the pathogen can be recognized by plant specific *R* gene products for resistance was continuously extended. Considering the structural composition of plant nucleotide-binding, leucine-rich repeat (NLR) intracellular immune receptors (NLRs) as *R* gene products, the integrated decoy model was developed (Cesari *et al.*, 2014). In this model, effector targeted proteins have been duplicated and fused to one NLR acting as bait to activate defense signaling upon effector binding at the second NLR. HMA domains were described as internal protein domains potentially functioning as integrated decoy domains (Cesari *et al.*, 2014; Maqbool *et al.*, 2015). During infections with *Magnaporthe oryzae* in rice, AVR1-CO39 and AVR-PikD are recognized by the NLRs RGA5 and PikP-1, both containing a HMA domain. The HMA domain was indeed found to be essential for effector binding (Guo *et al.*, 2018). Conformational changes were not observed in Pik-P-HMA upon effector binding supporting the hypothesis that NLR complexes might be re-arranged during effector-NLR interaction (Cesari *et al.*,

2014; Maqbool *et al.*, 2015). The mechanism by which downstream defense signaling is triggered remains unclear so far.

The effector HaRxL44 from *Hyaloperonospora arabidopsidis* was found to interact with several proteins from *Arabidopsis* including HMP35 and MED19a in the nucleus (Caillaud *et al.*, 2013). HaRxL44 serves as adaptor for the E3-ligases BOI and MBP1-like to mediate proteasomal degradation of MED19a leading to a shift from SA-responsive to jasmonate/ethylene (JA/Et)-signaling. Consequently, susceptibility to biotrophic pathogens is enhanced by attenuating SA-dependent gene expression (Caillaud *et al.*, 2013). It is generally assumed, that effector proteins target proteins in their host plant to increase virulence and to interfere with establishment of immune responses. Thus, the interaction between HaRxL44 and HMP35 hints that HMP35 is a component involved in immunity and interference is favorable for the pathogen's performance. The consequence of HaRxL44 interacting with HMP35 is not investigated yet but possibly undergoes a similar mode of interaction by serving as adapter to interfere with downstream defense components.

Recently, HMAD1 was identified as the closest relative of HMP35 (Li *et al.*, 2020). HMAD1 was shown to be a negative regulator of basal defense, *R*-gene mediated resistance and SAR (Imran *et al.*, 2016). Molecular data furthermore suggest that HMAD1 influences immunity by regulating the SA-dependent pathway but underlying mechanisms remain elusive (Imran *et al.*, 2016). Considering the close relation of HMAD1 and HMP35 it is feasible to assume that also HMP35 plays similar roles as negative regulator in immunity. This goes along with the observation of increased basal resistance in *hmp35*-1 and is furthermore supported by the SA to JA shift mediated by the interacting HaRxL44 (Caillaud *et al.*, 2013).

4.2.5. PUB54 mediates defense responses by regulation of HMP35

To sum up, the HMA domain is highly conserved but may be integrated in different types of proteins mediating multiple cellular processes. However, the mechanism by which pathogenic effectors and endogenous proteins interact with HMAs appears to be a relatively conserved mechanism (Guo *et al.*, 2018). Future investigation should aim to analyze the underlying mechanism by which HMP35 might contributes to immunity and if this mechanism depends on the HMA domain.

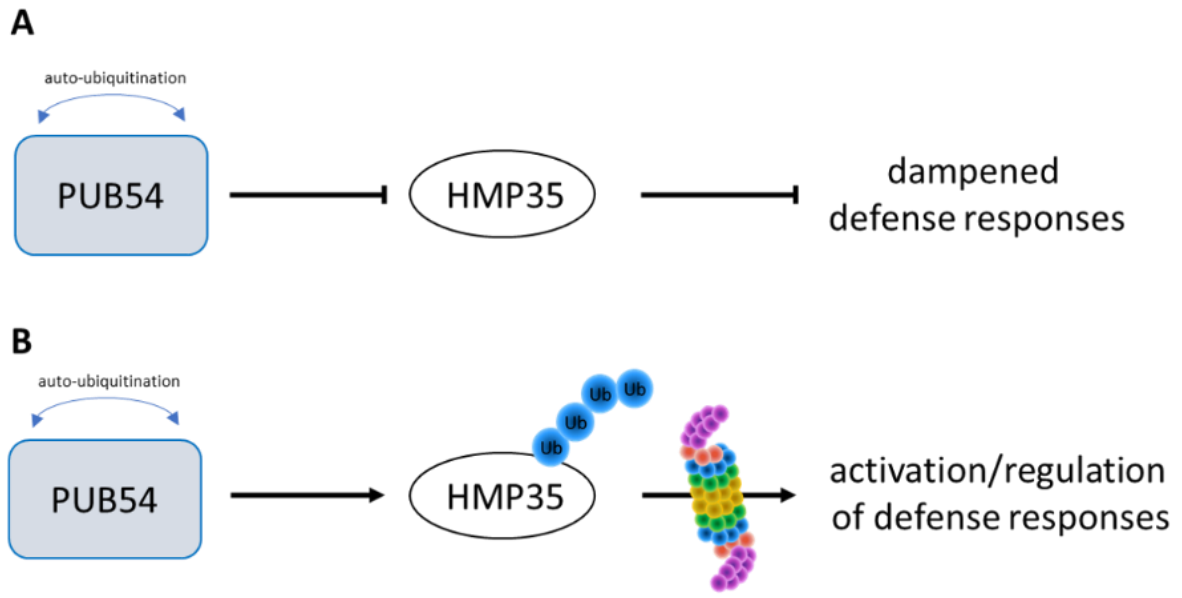

Figure 41: A model of how PUB54 might contribute to immune responses. Autoubiquitination of PUB54 self-regulates abundance and activity of the E3-ligase in unstressed conditions (A) and during infections with virulent *Pseudomonas* (B). During self-regulation of PUB54, the negative regulator of defense HMP35 accumulates and subsequently dampens immune responses (A). During infections, HMP35 is ubiquitinated by PUB54 and immune responses are activated (B).

Experiments performed in this project showed that HMP35 is potentially a negative regulator of immunity and is targeted and ubiquitinated by PUB54 to regulate downstream defense signaling. These data suggest a linear cascade of events implemented in a model. PUB54 and HMP35 both prevail in the nucleus. During unstressed conditions, PUB54 undergoes self-regulation by autoubiquitination (Figure 41A). Possibly, phosphorylation by an upstream kinase or other so far unknown signals shifts the auto-ubiquitination activity of PUB54 to substrate targeting. HMP35 likely acts as negative regulator suppressing defense in an HMA domain-mediated manner. Ubiquitination by PUB54 and subsequent degradation of HMP35 is required for activation of local defense responses during infections and might be involved in SAR (Figure 41B).

4.2.6. *ARI12* transcription can be primed and depends on SA- and Pip/NHP mediated pathways (induction by SAR metabolites)

Using RNAseq, *ariadne 12* (*ARI12*) was identified as differentially expressed E3-ubiquitin ligase during *Psm*-induced priming in systemic tissue from *Arabidopsis*. The initial observation was verified in an independent experiment showing gene induction in systemic tissue after priming or triggering and hyper-induction of gene expression in primed and triggered tissue (Figure 32). Weak gene induction during priming is likely a mechanism by which the plant prepares for potentially upcoming challenging infections to induce SAR in a cost effective manner (Hilker *et al.*, 2016). Furthermore, the observed hyper-induction is highly reminiscent of other well established marker genes such as *PR1*, *FMO1* and *ALD1* (Kiefer & Slusarenko, 2003; Mishina & Zeier, 2006). *ARI12* expression was found to be induced upon UV-B radiation in *Arabidopsis* leaves (Lang-Mladek *et al.*, 2012; Xie *et al.*, 2015). Furthermore, *ARI12* has been shown to be induced upon hypoxia in *ethylene response factor (ERF73*/*HRE1)-RNAi* lines showing increased ethylene sensitivity (Yang *et al.*, 2011). A link to biotic stress responses was not published yet. However, the molecular data obtained in this study strongly suggest a possible role of *ARI12* in local and systemic defense responses during infections with virulent *Pseudomonas*.

Among others, SA, Pip, and the active derivate NHP are central metabolites involved in induction of SAR in interdependent and synergistic signaling pathways (Vlot *et al.*, 2020). SA accumulates in local and systemic tissue during infections with (hemi-)biotrophic bacteria and is required but not sufficient for full SAR induction by activation of downstream SA-responsive genes (Bernsdorff *et al.*, 2016; Hao *et al.*, 2018). *ARI12* expression is not inducible by exogenous application of SA while *PR1* is strongly induced as expected (Figure 33). Thus, data implicate that *ARI12* is transcriptionally activated during priming in systemic tissue in a SA-independent manner. On the contrary, *npr1* mutants with defect in SA-dependent defense (Cao *et al.*, 1994; Pieterse *et al.*, 1998) show weak induction of *ARI12* during priming and triggering in this project (Figure 34). It has been shown, that a functional SA-pathway is required but not sufficient to mount full SAR-responses (Hao *et al.*, 2018) which is reflected in the *ARI12* expression. However, a functional Pip-pathway has been found to be essential for full induction of SAR (Bernsdorff *et al.*, 2016; Hartmann *et al.*, 2018). Present data indicate that expression of *ARI12* is not enhanced during priming and /or triggering in Pip-defective *fmo1* mutants. This is in line with transcriptional upregulation of *ARI12* after Pip treatment (Hartmann *et al.*, 2018). Interestingly, 24 genes were found to be upregulated during hypoxia in the ethylene sensitive *ERF73*/*HRE1-RNAi* line including *ARI12, FMO1,* and *CBP60g* (Yang *et al.*, 2011). CBP60g was recently found to function as key regulatory TF promoting Pip-biosynthesis (Sun *et al.*, 2018). *FMO1* is required for the conversion of Pip to

the active derivate NHP (Hartmann *et al.*, 2018). Mutual upregulation of gene transcription indicates a certain co-regulation during stress responses, thus supporting the potential involvement of *ARI12* in Pip-dependent regulation of SAR. Consequently, one can postulate that *ARI12* is induced during SAR in partially SA-dependent manner but fully depends on a functional Pip-pathway for gene induction.

4.2.7. ARI12 protein accumulates systemically during priming

Gene induction does not necessarily correlate with protein accumulation which can further be regulated by post-transcriptional processes *in vivo*. The experiments with *Arabidopsis K8* and *IIB1* carrying *pmARI12::ARI12-GFP* clearly indicate that endogenous ARI12 accumulates in systemic tissue after priming with *Psm*, SA, or Pip (Figure 35). This effect was stronger in *K8* than in *IIB1*. These so-called genomic position effects may result from the location of the inserted gene in a chromosome to different promotor, enhancer or coding regions of endogenous genes leading to varying levels of expression (Grigliatti & Mottus, 2013). It is hence important to investigate independent lines to bypass false implications depending on position effects. Genomic position effects possibly explain the different level of protein accumulation in *K8* and *IIB1*. However, the overall trend observed in both lines indicates that single metabolite-induced priming by watering with Pip or local infiltration of SA induces accumulation of ARI12-GFP in systemic tissue. It is not clear yet, if local application of SA promotes ARI12-accumulation in treated leaves due to differing observations in *K8* and *IIB1* and should therefore be investigated in future experiments. Interestingly, ARI12 protein levels are highest in systemic tissue after priming with *Psm* potentially indicating that either SA- and Pip-dependent signaling act synergistically or other SAR-involved factors contribute to ARI12 accumulation in systemic tissue. The SAR-involved mitogen-activated protein kinases (MKP3 and MPK6) have been suggested to accumulate as inactive cellular signal amplifiers during priming which are activated upon challenging infections for enhanced defense (Bruce *et al.*, 2007; Conrath, 2011; Conrath *et al.*, 2006). Recently, proteo-metabolomic analysis of transgenic rice expressing *AtNPR1* unraveled large scale accumulation of defense-related proteins during infections with *Rhizoctonia solani* (Karmakar *et al.*, 2019). Known defense related proteins such as MPK6, heat stress transcription factor A-2A (HSF2A) and a 14-3-3 protein (14-3-3-GF14f) were found to specifically accumulate after infection (Karmakar *et al.*, 2019). Protein accumulation is hence a prevalent mechanism in different organisms in response to infections. During transient expression in tobacco, localization of ARI12-GFP was determined to the nucleus and the cell periphery (Figure 36). Accumulation of ARI12 during SAR in different compartments of the plant cell is therefore a highly interesting observation worth for deeper investigations to understand the biological relevance.

4.2.8. ARI12 is involved in regulation of priming

Bacterial replication in systemic tissue of *ari12* unprimed plants is equal to wild type but resistance is slightly increased in primed plants when compared to Col-0 (Figure 37) indicating that ARI12 is not required for local defense. Both ARI12-OX lines display enhanced basal resistance and similar bacterial replication in primed plants comparable to primed Col-0. Thus, the question arises if the basal resistance is increased due to an autoimmune phenotype and priming is defective or if the plants are constitutively primed. Both effects have been found in transgenic plants with altered protein levels (i.e., knock out or overexpression) of defense-involved proteins such as *enhanced disease resistance 1 (edr1*) and the membrane bound nucleotide-binding domain leucine-rich repeat (NLR) *resistant to Pseudomonas syringae 2* (*RPS2*) (Frye & Innes, 1998; Li *et al.*, 2019). In *Arabidopsis*, *enhanced disease resistance 1 (edr1*) displays constitutively enhanced resistance toward *Pst* and only shows increased expression of *PR1* in response to infections assuming a role of EDR1 in priming (Conrath, 2006; Frye & Innes, 1998). Together with *edr1*, also *edr2* displays faster and stronger defense response upon infections without auto-activation of defense. Interestingly, this phenotype is highly similar to *ttm2,* impaired in the *tripolyphosphatase triphosphate tunnel metalloenzyme 2*. However, SAR is strongly enhanced in *ttm2* which is not the case for *edr1* and *edr2* (Ung *et al.*, 2014). These data therefore suggest that common phenotypes do not necessarily imply similar underlying molecular mechanisms. In terms of *ttm2*, it was concluded that *TTM2* acts in fine-tuning of defense responses (Ung *et al.*, 2014). Overexpression of the *Arabidopsis* NLR *RPS2* in rice has been shown to confer resistance against *M. oryzae* and to prime for defense responses without constitutive activation of defense (Li *et al.*, 2019). Instead, *AtRPS2* expression likely induces quick and strong induction of the defense-related genes upon pathogenic attack (Li *et al.*, 2019). *ari12* does not lead to an obvious SAR-phenotype but *ARI12*-overexpression confers increased resistance to *Pst.* Mutations of negative regulators often leads to constitutive defense activation (van Wersch *et al.*, 2016). *PR1* and *FMO1* are well-established marker genes to study SA-dependent defense induction and Pip/NHP dependent signaling during SAR (Bernsdorff *et al.*, 2016; Hartmann *et al.*, 2018; Kiefer & Slusarenko, 2003). Molecular data from *ari12* and ARI12-OX1 and 2 did not suggest constitutive *PR1* and *FMO1* expression in uninfected tissue indicating that altered *ARI12* expression does not induce an auto immune phenotype (Figure 38 Instead, plants might experience faster and /or stronger priming by *ARI12* expression as observed in *RPS2 expressing lines or edr1 / edr2 lines* (Ung *et al.*, 2014).

While *PR1* expression is not affected in *ari12, ARI12*-OX1 and *ARI12*-OX2 during priming and/or triggering, *FMO1* was found to be enhanced in *ari12* experiencing priming and in *ARI12*-OX lines upon infections. These data therefore indicate that presence of the level of ARI12 proteins does not influence SA-dependent signaling but Pip/NHP induced defense

response. *fmo1* has been found to display local resistance against *Psm* comparable to wild-type plants and *FMO1*-overexpression leads to enhanced disease resistance against *Pst* (Koch *et al.*, 2006; Mishina & Zeier, 2007). These resistance-phenotypes are highly reminiscent of *ari12* and *ARI12*-OX. Endogenous *ARI12* was found to be induced in systemic tissue upon priming and/or triggering dependent on functional *FMO1* (Figure 32 and Figure 34). Overall, a certain co-regulation of *FMO1* and *ARI12* and overlapping phenotypes of *fmo1* and *ari12* mutants and OX-lines suggest that *ARI12* might be involved in Pip/NHP-mediated SAR.

Induction of *ARI12* therefore appears to enable the plant to fine-tune Pip/NHP-dependent SAR as a positive regulator in systemic tissue and ARI12-OX likely mimics a primed state. This is in line with the observed increased resistance towards *Pst* in primed *ari12* (showing enhanced *FMO1* expression during priming) and increased resistance during ARI12-OX (with enhanced expression of *FMO1* at the infection site). Thus, physiological and molecular data strongly suggest that balanced ARI12 protein levels are required for onset of SAR by positively regulating the Pip/NHP-mediated branch of systemic defense.

4.2.9. ARI12 is an active E3-ubiquitin ligase targeting proteins to modulate SAR

4.2.9.1. ARI12 is an active E3 ligase *in vitro* and *in planta*

ARI12 has been shown to be an active E3 ubiquitin ligase *in vitro* functioning with a RING-HECT mechanism and requiring mono-ubiquitination for activation (Xie *et al.*, 2015). The E3 ligase activity and mono-ubiquitination of ARI12 was verified in this project in an *in vitro* ubiquitination assay and *in vivo* during transient expression in tobacco (Figure 39 and Figure 40). However, the specific ubiquitination site of ARI12 remained unknown. Transiently expressed ARI12-GFP was extracted from tobacco and subsequently measured by LC-MS/MS to identify the (auto-)ubiquitination site of ARI12 (Table 23). Sequence alignment of the ARI12 RING2 domain with homologues from other organisms showed that C281 is highly conserved among ARI ligases but is replaced in ARI12 by Serine (S281). While a lysine residue of the substrate is the canonical ubiquitination site, also non-canonical linkages can be formed between serine and the c-terminal glycine 76 of ubiquitin via an ester-bonds (Kravtsova-Ivantsiv & Ciechanover, 2012; McDowell & Philpott, 2013). S281 of ARI12 was consequently suggested as a potential ubiquitination site of ARI12 (Xie *et al.*, 2015). With RING1-IBR-RING2 (RBR) E3s found in all eukaryotes, the activity of this E3 ligase class was considered to rely on the conserved cysteine in the RING2 domain (Marín *et al.*, 2004;

Wenzel *et al.*, 2011). Autoinhibited RBR E3s require allosteric activation by ubiquitin or ubiquitin-like molecules to allow recruitment of E2~Ub thioester intermediates via the RING1. Ubiquitin is then transferred from E2 to the conserved cysteine in the RING2 domain which subsequently mediates the ubiquitin transfer to the bound substrate by nucleophilic attack (Cotton & Lechtenberg, 2020). However, despite lacking the conserved cysteine, ARI12 activity was found *in vitro* and *in vivo* nonetheless indicating functional E3 ligase activity. Active sites of enzymes contain amino acids able to bind substrates in order to catalyze the enzymatic step. Besides cysteine, also serine is capable of performing nucleophilic catalysis as required during E3-mediated substrate ubiquitination (Cotton & Lechtenberg, 2020). The peptide covering S281 of ARI12 was identified in the present MS-dataset without mass shift, which would be expected in peptides carrying a di-glycine residue resulting from ubiquitinated amino acids after tryptic digestion. To test if this peptide is also comprised in the sample with a GlyGly-residue the analysis was repeated integrating the mass shift potentially caused by a di-glycine residue. The second analysis emerged no mass shift for S281 but interestingly for K474 located in the c-terminal leucine-rich domain 2. ARI12 consists like other ARIs in *Arabidopsis* of a conserved acid-rich, leucine-rich1, RING1-IBR-RING2, coiled-coil, and leucine-rich2 region (Mladek *et al.*, 2003). The authors propose the leucine-rich2 region for protein regulation by post-translational modification (Mladek *et al.*, 2003). Hence, the identification of K474 as putative (auto-)ubiquitination site remains to be experimentally verified but suggest that ARI12 itself is regulated by the attachment of ubiquitin. This is further in line with the assumption that (auto-)ubiquitination is required for activation (Xie *et al.*, 2015). In the next step, ARI12-K474R mutants should be generated and tested in an *in vitro* ubiquitination assay and during transient expression *in vivo* for auto-ubiquitination activity to verify K474 as lysine residue required for ARI12 activation.

4.2.9.2. Potential substrates of ARI12 were identified using mass spectrometry

Experiments conducted in this project indicate that ARI12 is involved in onset of SAR by regulating the Pip/NHP-mediated branch of systemic defense by so far unknown underlying mechanisms. Data derived from experiments in this project suggest that the active E3-ubiquitin ligase ARI12 undergoes self-regulation and is thereby involved in defense and priming responses. (Figure 37, Figure 38, and Figure 39). Identification of potential substrates is thus central to evaluate and further understand the biological relevance of ARI12.

Transcription factors are nuclear key regulators of gene expression with either positive or negative effect in gene expression upon binding. Assuming a direct way of regulation, nuclear localized ARI12 might be involved in targeting and ubiquitination of TFs regulating

FMO1. The TF SAR-deficient 1 (SARD1) and Calmodulin Binding Protein60-like g (CBP60g) have been found to transcriptionally control biosynthesis of NHP by targeting *ADL1* and *FMO1* promotors (Sun *et al.*, 2015). RNAseq of Pip-primed plants revealed strong induction of stress related WRKY and NAC-family TFs (Hartmann *et al.*, 2018). Possibly, ARI12 could be involved in fine-tuning of defense responses by targeting TFs controlling Pip/NHP-related gene expression. An *in planta* approach used for potential substrates of ARI12 by transiently expressing GFP-ARI12 *N. benthamiana* followed by precipitation using a GFP-trap and subsequent LC-MS/MS analysis (Table 24). Via this method, ARI12, GFP, ubiquitin and 20 potentially interacting proteins were identified with high confidence. Ubiquitin 3 and 4 were identified with 93% coverage giving strong indications that (auto-)ubiquitinated ARI12 and/or ubiquitinated proteins were present in the tested samples. Among the 20 identified potential substrates most proteins have not been described in immune related context and no TF has been detected. However, identified proteins such as the heat-shock protein 81-2 (HSP81-2, also known as HSP90.2), the glyceraldehyde-3-phosphate dehydrogenase (GAPA-2), and catalases 2 and 3 (CAT2 and CAT3) represent interesting candidates and are therefore further discussed here.

The heat-shock protein 81-2 (HSP81-2 or HSP90.2) belonging to the HSP90 family was identified as potential substrate of ARI12. Expression is not induced by heat but by indole acetic acid (IAA) (El-Mergawi & Abd El-Wahed, 2020). Interestingly, SA and IAA share chorismate as common precursor (Pérez-Llorca *et al.*, 2019). The chaperone activity of HSP90 is required for activation of intracellular nucleotide binding domain, leucine rich repeat proteins (NB-LRR) in infections which are kept in inactive form in uninfected conditions (Hubert *et al.*, 2003; Kadota & Shirasu, 2012; Schulze-Lefert, 2004). The bacterial effector HopBF1 interacts with HSP90 for phosphorylation, thereby inhibiting the chaperone's ATPase activity (Lopez *et al.*, 2019). Thus, ARI12 might be a novel component involved in fine-tuning of NB-LRR activation especially in local defense responses by potentially targeting HSP90.2 for proteasomal degradation or re-localization depending on the type of mediated ubiquitination.

The glyceraldehyde-3-phosphate dehydrogenase (GAPA-2) of the GAPDH-family is involved in the Calvin cycle and has been identified as SA-binding protein (SABPs) but the specific effect of SA binding is unknown (Pokotylo *et al.*, 2019; Tian *et al.*, 2015). During glycolysis, glyceraldehyde 3-phosphate is converted to 1,3-bisphosphoglycerate by GAPDHs accompanied by reduction of NAD^+ to NADH (Rius *et al.*, 2008). The reverse reaction generates $NADP^+$ from NADPH by GAPDHs in the carbon cycle (Baalmann *et al.*, 1995). Consequently, the $NAD(P)^+$ /$NAD(P)H^+$ ratio and cellular redox could be shifted by regulation of GAPDH-levels such as GAPA-2. GAPA-2 was here detected as possible substrate of ARI12 thus suggesting that ARI12 could be involved in regulation of $NAD(P)^+$ /$NAD(P)H^+$ by

influencing substrate degradation or stabilization. $NAD(P)^+$ are universal electron carriers which can be released to the extracellular space ($eNAD(P)^+$) functioning as putative mobile SAR signal (Berger *et al.*, 2004; Billington *et al.*, 2006; Chenggang Wang *et al.*, 2019). Application of $eNAD(P)^+$ has been found to induce defense-like transcriptional changes (Zhang & Mou, 2009). The lectin receptor kinase VI.2 (LecRK-VI.2) is a potential receptor for mobile $eNAD(P)^+$ acting in concert with brassinosteroid insensitive1-associated kinase1 (BAK1) as central component in SAR (Wang *et al.*, 2019). BAK1 is a multi-functional adaptor protein with intracellular kinase domain interacting with and phosphorylating diverse proteins such as Catalase 2 (CAT2) and CAT3 (Zhang *et al.*, 2020). Both, CAT2 and CAT3 were identified as putative ARI substrate in the MS analysis. The hydrogen peroxide scavenging enzymes CAT2 and CAT3 regulate cellular H_2O_2 levels together with CAT1 thereby influencing cellular redox level (Du *et al.*, 2008; Frugoli *et al.*, 1996; Sies, 2017). Thus, redox changes may occur by shifted $NAD(P)^+$ /$NAD(P)H^+$ ratio or H_2O_2 levels during SAR. During redox change in SAR, the SA master regulator NPR1 is switched from oligomeric to monomeric state allowing for nuclear import which is required for SA-mediated SAR induction (Lee *et al.*, 2015). It is hence possible, that ARI12 is a novel component involved in regulation of GAPDH and CAT levels to regulate ROS and $eNAD(P)^+$ levels. ROS has been shown to induce SAR in concentration dependent manner and to function in a linear NO←→ROS→AzA→G3P signaling cascade in parallel with SA-mediated signaling (Wang *et al.*, 2014). Pip acts upstream of the self-amplifying NO←→ROS and operates in a feedback loop with G3P in systemic tissue during SAR (Wang *et al.*, 2018). Thus, literature provides excellent hints that ARI12 possibly contributes to SAR by mediating degradation or stabilization of substrates such as CAT2, CAT3, or GAPA-2 to regulate ROS and $NAD(P)^+$ /$NAD(P)H^+$ levels in a regulatory feedback-loop with Pip-mediated SAR acting in parallel with SA signaling. However, the interconnection of $eNAD(P)^+$ with other SAR components remain unclear (Wang *et al.*, 2019).

Direct interactions of ARI12 with CAT2, CAT3, or GAPA-2 remain to be experimentally verified in future investigations by applying several methods such as Y2H and BiFC. Verified interaction between ARI12 and the potential interacting proteins are highly interesting for further testing in *in vitro* ubiquitination assays in order to investigate if these proteins are targeted and ubiquitinated by ARI12 during these interaction events.

4.2.10. ARI12 is a novel component modulating Pip-depending SAR-pathways

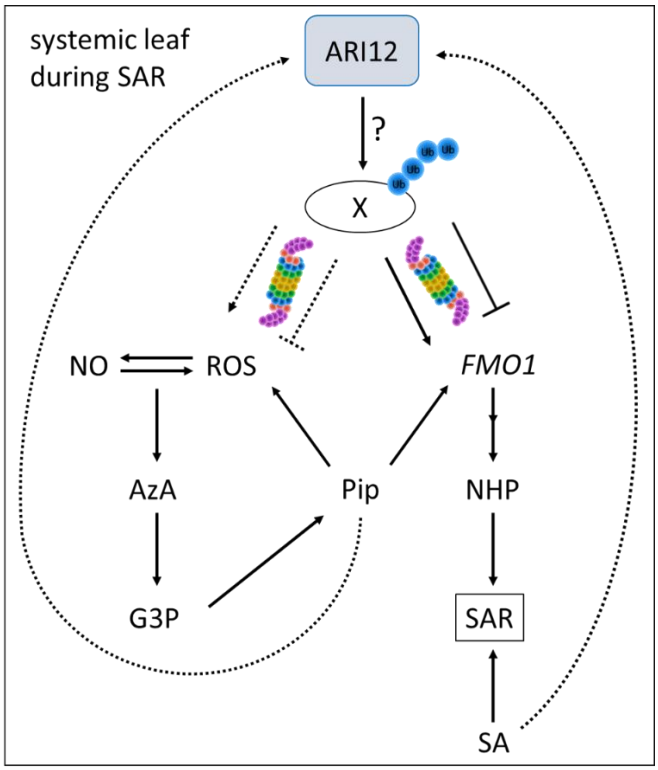

Figure 42: A model for the role of ARI12 during systemic defense. Infections with virulent bacteria induce *ARI12* and ARI12 protein accumulates dependent on and likely mediated by Pip and SA. ARI12 targets proteins for ubiquitination and thereby influences two interdependent branches of SAR. ARI12 regulates *FMO1* expression thereby affecting NHP-mediated SAR (Hartmann *et al.*, 2018). Additionally, ARI12 might influence ROS production which is involved in the linear NO←→ROS→AzA→G3P signaling cascade leading to increased Pip synthesis and subsequent increase in ROS production (Caixia Wang *et al.*, 2014, 2018). Hence, ARI12 is involved two feed-forward loops both mediating Pip/NHP-dependent SAR. Solid lines display observed signaling events while dashed lines indicate potential connections. The main text describes indicated events in detail.

Data from this project strongly suggest a regulatory role of *ARI12* in a feedback-loop in the onset of SAR after infection with (hemi-)biotrophic bacteria (Figure 42). Pip/NHP and SA-dependent signaling act in concert to induce SAR (Vlot *et al.*, 2020). Balanced ARI12 protein level is possibly required to maintain required gene expression of *FMO1* potentially mediated in a direct path by ARI12 controlling so far unknown transcription factors. Consequently, SAR induction by NHP could be regulated by ARI12. Another potential role of ARI12 could be targeting of proteins such as GAPA-2, CAT2, or CAT3 thereby regulating ROS. ROS has been shown to be involved in a cascade of NO←→ROS→AzA→G3P positively influencing Pip (Wang *et al.*, 2014). Thus, ARI12 could fine-tune Pip-mediated SAR in an indirect way via ROS. Vice versa, *ARI12* is controlled via SA- and Pip-dependent mechanisms. Taken together, ARI12 is likely a novel component involved in modulating Pip/NHP-dependent SAR in synergistic and interdependent feed-forward loops.

5. Appendix

Table 25: RNAseq - Top 100 differentially expressed genes in systemic tissue of Col-0 during priming (compared to systemic mock infiltrated Col-0). base mean >10; padj >0,1; sorted by Log2FC.

	Locus	Annotation	baseMean	log2Fold Change	padj
1	AT4G11170	Disease resistance protein (TIR-NBS-LRR class) family(AT4G11170)	16,01	7,26	4,6E-06
2	AT4G05540	P-loop containing nucleoside triphosphate hydrolases superfamily protein(AT4G05540)	11,83	6,83	3,9E-05
3	AT2G13810	AGD2-like defense response protein 1(ALD1)	125,87	6,45	2,8E-25
4	AT5G40010	AAA-ATPase 1(AATP1)	36,09	5,95	7,4E-08
5	AT4G21490	NAD(P)H dehydrogenase B3(NDB3)	19,90	5,74	2,9E-02
6	AT3G01420	Peroxidase superfamily protein(DOX1)	10,62	5,68	4,1E-03
7	AT3G28510	P-loop containing nucleoside triphosphate hydrolases superfamily protein(AT3G28510)	150,19	5,50	3,1E-06
8	AT3G45130	lanosterol synthase 1(LAS1)	23,60	5,44	5,7E-07
9	AT2G14610	pathogenesis-related protein 1(PR1)	2907,99	5,22	7,9E-04
10	AT5G51465		28,48	5,21	3,9E-07
11	AT1G33960	P-loop containing nucleoside triphosphate hydrolases superfamily protein(AIG1)	477,09	5,11	1,0E-11
12	AT4G13890	Pyridoxal phosphate (PLP)-dependent transferases superfamily protein(EDA36)	37,08	5,03	1,0E-09

13	AT2G29470	glutathione S-transferase tau 3(GSTU3)	11,97	5,03	4,2E-03
14	AT1G51860	Leucine-rich repeat protein kinase family protein(AT1G51860)	25,28	5,02	9,7E-07
15	AT1G19250	flavin-dependent monooxygenase 1(FMO1)	37,70	5,01	1,1E-07
16	AT5G11920	6-&1-fructan exohydrolase(cwINV6)	58,28	4,82	7,6E-15
17	AT1G17180	glutathione S-transferase TAU 25(GSTU25)	10,76	4,78	6,3E-03
18	AT4G16260	Glycosyl hydrolase superfamily protein(AT4G16260)	66,48	4,77	1,7E-02
19	AT1G65483	hypothetical protein(AT1G65483)	10,56	4,76	7,4E-04
20	AT1G73260	kunitz trypsin inhibitor 1(KTI1)	37,24	4,75	4,7E-03
21	AT1G66960	Terpenoid cyclases family protein(LUP5)	347,66	4,75	3,5E-49
22	AT1G09080	Heat shock protein 70 (Hsp 70) family protein(BIP3)	659,41	4,73	1,2E-59
23	AT4G00700	C2 calcium/lipid-binding plant phosphoribosyltransferase family protein(AT4G00700)	255,88	4,73	7,7E-40
24	AT2G30770	cytochrome P450 family 71 polypeptide(CYP71A13)	70,27	4,72	9,6E-04
25	AT2G03130	Ribosomal protein L12/ ATP-dependent Clp protease adaptor protein ClpS family protein(AT2G03130)	11,50	4,70	7,9E-03
26	AT3G13610	2-oxoglutarate (2OG) and Fe(II)-dependent oxygenase superfamily protein(AT3G13610)	32,46	4,69	2,8E-06
27	AT4G10500	2-oxoglutarate (2OG) and Fe(II)-dependent oxygenase superfamily protein(AT4G10500)	665,71	4,67	6,1E-88

28	AT1G14880	PLANT CADMIUM RESISTANCE 1(PCR1)	7154,24	4,66	7,0E-61
29	AT3G21080	ABC transporter-like protein(AT3G21080)	14,29	4,63	2,4E-04
30	AT3G55970	jasmonate-regulated gene 21(JRG21)	45,82	4,61	2,5E-02
31	AT5G24200	alpha/beta-Hydrolases superfamily protein(AT5G24200)	440,45	4,60	4,0E-16
32	AT2G43570	chitinase(CHI)	1603,39	4,57	1,0E-07
33	AT3G57260	beta-1,3-glucanase 2(BGL2)	8208,20	4,57	3,5E-68
34	AT3G11340	UDP-Glycosyltransferase superfamily protein(UGT76B1)	26,45	4,49	6,5E-08
35	AT1G66700	S-adenosyl-L-methionine-dependent methyltransferases superfamily protein(PXMT1)	22,17	4,47	3,6E-05
36	AT3G46080	C2H2-type zinc finger family protein(AT3G46080)	26,03	4,38	1,6E-05
37	AT4G22070	WRKY DNA-binding protein 31(WRKY31)	11,89	4,38	6,3E-03
38	AT4G04500	cysteine-rich RLK (RECEPTOR-like protein kinase) 37(CRK37)	143,97	4,31	1,3E-25
39	AT4G21850	methionine sulfoxide reductase B9(MSRB9)	101,31	4,30	8,9E-22
40	AT5G09290	Inositol monophosphatase family protein(AT5G09290)	77,92	4,22	5,2E-16
41	AT2G43140	basic helix-loop-helix (bHLH) DNA-binding superfamily protein(AT2G43140)	17,85	4,17	3,7E-06
42	AT5G47850	CRINKLY4 related 4(CCR4)	42,11	4,15	9,2E-11
43	AT3G02840	ARM repeat superfamily protein(AT3G02840)	13,05	4,12	1,2E-04
44	AT3G15536	ncRNA(AT3G15536)	176,46	4,11	4,6E-22

45	AT1G01680	plant U-box 54(PUB54)	151,74	4,11	1,7E-25
46	AT3G51860	cation exchanger 3(CAX3)	273,30	4,03	1,4E-41
47	AT3G24900	receptor like protein 39(RLP39)	82,17	4,02	2,8E-20
48	AT1G16420	metacaspase 8(MC8)	22,27	4,01	1,5E-06
49	AT5G25260	SPFH/Band 7/PHB domain-containing membrane-associated protein family(AT5G25260)	90,53	4,00	9,9E-19
50	AT5G54550	hypothetical protein (DUF295)(AT5G54550)	14,58	3,98	1,2E-02
51	AT3G25010	receptor like protein 41(RLP41)	1185,41	3,92	9,9E-66
52	AT1G32960	Subtilase family protein(SBT3.3)	180,75	3,88	2,3E-02
53	AT3G57240	beta-1,3-glucanase 3(BG3)	1709,52	3,87	7,0E-46
54	AT1G65610	Six-hairpin glycosidases superfamily protein(KOR2)	14,35	3,86	5,3E-05
55	AT1G44130	Eukaryotic aspartyl protease family protein(AT1G44130)	27,00	3,86	5,8E-05
56	AT3G48850	phosphate transporter 3;2(PHT3;2)	28,57	3,86	4,1E-06
57	AT2G35070	transmembrane protein(AT2G35070)	15,29	3,83	1,2E-03
58	AT1G21240	wall associated kinase 3(WAK3)	342,51	3,80	8,4E-27
59	AT3G50770	calmodulin-like 41(CML41)	31,77	3,80	1,8E-08
60	AT3G14280	LL-diaminopimelate aminotransferase(AT3G14280)	51,60	3,78	2,3E-11
61	AT3G09940	monodehydroascorbate reductase(MDHAR)	52,71	3,78	2,1E-11
62	AT4G23150	cysteine-rich RLK (RECEPTOR-like protein kinase) 7(CRK7)	418,03	3,78	4,0E-29
63	AT2G38240	2-oxoglutarate (2OG) and Fe(II)-dependent oxygenase superfamily protein(AT2G38240)	18,26	3,77	1,9E-03

64	AT4G10860	hypothetical protein(AT4G10860)	91,68	3,76	9,5E-02
65	AT5G22530	hypothetical protein(AT5G22530)	16,01	3,74	1,8E-05
66	AT1G79680	WALL ASSOCIATED KINASE (WAK)-LIKE 10(WAKL10)	13,04	3,74	1,1E-03
67	AT4G04540	cysteine-rich RLK (RECEPTOR-like protein kinase) 39(CRK39)	29,05	3,73	2,2E-08
68	AT2G45220	Plant invertase/pectin methylesterase inhibitor superfamily(AT2G45220)	65,78	3,71	6,0E-02
69	AT1G34180	NAC domain containing protein 16(NAC016)	31,68	3,71	3,3E-08
70	AT1G33950	Avirulence induced gene (AIG1) family protein(AT1G33950)	25,12	3,68	1,9E-05
71	AT1G47890	receptor like protein 7(RLP7)	26,40	3,66	4,6E-04
72	AT4G23310	cysteine-rich RLK (RECEPTOR-like protein kinase) 23(CRK23)	153,58	3,66	1,2E-23
73	AT2G32680	receptor like protein 23(RLP23)	2047,11	3,66	1,2E-80
74	AT4G37010	centrin 2(CEN2)	13,57	3,64	5,5E-04
75	AT2G33080	receptor like protein 28(RLP28)	18,28	3,63	3,6E-05
76	AT4G04510	cysteine-rich RLK (RECEPTOR-like protein kinase) 38(CRK38)	49,96	3,62	6,7E-11
77	AT1G13550	hypothetical protein (DUF1262)(AT1G13550)	11,64	3,62	4,2E-04
78	AT2G29350	senescence-associated gene 13(SAG13)	449,89	3,61	4,9E-04
79	AT5G66690	UDP-Glycosyltransferase superfamily protein(UGT72E2)	42,18	3,59	9,3E-02
80	AT1G21310	extensin 3(EXT3)	699,31	3,59	7,2E-05
81	AT5G38250	Protein kinase family protein(AT5G38250)	48,44	3,59	3,0E-11
82	AT2G34500	cytochrome P450, family 710, subfamily A, polypeptide	13,07	3,59	2,3E-02

		1(CYP710A1)			
83	AT5G48400	Glutamate receptor family protein(ATGLR1.2)	30,31	3,58	3,5E-04
84	AT1G57630	Toll-Interleukin-Resistance (TIR) domain family protein(AT1G57630)	111,06	3,57	2,4E-16
85	AT1G33840	LURP-one-like protein (DUF567)(AT1G33840)	28,38	3,57	3,1E-07
86	AT3G13950	ankyrin(AT3G13950)	52,98	3,57	4,7E-02
87	AT4G23140	cysteine-rich RLK (RECEPTOR-like protein kinase) 6(CRK6)	1515,21	3,54	7,1E-73
88	AT1G04600	myosin XI A(XIA)	174,02	3,53	1,5E-26
89	AT4G21840	methionine sulfoxide reductase B8(MSRB8)	53,52	3,52	9,2E-03
90	AT2G19190	FLG22-induced receptor-like kinase 1(FRK1)	66,36	3,51	3,3E-10
91	AT4G18250	receptor Serine/Threonine kinase-like protein(AT4G18250)	120,93	3,51	2,1E-20
92	AT1G09932	Phosphoglycerate mutase family protein(AT1G09932)	324,21	3,51	4,3E-32
93	AT3G61198	ncRNA(AT3G61198)	10,94	3,50	9,4E-04
94	AT5G10760	Eukaryotic aspartyl protease family protein(AT5G10760)	10717,95	3,50	2,0E-15
95	AT1G53625	hypothetical protein(AT1G53625)	16,00	3,48	3,9E-04
96	AT3G22600	Bifunctional inhibitor/lipid-transfer protein/seed storage 2S albumin superfamily protein(AT3G22600)	227,01	3,48	2,8E-04
97	AT1G57650	ATP binding protein(AT1G57650)	13,96	3,47	7,5E-04
98	AT5G23160	transmembrane protein(AT5G23160)	12,75	3,46	6,7E-04
99	AT2G04070	MATE efflux family	414,99	3,46	7,3E-02

		protein(AT2G04070)			
100	AT1G43910	P-loop containing nucleoside triphosphate hydrolases superfamily protein(AT1G43910)	164,17	3,45	4,8E-04

Table 26: RNAseq - Top 100 differentially expressed genes in systemic tissue of *rpt2a*-2 during priming (compared to systemic mock infiltrated *rpt2a*-2). base mean >10; padj >0,1; sorted by Log2FC.

	Locus	Annotation	baseMean	log2Fold Change	padj
1	AT5G40990	GDSL lipase 1(GLIP1)	38,62	39,75	2,0E-41
2	AT2G14610	pathogenesis-related protein 1(PR1)	75137,35	11,09	5,5E-09
3	AT5G59310	lipid transfer protein 4(LTP4)	168,19	10,54	1,1E-05
4	AT5G59320	lipid transfer protein 3(LTP3)	787,35	7,59	2,2E-07
5	AT3G28510	P-loop containing nucleoside triphosphate hydrolases superfamily protein(AT3G28510)	2146,00	7,47	4,1E-05
6	AT3G60470	transmembrane protein, putative (DUF247)(AT3G60470)	30,85	7,33	5,7E-05
7	AT3G11340	UDP-Glycosyltransferase superfamily protein(UGT76B1)	447,46	7,28	3,2E-04
8	AT2G26400	acireductone dioxygenase 3(ARD3)	833,70	7,02	1,7E-03
9	AT2G13810	AGD2-like defense response protein 1(ALD1)	1397,28	6,98	1,3E-04
10	AT5G11920	6-&1-fructan exohydrolase(cwINV6)	558,19	6,73	1,6E-05
11	AT5G51465		150,41	6,68	3,6E-04
12	AT1G05880	RING/U-box superfamily protein(ARI12)	170,44	6,65	8,6E-04
13	AT4G37010	centrin 2(CEN2)	365,24	6,53	4,4E-04

14	AT3G13610	2-oxoglutarate (2OG) and Fe(II)-dependent oxygenase superfamily protein(AT3G13610)	525,12	6,51	2,2E-03
15	AT1G26380	FAD-binding Berberine family protein(AT1G26380)	536,39	6,50	1,4E-04
16	AT1G47890	receptor like protein 7(RLP7)	419,14	6,41	5,0E-04
17	AT5G22545	hypothetical protein(AT5G22545)	28,04	6,39	5,7E-05
18	AT4G13890	Pyridoxal phosphate (PLP)-dependent transferases superfamily protein(EDA36)	20,30	6,33	1,0E-03
19	AT3G01830	Calcium-binding EF-hand family protein(AT3G01830)	94,12	6,31	9,5E-05
20	AT2G29460	glutathione S-transferase tau 4(GSTU4)	1064,01	6,14	2,4E-05
21	AT1G08173		13,42	6,11	6,3E-04
22	AT3G49160	pyruvate kinase family protein(AT3G49160)	155,55	6,11	2,7E-04
23	AT3G26830	Cytochrome P450 superfamily protein(PAD3)	3922,11	6,06	1,2E-05
24	AT4G04500	cysteine-rich RLK (RECEPTOR-like protein kinase) 37(CRK37)	479,76	6,02	5,4E-09
25	AT1G33840	LURP-one-like protein (DUF567)(AT1G33840)	27,06	5,97	2,7E-04
26	AT3G49340	Cysteine proteinases superfamily protein(AT3G49340)	46,97	5,93	1,6E-03
27	AT1G02850	beta glucosidase 11(BGLU11)	362,32	5,90	1,1E-08
28	AT1G66960	Terpenoid cyclases family protein(LUP5)	203,54	5,90	8,8E-07
29	AT3G25180	cytochrome P450, family 82, subfamily G, polypeptide 1(CYP82G1)	2730,19	5,85	1,2E-03
30	AT3G45330	Concanavalin A-like lectin protein	34,85	5,81	2,9E-03

		kinase family protein(AT3G45330)			
31	AT1G16420	metacaspase 8(MC8)	100,73	5,79	6,8E-06
32	AT2G18660	plant natriuretic peptide A(PNP-A)	970,20	5,78	4,7E-12
33	AT3G15536	ncRNA(AT3G15536)	318,34	5,66	1,0E-07
34	AT4G10500	2-oxoglutarate (2OG) and Fe(II)-dependent oxygenase superfamily protein(AT4G10500)	788,73	5,65	3,1E-08
35	AT4G10860	hypothetical protein(AT4G10860)	1097,59	5,64	1,4E-02
36	AT5G26690	Heavy metal transport/detoxification superfamily protein(AT5G26690)	295,36	5,62	3,1E-11
37	AT4G00700	C2 calcium/lipid-binding plant phosphoribosyltransferase family protein(AT4G00700)	918,56	5,58	1,5E-08
38	AT3G48850	phosphate transporter 3;2(PHT3;2)	510,35	5,58	7,6E-04
39	AT5G52730	Copper transport protein family(AT5G52730)	21,01	5,55	1,8E-03
40	AT3G13950	ankyrin(AT3G13950)	1371,82	5,54	5,6E-04
41	AT1G21240	wall associated kinase 3(WAK3)	2786,99	5,53	6,7E-13
42	AT5G22380	NAC domain containing protein 90(NAC090)	77,03	5,52	2,1E-10
43	AT1G32350	alternative oxidase 1D(AOX1D)	1680,93	5,50	2,2E-02
44	AT1G53620	transmembrane protein(AT1G53620)	32,51	5,49	2,0E-03
45	AT4G21840	methionine sulfoxide reductase B8(MSRB8)	165,84	5,49	2,1E-03
46	AT4G23310	cysteine-rich RLK (RECEPTOR-like protein kinase) 23(CRK23)	125,31	5,46	9,4E-08
47	AT3G09940	monodehydroascorbate reductase(MDHAR)	92,94	5,38	2,0E-03

48	AT3G46080	C2H2-type zinc finger family protein(AT3G46080)	524,18	5,36	2,9E-03
49	AT5G39670	Calcium-binding EF-hand family protein(AT5G39670)	162,53	5,36	8,2E-09
50	AT1G33960	P-loop containing nucleoside triphosphate hydrolases superfamily protein(AIG1)	4361,45	5,31	3,8E-09
51	AT1G66390	myb domain protein 90(MYB90)	131,01	5,31	5,0E-02
52	AT3G23250	myb domain protein 15(MYB15)	76,55	5,30	2,4E-03
53	AT3G57260	beta-1,3-glucanase 2(BGL2)	7585,64	5,28	8,4E-10
54	AT1G09080	Heat shock protein 70 (Hsp 70) family protein(BIP3)	595,45	5,27	1,1E-09
55	AT3G60966	RING/U-box superfamily protein(AT3G60966)	154,71	5,27	4,8E-04
56	AT5G15500	Ankyrin repeat family protein(AT5G15500)	88,62	5,24	8,4E-03
57	AT2G43000	NAC domain containing protein 42(NAC042)	462,37	5,24	3,8E-05
58	AT1G33730	cytochrome P450, family 76, subfamily C, polypeptide 5(CYP76C5)	187,98	5,23	2,2E-03
59	AT1G44130	Eukaryotic aspartyl protease family protein(AT1G44130)	416,46	5,21	2,2E-04
60	AT1G14880	PLANT CADMIUM RESISTANCE 1(PCR1)	15592,26	5,20	2,7E-06
61	AT5G22530	hypothetical protein(AT5G22530)	19,53	5,18	3,4E-04
62	AT2G24850	tyrosine aminotransferase 3(TAT3)	17926,50	5,16	2,8E-07
63	AT2G26480	UDP-glucosyl transferase 76D1(UGT76D1)	35,85	5,16	9,9E-03
64	AT5G52740	Copper transport protein family(AT5G52740)	53,10	5,12	3,8E-07

65	AT5G52760	Copper transport protein family(AT5G52760)	442,32	5,11	4,4E-12
66	AT5G23160	transmembrane protein(AT5G23160)	22,12	5,11	4,5E-03
67	AT5G62480	glutathione S-transferase tau 9(GSTU9)	95,89	5,11	2,2E-02
68	AT3G29250	NAD(P)-binding Rossmann-fold superfamily protein(SDR4)	848,51	5,00	1,9E-03
69	AT1G79680	WALL ASSOCIATED KINASE (WAK)-LIKE 10(WAKL10)	660,37	5,00	2,6E-03
70	AT5G55410	Bifunctional inhibitor/lipid-transfer protein/seed storage 2S albumin superfamily protein(AT5G55410)	21,03	4,97	1,6E-02
71	AT2G33080	receptor like protein 28(RLP28)	37,80	4,96	3,4E-03
72	AT5G40010	AAA-ATPase 1(AATP1)	500,78	4,96	8,8E-04
73	AT3G09960	Calcineurin-like metallo-phosphoesterase superfamily protein(AT3G09960)	138,57	4,94	3,3E-03
74	AT3G57240	beta-1,3-glucanase 3(BG3)	670,17	4,93	1,6E-04
75	AT3G11000	DCD (Development and Cell Death) domain protein(AT3G11000)	11,77	4,92	1,2E-03
76	AT1G73260	kunitz trypsin inhibitor 1(KTI1)	14745,06	4,91	1,1E-02
77	AT1G65483	hypothetical protein(AT1G65483)	251,18	4,91	4,1E-03
78	AT4G23150	cysteine-rich RLK (RECEPTOR-like protein kinase) 7(CRK7)	1144,58	4,88	2,4E-08
79	AT4G12490	Bifunctional inhibitor/lipid-transfer protein/seed storage 2S albumin superfamily protein(AT4G12490)	5457,59	4,85	2,1E-02
80	AT2G45220	Plant invertase/pectin methylesterase inhibitor	7272,90	4,82	1,3E-02

		superfamily(AT2G45220)			
81	AT1G43910	P-loop containing nucleoside triphosphate hydrolases superfamily protein(AT1G43910)	679,45	4,76	6,8E-06
82	AT5G09290	Inositol monophosphatase family protein(AT5G09290)	306,19	4,73	1,0E-09
83	AT4G21850	methionine sulfoxide reductase B9(MSRB9)	192,65	4,72	1,4E-07
84	AT3G61198	ncRNA(AT3G61198)	33,58	4,71	4,7E-03
85	AT2G04805		84,40	4,71	3,6E-03
86	AT4G12480	Bifunctional inhibitor/lipid-transfer protein/seed storage 2S albumin superfamily protein(EARLI1)	5178,78	4,70	2,7E-03
87	AT3G44326	F-box family protein(AT3G44326)	37,36	4,70	4,1E-03
88	AT2G23830	PapD-like superfamily protein(AT2G23830)	44,23	4,70	8,0E-03
89	AT1G71390	receptor like protein 11(RLP11)	29,79	4,65	4,3E-03
90	AT1G19250	flavin-dependent monooxygenase 1(FMO1)	2502,36	4,63	3,6E-02
91	AT4G23280	cysteine-rich RLK (RECEPTOR-like protein kinase) 20(CRK20)	36,73	4,61	4,4E-03
92	AT1G33950	Avirulence induced gene (AIG1) family protein(AT1G33950)	972,65	4,56	1,4E-02
93	AT4G18250	receptor Serine/Threonine kinase-like protein(AT4G18250)	304,33	4,55	3,7E-08
94	AT5G24080	Protein kinase superfamily protein(AT5G24080)	31,94	4,55	2,1E-02
95	AT3G51860	cation exchanger 3(CAX3)	3350,35	4,55	1,9E-07
96	AT5G52390	PAR1 protein(AT5G52390)	134,11	4,54	5,7E-03
97	AT2G32140	transmembrane receptor(AT2G32140)	308,06	4,54	3,0E-09

98	AT3G28580	P-loop containing nucleoside triphosphate hydrolases superfamily protein(AT3G28580)	489,65	4,53	2,9E-05
99	AT5G25260	SPFH/Band 7/PHB domain-containing membrane-associated protein family(AT5G25260)	590,86	4,52	1,4E-07
100	AT1G30850	root hair specific 4(RSH4)	31,51	4,52	3,4E-02

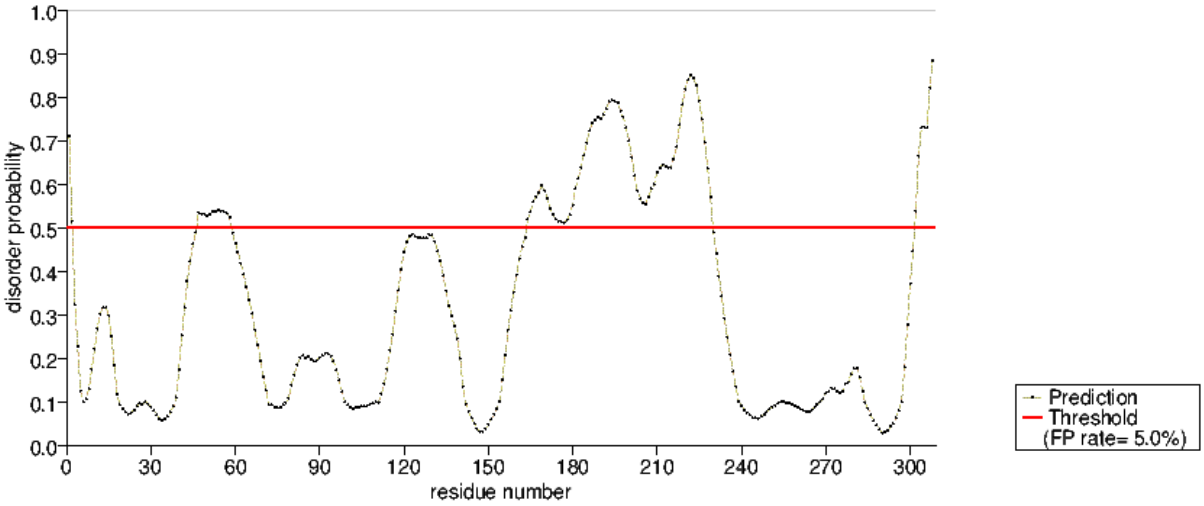

Figure 43: DisOrder prediction System (PrDOS) identified potentially disordered regions in PUB54.

6. Lists of figures and tables

List of figures

List of Tables

7. Bibliography

Adams, E. H. G., & Spoel, S. H. (2018). The ubiquitin-proteasome system as a transcriptional regulator of plant immunity. *Journal of Experimental Botany*, *69*(19), 4529–4537. https://doi.org/10.1093/jxb/ery216

Aguilar-Hernández, V., Aguilar-Henonin, L., & Guzmán, P. (2011). Diversity in the architecture of ATLs, a family of plant ubiquitin-ligases, leads to recognition and targeting of substrates in different cellular environments. *PLoS ONE*, *6*(8). https://doi.org/10.1371/journal.pone.0023934

Ali, S., Ganai, B. A., Kamili, A. N., Bhat, A. A., Mir, Z. A., Bhat, J. A., Tyagi, A., Islam, S. T., Mushtaq, M., Yadav, P., Rawat, S., & Grover, A. (2018). Pathogenesis-related proteins and peptides as promising tools for engineering plants with multiple stress tolerance. In *Microbiological Research* (Vols. 212–213, pp. 29–37). Elsevier GmbH. https://doi.org/10.1016/j.micres.2018.04.008

Antignani, V., Klocko, A. L., Bak, G., Chandrasekaran, S. D., Dunivin, T., & Nielsen, E. (2015). Recruitment of PLANT U-BOX13 and the PI4Kβ1/β2 phosphatidylinositol-4 kinases by the small GTPase RabA4B plays important roles during salicylic acid-mediated plant defense signaling in arabidopsis. *Plant Cell*, *27*(1), 243–261. https://doi.org/10.1105/tpc.114.134262

Aravind, L., & Koonin, E. V. (2000). The U box is a modified RING finger - A common domain in ubiquitination [1]. In *Current Biology* (Vol. 10, Issue 4, pp. R132–R134). Current Biology Ltd. https://doi.org/10.1016/S0960-9822(00)00398-5

Asher, G., Reuven, N., & Shaul, Y. (2006). 20S proteasomes and protein degradation "by default." In *BioEssays* (Vol. 28, Issue 8, pp. 844–849). Bioessays. https://doi.org/10.1002/bies.20447

Baalmann, E., Backhausen, J. E., Rak, C., Vetter, S., & Scheibe, R. (1995). Reductive modification and nonreductive activation of purified spinach chloroplast NADP-dependent glyceraldehyde-3-phosphate dehydrogenase. *Archives of Biochemistry and Biophysics*, *324*(2), 201–208. https://doi.org/10.1006/abbi.1995.0031

Babiychuk, E., Fuangthong, M., Van Montagu, M., Inzé, D., & Kushnir, S. (1997). Efficient gene tagging in Arabidopsis thaliana using a gene trap approach. *Proceedings of the National Academy of Sciences of the United States of America*, *94*(23), 12722–12727. https://doi.org/10.1073/pnas.94.23.12722

Bachmair, A., Novatchkova, M., Potuschak, T., & Eisenhaber, F. (2001). Ubiquitylation in plants: A post-genomic look at a post-translational modification. In *Trends in Plant Science* (Vol. 6, Issue 10, pp. 463–470). https://doi.org/10.1016/S1360-1385(01)02080-5

Banfield, M. J. (2015). Perturbation of host ubiquitin systems by plant pathogen/pest effector proteins. *Cellular Microbiology*, *17*(1), 18–25. https://doi.org/10.1111/cmi.12385

Barth, O., Vogt, S., Uhlemann, R., Zschiesche, W., & Humbeck, K. (2009). Stress induced and

nuclear localized HIPP26 from Arabidopsis thaliana interacts via its heavy metal associated domain with the drought stress related zinc finger transcription factor ATHB29. *Plant Molecular Biology*, *69*(1–2), 213–226. https://doi.org/10.1007/s11103-008-9419-0

Bent, A. F., & Clough, S. J. (1998). Agrobacterium Germ-Line Transformation: Transformation of Arabidopsis without Tissue Culture. In *Plant Molecular Biology Manual* (pp. 17–30). Springer Netherlands. https://doi.org/10.1007/978-94-011-5242-6_2

Berger, F., Ramírez-Hernández, M. H., & Ziegler, M. (2004). The new life of a centenarian: Signalling functions of NAD(P). In *Trends in Biochemical Sciences* (Vol. 29, Issue 3, pp. 111–118). Trends Biochem Sci. https://doi.org/10.1016/j.tibs.2004.01.007

Bernsdorff, F., Döring, A. C., Gruner, K., Schuck, S., Bräutigam, A., & Zeier, J. (2016). Pipecolic acid orchestrates plant systemic acquired resistance and defense priming via salicylic acid-dependent and -independent pathways. *Plant Cell*, *28*(1), 102–129. https://doi.org/10.1105/tpc.15.00496

Berrocal-Lobo, M., Stone, S., Yang, X., Antico, J., Callis, J., Ramonell, K. M., & Somerville, S. (2010). ATL9, a RING zinc finger protein with E3 ubiquitin ligase activity implicated in chitin- and NADPH oxidase-mediated defense responses. *PLoS ONE*, *5*(12). https://doi.org/10.1371/journal.pone.0014426

Besche, H. C., Sha, Z., Kukushkin, N. V, Peth, A., Hock, E., Kim, W., Gygi, S., Gutierrez, J. A., Liao, H., Dick, L., & Goldberg, A. L. (2014). Autoubiquitination of the 26S Proteasome on Rpn13 Regulates Breakdown of Ubiquitin Conjugates. *The EMBO Journal*, *33*(10), 1159–1176. https://doi.org/10.1002/embj.201386906

Beth Mudgett, M. (2005). NEW INSIGHTS TO THE FUNCTION OF PHYTOPATHOGENIC BACTERIAL TYPE III EFFECTORS IN PLANTS. *Annual Review of Plant Biology*, *56*(1), 509–531. https://doi.org/10.1146/annurev.arplant.56.032604.144218

Billington, R. A., Bruzzone, S., De Flora, A., Genazzani, A. A., Koch-Nolte, F., Ziegler, M., & Zocchi, E. (2006). Emerging functions of extracellular pyridine nucleotides. *Molecular Medicine*, *12*(11–12), 324–327. https://doi.org/10.2119/2006-00075.Billington

Birkenbihl, R. P., Kracher, B., & Somssich, I. E. (2017). Induced genome-wide binding of three arabidopsis WRKY transcription factors during early MAMP-triggered immunity. *Plant Cell*, *29*(1), 20–38. https://doi.org/10.1105/tpc.16.00681

Boller, T., & Felix, G. (2009). A Renaissance of Elicitors: Perception of Microbe-Associated Molecular Patterns and Danger Signals by Pattern-Recognition Receptors. *Annual Review of Plant Biology*, *60*(1), 379–406. https://doi.org/10.1146/annurev.arplant.57.032905.105346

Borden, K. L. B. (2000). RING domains: Master builders of molecular scaffolds? In *Journal of Molecular Biology* (Vol. 295, Issue 5, pp. 1103–1112). Academic Press. https://doi.org/10.1006/jmbi.1999.3429

Borden, K. L. B., & Freemont, P. S. (1996). The RING finger domain: A recent example of a sequence-structure family. *Current Opinion in Structural Biology*, *6*(3), 395–401. https://doi.org/10.1016/S0959-440X(96)80060-1

Breeden, L., & Nasmyth, K. (1985). Regulation of the yeast HO gene. *Cold Spring Harbor*

Symposia on Quantitative Biology, *50*, 643–650. https://doi.org/10.1101/SQB.1985.050.01.078

Brotman, Y., Landau, U., Cuadros-Inostroza, Ã., Takayuki, T., Fernie, A. R., Chet, I., Viterbo, A., & Willmitzer, L. (2013). Correction: Trichoderma-Plant Root Colonization: Escaping Early Plant Defense Responses and Activation of the Antioxidant Machinery for Saline Stress Tolerance. *PLoS Pathogens*, *9*(4). https://doi.org/10.1371/annotation/8b818c15-3fe0-4e56-9be2-e44fd1ed3fae

Bruce, T. J. A., Matthes, M. C., Napier, J. A., & Pickett, J. A. (2007). Stressful "memories" of plants: Evidence and possible mechanisms. In *Plant Science* (Vol. 173, Issue 6, pp. 603–608). Elsevier. https://doi.org/10.1016/j.plantsci.2007.09.002

Bull, P. C., & Cox, D. W. (1994). Wilson disease and Menkes disease: new handles on heavy-metal transport. In *Trends in Genetics* (Vol. 10, Issue 7, pp. 246–252). Elsevier Current Trends. https://doi.org/10.1016/0168-9525(94)90172-4

Cai, J., Jozwiak, A., Holoidovsky, L., Meijler, M. M., Meir, S., Rogachev, I., & Aharoni, A. (2020). Glycosylation of N-Hydroxy-Pipecolic Acid Equilibrates between Systemic Acquired Resistance Response and Plant Growth. *Molecular Plant*. https://doi.org/10.1016/j.molp.2020.12.018

Caillaud, M. C., Asai, S., Rallapalli, G., Piquerez, S., Fabro, G., & Jones, J. D. G. (2013). A Downy Mildew Effector Attenuates Salicylic Acid-Triggered Immunity in Arabidopsis by Interacting with the Host Mediator Complex. *PLoS Biology*, *11*(12). https://doi.org/10.1371/journal.pbio.1001732

Callis, J., Carpenter, T., Sun, C. W., & Vierstra, R. D. (1995). Structure and evolution of genes encoding polyubiquitin and ubiquitin- like proteins in Arabidopsis thaliana ecotype Columbia. *Genetics*, *139*(2), 921–939. /pmc/articles/PMC1206391/?report=abstract

Cao, H., Bowling, S. A., Gordon, A. S., & Dong' Dcmb, X. (1994). Characterization of an Arabidopsis Mutant That is Nonresponsive to Inducers of Systemic Acquired Resistance. In *The Plant Cell* (Vol. 6).

Cesari, S., Bernoux, M., Moncuquet, P., Kroj, T., & Dodds, P. N. (2014). A novel conserved mechanism for plant NLR protein pairs: The "integrated decoy" hypothesis. *Frontiers in Plant Science*, *5*(NOV). https://doi.org/10.3389/fpls.2014.00606

Champigny, M. J., Isaacs, M., Carella, P., Faubert, J., Fobert, P. R., & Cameron, R. K. (2013). Long distance movement of DIR1 and investigation of the role of DIR1-like during systemic acquired resistance in Arabidopsis. *Frontiers in Plant Science*, *4*(JUL). https://doi.org/10.3389/fpls.2013.00230

Chanda, B., Venugopal, S. C., Kulshrestha, S., Navarre, D. A., Downie, B., Vaillancourt, L., Kachroo, A., & Kachroo, P. (2008). Glycerol-3-phosphate levels are associated with basal resistance to the hemibiotrophic fungus Colletotrichum higginsianum in arabidopsis. *Plant Physiology*, *147*(4), 2017–2029. https://doi.org/10.1104/pp.108.121335

Chanda, B., Xia, Y., Mandal, M. K., Yu, K., Sekine, K. T., Gao, Q. M., Selote, D., Hu, Y., Stromberg, A., Navarre, D., Kachroo, A., & Kachroo, P. (2011). Glycerol-3-phosphate is a critical mobile inducer of systemic immunity in plants. *Nature Genetics*, *43*(5), 421–429. https://doi.org/10.1038/ng.798

Chang, M., Zhao, J., Chen, H., Li, G., Chen, J., Li, M., Palmer, I. A., Song, J., Alfano, J. R., Liu, F., & Fu, Z. Q. (2019). PBS3 Protects EDS1 from Proteasome-Mediated Degradation in Plant Immunity. *Molecular Plant*, *12*(5), 678–688. https://doi.org/10.1016/j.molp.2019.01.023

Chen, X., Li, C., Wang, H., & Guo, Z. (2019). WRKY transcription factors: evolution, binding, and action. *Phytopathology Research*, *1*(1), 1–15. https://doi.org/10.1186/s42483-019-0022-x

Chinchilla, D., Zipfel, C., Robatzek, S., Kemmerling, B., Nürnberger, T., Jones, J. D. G., Felix, G., & Boller, T. (2007). A flagellin-induced complex of the receptor FLS2 and BAK1 initiates plant defence. *Nature*, *448*(7152), 497–500. https://doi.org/10.1038/nature05999

Chisholm, S. T., Coaker, G., Day, B., & Staskawicz, B. J. (2006). Host-microbe interactions: Shaping the evolution of the plant immune response. In *Cell* (Vol. 124, Issue 4, pp. 803–814). Cell. https://doi.org/10.1016/j.cell.2006.02.008

Cho, S. K., Bae, H., Ryu, M. Y., Wook Yang, S., & Kim, W. T. K. (2015). PUB22 and PUB23 U-BOX E3 ligases directly ubiquitinate RPN6, a 26S proteasome lid subunit, for subsequent degradation in Arabidopsis thaliana. *Biochemical and Biophysical Research Communications*, *464*(4), 994–999. https://doi.org/10.1016/j.bbrc.2015.07.030

Chu, B. W., Kovary, K. M., Guillaume, J., Chen, L. C., Teruel, M. N., & Wandless, T. J. (2013). The E3 ubiquitin ligase UBE3C enhances proteasome processivity by ubiquitinating partially proteolyzed substrates. *Journal of Biological Chemistry*, *288*(48), 34575–34587. https://doi.org/10.1074/jbc.M113.499350

Ciechanover, A. (1998). The ubiquitin-proteasome pathway: On protein death and cell life. In *EMBO Journal* (Vol. 17, Issue 24, pp. 7151–7160). EMBO J. https://doi.org/10.1093/emboj/17.24.7151

Cohen, E., Bieschke, J., Perciavalle, R. M., Kelly, J. W., & Dillin, A. (2006). Opposing activities protect against age-onset proteotoxicity. *Science*, *313*(5793), 1604–1610. https://doi.org/10.1126/science.1124646

Coker, T. L. R., Cevik, V., Beynon, J. L., & Gifford, M. L. (2015). Spatial dissection of the Arabidopsis thaliana transcriptional response to downy mildew using Fluorescence Activated Cell Sorting. *Frontiers in Plant Science*, *6*(JULY), 527. https://doi.org/10.3389/fpls.2015.00527

Collins, G. A., & Tansey, W. P. (2006). The proteasome: A utility tool for transcription? In *Current Opinion in Genetics and Development* (Vol. 16, Issue 2, pp. 197–202). Elsevier Current Trends. https://doi.org/10.1016/j.gde.2006.02.009

Conrath, U. (2006). Systemic acquired resistance. In *Plant Signaling and Behavior* (Vol. 1, Issue 4, pp. 179–184). Taylor & Francis. https://doi.org/10.4161/psb.1.4.3221

Conrath, U. (2011). Molecular aspects of defence priming. *Trends in Plant Science*, *16*, 524–531. https://doi.org/10.1016/j.tplants.2011.06.004

Conrath, U., Beckers, G. J. M., Flors, V., García-Agustín, P., Jakab, G., Mauch, F., Newman, M. A., Pieterse, C. M. J., Poinssot, B., Pozo, M. J., Pugin, A., Schaffrath, U., Ton, J., Wendehenne, D., Zimmerli, L., & Mauch-Mani, B. (2006). Priming: Getting ready for battle. In *Molecular Plant-Microbe Interactions* (Vol. 19, Issue 10, pp. 1062–1071). Mol

Plant Microbe Interact. https://doi.org/10.1094/MPMI-19-1062

Conrath, U., Beckers, G. J. M., Langenbach, C. J. G., & Jaskiewicz, M. R. (2015). Priming for Enhanced Defense. *Annual Review of Phytopathology*, *53*(1), 97–119. https://doi.org/10.1146/annurev-phyto-080614-120132

Contreras-Cornejo, H. A., Macías-Rodríguez, L., Beltrán-Peña, E., Herrera-Estrella, A., & López-Bucio, J. (2011). Trichoderma-induced plant immunity likely involves both hormonal- and camalexindependent mechanisms in Arabidopsis thaliana and confers resistance against necrotrophic fungus Botrytis cinerea. *Plant Signaling and Behavior*, *6*(10), 1554–1563. https://doi.org/10.4161/psb.6.10.17443

Cotton, T. R., & Lechtenberg, B. C. (2020). Chain reactions: molecular mechanisms of RBR ubiquitin ligases. In *Biochemical Society Transactions* (Vol. 48, Issue 4, pp. 1737–1750). Portland Press Ltd. https://doi.org/10.1042/BST20200237

Dangl, J. L., & Jones, J. D. G. (2001). Plant pathogens and integrated defence responses to infection. In *Nature* (Vol. 411, Issue 6839, pp. 826–833). Nature Publishing Group. https://doi.org/10.1038/35081161

Danhorn, T., & Fuqua, C. (2007). Biofilm Formation by Plant-Associated Bacteria. *Annual Review of Microbiology*, *61*(1), 401–422. https://doi.org/10.1146/annurev.micro.61.080706.093316

Davies, K. J. A. (2001). Degradation of oxidized proteins by the 20S proteasome. *Biochimie*, *83*(3–4), 301–310. https://doi.org/10.1016/S0300-9084(01)01250-0

De Abreu-Neto, J. B., Turchetto-Zolet, A. C., De Oliveira, L. F. V., Bodanese Zanettini, M. H., & Margis-Pinheiro, M. (2013). Heavy metal-associated isoprenylated plant protein (HIPP): Characterization of a family of proteins exclusive to plants. *FEBS Journal*, *280*(7), 1604–1616. https://doi.org/10.1111/febs.12159

Dean, J. V., Shah, R. P., & Mohammed, L. A. (2003). Formation and vacuolar localization of salicylic acid glucose conjugates in soybean cell suspension cultures. *Physiologia Plantarum*, *118*(3), 328–336. https://doi.org/10.1034/j.1399-3054.2003.00117.x

Delaney, T. P., Uknes, S., Vernooij, B., Friedrich, L., Weymann, K., Negrotto, D., Gaffney, T., Gut-Rella, M., Kessmann, H., Ward, E., & Ryals, J. (1994). A central role of salicylic acid in plant disease resistance. *Science*, *266*(5188), 1247–1250. https://doi.org/10.1126/science.266.5188.1247

Desterro, J. M. P., Rodriguez, M. S., & Hay, R. T. (2000). Regulation of transcription factors by protein degradation. In *Cellular and Molecular Life Sciences* (Vol. 57, Issues 8–9, pp. 1207–1219). Birkhauser Verlag Basel. https://doi.org/10.1007/PL00000760

Devoto, A., Muskett, P. R., & Shirasu, K. (2003). Role of ubiquitination in the regulation of plant defence against pathogens. In *Current Opinion in Plant Biology* (Vol. 6, Issue 4, pp. 307–311). Elsevier Ltd. https://doi.org/10.1016/S1369-5266(03)00060-8

Dick, T. P., Nussbaum, A. K., Deeg, M., Heinemeyer, W., Groll, M., Schirle, M., Keilholz, W., Stevanović, S., Wolf, D. H., Huber, R., Rammensee, H. G., & Schild, H. (1998). Contribution of proteasomal β-subunits to the cleavage of peptide substrates analyzed with yeast mutants. *Journal of Biological Chemistry*, *273*(40), 25637–25646. https://doi.org/10.1074/jbc.273.40.25637

Ding, P., Rekhter, D., Ding, Y., Feussner, K., Busta, L., Haroth, S., Xu, S., Li, X., Jetter, R., Feussner, I., & Zhang, Y. (2016). Characterization of a pipecolic acid biosynthesis pathway required for systemic acquired resistance. *Plant Cell*, *28*(10), 2603–2615. https://doi.org/10.1105/tpc.16.00486

Ding, Y., Sun, T., Ao, K., Peng, Y., Zhang, Y., Li, X., & Zhang, Y. (2018). Opposite Roles of Salicylic Acid Receptors NPR1 and NPR3/NPR4 in Transcriptional Regulation of Plant Immunity. *Cell*, *173*(6), 1454-1467.e10. https://doi.org/10.1016/j.cell.2018.03.044

Dove, K. K., & Klevit, R. E. (2017). RING-Between-RING E3 Ligases: Emerging Themes amid the Variations. In *Journal of Molecular Biology* (Vol. 429, Issue 22, pp. 3363–3375). Academic Press. https://doi.org/10.1016/j.jmb.2017.08.008

Dove, K. K., Stieglitz, B., Duncan, E. D., Rittinger, K., & Klevit, R. E. (2016). Molecular insights into <scp>RBR</scp> E3 ligase ubiquitin transfer mechanisms. *EMBO Reports*, *17*(8), 1221–1235. https://doi.org/10.15252/embr.201642641

Du, Y. Y., Wang, P. C., Chen, J., & Song, C. P. (2008). Comprehensive functional analysis of the catalase gene family in Arabidopsis thaliana. *Journal of Integrative Plant Biology*, *50*(10), 1318–1326. https://doi.org/10.1111/j.1744-7909.2008.00741.x

Dubiella, U., Seybold, H., Durian, G., Komander, E., Lassig, R., Witte, C. P., Schulze, W. X., & Romeis, T. (2013). Calcium-dependent protein kinase/NADPH oxidase activation circuit is required for rapid defense signal propagation. *Proceedings of the National Academy of Sciences of the United States of America*, *110*(21), 8744–8749. https://doi.org/10.1073/pnas.1221294110

Duplan, V., & Rivas, S. (2014). E3 ubiquitin-ligases and their target proteins during the regulation of plant innate immunity. In *Frontiers in Plant Science* (Vol. 5, Issue FEB). Frontiers Research Foundation. https://doi.org/10.3389/fpls.2014.00042

Durrant, W. E., & Dong, X. (2004). Systemic acquired resistance. In *Annual Review of Phytopathology* (Vol. 42, pp. 185–209). Annu Rev Phytopathol. https://doi.org/10.1146/annurev.phyto.42.040803.140421

Durrant, Wendy E., Rowland, O., Piedras, P., Hammond-Kosack, K. E., & Jones, J. D. G. (2000). cDNA-AFLP reveals a striking overlap in race-specific resistance and wound response gene expression profiles. *Plant Cell*, *12*(6), 963–977. https://doi.org/10.1105/tpc.12.6.963

Edwards, K., Johnstone, C., & Thompson, C. (1991). A simple and rapid method for the preparation of plant genomic DNA for PCR analysis. In *Nucleic Acids Research* (Vol. 19, Issue 6, p. 1349). Oxford University Press. https://doi.org/10.1093/nar/19.6.1349

El-Mergawi, R. A., & Abd El-Wahed, M. S. A. (2020). Effect of exogenous salicylic acid or indole acetic acid on their endogenous levels, germination, and growth in maize. *Bulletin of the National Research Centre*, *44*(1), 1–8. https://doi.org/10.1186/s42269-020-00416-7

Eulgem, T., & Somssich, I. E. (2007). Networks of WRKY transcription factors in defense signaling. In *Current Opinion in Plant Biology* (Vol. 10, Issue 4, pp. 366–371). Curr Opin Plant Biol. https://doi.org/10.1016/j.pbi.2007.04.020

Feke, A., Liu, W., Hong, J., Li, M. W., Lee, C. M., Zhou, E. K., & Gendron, J. M. (2019). Decoys

provide a scalable platform for the identification of plant e3 ubiquitin ligases that regulate circadian function. *ELife*, *8*. https://doi.org/10.7554/eLife.44558

Ferrari, S., Galletti, R., Denoux, C., De Lorenzo, G., Ausubel, F. M., & Dewdney, J. (2007). Resistance to *Botrytis cinerea* Induced in Arabidopsis by Elicitors Is Independent of Salicylic Acid, Ethylene, or Jasmonate Signaling But Requires *PHYTOALEXIN DEFICIENT3*. *Plant Physiology*, *144*(1), 367–379. https://doi.org/10.1104/pp.107.095596

Fields, S., & Song, O. K. (1989). A novel genetic system to detect protein-protein interactions. *Nature*, *340*(6230), 245–246. https://doi.org/10.1038/340245a0

Finnegan, E. J., & Kovac, K. A. (2000). Plant DNA methyltransferases. *Plant Molecular Biology*, *43*(2–3), 189–201. https://doi.org/10.1023/a:1006427226972

Flor, H. H. (1971). Current Status of the Gene-For-Gene Concept. *Annual Review of Phytopathology*, *9*(1), 275–296. https://doi.org/10.1146/annurev.py.09.090171.001423

Freemont, P. S. (1993). The RING Finger. *Annals of the New York Academy of Sciences*, *684*(1 Zinc-Finger P), 174–192. https://doi.org/10.1111/j.1749-6632.1993.tb32280.x

Frugoli, J. A., Zhong, H. H., Nuccio, M. L., McCourt, P., McPeek, M. A., Thomas, T. L., & McClung, C. R. (1996). Catalase is encoded by a multigene family in Arabidopsis thaliana (L.) Heynh. *Plant Physiology*, *112*(1), 327–336. https://doi.org/10.1104/pp.112.1.327

Frye, C. A., & Innes, R. W. (1998). An arabidopsis mutant with enhanced resistance to powdery mildew. *Plant Cell*, *10*(6), 947–956. https://doi.org/10.1105/tpc.10.6.947

Fu, H., Reis, N., Lee, Y., Glickman, M. H., & Vierstra, R. D. (2001). Subunit interaction maps for the regulatory particle of the 26S proteasome and the COP9 signalosome. *EMBO Journal*, *20*(24), 7096–7107. https://doi.org/10.1093/emboj/20.24.7096

Fu, Z. Q., & Dong, X. (2013). Systemic acquired resistance: Turning local infection into global defense. In *Annual Review of Plant Biology* (Vol. 64, pp. 839–863). Annual Reviews . https://doi.org/10.1146/annurev-arplant-042811-105606

Fu, Z. Q., Yan, S., Saleh, A., Wang, W., Ruble, J., Oka, N., Mohan, R., Spoel, S. H., Tada, Y., Zheng, N., & Dong, X. (2012). NPR3 and NPR4 are receptors for the immune signal salicylic acid in plants. *Nature*, *486*(7402), 228–232. https://doi.org/10.1038/nature11162

Furlan, G., Nakagami, H., Eschen-Lippold, L., Jiang, X., Majovsky, P., Kowarschik, K., Hoehenwarter, W., Lee, J., & Trujillo, M. (2017). Changes in PUB22 ubiquitination modes triggered by MITOGEN-ACTIVATED PROTEIN KINASE3 dampen the immune response. *Plant Cell*, *29*(4), 726–745. https://doi.org/10.1105/tpc.16.00654

Furniss, J. J., Grey, H., Wang, Z., Nomoto, M., Jackson, L., Tada, Y., & Spoel, S. H. (2018). Proteasome-associated HECT-type ubiquitin ligase activity is required for plant immunity. *PLoS Pathogens*, *14*(11). https://doi.org/10.1371/journal.ppat.1007447

Gaffney, T., Friedrich, L., Vernooij, B., Negrotto, D., Nye, G., Uknes, S., Ward, E., Kessmann, H., & Ryals, J. (1993). Requirement of salicylic acid for the induction of systemic acquired resistance. *Science*, *261*(5122), 754–756. https://doi.org/10.1126/science.261.5122.754

Gao, Q. M., Zhu, S., Kachroo, P., & Kachroo, A. (2015). Signal regulators of systemic acquired

resistance. *Frontiers in Plant Science*, *6*(APR). https://doi.org/10.3389/fpls.2015.00228

Garcion, C., Lohmann, A., Lamodière, E., Catinot, J., Buchala, A., Doermann, P., & Métraux, J. P. (2008). Characterization and biological function of the Isochorismate Synthase2 gene of Arabidopsis. *Plant Physiology*, *147*(3), 1279–1287. https://doi.org/10.1104/pp.108.119420

Ge, X., Li, G. J., Wang, S. B., Zhu, H., Zhu, T., Wang, X., & Xia, Y. (2007). AtNUDT7, a negative regulator of basal immunity in arabidopsis, modulates two distinct defense response pathways and is involved in maintaining redox homeostasis. *Plant Physiology*, *145*(1), 204–215. https://doi.org/10.1104/pp.107.103374

Gietz, R. D., & Woods, R. A. (2002). Transformation of yeast by lithium acetate/single-stranded carrier DNA/polyethylene glycol method. *Methods in Enzymology*, *350*, 87–96. https://doi.org/10.1016/S0076-6879(02)50957-5

Gitschier, J., Moffat, B., Reilly, D., Wood, W. I., & Fairbrother, W. J. (1998). Solution structure of the fourth metal-binding domain from the Menkes copper-transporting ATPase. *Nature Structural Biology*, *5*(1), 47–54. https://doi.org/10.1038/nsb0198-47

Glickman, M. H. (2000). Getting in and out of the proteasome. *Seminars in Cell and Developmental Biology*, *11*(3), 149–158. https://doi.org/10.1006/scdb.2000.0161

Głowacki, S., Macioszek, V. K., & Kononowicz, A. K. (2011). R proteins as fundamentals of plant innate immunity. In *Cellular and Molecular Biology Letters* (Vol. 16, Issue 1, pp. 1–24). BioMed Central Ltd. https://doi.org/10.2478/s11658-010-0024-2

Göhre, V., Spallek, T., Häweker, H., Mersmann, S., Mentzel, T., Boller, T., de Torres, M., Mansfield, J. W., & Robatzek, S. (2008). Plant Pattern-Recognition Receptor FLS2 Is Directed for Degradation by the Bacterial Ubiquitin Ligase AvrPtoB. *Current Biology*, *18*(23), 1824–1832. https://doi.org/10.1016/j.cub.2008.10.063

Griebel, T., & Zeier, J. (2008). Light regulation and daytime dependency of inducible plant defenses in arabidopsis: Phytochrome signaling controls systemic acquired resistance rather than local defense. *Plant Physiology*, *147*(2), 790–801. https://doi.org/10.1104/pp.108.119503

Grigliatti, T., & Mottus, R. C. (2013). Position Effects. In *Brenner's Encyclopedia of Genetics: Second Edition* (pp. 418–420). Elsevier Inc. https://doi.org/10.1016/B978-0-12-374984-0.01198-0

Groll, M., Bajorek, M., Köhler, A., Moroder, L., Rubin, D. M., Huber, R., Glickman, M. H., & Finley, D. (2000). A gated channel into the proteasome core particle. *Nature Structural Biology*, *7*(11), 1062–1067. https://doi.org/10.1038/80992

Guerra, T., Schilling, S., Hake, K., Gorzolka, K., Sylvester, F. P., Conrads, B., Westermann, B., & Romeis, T. (2020). Calcium-dependent protein kinase 5 links calcium signaling with N-hydroxy-l-pipecolic acid- and SARD1-dependent immune memory in systemic acquired resistance. *New Phytologist*, *225*(1), 310–325. https://doi.org/10.1111/nph.16147

Guharoy, M., Bhowmick, P., & Tompa, P. (2016). Design principles involving protein disorder facilitate specific substrate selection and degradation by the ubiquitin-proteasome system. In *Journal of Biological Chemistry* (Vol. 291, Issue 13, pp. 6723–6731). American Society for Biochemistry and Molecular Biology Inc.

https://doi.org/10.1074/jbc.R115.692665

Guo, L., Cesari, S., De Guillen, K., Chalvon, V., Mammri, L., Ma, M., Meusnier, I., Bonnot, F., Padilla, A., Peng, Y. L., Liu, J., & Kroj, T. (2018). Specific recognition of two MAX effectors by integrated HMA domains in plant immune receptors involves distinct binding surfaces. *Proceedings of the National Academy of Sciences of the United States of America*, *115*(45), 11637–11642. https://doi.org/10.1073/pnas.1810705115

Guzmán, P. (2012). The prolific ATL family of RING-H2 ubiquitin ligases. *Plant Signaling and Behavior*, *7*(8), 1014. https://doi.org/10.4161/psb.20851

Guzmán, P. (2014). ATLs and BTLs, plant-specific and general eukaryotic structurally-related E3 ubiquitin ligases. In *Plant Science* (Vols. 215–216, pp. 69–75). Elsevier Ireland Ltd. https://doi.org/10.1016/j.plantsci.2013.10.017

Haas, A. L., Warms, J. V. B., & Rose, I. A. (1983). Ubiquitin Adenylate: Structure and Role in Ubiquitin Activation. *Biochemistry*, *22*(19), 4388–4394. https://doi.org/10.1021/bi00288a007

Hamilton, K. S., Ellison, M. J., Barber, K. R., Williams, R. S., Huzil, J. T., McKenna, S., Ptak, C., Glover, M., & Shaw, G. S. (2001). Structure of a conjugating enzyme-ubiquitin thiolester intermediate reveals a novel role for the ubiquitin tail. *Structure*, *9*(10), 897–904. https://doi.org/10.1016/S0969-2126(01)00657-8

Hao, Q., Wang, W., Han, X., Wu, J., Lyu, B., Chen, F., Caplan, A., Li, C., Wu, J., Wang, W., Xu, Q., & Fu, D. (2018). Isochorismate-based salicylic acid biosynthesis confers basal resistance to *Fusarium graminearum* in barley. *Molecular Plant Pathology*, *19*(8), 1995–2010. https://doi.org/10.1111/mpp.12675

Harris, M. A., Deegan, J. I., Ireland, A., Lomax, J., Ashburner, M., Tweedie, S., Carbon, S., Lewis, S., Mungall, C., Day-Richter, J., Eilbeck, K., Blake, J. A., Bult, C., Diehl, A. D., Dolan, M., Drabkin, H., Eppig, J. T., Hill, D. P., Ni, L., … McCarthy, F. (2008). The Gene Ontology project in 2008. *Nucleic Acids Research*, *36*(SUPPL. 1), D440–D444. https://doi.org/10.1093/nar/gkm883

Hartmann-Petersen, R., Hendil, K. B., & Gordon, C. (2003). Ubiquitin binding proteins protect ubiquitin conjugates from disassembly. *FEBS Letters*, *535*(1–3), 77–81. https://doi.org/10.1016/S0014-5793(02)03874-7

Hartmann, M., Zeier, T., Bernsdorff, F., Reichel-Deland, V., Kim, D., Hohmann, M., Scholten, N., Schuck, S., Bräutigam, A., Hölzel, T., Ganter, C., & Zeier, J. (2018). Flavin Monooxygenase-Generated N-Hydroxypipecolic Acid Is a Critical Element of Plant Systemic Immunity. *Cell*, *173*(2), 456-469.e16. https://doi.org/10.1016/j.cell.2018.02.049

Hatfield, P. M., Gosink, M. M., Carpenter, T. B., & Vierstra, R. D. (1997). The ubiquitin-activating enzyme (E1) gene family in Arabidopsis thaliana. *The Plant Journal*, *11*(2), 213–226. https://doi.org/10.1046/j.1365-313X.1997.11020213.x

He, B., & Guo, W. (2009). The exocyst complex in polarized exocytosis. In *Current Opinion in Cell Biology* (Vol. 21, Issue 4, pp. 537–542). NIH Public Access. https://doi.org/10.1016/j.ceb.2009.04.007

He, Q., McLellan, H., Boevink, P. C., Sadanandom, A., Xie, C., Birch, P. R. J., & Tian, Z. (2015).

U-box E3 ubiquitin ligase PUB17 acts in the nucleus to promote specific immune pathways triggered by Phytophthora infestans. *Journal of Experimental Botany*, *66*(11), 3189–3199. https://doi.org/10.1093/jxb/erv128

Hershko, A., Ciechanover, A., Heller, H., Haas, A. L., & Rose, I. A. (1980). Proposed role of ATP in protein breakdown: conjugation of protein with multiple chains of the polypeptide of ATP-dependent proteolysis. *Proceedings of the National Academy of Sciences of the United States of America*, *77*(4), 1783–1786. https://doi.org/10.1073/pnas.77.4.1783

Hershko, A., Ciechanover, A., & Varshavsky, A. (2000). The ubiquitin system. In *Nature Medicine* (Vol. 6, Issue 10, pp. 1073–1081). Nature Publishing Group. https://doi.org/10.1038/80384

Hershkos, A., Heller, H., Elias, S., & Ciechanover, A. (1983). Components of Ubiquitin-Protein Ligase System RESOLUTION, AFFINITY PURIFICATION, AND ROLE IN PROTEIN BREAKDOWN*. In *THE JOURNAL OF BIOLOGICAL CHEMISTRY* (Vol. 258, Issue 13). http://www.jbc.org/

Hicke, L. (2001). Protein regulation by monoubiquitin. In *Nature Reviews Molecular Cell Biology* (Vol. 2, Issue 3, pp. 195–201). Nature Publishing Group. https://doi.org/10.1038/35056583

Hilker, M., Schwachtje, J., Baier, M., Balazadeh, S., Bäurle, I., Geiselhardt, S., Hincha, D. K., Kunze, R., Mueller-Roeber, B., Rillig, M. C., Rolff, J., Romeis, T., Schmülling, T., Steppuhn, A., van Dongen, J., Whitcomb, S. J., Wurst, S., Zuther, E., & Kopka, J. (2016). Priming and memory of stress responses in organisms lacking a nervous system. *Biological Reviews*, *91*(4), 1118–1133. https://doi.org/10.1111/brv.12215

Hua, Z., & Vierstra, R. D. (2011). The cullin-RING ubiquitin-protein ligases. *Annual Review of Plant Biology*, *62*, 299–334. https://doi.org/10.1146/annurev-arplant-042809-112256

Huang, L., Kinnucan, E., Wang, G., Beaudenon, S., Howley, P. M., Huibregtse, J. M., & Pavletich, N. P. (1999). Structure of an E6AP-UbcH7 complex: Insights into ubiquitination by the E2-E3 enzyme cascade. *Science*, *286*(5443), 1321–1326. https://doi.org/10.1126/science.286.5443.1321

Hubert, D. A., Tornero, P., Belkhadir, Y., Krishna, P., Takahashi, A., Shirasu, K., & Dangl, J. L. (2003). Cytosolic HSP90 associates with and modulates the Arabidopsis RPM1 disease resistance protein. *EMBO Journal*, *22*(21), 5679–5689. https://doi.org/10.1093/emboj/cdg547

Husnjak, K., Elsasser, S., Zhang, N., Chen, X., Randles, L., Shi, Y., Hofmann, K., Walters, K. J., Finley, D., & Dikic, I. (2008). Proteasome subunit Rpn13 is a novel ubiquitin receptor. *Nature*, *453*(7194), 481–488. https://doi.org/10.1038/nature06926

Imran, Q. M., Falak, N., Hussain, A., Mun, B. G., Sharma, A., Lee, S. U., Kim, K. M., & Yun, B. W. (2016). Nitric oxide responsive heavy metal-associated gene AtHMAD1 contributes to development and disease resistance in Arabidopsis thaliana. *Frontiers in Plant Science*, *7*(NOVEMBER2016). https://doi.org/10.3389/fpls.2016.01712

Innes, R. (2018). The Positives and Negatives of NPR: A Unifying Model for Salicylic Acid Signaling in Plants. In *Cell* (Vol. 173, Issue 6, pp. 1314–1315). Cell Press. https://doi.org/10.1016/j.cell.2018.05.034

Ishida, T., & Kinoshita, K. (2007). PrDOS: Prediction of disordered protein regions from amino acid sequence. *Nucleic Acids Research*, *35*(SUPPL.2). https://doi.org/10.1093/nar/gkm363

Jones, J. D. G., & Dangl, J. L. (2006). The plant immune system. In *Nature* (Vol. 444, Issue 7117, pp. 323–329). https://doi.org/10.1038/nature05286

Jong, T. S., Lu, H., McDowell, J. M., & Greenberg, J. T. (2004). A key role for ALD1 in activation of local and systemic defenses in Arabidopsis. *Plant Journal*, *40*(2), 200–212. https://doi.org/10.1111/j.1365-313x.2004.02200.x

Jung, C., Zhao, P., Seo, J. S., Mitsuda, N., Deng, S., & Chua, N. H. (2015). PLANT U-BOX PROTEIN10 regulates MYC2 stability in arabidopsis. *Plant Cell*, *27*(7), 2016–2031. https://doi.org/10.1105/tpc.15.00385

Jung, H. W., Tschaplinski, T. J., Wang, L., Glazebrook, J., & Greenberg, J. T. (2009). Priming in systemic plant immunity. *Science*, *324*(5923), 89–91. https://doi.org/10.1126/science.1170025

Kadota, Y., & Shirasu, K. (2012). The HSP90 complex of plants. In *Biochimica et Biophysica Acta - Molecular Cell Research* (Vol. 1823, Issue 3, pp. 689–697). Elsevier. https://doi.org/10.1016/j.bbamcr.2011.09.016

Karimi, M., Inzé, D., & Depicker, A. (2002). GATEWAY^{TM} vectors for Agrobacterium-mediated plant transformation. In *Trends in Plant Science* (Vol. 7, Issue 5, pp. 193–195). Elsevier Ltd. https://doi.org/10.1016/S1360-1385(02)02251-3

Karmakar, S., Datta, K., Molla, K. A., Gayen, D., Das, K., Sarkar, S. N., & Datta, S. K. (2019). Proteo-metabolomic investigation of transgenic rice unravels metabolic alterations and accumulation of novel proteins potentially involved in defence against Rhizoctonia solani. *Scientific Reports*. https://doi.org/10.1038/s41598-019-46885-3

Khoury, G. A., Baliban, R. C., & Floudas, C. A. (2011). Proteome-wide post-translational modification statistics: Frequency analysis and curation of the swiss-prot database. *Scientific Reports*, *1*. https://doi.org/10.1038/srep00090

Kiefer, I. W., & Slusarenko, A. J. (2003). The pattern of systemic acquired resistance induction within the Arabidopsis rosette in relation to the pattern of translocation. *Plant Physiology*, *132*(2), 840–847. https://doi.org/10.1104/pp.103.021709

Kim, D. S., & Hwang, B. K. (2014). An important role of the pepper phenylalanine ammonia-lyase gene (PAL1) in salicylic acid-dependent signalling of the defence response to microbial pathogens. *Journal of Experimental Botany*, *65*(9), 2295–2306. https://doi.org/10.1093/jxb/eru109

Kim, D. Y., Scalf, M., Smith, L. M., & Vierstra, R. D. (2013). Advanced proteomic analyses yield a deep catalog of ubiquitylation targets in Arabidopsis. *Plant Cell*, *25*(5), 1523–1540. https://doi.org/10.1105/tpc.112.108613

Kim, M. H., Jeon, J., Lee, S., Lee, J. H., Gao, L., Lee, B. H., Park, J. M., Kim, Y. J., & Kwak, J. M. (2019). Proteasome subunit RPT2a promotes PTGS through repressing RNA quality control in Arabidopsis. *Nature Plants*, *5*(12), 1273–1282. https://doi.org/10.1038/s41477-019-0546-1

Kim, Y., Gilmour, S. J., Chao, L., Park, S., & Thomashow, M. F. (2019). Arabidopsis CAMTA Transcription Factors Regulate Pipecolic Acid Biosynthesis and Priming of Immunity Genes. *Molecular Plant*, *13*(1). https://doi.org/10.1016/j.molp.2019.11.001

Kirkin, V., McEwan, D. G., Novak, I., & Dikic, I. (2009). A Role for Ubiquitin in Selective Autophagy. In *Molecular Cell* (Vol. 34, Issue 3, pp. 259–269). Elsevier. https://doi.org/10.1016/j.molcel.2009.04.026

Knepper, C., & Day, B. (2010). From Perception to Activation: The Molecular-Genetic and Biochemical Landscape of Disease Resistance Signaling in Plants. *The Arabidopsis Book*, *8*(8), e012. https://doi.org/10.1199/tab.0124

Koch, M., Vorwerk, S., Masur, C., Sharifi-Sirchi, G., Olivieri, N., & Schlaich, N. L. (2006). A role for a flavin-containing mono-oxygenase in resistance against microbial pathogens in Arabidopsis. *Plant Journal*, *47*(4), 629–639. https://doi.org/10.1111/j.1365-313X.2006.02813.x

Kraft, E., Stone, S. L., Ma, L., Su, N., Gao, Y., Lau, O. S., Deng, X. W., & Callis, J. (2005). Genome analysis and functional characterization of the E2 and RING-type E3 ligase ubiquitination enzymes of Arabidopsis. *Plant Physiology*, *139*(4), 1597–1611. https://doi.org/10.1104/pp.105.067983

Kravtsova-Ivantsiv, Y., & Ciechanover, A. (2012). Non-canonical ubiquitin-based signals for proteasomal degradation. *Journal of Cell Science*, *125*(3), 539–548. https://doi.org/10.1242/jcs.093567

Kumar, D., & Klessig, D. F. (2003). High-affinity salicylic acid-binding protein 2 is required for plant innate immunity and has salicylic acid-stimulated lipase activity. *Proceedings of the National Academy of Sciences of the United States of America*, *100*(26), 16101–16106. https://doi.org/10.1073/pnas.0307162100

Kurepa, J., Toh-E, A., & Smalle, J. A. (2008). 26S proteasome regulatory particle mutants have increased oxidative stress tolerance. *Plant Journal*, *53*(1), 102–114. https://doi.org/10.1111/j.1365-313X.2007.03322.x

Kurepa, J., Wang, S., Li, Y., & Smalle, J. (2009). Proteasome regulation, plant growth and stress tolerance. In *Plant Signaling and Behavior* (Vol. 4, Issue 10, pp. 924–927). Taylor & Francis. https://doi.org/10.4161/psb.4.10.9469

Kurepa, J., Wang, S., Li, Y., Zaitlin, D., Pierce, A. J., & Smalle, J. A. (2009). Loss of 26S proteasome function leads to increased cell size and decreased cell number in Arabidopsis shoot organs 1[C][W][OA]. *Plant Physiology*, *150*(1), 178–189. https://doi.org/10.1104/pp.109.135970

Lang-Mladek, C., Xie, L., Nigam, N., Chumak, N., Binkert, M., Neubert, S., & Hauser, M.-T. (2012). UV-B signaling pathways and fluence rate dependent transcriptional regulation of ARIADNE12. *Physiologia Plantarum*, *145*(4), 527–539. https://doi.org/10.1111/j.1399-3054.2011.01561.x

Lasker, K., Förster, F., Bohn, S., Walzthoeni, T., Villa, E., Unverdorben, P., Beck, F., Aebersold, R., Sali, A., & Baumeister, W. (2012). Molecular architecture of the 26S proteasome holocomplex determined by an integrative approach. *Proceedings of the National Academy of Sciences of the United States of America*, *109*(5), 1380–1387.

https://doi.org/10.1073/pnas.1120559109

Lee, D. H., Choi, H. W., & Hwang, B. K. (2011). The pepper E3 ubiquitin ligase RING1 gene, caRING1, is required for cell death and the salicylic acid-dependent defense response. *Plant Physiology*, *156*(4), 2011–2025. https://doi.org/10.1104/pp.111.177568

Lee, H. J., Park, Y. J., Seo, P. J., Kim, J. H., Sim, H. J., Kim, S. G., & Park, C. M. (2015). Systemic immunity requires SnRK2.8-mediated nuclear import of NPR1 in arabidopsis. *Plant Cell*, *27*(12), 3425–3438. https://doi.org/10.1105/tpc.15.00371

Li, J., Zhang, M., Sun, J., Mao, X., Wang, J., Liu, H., Zheng, H., Li, X., Zhao, H., & Zou, D. (2020). Heavy Metal Stress-Associated Proteins in Rice and Arabidopsis: Genome-Wide Identification, Phylogenetics, Duplication, and Expression Profiles Analysis. *Frontiers in Genetics*, *11*, 477. https://doi.org/10.3389/fgene.2020.00477

Li, P., Liu, C., Deng, W. H., Yao, D. M., Pan, L. L., Li, Y. Q., Liu, Y. Q., Liang, Y., Zhou, X. P., & Wang, X. W. (2019). Plant begomoviruses subvert ubiquitination to suppress plant defenses against insect vectors. *PLoS Pathogens*, *15*(2). https://doi.org/10.1371/journal.ppat.1007607

Li, Wei, Ahn, I. P., Ning, Y., Park, C. H., Zeng, L., Whitehill, J. G. A., Lu, H., Zhao, Q., Ding, B., Xie, Q., Zhou, J. M., Dai, L., & Wang, G. L. (2012). The U-Box/ARM E3 ligase PUB13 regulates cell death, defense, and flowering time in Arabidops. *Plant Physiology*, *159*(1), 239–250. https://doi.org/10.1104/pp.111.192617

Li, Wenfeng, & Schmidt, W. (2010). A lysine-63-linked ubiquitin chain-forming conjugase, UBC13, promotes the developmental responses to iron deficiency in Arabidopsis roots. *Plant Journal*, *62*(2), 330–343. https://doi.org/10.1111/j.1365-313X.2010.04150.x

Li, Z., Huang, J., Wang, Z., Meng, F., Zhang, S., Wu, X., Zhang, Z., & Gao, Z. (2019). Overexpression of Arabidopsis nucleotide-binding and leucine-rich repeat genes RPS2 and RPM1(D505v) confers broad-spectrum disease resistance in rice. *Frontiers in Plant Science*, *10*. https://doi.org/10.3389/fpls.2019.00417

Liao, D., Cao, Y., Sun, X., Espinoza, C., Nguyen, C. T., Liang, Y., & Stacey, G. (2017). Arabidopsis E3 ubiquitin ligase PLANT U-BOX13 (PUB13) regulates chitin receptor LYSIN MOTIF RECEPTOR KINASE5 (LYK5) protein abundance. *New Phytologist*, *214*(4), 1646–1656. https://doi.org/10.1111/nph.14472

Lim, G. H., Shine, M. B., De Lorenzo, L., Yu, K., Cui, W., Navarre, D., Hunt, A. G., Lee, J. Y., Kachroo, A., & Kachroo, P. (2016). Plasmodesmata Localizing Proteins Regulate Transport and Signaling during Systemic Acquired Immunity in Plants. *Cell Host and Microbe*, *19*(4), 541–549. https://doi.org/10.1016/j.chom.2016.03.006

Lin, S. J., & Culotta, V. C. (1995). The ATX1 gene of Saccharomyces cerevisiae encodes a small metal homeostasis factor that protects cells against reactive oxygen toxicity. *Proceedings of the National Academy of Sciences of the United States of America*, *92*(9), 3784–3788. https://doi.org/10.1073/pnas.92.9.3784

Lin, S. S., Martin, R., Mongrand, S., Vandenabeele, S., Chen, K. C., Jang, I. C., & Chua, N. H. (2008). RING1 E3 ligase localizes to plasma membrane lipid rafts to trigger FB1-induced programmed cell death in Arabidopsis. *Plant Journal*, *56*(4), 550–561. https://doi.org/10.1111/j.1365-313X.2008.03625.x

Linke, K., Mace, P. D., Smith, C. A., Vaux, D. L., Silke, J., & Day, C. L. (2008). Structure of the MDM2/MDMX RING domain heterodimer reveals dimerization is required for their ubiquitylation in trans. *Cell Death and Differentiation*, *15*(5), 841–848. https://doi.org/10.1038/sj.cdd.4402309

Liu, Hongxia, Ravichandran, S., Teh, O. K., McVey, S., Lilley, C., Teresinski, H. J., Gonzalez-Ferrer, C., Mullen, R. T., Hofius, D., Prithiviraj, B., & Stonea, S. L. (2017). The RING-Type E3 Ligase XBAT35.2 is involved in cell death induction and pathogen response. *Plant Physiology*, *175*(3), 1469–1483. https://doi.org/10.1104/pp.17.01071

Liu, Huizhi, Zhang, H., Yang, Y., Li, G., Yang, Y., Wang, X., Basnayake, B. M. V. S., Li, D., & Song, F. (2008). Functional analysis reveals pleiotropic effects of rice RING-H2 finger protein gene OsBIRF1 on regulation of growth and defense responses against abiotic and biotic stresses. *Plant Molecular Biology*, *68*(1–2), 17–30. https://doi.org/10.1007/s11103-008-9349-x

Liu, P. P., von Dahl, C. C., & Klessig, D. F. (2011). The extent to which methyl salicylate is required for signaling systemic acquired resistance is dependent on exposure to light after infection. *Plant Physiology*, *157*(4), 2216–2226. https://doi.org/10.1104/pp.111.187773

Liu, Y., & Li, J. (2014). Endoplasmic reticulum-mediated protein quality control in Arabidopsis. In *Frontiers in Plant Science* (Vol. 5, Issue APR). Frontiers Research Foundation. https://doi.org/10.3389/fpls.2014.00162

Lopez, V. A., Park, B. C., Nowak, D., Sreelatha, A., Zembek, P., Fernandez, J., Servage, K. A., Gradowski, M., Hennig, J., Tomchick, D. R., Pawłowski, K., Krzymowska, M., & Tagliabracci, V. S. (2019). A Bacterial Effector Mimics a Host HSP90 Client to Undermine Immunity. *Cell*, *179*(1), 205-218.e21. https://doi.org/10.1016/j.cell.2019.08.020

Love, M. I., Huber, W., & Anders, S. (2014). Moderated estimation of fold change and dispersion for RNA-seq data with DESeq2. *Genome Biology*, *15*(12), 550. https://doi.org/10.1186/s13059-014-0550-8

Lu, D., Lin, W., Gao, X., Wu, S., Cheng, C., Avila, J., Heese, A., Devarenne, T. P., He, P., & Shan, L. (2011). Direct ubiquitination of pattern recognition receptor FLS2 attenuates plant innate immunity. *Science*, *332*(6036), 1439–1442. https://doi.org/10.1126/science.1204903

Lu, D., Wu, S., Gao, X., Zhang, Y., Shan, L., & He, P. (2010). A receptor-like cytoplasmic kinase, BIK1, associates with a flagellin receptor complex to initiate plant innate immunity. *Proceedings of the National Academy of Sciences of the United States of America*, *107*(1), 496–501. https://doi.org/10.1073/pnas.0909705107

Luo, H., Laluk, K., Lai, Z., Veronese, P., Song, F., & Mengiste, T. (2010). The arabidopsis botrytis susceptible1 interactor defines a subclass of RING E3 ligases that regulate pathogen and stress responses. *Plant Physiology*, *154*(4), 1766–1782. https://doi.org/10.1104/pp.110.163915

Ma, X., Claus, L. A. N., Leslie, M. E., Tao, K., Wu, Z., Liu, J., Yu, X., Li, B., Zhou, J., Savatin, D. V., Peng, J., Tyler, B. M., Heese, A., Russinova, E., He, P., & Shan, L. (2020). Ligand-induced monoubiquitination of BIK1 regulates plant immunity. *Nature*, *581*(7807), 199–203.

https://doi.org/10.1038/s41586-020-2210-3

Maekawa, S., Sato, T., Asada, Y., Yasuda, S., Yoshida, M., Chiba, Y., & Yamaguchi, J. (2012). The Arabidopsis ubiquitin ligases ATL31 and ATL6 control the defense response as well as the carbon/nitrogen response. *Plant Molecular Biology*, *79*(3), 217–227. https://doi.org/10.1007/s11103-012-9907-0

Mandal, M. K., Chanda, B., Xia, Y., Yu, K., Sekine, K. T., Gao, Q. M., Selote, D., Kachroo, A., & Kachroo, P. (2011). Glycerol-3-phosphate and systemic immunity. *Plant Signaling and Behavior*, *6*(11), 1871–1874. https://doi.org/10.4161/psb.6.11.17901

Mao, G., Meng, X., Liu, Y., Zheng, Z., Chen, Z., & Zhang, S. (2011). Phosphorylation of a WRKY transcription factor by two pathogen-responsive MAPKs drives phytoalexin biosynthesis in Arabidopsis. *Plant Cell*, *23*(4), 1639–1653. https://doi.org/10.1105/tpc.111.084996

Maqbool, A., Saitoh, H., Franceschetti, M., Stevenson, C. E. M., Uemura, A., Kanzaki, H., Kamoun, S., Terauchi, R., & Banfield, M. J. (2015). Structural basis of pathogen recognition by an integrated HMA domain in a plant NLR immune receptor. *ELife*, *4*(AUGUST2015). https://doi.org/10.7554/eLife.08709

Marín, I. (2010). Diversification and specialization of plant RBR ubiquitin ligases. *PLoS ONE*, *5*(7). https://doi.org/10.1371/journal.pone.0011579

Marín, I., Lucas, J. I., Gradilla, A. C., & Ferrús, A. (2004). Parkin and relatives: The RBR family of ubiquitin ligases. In *Physiological Genomics* (Vol. 17, Issue 3, pp. 253–263). Physiol Genomics. https://doi.org/10.1152/physiolgenomics.00226.2003

Marino, D., Peeters, N., & Rivas, S. (2012). Ubiquitination during plant immune signaling. *Plant Physiology*, *160*(1), 15–27. https://doi.org/10.1104/pp.112.199281

Marshall, R. S., & Vierstra, R. D. (2019). Dynamic regulation of the 26S proteasome: From synthesis to degradation. In *Frontiers in Molecular Biosciences* (Vol. 6, Issue JUN). Frontiers Media S.A. https://doi.org/10.3389/fmolb.2019.00040

Mbengue, M., Camut, S., de Carvalho-Niebel, F., Deslandes, L., Solène, F., Klaus-Heisen, D., Moreau, S., Rivas, S., Timmers, T., Hervé, C., Cullimore, J., & Lefebvre, B. (2010). The medicago truncatula E3 ubiquitin ligase PUB1 interacts with the LYK3 symbiotic receptor and negatively regulates infection and nodulation. *Plant Cell*, *22*(10), 3474–3488. https://doi.org/10.1105/tpc.110.075861

McDowell, G. S., & Philpott, A. (2013). Non-canonical ubiquitylation: Mechanisms and consequences. In *International Journal of Biochemistry and Cell Biology* (Vol. 45, Issue 8, pp. 1833–1842). Elsevier Ltd. https://doi.org/10.1016/j.biocel.2013.05.026

Meng, X., & Zhang, S. (2013). MAPK Cascades in Plant Disease Resistance Signaling. *Annual Review of Phytopathology*, *51*(1), 245–266. https://doi.org/10.1146/annurev-phyto-082712-102314

Mengiste, T., Chen, X., Salmeron, J., & Dietrich, R. (2003). The Botrytis Susceptible1 Gene Encodes an R2R3MYB Transcription Factor Protein That Is Required for Biotic and Abiotic Stress Responses in Arabidopsis. *Plant Cell*, *15*(11), 2551–2565. https://doi.org/10.1105/tpc.014167

Meuwly, P., & Métraux, J. P. (1993). Ortho-anisic acid as internal standard for the

simultaneous quantitation of salicylic acid and its putative biosynthetic precursors in cucumber leaves. *Analytical Biochemistry*, *214*(2), 500–505. https://doi.org/10.1006/abio.1993.1529

Miao, Y., & Zentgraf, U. (2010). A HECT E3 ubiquitin ligase negatively regulates Arabidopsis leaf senescence through degradation of the transcription factor WRKY53. *Plant Journal*, *63*(2), 179–188. https://doi.org/10.1111/j.1365-313X.2010.04233.x

Miller, G., Schlauch, K., Tam, R., Cortes, D., Torres, M. A., Shulaev, V., Dangl, J. L., & Mittler, R. (2009). The plant NADPH oxidase RBOHD mediates rapid systemic signaling in response to diverse stimuli. *Science Signaling*, *2*(84). https://doi.org/10.1126/scisignal.2000448

Mishina, T. E., & Zeier, J. (2006). The Arabidopsis flavin-dependent monooxygenase FMO1 is an essential component of biologically induced systemic acquired resistance. *Plant Physiology*, *141*(4), 1666–1675. https://doi.org/10.1104/pp.106.081257

Mishina, T. E., & Zeier, J. (2007). Pathogen-associated molecular pattern recognition rather than development of tissue necrosis contributes to bacterial induction of systemic acquired resistance in Arabidopsis. *Plant Journal*, *50*(3), 500–513. https://doi.org/10.1111/j.1365-313X.2007.03067.x

Mladek, C., Guger, K., & Hauser, M. T. (2003). Identification and characterization of the ARIADNE gene family in Arabidopsis. A group of putative E3 ligases. *Plant Physiology*, *131*(1), 27–40. https://doi.org/10.1104/pp.012781

Moreno, A. A., Mukhtar, M. S., Blanco, F., Boatwright, J. L., Moreno, I., Jordan, M. R., Chen, Y., Brandizzi, F., Dong, X., Orellana, A., & Pajerowska-Mukhtar, K. M. (2012). IRE1/bZIP60-mediated unfolded protein response plays distinct roles in plant immunity and abiotic stress responses. *PLoS ONE*, *7*(2). https://doi.org/10.1371/journal.pone.0031944

Mudgil, Y., Shiu, S. H., Stone, S. L., Salt, J. N., & Goring, D. R. (2004). A Large Complement of the Predicted Arabidopsis ARM Repeat Proteins Are Members of the U-Box E3 Ubiquitin Ligase Family. *Plant Physiology*, *134*(1), 59–66. https://doi.org/10.1104/pp.103.029553

Mural, R. V., Liu, Y., Rosebrock, T. R., Brady, J. J., Hamera, S., Connor, R. A., Martin, G. B., & Zeng, L. (2013). The tomato Fni3 Lysine-63-specific ubiquitin-conjugating enzyme and suv ubiquitin E2 variant positively regulate plant immunity. *Plant Cell*, *25*(9), 3615–3631. https://doi.org/10.1105/tpc.113.117093

Nafisi, M., Goregaoker, S., Botanga, C. J., Glawischnig, E., Olsen, C. E., Halkier, B. A., & Glazebrook, J. (2007). Arabidopsis cytochrome P450 monooxygenase 71A13 catalyzes the conversion of indole-3-acetaldoxime in camalexin synthesis. *Plant Cell*, *19*(6), 2039–2052. https://doi.org/10.1105/tpc.107.051383

Nakamura, S., Mano, S., Tanaka, Y., Ohnishi, M., Nakamori, C., Araki, M., Niwa, T., Nishimura, M., Kaminaka, H., Nakagawa, T., Sato, Y., & Ishiguro, S. (2010). Gateway binary vectors with the bialaphos resistance gene, bar, as a selection marker for plant transformation. *Bioscience, Biotechnology and Biochemistry*, *74*(6), 1315–1319. https://doi.org/10.1271/bbb.100184

Návarová, H., Bernsdorff, F., Döring, A. C., & Zeier, J. (2013). Pipecolic acid, an endogenous

mediator of defense amplification and priming, is a critical regulator of inducible plant immunity. *Plant Cell*, *24*(12), 5123–5141. https://doi.org/10.1105/tpc.112.103564

Nawrath, C., Heck, S., Parinthawong, N., & Métraux, J. P. (2002). EDS5, an essential component of salicylic acid-dependent signaling for disease resistance in arabidopsis, is a member of the MATE transporter family. *Plant Cell*, *14*(1), 275–286. https://doi.org/10.1105/tpc.010376

Nawrath, C., & Métraux, J.-P. (1999). Salicylic Acid Induction-Deficient Mutants of Arabidopsis Express PR-2 and PR-5 and Accumulate High Levels of Camalexin after Pathogen Inoculation. In *The Plant Cell* (Vol. 11). www.plantcell.org

Ng, D. W. K., Abeysinghe, J. K., & Kamali, M. (2018). Regulating the regulators: The control of transcription factors in plant defense signaling. In *International Journal of Molecular Sciences* (Vol. 19, Issue 12). MDPI AG. https://doi.org/10.3390/ijms19123737

Nürnberger, T., & Brunner, F. (2002). Innate immunity in plants and animals: Emerging parallels between the recognition of general elicitors and pathogen-associated molecular patterns. In *Current Opinion in Plant Biology* (Vol. 5, Issue 4, pp. 318–324). Elsevier Ltd. https://doi.org/10.1016/S1369-5266(02)00265-0

O'Brien, J. A., Daudi, A., Butt, V. S., & Bolwell, G. P. (2012). Reactive oxygen species and their role in plant defence and cell wall metabolism. *Planta*, *236*(3), 765–779. https://doi.org/10.1007/s00425-012-1696-9

Ogawa, T., Muramoto, K., Takada, R., Nakagawa, S., Shigeoka, S., & Yoshimura, K. (2016). Modulation of NADH Levels by Arabidopsis Nudix Hydrolases, AtNUDX6 and 7, and the Respective Proteins Themselves Play Distinct Roles in the Regulation of Various Cellular Responses Involved in Biotic/Abiotic Stresses. *Plant and Cell Physiology*, *57*(6), 1295–1308. https://doi.org/10.1093/pcp/pcw078

Orosa, B., He, Q., Mesmar, J., Gilroy, E. M., McLellan, H., Yang, C., Craig, A., Bailey, M., Zhang, C., Moore, J. D., Boevink, P. C., Tian, Z., Birch, P. R. J., & Sadanandom, A. (2017). BTB-BACK Domain Protein POB1 Suppresses Immune Cell Death by Targeting Ubiquitin E3 ligase PUB17 for Degradation. *PLoS Genetics*, *13*(1). https://doi.org/10.1371/journal.pgen.1006540

Pandey, S. P., Roccaro, M., Schön, M., Logemann, E., & Somssich, I. E. (2010). Transcriptional reprogramming regulated by WRKY18 and WRKY40 facilitates powdery mildew infection of Arabidopsis. *Plant Journal*, *64*(6), 912–923. https://doi.org/10.1111/j.1365-313X.2010.04387.x

Pandey, S. P., & Somssich, I. E. (2009). The role of WRKY transcription factors in plant immunity. *Plant Physiology*, *150*(4), 1648–1655. https://doi.org/10.1104/pp.109.138990

Park, S. W., Kaimoyo, E., Kumar, D., Mosher, S., & Klessig, D. F. (2007). Methyl salicylate is a critical mobile signal for plant systemic acquired resistance. *Science*, *318*(5847), 113–116. https://doi.org/10.1126/science.1147113

Passmore, L. A., & Barford, D. (2004). Getting into position: the catalytic mechanisms of protein ubiquitylation. In *Biochem. J* (Vol. 379).

Pedersen, C. N. S., Axelsen, K. B., Harper, J. F., & Palmgren, M. G. (2012). Evolution of Plant

P-Type ATPases. *Frontiers in Plant Science*, *3*(FEB), 31. https://doi.org/10.3389/fpls.2012.00031

Pérez-Llorca, M., Muñoz, P., Müller, M., & Munné-Bosch, S. (2019). Biosynthesis, metabolism and function of auxin, salicylic acid and melatonin in climacteric and non-climacteric fruits. In *Frontiers in Plant Science* (Vol. 10, p. 136). Frontiers Media S.A. https://doi.org/10.3389/fpls.2019.00136

Pétriacq, P., Ton, J., Patrit, O., Tcherkez, G., & Gakière, B. (2016). NAD acts as an integral regulator of multiple defense layers. *Plant Physiology*, *172*(3), 1465–1479. https://doi.org/10.1104/pp.16.00780

Petroski, M. D., & Deshaies, R. J. (2005). Function and regulation of cullin-RING ubiquitin ligases. In *Nature Reviews Molecular Cell Biology* (Vol. 6, Issue 1, pp. 9–20). Nature Publishing Group. https://doi.org/10.1038/nrm1547

Pickart, C. M., & Fushman, D. (2004). Polyubiquitin chains: Polymeric protein signals. In *Current Opinion in Chemical Biology* (Vol. 8, Issue 6, pp. 610–616). Curr Opin Chem Biol. https://doi.org/10.1016/j.cbpa.2004.09.009

Pieterse, C. M. J., Van Wees, S. C. M., Van Pelt, J. A., Knoester, M., Laan, R., Gerrits, H., Weisbeek, P. J., & Van Loon, L. C. (1998). A novel signaling pathway controlling induced systemic resistance in arabidopsis. *Plant Cell*, *10*(9), 1571–1580. https://doi.org/10.1105/tpc.10.9.1571

Pokotylo, I., Kravets, V., & Ruelland, E. (2019). Salicylic acid binding proteins (SABPs): The hidden forefront of salicylic acid signalling. In *International Journal of Molecular Sciences* (Vol. 20, Issue 18). MDPI AG. https://doi.org/10.3390/ijms20184377

Poppek, D., & Grune, T. (2006). Proteasomal defense of oxidative protein modifications. In *Antioxidants and Redox Signaling* (Vol. 8, Issues 1–2, pp. 173–184). Antioxid Redox Signal. https://doi.org/10.1089/ars.2006.8.173

Puig, S., Mira, H., Dorcey, E., Sancenón, V., Andrés-Colás, N., Garcia-Molina, A., Burkhead, J. L., Gogolin, K. A., Abdel-Ghany, S. E., Thiele, D. J., Ecker, J. R., Pilon, M., & Peñarrubia, L. (2007). Higher plants possess two different types of ATX1-like copper chaperones. *Biochemical and Biophysical Research Communications*, *354*(2), 385–390. https://doi.org/10.1016/j.bbrc.2006.12.215

Rekhter, D., Lüdke, D., Ding, Y., Feussner, K., Zienkiewicz, K., Lipka, V., Wiermer, M., Zhang, Y., & Feussner, I. (2019). Isochorismate-derived biosynthesis of the plant stress hormone salicylic acid. *Science*, *365*(6452), 498–502. https://doi.org/10.1126/science.aaw1720

Rieu, I., & Powers, S. J. (2009). Real-time quantitative RT-PCR: Design, calculations, and statistics. *Plant Cell*, *21*(4), 1031–1033. https://doi.org/10.1105/tpc.109.066001

Rius, S. P., Casati, P., Iglesias, A. A., & Gomez-Casati, D. F. (2008). Characterization of Arabidopsis lines deficient in GAPC-1, a cytosolic NAD-dependent glyceraldehyde-3-phosphate dehydrogenase. *Plant Physiology*, *148*(3), 1655–1667. https://doi.org/10.1104/pp.108.128769

Romero-Barrios, N., & Vert, G. (2018). Proteasome-independent functions of lysine-63 polyubiquitination in plants. In *New Phytologist*. https://doi.org/10.1111/nph.14915

Rosebrock, T. R., Zeng, L., Brady, J. J., Abramovitch, R. B., Xiao, F., & Martin, G. B. (2007). A bacterial E3 ubiquitin ligase targets a host protein kinase to disrupt plant immunity. *Nature*, *448*(7151), 370–374. https://doi.org/10.1038/nature05966

Rustérucci, C., Aviv, D. H., Holt, B. F., Dangl, J. L., & Parker, J. E. (2001). The Disease Resistance Signaling Components EDS1 and PAD4 Are Essential Regulators of the Cell Death Pathway Controlled by LSD1 in Arabidopsis . *The Plant Cell*, *13*(10), 2211–2224. https://doi.org/10.1105/tpc.010085

Ryals, J. A., Neuenschwander, U. H., Willits, M. G., Molina, A., Steiner, H. Y., & Hunt, M. D. (1996). Systemic acquired resistance. In *Plant Cell* (Vol. 8, Issue 10, pp. 1809–1819). American Society of Plant Physiologists. https://doi.org/10.1105/tpc.8.10.1809

Sadanandom, A., Bailey, M., Ewan, R., Lee, J., & Nelis, S. (2012). The ubiquitin-proteasome system: central modifier of plant signalling. *New Phytologist*, *196*(1), 13–28. https://doi.org/10.1111/j.1469-8137.2012.04266.x

Sako, K., Maki, Y., Kanai, T., Kato, E., Maekawa, S., Yasuda, S., Sato, T., Watahiki, M. K., & Yamaguchi, J. (2012). Arabidopsis RPT2a, 19S Proteasome Subunit, Regulates Gene Silencing via DNA Methylation. *PLoS ONE*, *7*(5), e37086. https://doi.org/10.1371/journal.pone.0037086

Saleh, A., Withers, J., Mohan, R., Marqués, J., Gu, Y., Yan, S., Zavaliev, R., Nomoto, M., Tada, Y., & Dong, X. (2015). Posttranslational modifications of the master transcriptional regulator NPR1 enable dynamic but tight control of plant immune responses. *Cell Host and Microbe*, *18*(2), 169–182. https://doi.org/10.1016/j.chom.2015.07.005

Salinas-Mondragón, R. E., Garcidueñas-Piña, C., & Guzmán, P. (1999). Early elicitor induction in members of a novel multigene family coding for highly related RING-H2 proteins in Arabidopsis thaliana. *Plant Molecular Biology*, *40*(4), 579–590. https://doi.org/10.1023/A:1006267201855

Samuel, M. A., Mudgil, Y., Salt, J. N., Delmas, F., Ramachandran, S., Chilelli, A., & Goring, D. R. (2008). Interactions between the S-domain receptor kinases and AtPUB-ARM E3 ubiquitin ligases suggest a conserved signaling pathway in arabidopsis. *Plant Physiology*, *147*(4), 2084–2095. https://doi.org/10.1104/pp.108.123380

Sanger, F., Nicklen, S., & Coulson, A. R. (1977). *DNA sequencing with chain-terminating inhibitors (DNA polymerase/nucleotide sequences/bacteriophage 4X174)* (Vol. 74, Issue 12).

Schuhegger, R., Nafisi, M., Mansourova, M., Petersen, B. L., Olsen, C. E., Svatoš, A., Halkier, B. A., & Glawischnig, E. (2006). CYP71B15 (PAD3) catalyzes the final step in camalexin biosynthesis. *Plant Physiology*, *141*(4), 1248–1254. https://doi.org/10.1104/pp.106.082024

Schulze-Lefert, P. (2004). Plant Immunity: The Origami of Receptor Activation. *Current Biology*, *14*(1), R22–R24. https://doi.org/10.1016/j.cub.2003.12.017

Seok, K. C., Moon, Y. R., Song, C., Kwak, J. M., & Woo, T. K. (2008). Arabidopsis PUB22 and PUB23 are homologous U-Box E3 ubiquitin ligases that play combinatory roles in response to drought stress. *Plant Cell*, *20*(7), 1899–1914. https://doi.org/10.1105/tpc.108.060699

Serrano, I., Campos, L., & Rivas, S. (2018). Roles of E3 ubiquitin-ligases in nuclear protein homeostasis during plant stress responses. In *Frontiers in Plant Science* (Vol. 9). Frontiers Media S.A. https://doi.org/10.3389/fpls.2018.00139

Serrano, I., Gu, Y., Qi, D., Dubiella, U., & Innes, R. W. (2014). The arabidopsis EDR1 protein kinase negatively regulates the ATL1 e3 ubiquitin ligase to suppress cell death. *Plant Cell*, *26*(11), 4532–4546. https://doi.org/10.1105/tpc.114.131540

Serrano, M., Parra, S., Alcaraz, L. D., & Guzmán, P. (2006). The ATL gene family from Arabidopsis thaliana and Oryza sativa comprises a large number of putative ubiquitin ligases of the RING-H2 type. *Journal of Molecular Evolution*, *62*(4), 434–445. https://doi.org/10.1007/s00239-005-0038-y

Shah, J., & Zeier, J. (2013). Long-distance communication and signal amplification in systemic acquired resistance. In *Frontiers in Plant Science* (Vol. 4, Issue FEB). Frontiers Research Foundation. https://doi.org/10.3389/fpls.2013.00030

Shen, Q. H., Saijo, Y., Mauch, S., Biskup, C., Bieri, S., Keller, B., Seki, H., Ülker, B., Somssich, I. E., & Schulze-Lefert, P. (2007). Nuclear activity of MLA immune receptors links isolate-specific and basal disease-resistance responses. *Science*, *315*(5815), 1098–1103. https://doi.org/10.1126/science.1136372

Shen, W. H., Parmentier, Y., Hellmann, H., Lechner, E., Dong, A., Masson, J., Granier, F., Lepiniec, L., Estelle, M., & Genschik, P. (2002). Null mutation of AtCUL1 causes arrest in early embryogenesis in Arabidopsis. *Molecular Biology of the Cell*, *13*(6), 1916–1928. https://doi.org/10.1091/mbc.E02-02-0077

Shi, Y., Chen, X., Elsasser, S., Stocks, B. B., Tian, G., Lee, B. H., Shi, Y., Zhang, N., De Poot, S. A. H., Tuebing, F., Sun, S., Vannoy, J., Tarasov, S. G., Engen, J. R., Finley, D., & Walters, K. J. (2016). Rpn1 provides adjacent receptor sites for substrate binding and deubiquitination by the proteasome. *Science*, *351*(6275). https://doi.org/10.1126/science.aad9421

Shi, Z., Maximova, S., Liu, Y., Verica, J., & Guiltinan, M. J. (2013). The salicylic acid receptor NPR3 is a negative regulator of the transcriptional defense response during early flower development in Arabidopsis. *Molecular Plant*, *6*(3), 802–816. https://doi.org/10.1093/mp/sss091

Shringarpure, R., Grune, T., Mehlhase, J., & Davies, K. J. A. (2003). Ubiquitin conjugation is not required for the degradation of oxidized proteins by proteasome. *Journal of Biological Chemistry*, *278*(1), 311–318. https://doi.org/10.1074/jbc.M206279200

Sies, H. (2017). Hydrogen peroxide as a central redox signaling molecule in physiological oxidative stress: Oxidative eustress. In *Redox Biology* (Vol. 11, pp. 613–619). Elsevier B.V. https://doi.org/10.1016/j.redox.2016.12.035

Transport of chemical signals in systemic acquired resistance, 59 Journal of Integrative Plant Biology 336 (2017). https://doi.org/10.1111/jipb.12537

Smalle, J., Kurepa, J., Yang, P., Babiychuk, E., Kushnir, S., Durski, A., & Vierstra, R. D. (2002). Cytokinin growth responses in Arabidopsis involve the 26S proteasome subunit RPN12. *Plant Cell*, *14*(1), 17–32. https://doi.org/10.1105/tpc.010381

Smalle, J., Kurepa, J., Yang, P., Emborg, T. J., Babiychuk, E., Kushnir, S., & Vierstra, R. D.

(2003). The pleiotropic role of the 26S proteasome subunit RPN10 in Arabidopsis growth and development supports a substrate-specific function in abscisic acid signaling. *Plant Cell*, *15*(4), 965–980. https://doi.org/10.1105/tpc.009217

Smalle, J., & Vierstra, R. D. (2004). THE UBIQUITIN 26S PROTEASOME PROTEOLYTIC PATHWAY. *Annual Review of Plant Biology*, *55*(1), 555–590. https://doi.org/10.1146/annurev.arplant.55.031903.141801

Smith, D. M., Chang, S. C., Park, S., Finley, D., Cheng, Y., & Goldberg, A. L. (2007). Docking of the Proteasomal ATPases' Carboxyl Termini in the 20S Proteasome's α Ring Opens the Gate for Substrate Entry. *Molecular Cell*, *27*(5), 731–744. https://doi.org/10.1016/j.molcel.2007.06.033

Son, O., Cho, S. K., Kim, S. J., & Kim, W. T. (2010). In vitro and in vivo interaction of AtRma2 E3 ubiquitin ligase and auxin binding protein 1. *Biochemical and Biophysical Research Communications*, *393*(3), 492–497. https://doi.org/10.1016/j.bbrc.2010.02.032

Sonoda, Y., Sako, K., Maki, Y., Yamazaki, N., Yamamoto, H., Ikeda, A., & Yamaguchi, J. (2009). Regulation of leaf organ size by the Arabidopsis RPT2a 19S proteasome subunit. *The Plant Journal*, *60*(1), 68–78. https://doi.org/10.1111/j.1365-313X.2009.03932.x

Spoel, S. H., Mou, Z., Tada, Y., Spivey, N. W., Genschik, P., & Dong, X. (2009). Proteasome-Mediated Turnover of the Transcription Coactivator NPR1 Plays Dual Roles in Regulating Plant Immunity. *Cell*, *137*(5), 860–872. https://doi.org/10.1016/j.cell.2009.03.038

Spratt, D. E., Walden, H., & Shaw, G. S. (2014). RBR E3 ubiquitin ligases: New structures, new insights, new questions. In *Biochemical Journal* (Vol. 458, Issue 3, pp. 421–437). Portland Press Ltd. https://doi.org/10.1042/BJ20140006

Stegmann, M., Anderson, R. G., Ichimura, K., Pecenkova, T., Reuter, P., Žárský, V., McDowell, J. M., Shirasu, K., & Trujillo, M. (2012). The ubiquitin ligase PUB22 targets a subunit of the exocyst complex required for PAMP-triggered responses in arabidopsis c w. *Plant Cell*, *24*(11), 4703–4716. https://doi.org/10.1105/tpc.112.104463

Stone, S. L. (2014). The role of ubiquitin and the 26S proteasome in plant abiotic stress signaling. In *Frontiers in Plant Science* (Vol. 5, Issue APR). Frontiers Research Foundation. https://doi.org/10.3389/fpls.2014.00135

Su, W., Liu, Y., Xia, Y., Hong, Z., & Li, J. (2011a). Conserved endoplasmic reticulum-associated degradation system to eliminate mutated receptor-like kinases in Arabidopsis. *Proceedings of the National Academy of Sciences of the United States of America*, *108*(2), 870–875. https://doi.org/10.1073/pnas.1013251108

Sun, T., Busta, L., Zhang, Q., Ding, P., Jetter, R., & Zhang, Y. (2018). TGACG-BINDING FACTOR 1 (TGA1) and TGA4 regulate salicylic acid and pipecolic acid biosynthesis by modulating the expression of SYSTEMIC ACQUIRED RESISTANCE DEFICIENT 1 (SARD1) and CALMODULIN-BINDING PROTEIN 60g (CBP60g). *New Phytologist*, *217*(1), 344–354. https://doi.org/10.1111/nph.14780

Sun, T., Huang, J., Xu, Y., Verma, V., Jing, B., Sun, Y., Ruiz Orduna, A., Tian, H., Huang, X., Xia, S., Schafer, L., Jetter, R., Zhang, Y., & Li, X. (2019). Redundant CAMTA Transcription Factors Negatively Regulate the Biosynthesis of Salicylic Acid and N-Hydroxypipecolic Acid by Modulating the Expression of SARD1 and CBP60g. *Molecular Plant*, *13*(1).

https://doi.org/10.1016/j.molp.2019.10.016

Sun, T., Li, Y., Zhang, Q., Ding, Y., Zhang, Y., & Zhang, Y. (2015). ChIP-seq reveals broad roles of SARD1 and CBP60g in regulating plant immunity. *Nature Communications*, *6*(1), 1–12. https://doi.org/10.1038/ncomms10159

Sun, X. M., Butterworth, M., MacFarlane, M., Dubiel, W., Ciechanover, A., & Cohen, G. M. (2004). Caspase activation inhibits proteasome function during apoptosis. *Molecular Cell*, *14*(1), 81–93. https://doi.org/10.1016/S1097-2765(04)00156-X

Tanaka, S., Han, X., & Kahmann, R. (2015). Microbial effectors target multiple steps in the salicylic acid production and signaling pathway. *Frontiers in Plant Science*, *6*(MAY), 1–10. https://doi.org/10.3389/fpls.2015.00349

Tehseen, M., Cairns, N., Sherson, S., & Cobbett, C. S. (2010). Metallochaperone-like genes in Arabidopsis thaliana. *Metallomics*, *2*(8), 556–564. https://doi.org/10.1039/c003484c

Thatcher, L. F., Kamphuis, L. G., Hane, J. K., Oñate-Sánchez, L., & Singh, K. B. (2015). *The Arabidopsis KH-Domain RNA-Binding Protein ESR1 Functions in Components of Jasmonate Signalling, Unlinking Growth Restraint and Resistance to Stress*. https://doi.org/10.1371/journal.pone.0126978

Tian, M., Sasvari, Z., Gonzalez, P. A., Friso, G., Rowland, E., Liu, X. M., Van Wijk, K. J., Nagy, P. D., & Klessig, D. F. (2015). Salicylic acid inhibits the replication of Tomato bushy stunt virus by directly targeting a host component in the replication complex. *Molecular Plant-Microbe Interactions*, *28*(4), 379–386. https://doi.org/10.1094/MPMI-09-14-0259-R

Tomko, R. J., & Hochstrasser, M. (2013). Molecular architecture and assembly of the eukaryotic proteasome. In *Annual Review of Biochemistry* (Vol. 82, pp. 415–445). Annu Rev Biochem. https://doi.org/10.1146/annurev-biochem-060410-150257

Tomko, R. J., Taylor, D. W., Chen, Z. A., Wang, H. W., Rappsilber, J., & Hochstrasser, M. (2015). A Single α Helix Drives Extensive Remodeling of the Proteasome Lid and Completion of Regulatory Particle Assembly. *Cell*, *163*(2), 432–444. https://doi.org/10.1016/j.cell.2015.09.022

Tripathi, D., Raikhy, G., & Kumar, D. (2019). Chemical elicitors of systemic acquired resistance—Salicylic acid and its functional analogs. In *Current Plant Biology* (Vol. 17, pp. 48–59). Elsevier B.V. https://doi.org/10.1016/j.cpb.2019.03.002

Trujillo, M. (2018). News from the PUB: Plant U-box type E3 ubiquitin ligases. In *Journal of Experimental Botany* (Vol. 69, Issue 3, pp. 371–384). Oxford University Press. https://doi.org/10.1093/jxb/erx411

Trujillo, M., Ichimura, K., Casais, C., & Shirasu, K. (2008). Negative Regulation of PAMP-Triggered Immunity by an E3 Ubiquitin Ligase Triplet in Arabidopsis. *Current Biology*, *18*(18), 1396–1401. https://doi.org/10.1016/j.cub.2008.07.085

Trujillo, M., & Shirasu, K. (2010). Ubiquitination in plant immunity. In *Current Opinion in Plant Biology* (Vol. 13, Issue 4, pp. 402–408). Elsevier Ltd. https://doi.org/10.1016/j.pbi.2010.04.002

Ueda, M., Matsui, K., Ishiguro, S., Kato, T., Tabata, S., Kobayashi, M., Seki, M., Shinozaki, K., &

Okada, K. (2011). Arabidopsis RPT2a encoding the 26S proteasome subunit is required for various aspects of root meristem maintenance, and regulates gametogenesis redundantly with its homolog, RPT2b. *Plant and Cell Physiology*, *52*(9), 1628–1640. https://doi.org/10.1093/pcp/pcr093

Ueda, M., Matsui, K., Ishiguro, S., Sano, R., Wada, T., Paponov, I., Palme, K., & Okada, K. (2004). The HALTED ROOT gene encoding the 26S proteasome subunit RPT2a is essential for the maintenance of Arabidopsis meristems. *Development*, *131*(9), 2101–2111. https://doi.org/10.1242/dev.01096

Ung, H., Moeder, W., & Yoshioka, K. (2014). Arabidopsis triphosphate tunnel metalloenzyme2 is a negative regulator of the salicylic acid-mediated feedback amplification loop for defense responses. *Plant Physiology*, *166*(2), 1009–1021. https://doi.org/10.1104/pp.114.248757

Üstün, S., Bartetzko, V., & Börnke, F. (2013). The Xanthomonas campestris Type III Effector XopJ Targets the Host Cell Proteasome to Suppress Salicylic-Acid Mediated Plant Defence. *PLoS Pathogens*, *9*(6), e1003427. https://doi.org/10.1371/journal.ppat.1003427

Üstün, S., Bartetzko, V., & Börnke, F. (2015). The Xanthomonas effector XopJ triggers a conditional hypersensitive response upon treatment of N. benthamiana leaves with salicylic acid. *Frontiers in Plant Science*, *6*(AUG), 599. https://doi.org/10.3389/fpls.2015.00599

Üstün, S., & Börnke, F. (2014). Interactions of Xanthomonas type-III effector proteins with the plant ubiquitin and ubiquitin-like pathways. *Frontiers in Plant Science*, *5*(DEC), 736. https://doi.org/10.3389/fpls.2014.00736

Üstün, S., & Börnke, F. (2015). The Xanthomonas campestris type III effector XopJ proteolytically degrades proteasome subunit RPT6. *Plant Physiology*, *168*(1), 107–119. https://doi.org/10.1104/pp.15.00132

Üstün, S., Hafrén, A., Liu, Q., Marshall, R. S., Minina, E. A., Bozhkov, P. V., Vierstra, R. D., & Hofius, D. (2018). Bacteria exploit autophagy for proteasome degradation and enhanced virulence in plants. *Plant Cell*, *30*(3), 668–685. https://doi.org/10.1105/tpc.17.00815

Üstün, S., Sheikh, A., Gimenez-Ibanez, S., Jones, A., Ntoukakis, V., & Börnke, F. (2016). The proteasome acts as a hub for plant immunity and is targeted by pseudomonas type III effectors. *Plant Physiology*, *172*(3), 1941–1958. https://doi.org/10.1104/pp.16.00808

Van Der Hoorn, R. A. L., & Kamoun, S. (2008). From guard to decoy: A new model for perception of plant pathogen effectors. *Plant Cell*, *20*(8), 2009–2017. https://doi.org/10.1105/tpc.108.060194

van Wersch, R., Li, X., & Zhang, Y. (2016). Mighty dwarfs: Arabidopsis autoimmune mutants and their usages in genetic dissection of plant immunity. In *Frontiers in Plant Science* (Vol. 7, Issue NOVEMBER2016). Frontiers Media S.A. https://doi.org/10.3389/fpls.2016.01717

Verdecia, M. A., Joazeiro, C. A. P., Wells, N. J., Ferrer, J. L., Bowman, M. E., Hunter, T., & Noel, J. P. (2003). Conformational flexibility underlies ubiquitin ligation mediated by the

WWP1 HECT domain E3 ligase. *Molecular Cell*, *11*(1), 249–259. https://doi.org/10.1016/S1097-2765(02)00774-8

Verma, R., Aravind, L., Oania, R., McDonald, W. H., Yates, J. R., Koonin, E. V., & Deshaies, R. J. (2002). Role of Rpn11 metalloprotease in deubiquitination and degradation by the 26S proteasome. *Science*, *298*(5593), 611–615. https://doi.org/10.1126/science.1075898

Vierstra, R. D. (2009). The ubiquitin-26S proteasome system at the nexus of plant biology. In *Nature Reviews Molecular Cell Biology* (Vol. 10, Issue 6, pp. 385–397). Nat Rev Mol Cell Biol. https://doi.org/10.1038/nrm2688

Vierstra, R. D. (2012). The expanding universe of ubiquitin and ubiquitin-like modifiers. In *Plant Physiology* (Vol. 160, Issue 1, pp. 2–14). American Society of Plant Biologists. https://doi.org/10.1104/pp.112.200667

Vlot, A. C., Sales, J. H., Lenk, M., Bauer, K., Brambilla, A., Sommer, A., Chen, Y., Wenig, M., & Nayem, S. (2020). Systemic propagation of immunity in plants. *New Phytologist*, nph.16953. https://doi.org/10.1111/nph.16953

Vlot, A. C., Liu, P. P., Cameron, R. K., Park, S. W., Yang, Y., Kumar, D., Zhou, F., Padukkavidana, T., Gustafsson, C., Pichersky, E., & Klessig, D. F. (2008). Identification of likely orthologs of tobacco salicylic acid-binding protein 2 and their role in systemic acquired resistance in Arabidopsis thaliana. *Plant Journal*, *56*(3), 445–456. https://doi.org/10.1111/j.1365-313X.2008.03618.x

Vogel, C., & Marcotte, E. M. (2012). Insights into the regulation of protein abundance from proteomic and transcriptomic analyses. *Nature Reviews Genetics*, *13*(4), 227–232. https://doi.org/10.1038/nrg3185

Voges, D., Zwickl, P., & Baumeister, W. (1999). The 26S proteasome: A molecular machine designed for controlled proteolysis. In *Annual Review of Biochemistry* (Vol. 68, pp. 1015–1068). Annu Rev Biochem. https://doi.org/10.1146/annurev.biochem.68.1.1015

Voinnet, O., Rivas, S., Mestre, P., & Baulcombe, D. (2003). An enhanced transient expression system in plants based on suppression of gene silencing by the p19 protein of tomato bushy stunt virus. *Plant Journal*, *33*(5), 949–956. https://doi.org/10.1046/j.1365-313X.2003.01676.x

Wang, Caixia, El-Shetehy, M., Shine, M. B., Yu, K., Navarre, D., Wendehenne, D., Kachroo, A., & Kachroo, P. (2014). Free Radicals Mediate Systemic Acquired Resistance. *Cell Reports*, *7*(2), 348–355. https://doi.org/10.1016/j.celrep.2014.03.032

Wang, Caixia, Liu, R., Lim, G. H., De Lorenzo, L., Yu, K., Zhang, K., Hunt, A. G., Kachroo, A., & Kachroo, P. (2018). Pipecolic acid confers systemic immunity by regulating free radicals. *Science Advances*, *4*(5). https://doi.org/10.1126/sciadv.aar4509

Wang, Chenggang, Huang, X., Li, Q., Zhang, Y., Li, J. L., & Mou, Z. (2019). Extracellular pyridine nucleotides trigger plant systemic immunity through a lectin receptor kinase/BAK1 complex. *Nature Communications*, *10*(1), 4810. https://doi.org/10.1038/s41467-019-12781-7

Wang, J., Grubb, L. E., Wang, J., Zipfel, C., Monaghan, J., & Correspondence, J.-M. Z. (2018). A Regulatory Module Controlling Homeostasis of a Plant Immune Kinase. *Molecular Cell*, *69*, 493–504. https://doi.org/10.1016/j.molcel.2017.12.026

Wang, W., Liu, N., Gao, C., Cai, H., Romeis, T., & Tang, D. (2020). The *Arabidopsis* exocyst subunits EXO70B1 and EXO70B2 regulate FLS2 homeostasis at the plasma membrane. *New Phytologist*, *227*(2), 529–544. https://doi.org/10.1111/nph.16515

Wang, Y., Schuck, S., Wu, J., Yang, P., Döring, A. C., Zeier, J., & Tsuda, K. (2018). A MPK3/6-WRKY33-ALD1-Pipecolic Acid Regulatory Loop Contributes to Systemic Acquired Resistance. *The Plant Cell*, *30*(10), 2480–2494. https://doi.org/10.1105/tpc.18.00547

Wen, R., Torres-Acosta, J. A., Pastushok, L., Lai, X., Pelzer, L., Wang, H., & Xiao, W. (2008). Arabidopsis UEV1D promotes lysine-63-linked polyubiquitination and is involved in DNA damage response. *Plant Cell*, *20*(1), 213–224. https://doi.org/10.1105/tpc.107.051862

Wenzel, D. M., & Klevit, R. E. (2012). Following Ariadne's thread: A new perspective on RBR ubiquitin ligases. In *BMC Biology* (Vol. 10, p. 24). BioMed Central. https://doi.org/10.1186/1741-7007-10-24

Wenzel, D. M., Lissounov, A., Brzovic, P. S., & Klevit, R. E. (2011). UBCH7 reactivity profile reveals parkin and HHARI to be RING/HECT hybrids. *Nature*, *474*(7349), 105–108. https://doi.org/10.1038/nature09966

Westman, S. M., Kloth, K. J., Hanson, J., Ohlsson, A. B., & Albrectsen, B. R. (2019). Defence priming in Arabidopsis – a Meta-Analysis. *Scientific Reports*, *9*(1), 1–13. https://doi.org/10.1038/s41598-019-49811-9

Wiborg, J., O'Shea, C., & Skriver, K. (2008). Biochemical function of typical and variant Arabidopsis thaliana U-box E3 ubiquitin-protein ligases. *Biochemical Journal*, *413*(3), 447–457. https://doi.org/10.1042/BJ20071568

Wilkins, M. R., Lindskog, I., Gasteiger, E., Bairoch, A., Sanchez, J. C., Hochstrasser, D. F., & Appel, R. D. (1997). Detailed peptide characterization using PEPTIDEMASS - A World-Wide-Web-accessible tool. *Electrophoresis*, *18*(3–4), 403–408. https://doi.org/10.1002/elps.1150180314

Williams, L. E., Pittman, J. K., & Hall, J. L. (2000). Emerging mechanisms for heavy metal transport in plants. In *Biochimica et Biophysica Acta - Biomembranes* (Vol. 1465, Issues 1–2, pp. 104–126). Elsevier. https://doi.org/10.1016/S0005-2736(00)00133-4

Winter, D., Vinegar, B., Nahal, H., Ammar, R., Wilson, G. V., & Provart, N. J. (2007). An "Electronic Fluorescent Pictograph" Browser for Exploring and Analyzing Large-Scale Biological Data Sets. *PLoS ONE*, *2*(8), e718. https://doi.org/10.1371/journal.pone.0000718

Withers, J., & Dong, X. (2016). Posttranslational Modifications of NPR1: A Single Protein Playing Multiple Roles in Plant Immunity and Physiology. In *PLoS Pathogens* (Vol. 12, Issue 8). Public Library of Science. https://doi.org/10.1371/journal.ppat.1005707

Witzel, K., Üstün, S., Schreiner, M., Grosch, R., Börnke, F., & Ruppel, S. (2017). A proteomic approach suggests unbalanced proteasome functioning induced by the growth-promoting bacterium kosakonia radicincitans in arabidopsis. *Frontiers in Plant Science*, *8*. https://doi.org/10.3389/fpls.2017.00661

Wu, Y., Zhang, D., Chu, J. Y., Boyle, P., Wang, Y., Brindle, I. D., De Luca, V., & Després, C. (2012). The Arabidopsis NPR1 Protein Is a Receptor for the Plant Defense Hormone Salicylic Acid. *Cell Reports*, *1*(6), 639–647. https://doi.org/10.1016/j.celrep.2012.05.008

Xie, L., Lang-Mladek, C., Richter, J., Nigam, N., & Hauser, M. T. (2015). UV-B induction of the E3 ligase ARIADNE12 depends on CONSTITUTIVELY PHOTOMORPHOGENIC 1. *Plant Physiology and Biochemistry*, *93*, 18–28. https://doi.org/10.1016/j.plaphy.2015.03.006

Xin, X.-F., & He, S. Y. (2013). Pseudomonas syringae pv. tomato DC3000: A Model Pathogen for Probing Disease Susceptibility and Hormone Signaling in Plants. *Annual Review of Phytopathology*, *51*(1), 473–498. https://doi.org/10.1146/annurev-phyto-082712-102321

Xiong, Q., Li, W., Li, P., Yang, M., Wu, C., & Eichinger, L. (2018). The Role of ATG16 in Autophagy and The Ubiquitin Proteasome System. *Cells*, *8*(1), 2. https://doi.org/10.3390/cells8010002

Yang, C. W., González-Lamothe, R., Ewan, R. A., Rowland, O., Yoshioka, H., Shenton, M., Ye, H., O'Donnell, E., Jones, J. D. G., & Sadanandom, A. (2006). The E3 ubiquitin ligase activity of Arabidopsis PLANT U-BOX17 and its functional tobacco homolog ACRE276 are required for cell death and defense. *Plant Cell*, *18*(4), 1084–1098. https://doi.org/10.1105/tpc.105.039198

Yang, C. Y., Hsu, F. C., Li, J. P., Wang, N. N., & Shih, M. C. (2011). The AP2/ERF transcription factor AtERF73/HRE1 modulates ethylene responses during hypoxia in Arabidopsis. *Plant Physiology*, *156*(1), 202–212. https://doi.org/10.1104/pp.111.172486

Yang, P., Fu, H., Walker, J., Papa, C. M., Smalle, J., Ju, Y. M., & Vierstra, R. D. (2004). Purification of the Arabidopsis 26 S proteasome: Biochemical and molecular analyses revealed the presence of multiple isoforms. *Journal of Biological Chemistry*, *279*(8), 6401–6413. https://doi.org/10.1074/jbc.M311977200

Yao, C., Wu, Y., Nie, H., & Tang, D. (2012). RPN1a, a 26S proteasome subunit, is required for innate immunity in Arabidopsis. *Plant Journal*, *71*(6), 1015–1028. https://doi.org/10.1111/j.1365-313X.2012.05048.x

Ye, Y., & Rape, M. (2009). Building ubiquitin chains: E2 enzymes at work. In *Nature Reviews Molecular Cell Biology* (Vol. 10, Issue 11, pp. 755–764). Nat Rev Mol Cell Biol. https://doi.org/10.1038/nrm2780

Yee, D., & Goring, D. R. (2009). The diversity of plant U-box E3 ubiquitin ligases: From upstream activators to downstream target substrates. *Journal of Experimental Botany*, *60*(4), 1109–1121. https://doi.org/10.1093/jxb/ern369

Yeh, Y.-H., Chang, Y.-H., Huang, P.-Y., Huang, J.-B., & Zimmerli, L. (2015). Enhanced Arabidopsis pattern-triggered immunity by overexpression of cysteine-rich receptor-like kinases. *Frontiers in Plant Science*, *6*(MAY), 1–12. https://doi.org/10.3389/fpls.2015.00322

Yoon, S. H., & Chung, T. (2019). Protein and RNA Quality Control by Autophagy in Plant Cells. In *Molecules and cells* (Vol. 42, Issue 4, pp. 285–291). NLM (Medline). https://doi.org/10.14348/molcells.2019.0011

Yu, F., & Xie, Q. (2017). Non-26S Proteasome Endomembrane Trafficking Pathways in ABA Signaling. In *Trends in Plant Science*. https://doi.org/10.1016/j.tplants.2017.08.009

Zeier, J., Pink, B., Mueller, M. J., & Berger, S. (2004). Light conditions influence specific defence responses in incompatible plant-pathogen interactions: Uncoupling systemic

resistance from salicylic acid and PR-1 accumulation. *Planta*, *219*(4), 673–683. https://doi.org/10.1007/s00425-004-1272-z

Zhang, S., Li, C., Ren, H., Zhao, T., Li, Q., Wang, S., Zhang, Y., Xiao, F., & Wang, X. (2020). BAK1 Mediates Light Intensity to Phosphorylate and Activate Catalases to Regulate Plant Growth and Development. *International Journal of Molecular Sciences*, *21*(4), 1437. https://doi.org/10.3390/ijms21041437

Zhang, X., & Mou, Z. (2009). Extracellular pyridine nucleotides induce PR gene expression and disease resistance in Arabidopsis. *Plant Journal*, *57*(2), 302–312. https://doi.org/10.1111/j.1365-313X.2008.03687.x

Zhang, Y., Cheng, Y. T., Qu, N., Zhao, Q., Bi, D., & Li, X. (2006). Negative regulation of defense responses in Arabidopsis by two NPR1 paralogs. *Plant Journal*, *48*(5), 647–656. https://doi.org/10.1111/j.1365-313X.2006.02903.x

Zhang, Y., Fan, W., Kinkema, M., Li, X., & Dong, X. (1999). Interaction of NPR1 with basic leucine zipper protein transcription factors that bind sequences required for salicylic acid induction of the PR-1 gene. *Proceedings of the National Academy of Sciences of the United States of America*, *96*(11), 6523–6528. https://doi.org/10.1073/pnas.96.11.6523

Zhou, J., Lu, D., Xu, G., Finlayson, S. A., He, P., & Shan, L. (2015). The dominant negative ARM domain uncovers multiple functions of PUB13 in Arabidopsis immunity, flowering, and senescence. *Journal of Experimental Botany*, *66*(11), 3353–3366. https://doi.org/10.1093/jxb/erv148

Zientara-Rytter, K., & Subramani, S. (2019). The Roles of Ubiquitin-Binding Protein Shuttles in the Degradative Fate of Ubiquitinated Proteins in the Ubiquitin-Proteasome System and Autophagy. *Cells*, *8*(1), 40. https://doi.org/10.3390/cells8010040

Zorrig, W., Abdelly, C., & Berthomieu, P. (2011). The phylogenetic tree gathering the plant Zn/Cd/Pb/Co P 1B- ATPases appears to be structured according to the botanical families. *Comptes Rendus - Biologies*, *334*(12), 863–871. https://doi.org/10.1016/j.crvi.2011.09.004

Zschiesche, W., Barth, O., Daniel, K., Böhme, S., Rausche, J., & Humbeck, K. (2015). The zinc-binding nuclear protein HIPP3 acts as an upstream regulator of the salicylate-dependent plant immunity pathway and of flowering time in *Arabidopsis thaliana*. *New Phytologist*, *207*(4), 1084–1096. https://doi.org/10.1111/nph.13419

8. Danksagung

An dieser Stelle möchte ich allen danken, die zum Gelingen dieser Arbeit beigetragen haben.

Zunächst gilt mein Dank Prof. Dr. Frederik Börnke für die Möglichkeit zur Promotion in seiner Arbeitsgruppe, für die Betreuung und Korrektur dieser Arbeit. Vielen Dank für das tolle Projekt, für das gemeinsame Einarbeiten in die Welt des RNAseq, für die Möglichkeit miteinanders als auch auf Konferenzen meine Arbeit zu diskutieren und für die gute Zeit, die ich seit Beginn meiner Masterarbeit in der Arbeitsgruppe erleben durfte.

Prof. Dr. Tina Romeis und PD Dr. Marcel Wiermer danke ich sehr für die Bereitschaft zur Begutachtung meiner Dissertation.

Mein ganz herzlicher Dank geht an die aktuellen und ehemaligen Mitglieder der AG Börnke, mit denen ich die letzten Jahre am IGZ erlebte. Danke für das gemeinsame Leiden, wenn ein Experiment wieder nicht geklappt hat und die geteilte überschwängliche Freude, wenn ein Problem gelöst wurde, für das bange Warten am Imager, für die unendlichen Diskussionen der neuesten Ergebnisse, für helfende Hände, für unendlich viel Kaffee und Eis. Und nicht zu vergesen sind die fleißigen Korrekturleser!

Weiterhin danke ich den Mitarbeitern am IGZ für die Arbeitsatmosphäre und die Unterstützung, ohne die einige Experimente nicht geklappt hätten. Des Weiteren danke ich dem SFB973 für die finanzielle Unterstützung und den kontinuierlichen wissenschaftlichen Austausch.

Ein besonders großes Dankeschön geht an meine Eltern und engsten Freunde. Ich bin so glücklich, dass ich immer eure volle Unterstützung gespürt habe. Ihr habt mir erst durch euren Rückhalt die Möglichkeit dazu gegeben, diese Arbeit abzuschließen.

Mein allergrößter Dank geht an Basti. Du hast mich in der ganzen Zeit deine bedingungslose Unterstützung spüren lassen und hast so viele Alltagsprobleme von mir ferngehalten. Danke für die Liebe, Motivation und Energie, die du mit mir teilst.

Eidesstattliche Erklärung

Hiermit versichere ich, die vorliegende Arbeit selbstständig angefertigt und keine anderen als die angegebenen Quellen und Hilfsmittel verwendet zu haben. Ich versichere ebenfalls, dass die Arbeit an keiner anderen Hochschule als der Universität Potsdam eingereicht wurde.

Berlin, _____

Daniela Spinti